STUDIES ON THE MAIN GROUP-BASED AROMATIC COMPOUNDS: 1,4,2-DIAZABOROLE AND GERMANIUM(0) SPECIES SU BOCHAO 2018

NANYANG
TECHNOLOGICAL
UNIVERSITY
SINGAPORE

STUDIES ON THE MAIN GROUP-BASED AROMATIC COMPOUNDS: 1,4,2-DIAZABOROLE AND GERMANIUM(0) SPECIES

SU BOCHAO

SCHOOL OF PHYSICAL AND MATHEMATICAL SCIENCES

2018

STUDIES ON THE MAIN GROUP-BASED AROMATIC COMPOUNDS: 1,4,2-DIAZABOROLE AND GERMANIUM(0) SPECIES

SU BOCHAO

SU BOCHAO

School of Physical and Mathematical Sciences

A thesis submitted to the Nanyang Technological University
in partial fulfilment of the requirements for the degree of
Doctor of Philosophy

2018

Acknowledgements

Firstly, I would like to express my gratitude towards my supervisor, Associate Professor Rei Kinjo, for accepting me as his Ph.D student and leading me into the main group research area. During my Ph.D journey, he always supported me by giving me a lot of valuable advice and opportunities, which have encouraged me to be a better researcher. Without his continuous supports, this Ph.D thesis would not have been possible.

I would like to thank my colleagues in these years through my Ph.D study. I have learnt a lot from them. Without their help, it would be tough for me. I want to thank the former members Dr. Kong Lingbing, Dr. Chong Che Chang, Dr. Cui Jingjing, Mr. Wang Liliang, Dr. Chandrakanta Dash, and Mr. Hu Haitao; and current members Dr. Wang Baolin, Dr. Lu Wei, Dr. Rao Bin, Dr. Su Yuanting, Mr. Wu Di, Ms. Gillian Goh Kor Hwee and Ms. Kei Ohta.

I would like to thank all CBC technical and administrative staffs: especially, Dr. Li Yongxin and Dr. Rakesh Ganguly for their help in X-ray crystallography analysis, Ms. Goh Ee Ling, Mr. Ong Yiren Derek and Mr. Keith Leung for their suport in NMR analysis, and Ms. Zhu Wenwei and Ms. Pui Pang Yi for their assistance in the HRMS analysis. I would also like to thank Nanyang Technological University for providing me a research scholarship to support me to pursue my degree.

Lastly, I would like to express my sincere thanks to my family for their always support which has given me the strength to overcome every difficult moment during this journey. Especially, I thank deeply from my heart to Zhang Xiuli, my wife, for her so much love, support and trust. I thank my parents for their always support and encouragement in every single moment.

Table of Contents

List of Abbreviations

NMR	Nuclear magnetic resonance
δ	chemical shift
eq.	equivalent
g	gram
h	hour
IR	infra-red
J	coupling constant
s	singlet
d	doublet
q	quartet
m	multiplet
t	triplet
br	broad
Hz	Hertz
MHz	megahertz
calcd	calculated
NBO	Natural Bond orbital
HOMO	Highest Occupied Molecular Orbital
LUMO	Lowest Unoccupied Molecular Orbital
r.t.	room temperature
HRMS	High Resolution Mass Spectrometry
μL	microliter
M+	parent ion peak in mass spectrum
mL	milliliter
mmol	millimole
mol%	mole percent
M.p.	melting point
m/z	mass to charge ratio (mass spectrum)
^{i}Pr	isopropyl
^{t}Bu	*tert*-butyl
^{n}Bu	n-butyl
Mes	2,4,6-trimethylphenyl

Abstract

Aromaticity is one of most important concepts in the chemistry. Recently, a variety of aromatic molecules containing main group elements have been extensively studied, which show some unique electronic property. However, in contrast to the classical methods widely applied in organic chemistry, the preparation of such aromatic compounds seems a big challenge due to the requirement of the novel synthetic approaches. Given the importance of aromatic compounds involving main group elements, the development of unique framework is desirable from both fundamental and application points of views.

Among them, by installation of a boron atom into ring system with the electronegative nitrogen atom, a series of aromatic B,N-containing heterocycles have been developed with the dramatic advance in synthetic route. In this thesis, a new family of aromatic five-membered B,N-heterocyclic rings, namely 1,4,2-diazaboroles, were introduced and fully characterized. Due to their unique electronic structures, the interesting reactivity was also studied including nucleophilic reactivity of the boron center, borylene insertion, photo-induced isomerization and elimination.

Moreover, by utilization of an imino-N-heterocyclic carbene, we successfully isolated a novel germanium(0) species which can be viewed as a mesoionic germylene. The solid-state structure and computational studies disclosed that the electron delocalization over the C_2N_2Ge ring with the participation of one lone pair on Ge atom, thus supporting its aromaticity. Its nucleophilic properties as one or two lone pairs donor were confirmed by the reactions with MeOTf and transition metal complexes (Cr, Mo, W, Ir).

Thus, in this thesis we have demonstrated that by use of N-heterocyclic carbene as the supporting ligand several novel aromatic species containing boron or germanium elements could be isolated successfully. Some unusual reactivity has been also investigated due to their unique electronic structures.

Chapter 1 Introduction†

Aromaticity is one of the most significant concepts in chemistry. Benzene (C_6H_6), a representative aromatic molecule, was first described by Fradary in 1825,[1] and in 1865, Kekulé proposed its cyclic structure.[2] Decades later, Hückel and Pauling revealed the structure of benzene and clarified the unusual stability based on theoretical calculations.[3] Since then, various aromatic hydrocarbons have been recognized which in general display the intrinsic planar structures,[4] high thermal stabilities,[4a,5] and unique magnetic properties[4a,6] concomitant with π-electron delocalization.[7] As such, Schleyer and co-workers proposed that the nucleus independent chemical shift (NICS) could be a useful indicator to assess the aromatic nature of those molecules.[8]

Beyond the aromatic hydrocarbons, a variety of aromatic hydrocarbons involving heteroatoms (boron and group 14 elements) have been extensively developed, which has enriched the chemistry of aromatic molecules. Owing to the fundamental differences such as electronegativity, size, and polarizability between carbon and the heteroatoms, many of them possess the intrisinic reactivity and physical properties. Thus, exploration of noval heterocycles are highly desired from both fundamental and applied points of view.

1.1 Various synthetic routes to the aromatic five-, six-membered B,N-heterocycles.

On the basis of the isoelectronic and isosteric relationships of CC and BN systems, by incorporating a boron atom into ring system with the electronegative nitrogen atom many B,N-

† Portions of this chapter are taken with permission from: Su. B.; Kinjo, R. Synthesis, **2017**, *49*, 2985 − 3034. Copy→right (2017) Georg Thieme Verlag KG Stuttgart • New York.

containing aromatic molecules have been developed with the dramatic advance in synthetic routes.[9] Significantly, as normally the boron atoms accept electrons while nitrogen atoms donate electrons, the overall electronic structures are quite different from their all-carbon counterparts. The strong dipole moments in the B,N-heterocycles result in their higher reactivity than their hydrocarbon counterparts.[9d] Therefore, their aromaticity, substitution reaction s (such as higher selectivity) and diverse coordination structures compared to their all-carbon counterparts have been widely investigated, which have greatly enriched our fundamental understanding of their electronic structures.[9] In addition, B,N-heterocycles are considered as the potential candidates for application in coordination chemistry, biomedical research, and materials science. Especially, such molecules are expected to be applied as building blocks for the high functional materials, such as π-conjugated frameworks with unique photophysical and electronic properties.

1.1.1 1,2-Azaborolyls

1,2-azaborolyl compounds, as one of the most important surrogates for cyclopentadienyl (Cp) ligands, have been widely studied for a long time due to their coordination ability to metals.[10] During early studies by Schmid in 1980s,[11] the lithium 1,2-azaborolides **2** were synthesized by deprotonation of **1** with lithium tetramethylpiperidine (LTMP) (Scheme 1.1a). In 2000, Ashe's group reported an efficient synthetic procedure of 1,2-azaborolides **5** based on the ring closing metathesis (RCM) (Scheme 1.1b).[12] Vinyl or allyl aminoboranes **3** were subjected to the Grubbs catalyst to form the five-membered heterocycles **4**. Subsequent deprotonation of **4** with lithium diisopropylamide (LDA) afforded the corresponding 1,2-azaborolides **5**. One year later, Fu and co-workers reported that the substituent on the B atom in 1,2-azaborolides can be readily modified using the precursor **6** involving a B-Cl bond (Scheme 1.1c).[13] After nucleophilic substitution on the B center to afford **7**, the corresponding lithium salt **8** was obtained by deprotonation with an appropriate base. This synthetic procedure has enriched the diversity of the 1,2-azaborolide species.

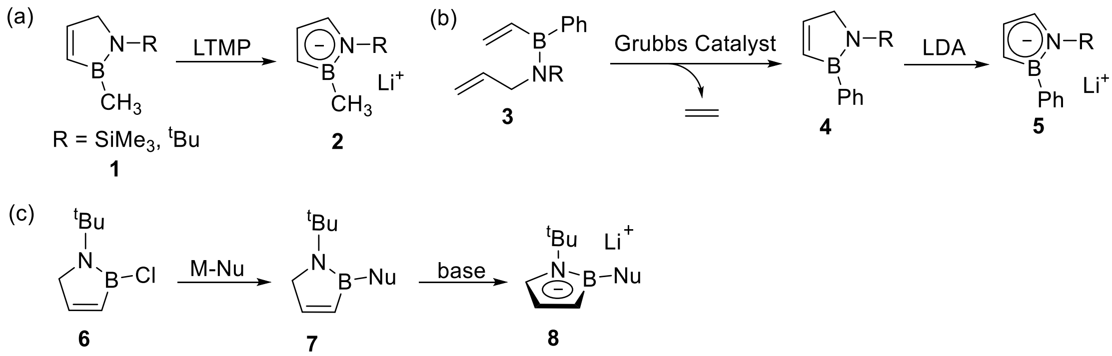

Scheme 1.1 (a) Preparation of B-methyl 1,2-azaborolide **2** by deprotonation of **1**. (b) Preparation of **5** via ring closing metathesis. (c) Preparation of various B-substituted 1,2-azaborolides **8**.

Although several B- and N-substituted 1,2-azaborolides have been developed, synthetic routes to *C*-substituted 1,2-azaborolides are still limited to a handful reports. In 2008, Fang's group reported two synthetic methods for the preparation of tri- and tetra-substituted 1,2-azaborolyls.[14] Starting from allylamines, 1,2-azaborole derivatives **9** featuring a methyl group at the 4-position was synthesized via dilithiation-directed cyclization, B/Sn transmetalation, followed by substitution of the chloro group by nucleophiles (Scheme 1.2). Deprotonation of **9** with $KN(SiMe_3)_2$ or LDA yielded the tri-substituted 1,2-azaborolides **10**. Further methylation of trimetyl-1,2-azaborolyl with MeI followed by deprotonation with LDA afforded tetramethylated 1,2-azaboride **11**, which could react with $(C_5Me_4H)HfCl_3$ to give the corresponding hafnium metallocene complex. Meanwhile, the synthesis of 1,2-azaborolides featuring a substituent at 3-position as well as tetra-substituted 1,2-azaborolides was not accessible by the above mentioned synthetic protocol. Gratifyingly, the same group discovered an alternative method for the preparation of tetrasubstituted azaborolide systems. They utilized 1,2-azazircona-4-cyclopentenes **11**, which are readily available from Cp_2Zr^{II}-mediated cyclization of α,β-unsaturated imine molecules. B/Zr transmetalation of **11** furnished **12**, which yielded the isomer **13** (only for R = H) at the elevated temperature (Scheme 1.3).[14] Subsequent deprotonation of **12** with $KN(SiMe_3)_2$ or LDA afforded **14** in good yields.

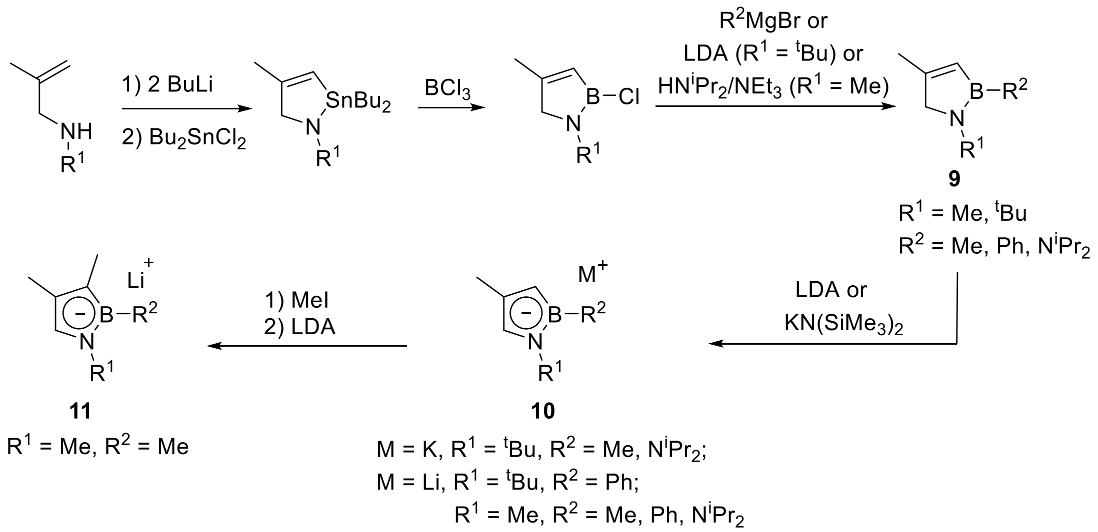

Scheme 1.2 Synthesis of tri-and tetra-substituted 1,2-azaborolides **10** and **11**

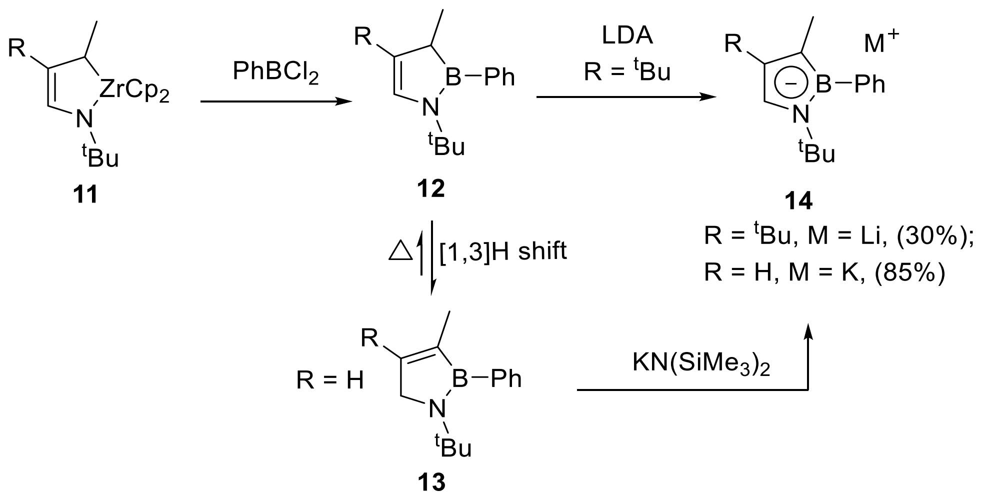

Scheme 1.3 Synthesis of tetra-substituted 1,2-azaborolides **14** via B/Zr transmetalation

Recently, Cui et al. reported the preparation of 1,2-azaborolide derivative involving a B-Cl bond.[15] Lithiation of **15** followed by treatment with boron trichloride generated **16** in which the imine moiety intramolecularly coordinated to the boron center to form a five-membered cyclic structure (Scheme 1.4). Reduction of **16** with potassium metal yielded the 2-chloro-azaborolyl anion **17**. The solid-state structure of **17** revealed the polymeric structure in which the potassium cation acts as a linker by coordinating to the azaborolide ring in η^5-fashion, the aryl ring on the N atom, and the Cl atom. The ^{11}B NMR spectrum of **17** displays a broad signal at 18.3 ppm, which is shifted high field with respect to those of the reported azaborolyl alkali metal species (ca. 25–30 ppm).

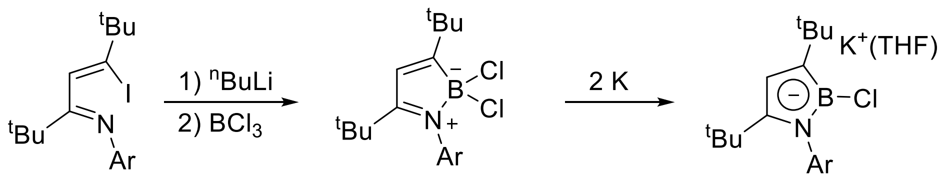

15 **16** (80%) **17** (61%)

Ar = 2,6-$Me_2C_6H_3$

Scheme 1.4 Synthesis of 2-chloro-1,2-azaborolide **17**

1.1.2 Diazaboroles

Diazaboroles can be deemed B,N-heterocyclic counterparts of pyrrole. Synthesis and reactivity of diazaboroles have been comprehensively studied.[9c,10b] In 1973, Merriam and Niedenzu reported the first synthesis of 1,3,2-diazaborole **19** via catalytically dehydrogenation of saturated diazaborole **18** (Scheme 1.5a).[16] Later, an alternative route was developed by Weber and Schmid; thus, 1,3,2-diazaborole **22** was synthesized by reduction of 2-halo-1,3,2-diazaborolium salts **21** which was formed by the reaction of *N,N'*-diphenylbiacetyldiimine **20** with $MeBBr_2$ (Scheme 1.5b).[17] Since then, 1,3,2-diazaborole derivatives bearing various substituents on the backbone have been reported.[18]

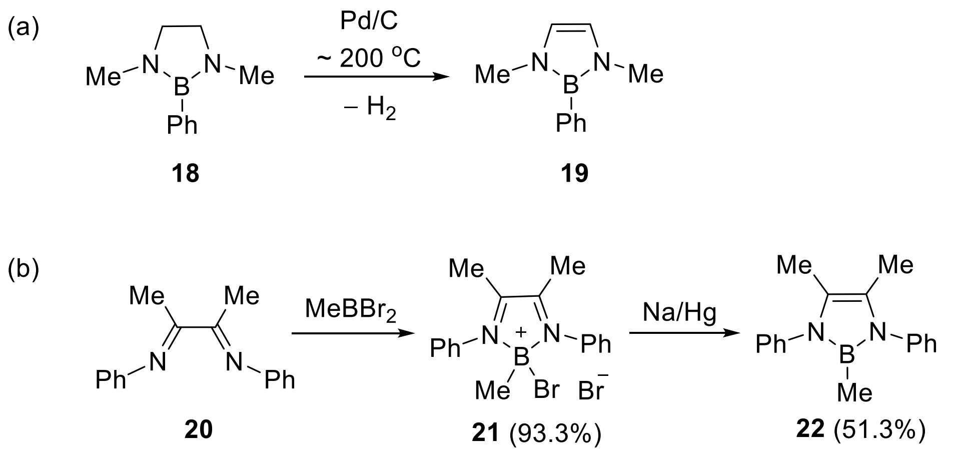

Scheme 1.5 (a) Preparation of 1,3,2-diazaboroles **19** by catalytically dehydrogenation of **18** (b) Preparation of 1,3,2-diazaboroles **22** by reduction of **21**

In 1997, Weber's group developed a new method to synthesize 2-bromo-1,3,2-diazaboroles.[19] Reduction of the 1,4-diazabutadienes **23** with lithium followed by subsequent cyclisation of the dilithio salts **24** with boron tribromide afforded **25** (Scheme 1.6). Isolation of 1,3,2-diazaboroles with halide substituents at the boron center has allowed synthesizing broad 1,3,2-diazaborole derivatives: thus, a variety of 1,3,2-diazaboroles can be accessible by the halide substitution with a hydride, carbon-, nitrogen- and other nucleophiles, which is summarized in a review by Weber.[10b]

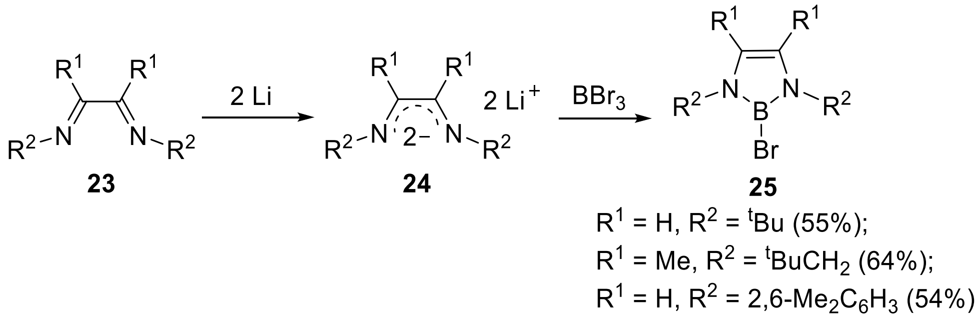

Scheme 1.6 Synthesis of 1,3,2-diazaboroles **25** by cyclocondensation of dilithio salts with BBr_3

Pentaaryl-substituted diazaboroles had been rarely reported until the new synthetic strategy was elegantly developed by the group of Cui in 2012.[20] The reactions of $ArBBr_2$ (Ar = Ph, Mes) with imidoylstannane reagents **26**, readily available by the reaction of imidazoyl chorides with Me_3SnLi, afforded the pentaaryldiazaboroles **27** via the C–C bond formation and ring closure (Scheme 1.7). Pentaarydiazaboroles **27** show luminescence both in the solid state and solution, which is red-shifted in comparison to that of other 4,5-dihydro diazaborole derivatives. DFT calculations revealed that the significant contribution of 4,5-aryl rings to the LUMOs may decrease the energy level, resulting in their red-shifted absorption and emission bands. Bis-diazaboroles **28** with a phenylene linker were obtained by the same method.

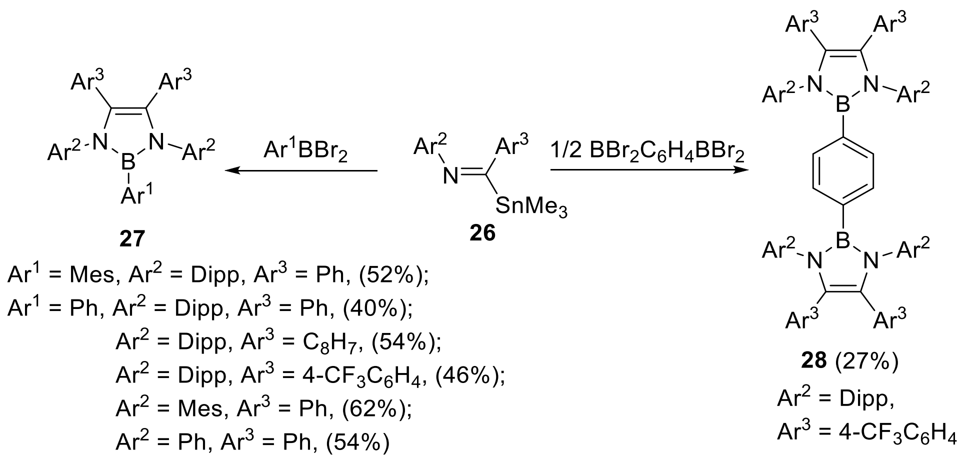

Scheme 1.7 Synthesis of the peripheral aryl-substituted diazaboroles **27** and **28**

1.1.3 1,2,4,3-triazaboroles

In addition to the azaborolyls ligand and 1,3,2-diazaboroles mentioned above, 1,2,4,3-triazaboroles also have been studied a long time ago. In 1963, the first 1,2,4,3-triazaborole, namely 2,3,4,5-tetraphenyl-1,2,4,3-triazaborole **30**, was obtained in 5% yield by pyrolysis of a mixture of 2,5-diphenyltetrazole **29** with the pyridine adduct of diphenylboron azide (Scheme 1.8a). [21] Later, a more general synthetic route was developed by Dewar's group (Scheme 1.8b).[22] Cyclocondensation of amidrazones **31** with RBX_2 derivatives afforded various 1,2,4,3-triazaboroles **32**. A similar protocol using oxamidrazones with boronic acid could be applied for the synthesis of the bisboratriazaroles **33**.[23] In 1999, Weber's group reported more detailed studies on the synthesis and reactivity of 1,2,4,3-triazaboroles including the first example of 3-halo-1,2,4,3-triazaboroles (Scheme 1.8c).[24] Cyclocondensation of N^1,N^3-diphenylformamidrazone **34** with dibromophenylborane or dibromomethylborane yielded the 1,2,4,3-triazaboroles **35** while the reaction of **34** with BCl_3 led to the formation of the 3-halo-1,2,4,3-triazaborole **36**, which could be utilized as a precursor for preparation of other B-substituted 1,2,4,3-triazaboroles.

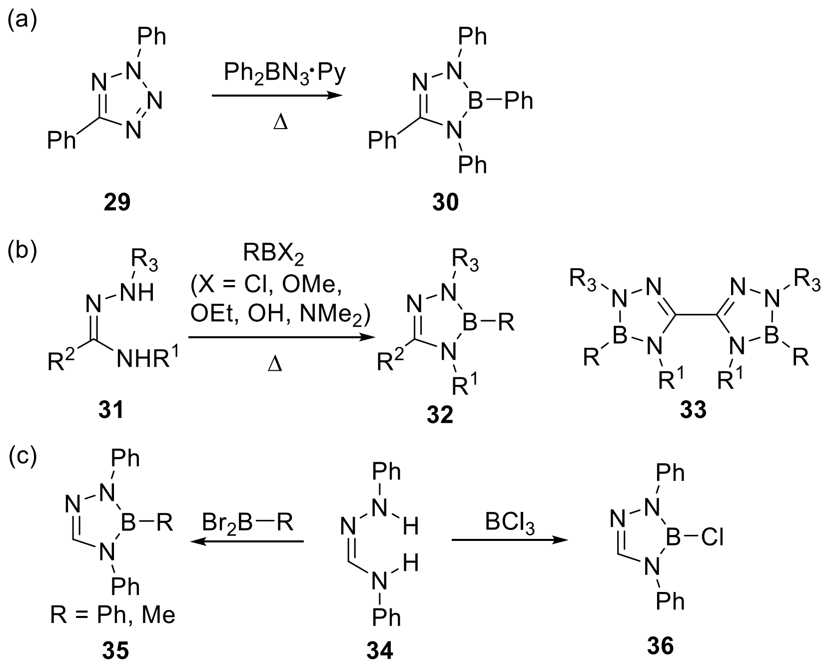

Scheme 1.8 (a) Synthesis of the first example of 1,2,4,3-triazaborole **30**. (b) Synthesis of 1,2,4,3-triazaboroles **32** and **33** by cyclocondensation of amidrazones **31** with RBX_2 (c) Synthesis of the first example of 3-halo-1,2,4,3-triazaborole **36**.

1.1.4 1,2-azaborinine derivatives

1,2-Dihydro-1,2-azaborine (abbreviated as 1,2-azaborinines hereafter), bearing the structure isoelectronic with benzene, has attracted considerable interest in recent years for their potential application in optical, electronic devices and biological systems.[25] The first synthesis of monocyclic 1,2-azaborinines was reported by Dewar and White in the early 1960s.[26] Subsequently, several fused-ring 1,2-azaborinines were reported.[27] Recently, two general synthetic methods have been developed by Ashe's group. In 2000, the same group reported the synthesis of 1,2-azaborinines via ring-closing metathesis and subsequent oxidation process (Scheme 1.9).[12] Treatment of aminoborane **37** with the first-generation Grubbs catalyst afforded the ring-closed product **38**. Subsequent oxidation of **38** with DDQ yielded the 1,2-azaborinine **39**. Later, the same group discovered that 1,2-azaborinines could be formed via ring expansion of the corresponding lithium azaborolides (Scheme 1.10).[28] Ring-closing metathesis of aminoboranes **40** using the first-generation Grubbs catalyst gave the corresponding ring-closed products **41**, which were then deprotonated by LDA to form the azaborolides **42**. The reaction of **42** with CH_2Cl_2 in the presence of a base such as LDA or LiTMP yielded the products **43**. It was also reported by the same group that 1,2-azaborinines could undergo classical electrophilic aromatic substitution reactions to form a variety of 3- and 5- substituted derivatives.[29]

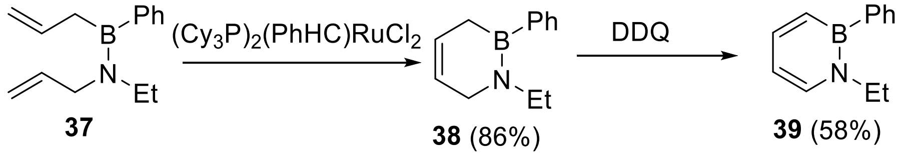

DDQ = 2,3-Dichloro-5,6-dicyano-1,4-benzoquinone

Scheme 1.9 Synthesis of 1,2-azaborinine **39** via oxidization of B,N-heterocycle **38**

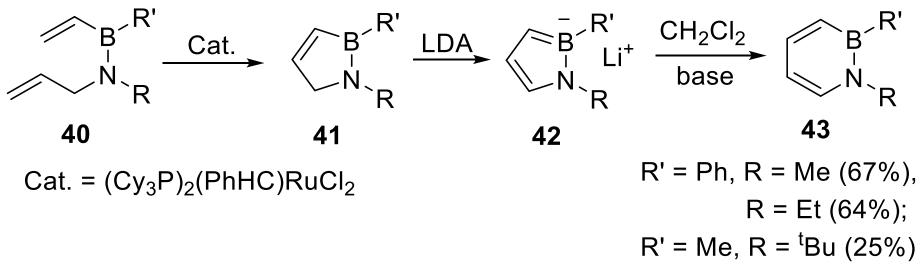

Scheme 1.10 Synthesis of 1,2-azaborinines **43** via ring expansion of lithium azaborolides **42**.

In 2007, Liu's group reported a synthetic protocol for B-substituted 1,2-azaborinines which has led to expand the diversity of the substituents on the boron (Scheme 1.11).[30] Synthetic strategy for B-chloro1,2-azaborinines **46** is based on a ring-closing metathesis of the aminoborane **44** followed by oxidation reaction. With the first-generation Grubbs catalyst, the ring-closed product **45** was generated smoothly from **44**. However, the aromatization of **45** with the oxidation with DDQ as Ashe et al. reported was unsuccessful. By optimization of the reaction conditions, it was found that Pd black efficiently catalyzes the aromatization of **45** to afford **46** in the presence of the hydrogen acceptor such as cyclohexene. From **46** bearing a good leaving Cl group on the boron center, a variety of 1,2-azaborinines **47** could be easily obtained by nucleophilic substitution reaction. Displacement of the chloride in **46** with nucleophiles including alkyl-, vinyl-, aryl-, alkynyl-, and heteroatom-based ones occurred smoothly, and a variety of B-substituted 1,2-azaborinines **47** (R = Et) were obtained. Significantly, Liu et al. reported the reaction of **45** with $LiBHEt_3$ followed by oxidation furnished the first 1,2-azaborinine bearing a B–H bond **47** (Nu = H, R = ^{t}Bu), and examined the potential application of **47** (Nu = H, R = ^{t}Bu) as hydrogen storage material.[31] Analyses on crystal structures of 1,2-azaborinines as well as their pre-aromatic heterocycles involving only one C=C unit in the BNC_4 ring revealed the electron delocalization character.[32]

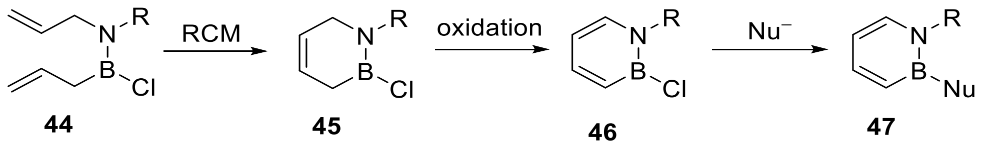

Scheme 1.11 Synthesis of B-substituted 1,2-azaborinines **47**

Although various B-substituted 1,2-azaborinines have been developed by the methods mentioned above, the variety of derivatives featuring aryl group on the boron is narrow because the aryl-based nucleophiles are limited to the corresponding organomagnesium and organolithium reagents. To circumvent this issue, Liu's group developed a general synthetic method of the BN biphenyls **49** via a rhodium-catalyzed cross-coupling reaction between B-Cl-substituted 1,2-azaborinines **46** and arylstannanes **48** (Scheme 1.12).[33] The chlorobis(ethylene)rhodium(I) dimer complex in combination with BIPHEP (2,2'-bis(diphenylphosphino)-1,1'-biphenyl) as the optimal ligand was employed as catalyst. This method has allowed accessing the derivatives which are otherwise difficult to be prepared by the previously developed method, and hence the scope of aryl substituents on the boron in azaborinine ring has been dramatically expanded.

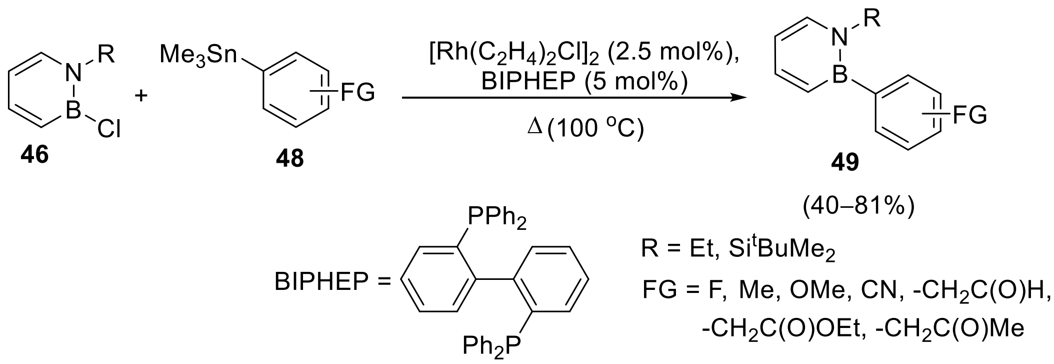

Scheme 1.12 Catalytic synthesis of the BN biphenyls **49**

Recently, Braunschweig et al. reported the preparation of a series of highly-arylated 1,2-azaborinines **52** by ring expansion reactions of inherently electron-deficient boroles **50** with azides **51**.[34] Depending on the substituents on the B atom of boroles as well as azides, two different kinds of 1,2-azaboines **52** and **53** were formed (Scheme 1.13). Compounds **52** (R^1 = Ph, R^2 =Ph, Mes, Me_3Si; R^1 = Mes, R^2 = Me_3Si, 4-^{i}Pr-Ph) were formed via spontaneous elimination of nitrogen. Based on the experimental and theoretical studies, the mechanism for the formation of **52** (R^1 = Ph, R^2 = Me_3Si) has been proposed.[35] The initial step involves the coordination of the α-nitrogen atom of azide **51** to the empty p_z orbital of the boron in **50**. Meanwhile, reactions of the borole **50** (R^1 = Mes) with the bulky group-substituted azides afforded the different kind of 1,2-azaborinines **53** (R = Mes, 2,6-Br_2-4-Me-Ph, 2,6-Br_2-4-^{i}Pr-Ph) containing a RN=N–N motif which can be described as a triazene. Compound **53** (R = Mes) is unstable in solution at room temperature, and decomposes into indazole **54** and 1-hydro-1,2-azaborinine **55**. The formation of these two products involves a C–H activation of one of the *ortho* methyl groups in the mesityl residue of the azo substituent. Interestingly, the replacement of methyl groups at the *ortho* position in the aryl azide with bromo group greatly increases the stability of **53** (R = 2,6-Br_2-4-Me-Ph, 2,6-Br_2-4-^{i}Pr-Ph). Computational studies revealed that the formation of the kinetically favoured azo-azaborinine **53** is due to the steric restraints imposed by the *ortho* substituents in the aryl ligands of both the borole and azide molecule.

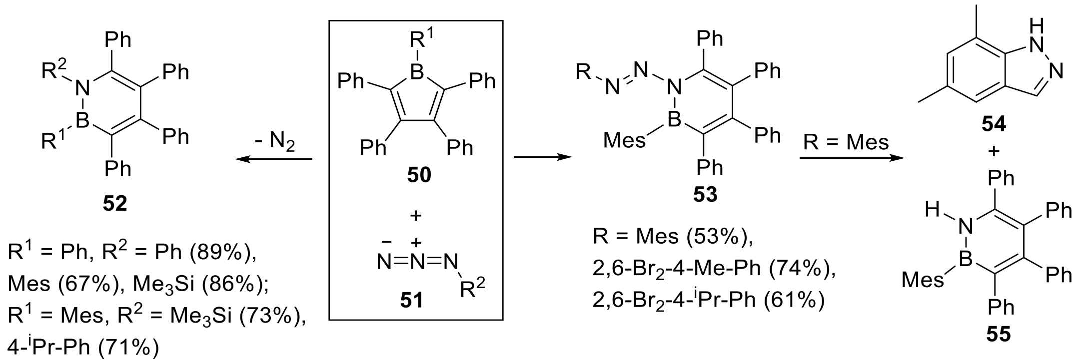

Scheme 1.13 Ring-expansion of boroles **50** with azides **51**

Later, the same group developed a new catalytic reaction for the synthesis of functionalized 1,2-diazaborinines.[36] The reaction of the ethynylferrocene **56** with the iminoborane **57** in the presence of a rhodium catalyst $[(^iPr_3P)_2RhCl]_2$ afforded the first example of ferrocene-functionalized azaborinine **59** via subsequent [2+2]/[2+4] cycloaddition reactions (Scheme 1.14). It has been confirmed that the stoichiometric reaction among **56**, **57** and $[(^iPr_3P)_2RhCl]_2$ led to the formation of the rhodium complex **58**. A mechanistic study was carried out by the reaction of **58** with [D$_1$]-ethynylferrocene under similar conditions, from which deuterated **59** with a deuterium at 3-position was obtained. This observation clearly indicated that the first formation of **58** is followed by the insertion of second **56** concomitant with the cleavage of the B–C bond in the catalytic reaction. In addition, it was found that upon heating at 200 ºC, **59** can be easily converted to 2-tert-butyl-4,6-diferrocenyl-1-hydro-1,2-azaborinine **60**.

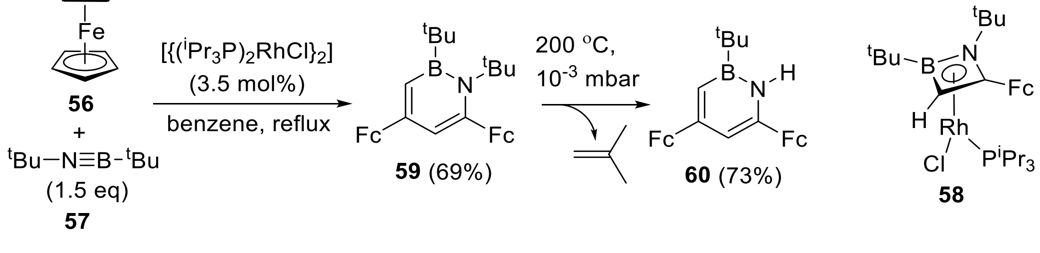

Scheme 1.14 Synthesis of the ferrocene-functionalized 1,2-azaborinine **59**

With the unsymmetrical iminoborane, the same strategy can be applied for the regio-selective construction of functionalized 1,2-azaborinines.[37] Rhodium-catalyzed reactions of the unsymmetrical iminoborane **61** with acetylene **62** yielded the new 1,2-azaborinines **63** (Scheme 1.15a). Through control of the stepwise reaction sequence, 1,2-azaborinines with functional groups at the 4- and/or 6-position can be obtained. Treatment of $[(^iPr_3P)_2RhCl]_2$ with **61** and **62** gave η^4-1,2-azaborete complexes **64**, which were fully characterized by NMR spectra and X-ray crystallography (Scheme 1.15b). Finally, the late-stage cycloaddition of **64** with various terminal alkynes led to the 1,2-azaborinines **65**.

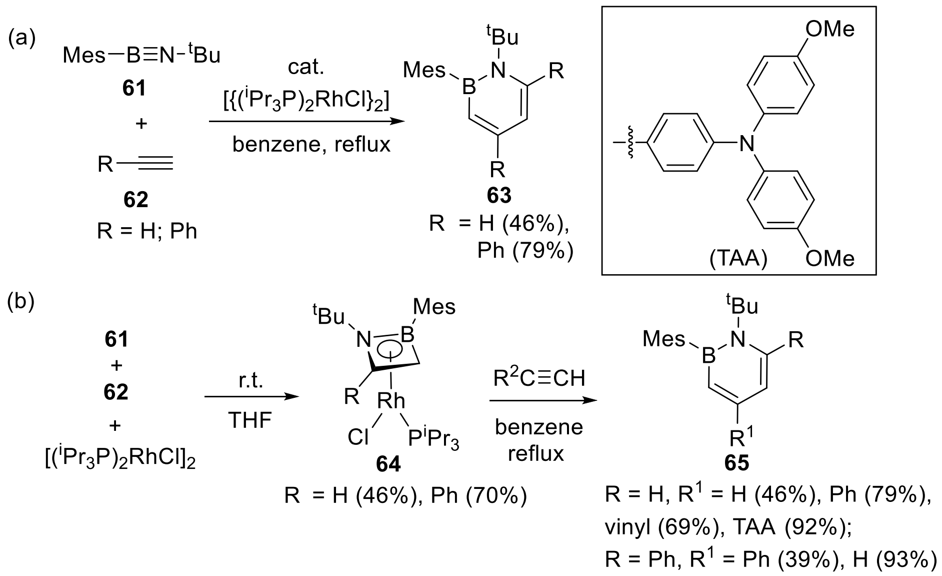

Scheme 1.15 (a) Synthesis of 1,2-azaborinines **63** (b) Synthesis of 1,2-azaborinines **65** through η^4-1,2-azaborete complexes **64**

1.1.5 1,3-azaborinine derivatives

Compared with the intensive studies on 1,2-azaborinines, the synthesis of 1,3-azaborinines have been rarely reported. In 2011, The first isolation of 1,3-azaborinine derivative was reported by Liu's group (Scheme 1.16a).[38] Reaction of *N*-methylallylamine **66** with 1,2,3-

benzotriazole **67** afforded a mixture of **68** and **68'**. Treatment of the mixture with Bu_3SnLi gave **69**. Lithium/tin exchange of **69** with n-hexyllithium followed by treatment of electrophile **70** furnished the coupling product **71**. After protection of the N lone pair in **71** with triflic acid, ring-closing metathesis in the presence of the Grubbs first-generation catalyst followed by deprotonation with DBU afforded a cyclic compound **72**. Dehydrogenation of **72** with Pd/C catalyst yielded 1,3-azaborinine **73** together with the reduced byproduct **74**. The substitution reaction of **73** with a variety of nucleophiles rarely occurred under basic and neutral conditions, probably due to the poor leaving ability of the diisopropylamino group. Compound **73** readily reacted with acetic acid to give B-OAc substituted azaborinine derivative **75**, which may further react with $LiAlH_4$ to produce compound **76** (Scheme 1.16b).[39] By contrast, treatment of **75** with other stronger bases such as $^{n}BuLi$ generated only a trace amount of substitution products. Notably, by introduction of a bulkier carboxylate group $^{t}BuCO_2$ instead of OAc group, the substitution reaction of **73** could smoothly undergo to furnish various products **77** (Scheme 1.16b).[40]

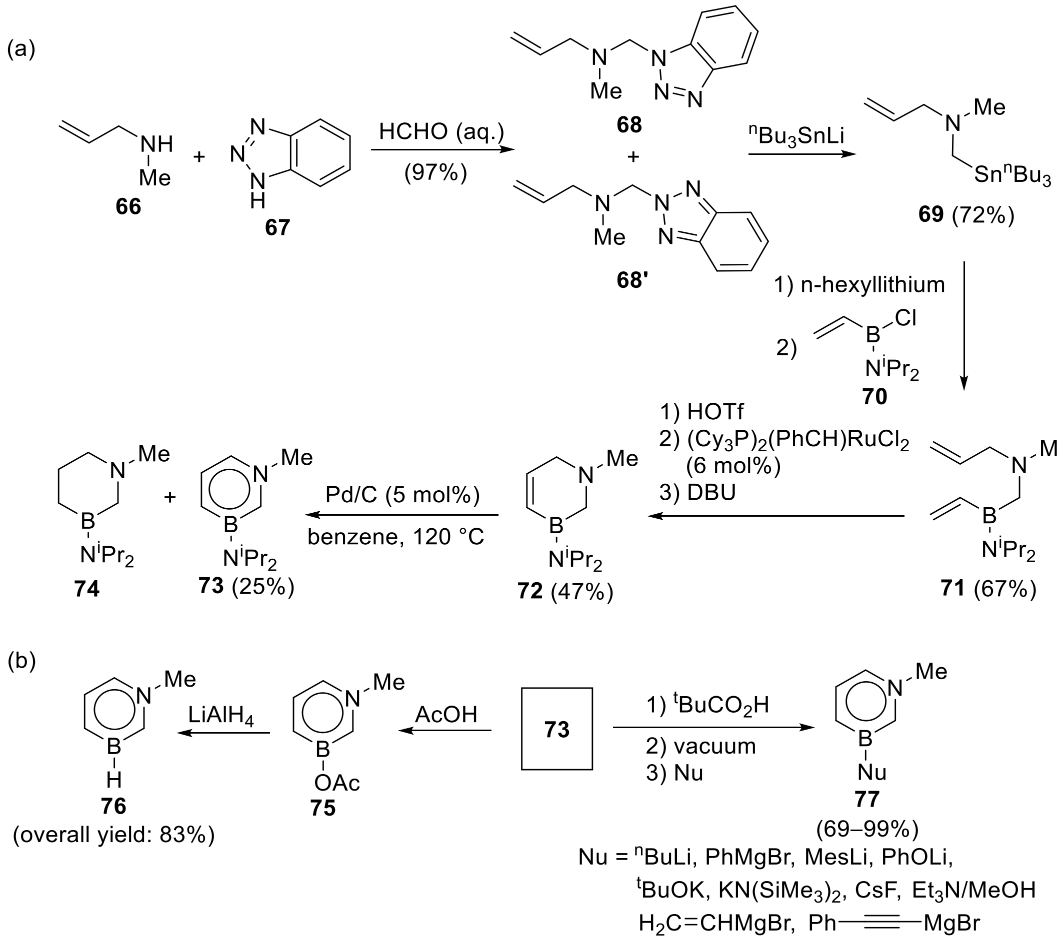

Scheme 1.16 (a) Synthesis of the first example of 1,3-azaborinine **73** (b) Synthesis of various B-substituted 1,3-azaborinines **75**, **76** and **77** by the nucleophilic substitution reaction

1.1.6 1,4-azaborinine derivatives

Although the polycyclic dibenzofused 1,4-azaborinine derivatives were reported long time ago,[41] simple monocyclic 1,4-azaborinines have been unexplored until the first isolation of 1,4-azaborinine reported by Braunschweig's group in 2012.[42] Isolable 1,4-Azaborinine **78** was prepared by the cyclization reaction of $^{t}BuB{\equiv}N^{t}Bu$ with acetylene catalyzed by $[(^{i}Pr_3P)_2RhCl]_2$ (Scheme 1.17). In the ^{11}B NMR spectrum, a singlet appears at $\delta = 48$ ppm. Compound **78** is chemically stable and does not react with water, air, or even trifluoroacetic acid. By controlling the reaction condition, the rhodium η^4-1,2-azaborete complex **79** was successfully isolated, indicating that the **79** was the key intermediate for the formation of **78**.

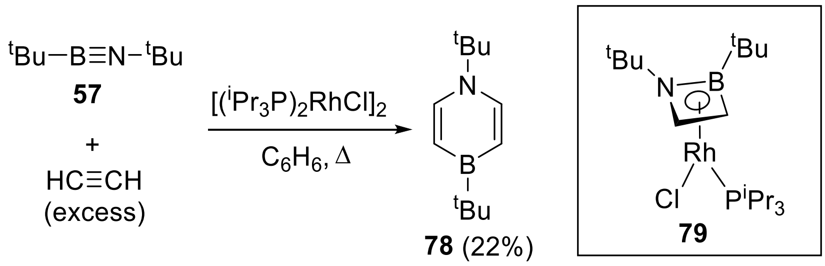

Scheme 1.17 Rh-mediated synthesis of a 1,4-azaborinine **78**

Very recently, Liu's group developed a simple and general method for the synthesis of various monocyclic 1,4-azaborinines (Scheme 1.18).[43] B-amino-1,4-azaborinine **84** was formed over three steps. Reaction of methylamine **80** with 2,3-dibromopropene **81** afforded a bis(allyl)amine **82**. Subsequent metal-halogen exchange followed by quenching with $^{i}Pr_2NBCl_2$ gave BN heteocycle **83** in good yield. Olefin isomerization of **83** with the Ru^{II} catalyst furnished a product **84**. Following the similar synthetic route, 1,4-azaborinines with a wide range of substituent on the nitrogen atom could be obtained by displacement of **80** with other amines, such as benzylamine, allylamine, aniline, *para*-methoxyaniline, and *para*-trifluoromethylaniline. On the other hand, modification of the substituents on the boron atom could be achieved with compounds **85** featuring good leaving groups (-OMe, -Cl). Reaction of **84** with MeOH or HCl furnished **85**, which was then treated with a variety of nucleophiles to afford a vaiety of *B*-substituted 1,4-azaborinines **86**.

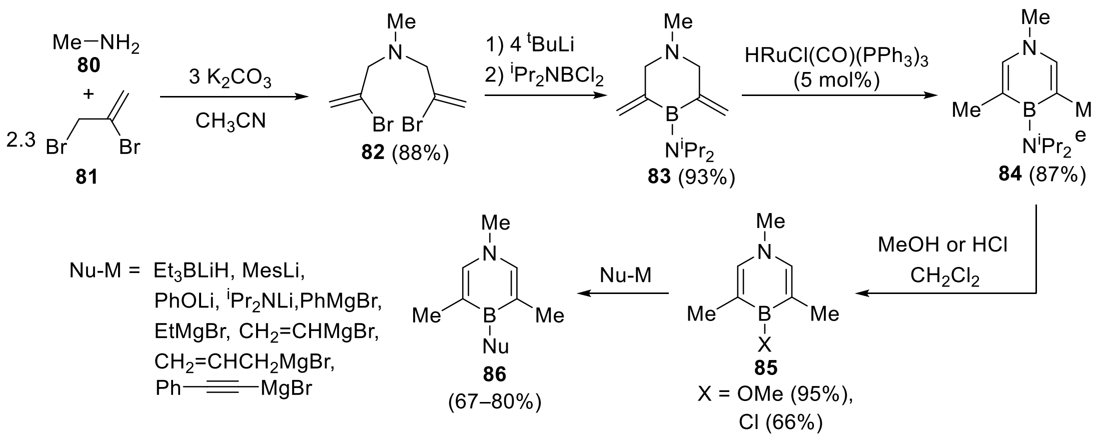

Scheme 1.18 Synthesis and nucleophilic substitution reaction of 1,4-azaborinine **84**

1.1.7 1,3,2,5-diazadiborinine and 1,4,2,5-diazadiborinine derivatives

Recently, our group developed two novel aromatic BN heterocycles based on the $B_2C_2N_2$ six-membered skeleton, namely 1,3,2,5-diazadiborinine and 1,4,2,5-diazadiborinine.[44] 1,3,2,5-diazadiborinine **90** was prepared by the synthetic procedure shown in Scheme 1.19a. The reaction of two equivalents of 2-lithio-4,4'-dimethyl-2-oxazolide **87** with dichlorophenylborane afforded the lithium salt **88**, which after treatment of one equivalent of dichlorophenylborane generated **89**. Reduction of **89** with six equivalents of KC_8 afforded 1,3,2,5-diazadiborinine **90** featuring a formal B(+I)/B(+III) mixed valence system. 1,4,2,5-diazadiborinine **92** was prepared by reduction of compound **91** with excess amounts of KC_8 in benzene (Scheme 1.19b).[45] The ^{11}B NMR spectrum of **92** displays a singlet at $\delta = 18.3$ ppm, clearly indicating that two boron atoms in **92** are magnetically equivalent. X-ray crystallography confirmed the coplanar $B_2C_2N_2$ ring. DFT studies revealed that the HOMO is mainly a π-orbital over the six-membered $B_2C_2N_2$ ring and the NICS values for the central $B_2C_2N_2$ ring are comparable to those of benzene, indicating the considerable aromatic nature.

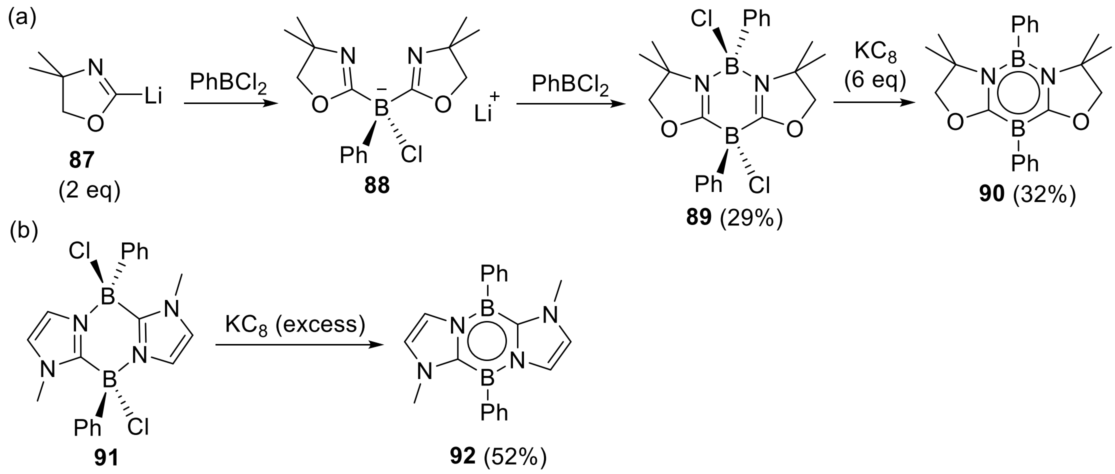

Scheme 1.19 (a) Synthesis of 1,3,2,5-diazadiborinine **90** (b) Synthesis of 1,4,2,5-diazadiborinine **92**

1.2 Preparation of various aromatic five-membered heterocyclic rings involving heavy group 14 elements (Si, Ge)

Aromatic compounds contaning heavier group 14 elements (Si, Ge) have received considerable attention recently.[46] However, the design and synthesis of such compounds remains challenging in comparison with its carbon analogue, mainly due to their distinct electronegativity, size, polarizability, as well as the difficulty of the formation of sp^2-hybridization. Because of these intrinsic properties, the resulting compounds are usually highly reactive and unstable compared to their carbon analogue. To overcome the difficulty in isolation of the reactive Si- and Ge-containing aromatic compounds, two major strategies, namely kinetic stabilization and thermodynamic stabilization, should be taken into consideration.[46b] The former is mainly achieved using bulky groups to prevent its oligomerization or reactions with other reagents. The later means the stabilization of the ground state by the mesomeric effect of the electron-donating or -withdrawing neighbouring heteroatoms. In many cases, application of the protective bulky substitutes is the strategy for the successful synthesis of heavier main group compounds. For instance, installation of the bulky substitute Tbt (2,4,6-tris[bis(trimethylsilyl)methyl]phenyl) on the silicon atom allows the isolation of the reactive silabenzene or silanaphthalene. However, sometimes slightly modification of the electronic property of attached substitutes on the heavier atoms will also be efficient for the improvement of their stabilization. Based on both strategies, several aromatic five-membered heterocyclic rings containing Si, Ge elements have been isolated, including unsaturated N-heterocyclic silylenes and germylenes as well as anions and dianions of group 14 metalloles. Among them, the silole monoanions show various degrees of aromaticity depending on the substituted groups, however, only negligible aromatic character is shown in monoanions of germoles.

1.2.1 N-heterocyclic silylenes and germylenes

As the unsaturated N-heterocyclic silylenes and gemylenes contain six π-electrons in the ring, their thermal stability is improved compared with their saturated analogues mainly due to the cyclic six π-electrons aromaticity, which has been investigated by both experimental and theoretical methods, such as ^{1}H NMR chemical shift, photoelectron spectra, core excitation spectra, ab initio molecular orbital calculations, and nucleus-independent chemical shift (NICS) calculations.[47] The general preparation of these aromatic compounds is based on the reduction of their cyclic diamino halide group 14 compounds.

The unsaturated N-heterocyclic silylene was firstly reported by Denk's group[48] and West's group.[49] The reaction of glyoxal **93** with *tert*-butylamine afforded the diimine **94** (Scheme 1.20). Lithiation of **94** gave the dilithium derivative **95**, which further reacted with silicon tetrachloride to furnish a cyclic silicon product **96**. Reduction of **96** with potassium metal in refluxing THF resulted in the target silylene **97**. The final reduction process requires the careful monitoring with ^{1}H NMR, due to the difficulty in separation of **96** and **97** as well as the possibility of over-reduction of **97**. In the solid-state structure, the longer C–C bond length and shorter Si–N bond length of **97** than those of **96** were observed, indicating the delocalization of the π-electrons over the C_2N_2Si ring. Later, the photoelectron spectra and theoretical calculation of **97** confirmed the presence of significant Si–N π bonding interaction and 6π electrons delocalization over the five-membered ring.[50]

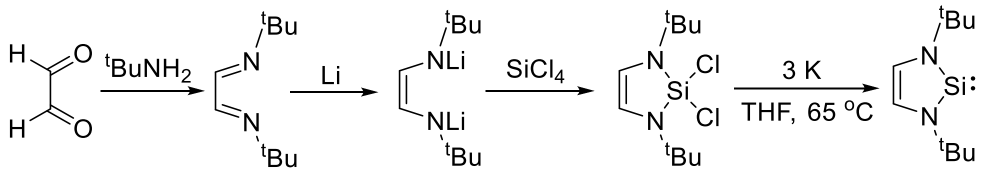

Scheme 1.20 Synthesis of the unsaturated silylene **97**

In 2004, a cationic aromatic compound **99**, namely 2-silaimidazolium cation, was reported by Komatsu's group.[51] **98** was synthesized by reaction of **97** with bis(trimethylsilyl)methyl chloride (Scheme 1.21). Then, chloride abstraction from **98** with [triethylsilylbenzene]$^{+}$•TPFPB^{-} resulted in the cationic species **99**, which was confirmed by multiple NMR spectroscopy. **99** is stable in solution and the solid state below −10 °C, but decompose at higher temperatures. In the optimized structure of **99**, all the atoms of the C_2N_2Si five-membered ring are coplanar and the silicon atom possesses a tricoordinate planar geometry. The negative NICS(1) value of −6.5 indicates the aromatic property of **99**.

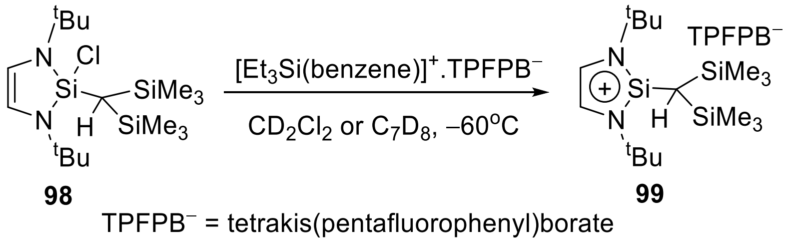

Scheme 1.21 Synthesis of the 2-silaimidazolium cation **99**

Herrmann's group reported the preparation of the first unsaturated N-heterocyclic germylene via different synthetic routes.[52] Interestingly, **102** could be obtained as the by-product by dehydrogenation during the preparation of the saturated germylene **101** from the reaction of germanium dichloride•1,4-dioxane complex ($GeCl_2$•1,4-dioxane) with the dilithium salt **100** (Scheme 1.22). The reaction of **101** with $[(CH_3)_3Si]_2NLi$ also afforded **102**. The most convenient and general method for preparation of **102** is the direct treatment of $GeCl_2$•1,4-dioxane with the unsaturated dilithium salt **95**. **102** is thermodynamically more stable than **101**, and therefore **101** is converted to **102** upon heating to 60 °C. X-ray structure analysis of **102** revealed that the atoms of the C_2N_2Ge five-membered ring are coplanar. In addition, DFT calculations and experimental results (planarity, ^{15}N NMR data) support its aromatic character.

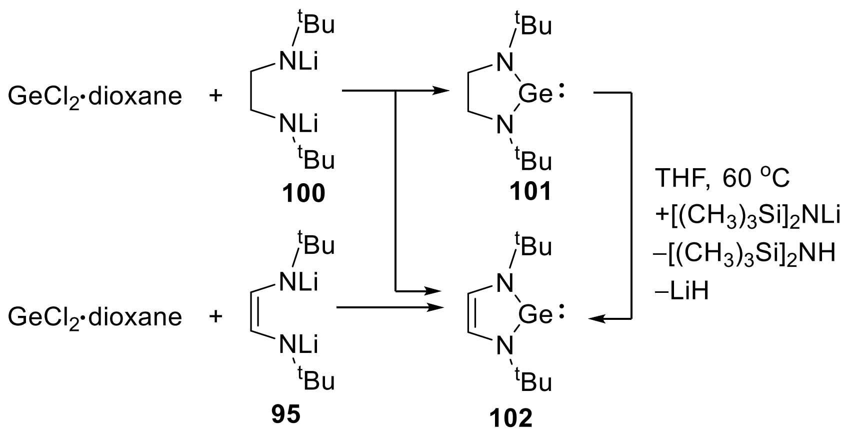

Scheme 1.22 Synthesis of the first unsaturated germylene **102**

1.2.2 Silole anions and germole anions

As the heavier congener of the cyclopentadienyl anion, the group 14 metallole mono- and dianions has attracted increasing attention recently. In 1993, Boudjouk's group reported the first preparation of a silole anion, which was obtained by reduction of bis(1-tert-butyl-2,3,4,5-tetraphenyl-1-silacyclopentadienyl) **103** with sodium in THF (Scheme 1.23a).[53] The ^{29}Si NMR chemical shift (δ =26.12 ppm) of **104** is significantly shifted downfield relative to that (δ =22.50 ppm) of **103**, suggesting the negative charge is delocalized into the butadiene unit by an incorporation of silicon p-orbital. Thus, **104** shows some aromatic character. Later, the C-alkylated silole anion **106** was synthesized by the Si−Si bond cleavage of **105** with benzylpotassium (Scheme 1.23b).[54] Interestingly, the ^{29}Si NMR signal (δ = −41.52 ppm) of **106** is shifted upfield compared to that (δ = −34.26 ppm) of **105**. This phenomenon is different from that of **104**, indicating that the high localization of negative charge on the silicon. The solid-state structure of **106** discloses the non-aromaticity of the anion as supported by the significant C−C bond alternation in the C_4Si ring and the pyramidal geometry at the silicon center. The different aromatic properties of **104** and **106** show that the substitutes on the rings are important to influence the aromaticity of the anions.

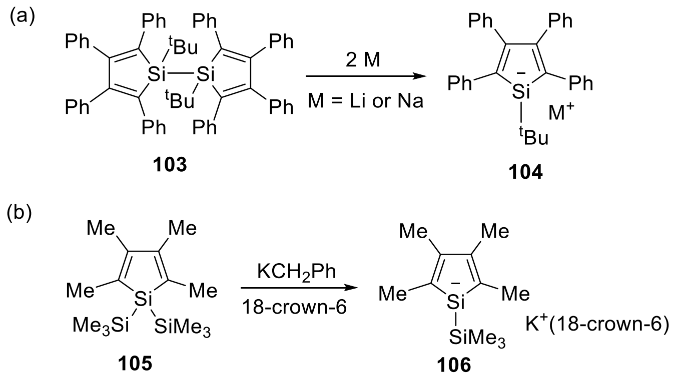

Scheme 1.23 (a) Synthesis of the silole anion **104**. (b) Synthesis of the silole anion**106**

The pioneering studies on the synthesis of C-phenylated germole anions were performed by the groups of Curtis and Jutzi, where the in-situ generated anions were confirmed by the trapping reaction with Me_3SiCl.[55] In 1990, Dartiguenave group reported the first stable C-methylated germole anions **109**.[56] Treatment of **107** with one equivalent of Grignard reagent followed by reduction with $LiAlH_4$ afforded the precursor **108** in good yield (Scheme 1.24). Then, the reaction of **108** with *n*-butyllithium in THF generated the germole anion **109**. The deshielding of C_α and C_β should be attributed to the delocalization of the negative charge on the germanium atom.

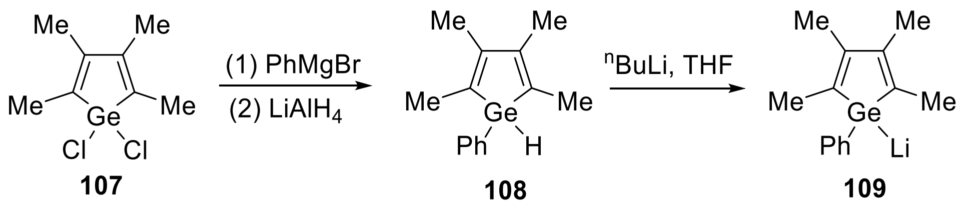

Scheme 1.24 Synthesis of the germole anion **109**

Later, a series of germole anions were prepared and their solid structures were confirmed by X-ray diffraction analysis (Scheme 1.25).[54b,57] **112a** and **113a** were produced by treatment of **110** and **111** with butyllithium and crown ether, respectively. Deprotonation of **110** and **111** with potassium salts such as $KN(SiMe_3)_2$ and KCH_2Ph gave the anions **112b** and **113b,** respectively. Alternatively, reductive cleavage of Ge–Ge bond in **114** with sodium in the presence of 15-crown-5 led to the formation of **115**. The ^{13}C NMR signals for the C_4Ge ring of **115** are somewhat shifted downfield compared with those of the precursors, suggesting that those anions possess the non-aromaticity with the localization of negative charge on the germanium center. In the solid-state structure, the germanium center possess a pyramidal geometry and a sharp angle between the C_4Ge plane and the Ge−R bond is observed. In addition, the distances C−C bond in the five-membered ring suggest a remarkable diene character. Thus, the experimental results indicate the non-aromaticity of the germole anions.

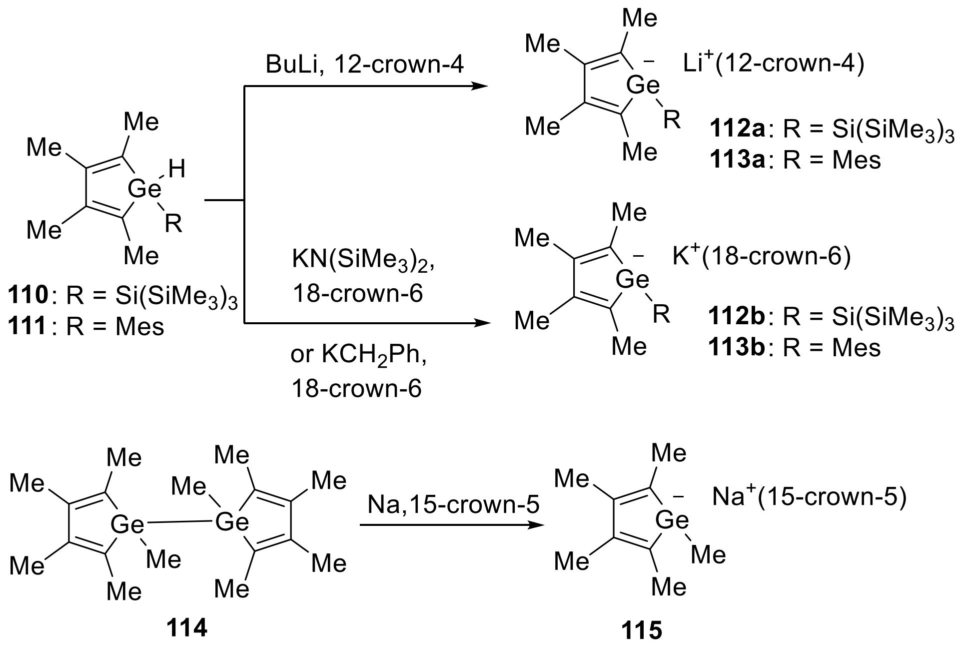

Scheme 1.25 Synthesis of the germole anion **112, 113** and **115**

In sharp contrast to the silole and germole mono-anion, their dianions show significant aromatic character, which is mainly due to the reduced pyramidal geometry or complete planarity of the silicon and germanium atoms leading to the better conjugation of the p-orbitals of the carbon and E (E = Si, Ge) atoms in the dianions. Compound **117** (M = Na) represents the first preparation of the silole dianion, which was formed by reduction of the 1,1-dichlorosilole **116** with sodium (Scheme 1.26a).[58] Four years later, the silole dianion **117** (M = Li) was reported and its aromaticity was discussed.[59] The ^{29}Si NMR spectrum shows only one signal at 68.54 ppm, significantly shifted downfield relative to that (6.80 ppm) of **116**. The ^{13}C NMR signals of C_α and C_β atoms in the C_4Si ring were shifted upfield, suggesting the somewhat aromatic property. X-ray diffraction analysis of **117** (M = Li) revealed two kinds of coordination situation for lithium atoms. One of the lithium atoms is coordinated to silole ring in η^5-fashion and the other is coordinated to the silicon atom in η^1-fashion. All the C–C distances in the C_4Si ring are very similar and in the range of 1.426–1.448 Å. The experimental results support the aromatic property of **117** (M = Li). In addition, the C-methylated silole dianion **119** was prepared by treatment of 1,2-dibromosilole **108** with potassium (Scheme 1.26b).[54] Crystals of **120** were isolated after the complexation of **119** with 18-crown-6. The solid-state structure disclosed the slight bond length alternation in the C_4Si ring, which is possibly because of the delocalization of π-electrons overall the five-membered ring. In contrast to the structure of **117** (M = Li), the potassium cation features an η^5-coordination on both sides of the ring.

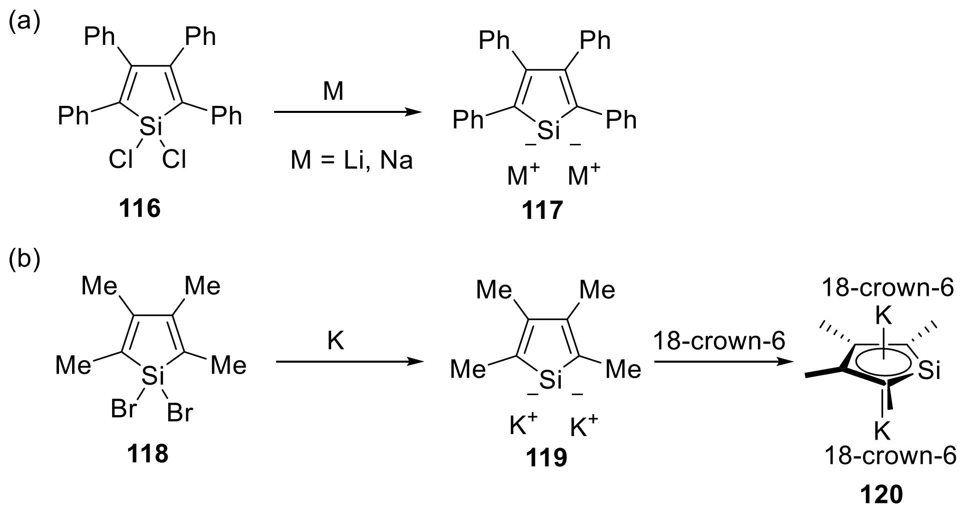

Scheme 1.26 (a) Synthesis of the silole dianion **117**. (b) Synthesis of the silole dianions **119** and **120**

The first reported germole dianion was prepared by the reaction of 1,1-dichlorogermole **121** with lithium (Scheme 1.27a).[60] Sonication of a THF solution of **121** with lithium resulted in a dark-red solution, which further reacted with R–X to afford **123**. The formation of **123** indicated the generation of the germole dianion **122**. Crystals suitable for X-ray diffraction analysis were obtained from dioxane solution.[61] The solid-state structure revealed two distinct structures depending on the crystallization temperature. At low temperature (–20 ºC), two lithium atoms are located at both sides of the five-membered ring in η^5-fashion. By contrast, at room temperature (25 ºC), two lithium atoms show different coordination situations: one is bonded to the ring in η^5-fashion and the other is bonded to the germanium atom in η^1-fashion. In both situations, the high delocalization of electrons in the ring results in nearly equal C–C bond distances. The C-methylated germole dianion **124** was prepared by treatment of **107** with potassium (Scheme 1.27b).[54b]. Complexation of **124** with 18-crown-6 resulted in the formation of crystalline bis(germole dianion) **125**. The solid-state structure revealed a slight bond length alternation in the germole ring suggests the aromatic nature of **125**.

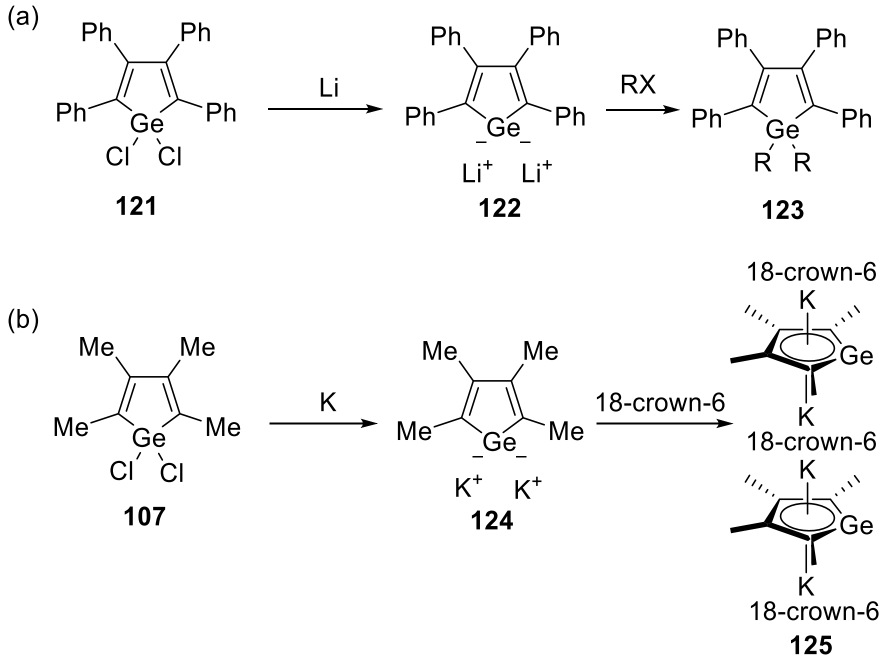

Scheme 1.27 (a) Synthesis and reactivity of the germole dianion **122**. (b) Synthesis of the germole dianions **124** and **125**

1.2.3 Disilagermacyclopentadienide and trisilacyclopentadienide

In 2005, Sekiguchi group reported a novel heavy group 14 analogue of the cyclopentadienide ion containing two Si atoms and one Ge atom.[62] Reduction of **126** with two equivalents of KC_8 in THF smoothly produced the anionic species **127**, which has a poor crystallization property (Scheme 1.28). Treatment of **127** with an excess of LiBr resulted in the clean formation of the corresponding Li derivative **128**. X-ray crystallography revealed that the five-membered ring of **128** is nearly planar and the Li atom is coordinated to the ring in η^5-fashion. To get deep insight into the electronic structure of **128**, DFT calculation was performed. The negative NICS(1) value (−12) of **128** supports its aromatic character.

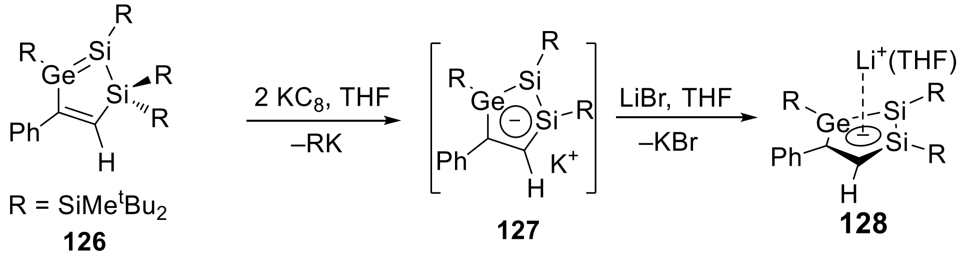

Scheme 1.28 Synthesis of 1,2-disila-3-germacyclopentadienide **128**

Later, the Sekiguchi group reported a totally different approach for the synthesis of a novel aromatic trisilacyclopentadienide ion **131** (Scheme 1.29).[63] Heating of the 1,2,3-trisilabicyclo[1.1.0]butane derivative **129** at 130 ºC for 8 h in the presence of excess 3-hexyne as a trapping agent afforded the air-sensitive 1,2,3-trisilacyclopenta1,4-diene **130**. X-ray ananlysis of **130** showed that the C_2Si_3 five-membered ring is planar and there is no conjugation between the Si=Si and C=C bonds base on their bond lengths. Reduction of **130** with two equivalents of KC_8 followed by the cation exchange reaction with LiBr resulted in the targeted compound **131**. The solid-state structure of **131b** was confirmed by X-ray analysis, which reveals an η^5-coordination of the C_2Si_3 ring to the lithium cation. The C_2Si_3 five-membered ring retains its planarity and the C=C and Si=Si double bond lengths increase along with the shortening of the Si–C and Si–Si single bonds compared with those of **130**, supporting the delocalization of the 6π-electrons in the ring. Treatment of **131a** with 12-crown-4 afford non-aromatic species **132**, which represents the first example of a cyclic disilenide derivative. The formation of **132** revealed that the Li$^+$ countercation plays a decisive role in the stabilization of the aromatic **131**.

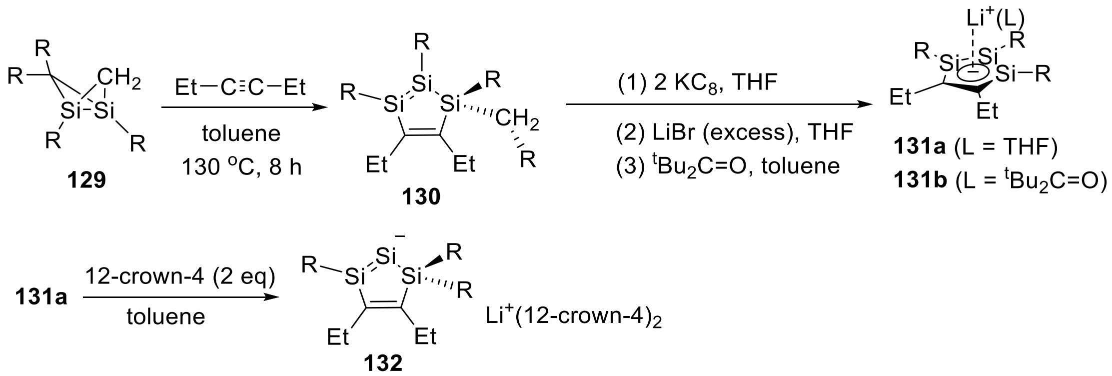

Scheme 1.29 Synthesis and reactivity of trisilacyclopentadienide ion **131**

1.3 Objectives of thesis project

Construction of the aromatic heterocyclic rings is of great importance both in fundamental research and application area. Remarkably, it has been demonstrated that aromatic B,N-heterocyclic rings have unique electronic structures, which are quite different from conventional aromatic hydrocarbons. Hence, they are expected to be utilized as potential candidates for application in coordination chemistry, materials science, and biomedical research. Given the importance of development of novel B,N-heterocycles, we designed a new aromatic framework, namely 1,4,2-diazaborole, which is the isomer of 1,3,2-diazaborole (Figure 1.1a). This targeted compound is inaccessible by use of tranditional organic synthetic method. To overcome this challenge, we employed an imino-N-heterocyclic carbene as the supporting ligand, as once the five-membered ring is formed (see the resonance structures in Figure 1.1a), the electrons will be efficiently delocalized on the π orbital of C=N bond as well as the p orbital of carbene carbon. The diverse reactivity was also investigated in detail.

Although several aromatic compounds of heavier group 14 elements (Si, Ge) have been synthesized and investigated, the chemistry in this field is still in its infancy and more novel compounds are highly desired from both experimental and theoretical points of view. Here, we designed a novel mesoionic germylene, which can also be viewed as a germanium(0) species (Figure 1.1b). To construct this hitherto unknown germanium-containing aromatic molecule, we utilized the same carbene as the supporting ligand (see the resonance structures in Figure 1.1). Once the desired structure is formed, one lone pair of the Ge atom will be delocalized over the five-membered system. Its aromaticity was evaluated by means of the experimental and DFT calculation analysis. Moreover, its four electrons donating ability was also demonstrated by the reactivity towards the electrophiles.

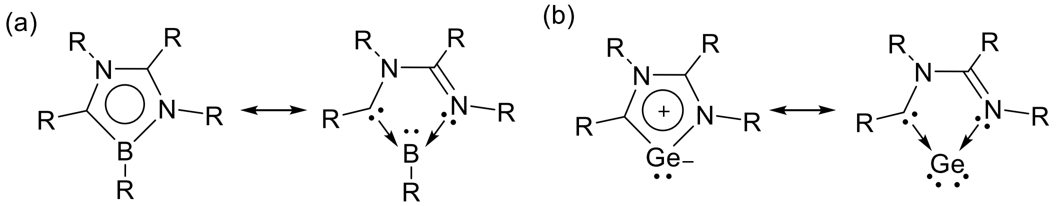

Figure 1.1 (a) Simplified structure of the targeted 1,4,2-diazaborole and its resonance structure; (b) Simplified structure of the targeted mesoionic germylene and its resonance structure.

1.4 References

(1) Faraday, M, *Phil. Trans. R. Soc. Lond*. **1825**, *115*, 440 – 446.

(2) Kekulé, A. *Bull. Soc. Chim. Fr.* **1865**, *3*, 98 – 110.

(3) a) Hückel, E. *Zeitschrift für Physik* **1931**, *70*, 204 – 286; b) Hückel, E. *Zeitschrift für Physik* **1931**, *72*, 310 – 337; c) Hückel, E. *Zeitschrift für Physik* **1932**, *76*, 628 – 648; d) Pauling, L. *J. Am. Chem. Soc.* **1926**, *48*, 1132 – 1143; e) Pauling, L.; Wheland, G. W. *J. Chem. Phys.*

1933, *1*, 362 – 374.

(4) a) Stanger, A. *Chem. Commun.* **2009**, 1939 – 1947; b) Krygowski, T. M.; Szatylowicz, H.; Stasyuk, O. A.; Dominikowska, J.; Palusiak, M. *Chem. Rev.* **2014**, *114*, 6383 – 6422.

(5) Cyrański, M. K. *Chem. Rev.* **2005**, *105*, 3773 – 3811.

(6) Gershoni-Poranne, R.; Stanger, A. *Chem. Soc. Rev.* **2015**, *44*, 6597 – 6615.

(7) a) Poater, J.; Fradera, X.; Duran, M.; Solà, M. *Chem. Eur. J.* **2003**, *9*, 400 – 406; b) Feixas, F.; Matito, E.; Poater, J.; Sola, M. *Chem. Soc. Rev.* **2015**, *44*, 6434 – 6451.

(8) a) Schleyer, P. v. R; Jiao, H. *Pure Appl. Chem.* **1996**, *68*, 209 – 218; b) Schleyer, P. v. R.; Maerker, C.; Dransfeld, A.; Jiao, H.; Hommes, N. J. R. v. E. *J. Am. Chem. Soc.* **1996**, *118*, 6317 – 6318.

(9) a) Bosdet, M. J. D.; Piers, W. E. *Can. J. Chem.* **2009**, *87*, 8 – 29; b) Abbey, E. R.; Liu, S.-Y. *Org. Biomol. Chem.* **2013**, *11*, 2060 – 2069; c) Weber, L. *Coord. Chem. Rev.* **2001**, *215*, 39 – 77; d) Campbell, P. G.; Marwitz, A. J. V.; Liu, S.-Y. *Angew. Chem., Int. Ed.* **2012**, *51*, 6074 – 6092.

(10) a) Ashe, A. J. *Organometallics* **2009**, *28*, 4236 – 4248; b) Weber, L. *Coord. Chem. Rev.* **2008**, *252*, 1 – 31.

(11) Schulze, J.; Schmid, G. *J. Organomet. Chem.* **1980**, *193*, 83 – 91.

(12) Ashe, A. J.; Fang *Org. Lett.* **2000**, *2*, 2089 – 2091.

(13) Liu, S.-Y.; Hills, I. D.; Fu, G. C. *Organometallics* **2002**, *21*, 4323 – 4325.

(14) Fang, X.; Assoud, J. *Organometallics* **2008**, *27*, 2408 – 2410.

(15) Xie, L.; Zhang, J.; Cui, C. *Chem. Eur. J.* **2014**, *20*, 9500 – 9504.

(16) Merriam, J. S.; Niedenzu, K. *J. Organomet. Chem.* **1973**, *51*, C1 – C2.

(17) Weber, L.; Schmid, G. *Angew. Chem. Int. Ed. Engl.* **1974**, *13*, 467 – 476.

(18) a) Niedenzu, K.; Merriam, J. S. *Z. Anorg. Allg. Chem.* **1974**, *406*, 251 – 259; b) Schmid, G.; Polk, M.; Boese, R. *Inorg. Chem.* **1990**, *29*, 4421 – 4429; c) Schmid, G.; Schulze, J. *Chem. Ber.* **1977**, *110*, 2744 – 2750.

(19) Weber, L.; Dobbert, E.; Stammler, H.-G.; Neumann, B.; Boese, R.; Bläser, D. *Chem. Ber.* **1997**, *130*, 705 – 710.

(20) Tian, D.; Jiang, J.; Hu, H.; Zhang, J.; Cui, C. *J. Am. Chem. Soc.***2012**, *134*, 14666 – 14669.

(21) Paetzold, P. I. *Z. Anorg. Allg. Chem.* **1963**, *326*, 64 – 69.

(22) Dewar, M. J. S.; Golden, R.; Spanninger, P. A. *J. Am. Chem. Soc.***1971**, *93*, 3298 – 3299.

(23) Dewar, M. J. S.; Spanninger, P. A. *Tetrahedron* **1972**, *28*, 959 – 961.

(24) Weber, L.; Schnieder, M.; Stammler, H.-G.; Neumann, B.; Schoeller, W. W. *Eur. J. Inorg. Chem.* **1999**, *1999*, 1193 – 1198.

(25) a) Liu, L.; Marwitz, A. J. V.; Matthews, B. W.; Liu, S.-Y. *Angew.Chem. Int. Ed.* **2009**, 4*8*, 6817 – 6819; b) Knack, D. H.; Marshall, J. L.; Harlow, G. P.; Dudzik, A.; Szaleniec, M.; Liu, S.-Y.; Heider, J. *Angew. Chem. Int. Ed.* **2013**, *52*, 2599 – 2601; c) Wang, X.-Y.; Wang, J.-Y.; Pei, J. *Chem. - Eur. J.* **2015**, *21*, 3528 – 3539.

(26) a) Dewar, M. J. S.; Marr, P. A. *J. Am. Chem. Soc.* **1962**, *84*, 3782 – 3782; b) Davies, K. M.; Dewar, M. J. S.; Rona, P. *J. Am. Chem. Soc.***1967**, *89*, 6294 – 6297; c) White, D. G. *J. Am. Chem. Soc.* **1963**, *85*, 3634 – 3636.

(27) Fritsch, A. J. *Chem. Heterocycl. Compd.* **1977**, *30*, 381 – 440.

(28) Ashe, A. J.; Fang, X.; Fang, X.; Kampf, J. W. *Organometallics* **2001**, *20*, 5413 – 5418.

(29) Pan, J.; Kampf, J. W.; Ashe, A. J. *Org. Lett.* **2007**, *9*, 679 – 681.

(30) Marwitz, A. J. V.; Abbey, E. R.; Jenkins, J. T.; Zakharov, L. N.; Liu, S.-Y. *Org. Lett.* **2007**, *9*, 4905 – 4908.

(31) Campbell, P. G.; Zakharov, L. N.; Grant, D. J.; Dixon, D. A.; Liu, S.-Y. *J. Am. Chem. Soc.* **2010**, *132*, 3289 – 3291.

(32) Abbey, E. R.; Zakharov, L. N.; Liu, S.-Y. *J. Am. Chem. Soc.* **2008**, *130*, 7250 – 7252.

(33) Rudebusch, G. E.; Zakharov, L. N.; Liu, S.-Y. *Angew. Chem. Int. Ed*. **2013**, *52*, 9316 – 9319.

(34) a) Braunschweig, H.; Horl, C.; Mailander, L.; Radacki, K.; Wahler, J. *Chem. Eur. J.* **2014**, *20*, 9858 – 9861; b) Braunschweig, H.; Celik, M. A.; Hupp, F.; Krummenacher, I.; Mailander, L. *Angew. Chem. Int. Ed.* **2015**, *54*, 6347 – 6351; c) Barnard, J. H.; Yruegas, S.; Huang, K.; Martin, C. D. *Chem. Commun.* **2016**, *52*, 9985 – 9991.

(35) Couchman, S. A.; Thompson, T. K.; Wilson, D. J. D.; Dutton, J. L.; Martin, C. D. *Chem. Commun.* **2014**, *50*, 11724 – 11726.

(36) Braunschweig, H.; Geetharani, K.; Jimenez-Halla, J. O. C.; Schafer, M. *Angew. Chem. Int. Ed.* **2014**, *53*, 3500 – 3504.

(37) Schafer, M.; Schafer, J.; Dewhurst, R. D.; Ewing, W. C.; Krahfus, M.; Kuntze-Fechner, M. W.; Wehner, M.; Lambert, C.; Braunschweig, H. *Chem. Eur. J.* **2016**, *22*, 8603 – 8609.

(38) Xu, S.; Zakharov, L. N.; Liu, S.-Y. *J. Am. Chem. Soc.* **2011**, *133*, 20152 – 20155.

(39) Chrostowska, A.; Xu, S.; Lamm, A. N.; Maziere, A.; Weber, C. D.; Dargelos, A.; Baylere, P.; Graciaa, A.; Liu, S.-Y. *J. Am. Chem. Soc.* **2012**, *134*, 10279 – 10285.

(40) Xu, S.; Mikulas, T. C.; Zakharov, L. N.; Dixon, D. A.; Liu, S.-Y. *Angew. Chem. Int. Ed.* **2013**, *52*, 7527 – 7531.

(41) a) Maitlis, P. M. *J. Chem. Soc.* **1961**, 425 – 429; (b)Kranz, M.; Hampel, F.; Clark, T. *J. Chem. Soc., Chem. Commun.* **1992**, 1247 – 1248.

(42) Braunschweig, H.; Damme, A.; Jimenez-Halla, J. O. C.; Pfaffinger, B.; Radacki, K.; Wolf, J. *Angew. Chem. Int. Ed.* **2012**, *51*, 10034 – 10037.

(43) Liu, X.; Zhang, Y.; Li, B.; Zakharov, L. N.; Vasiliu, M.; Dixon, D. A.; Liu, S.-Y. *Angew. Chem. Int. Ed.* **2016**, *55*, 8333 – 8337.

(44) Wu, D.; Kong, L.; Li, Y.; Ganguly, R.; Kinjo, R. *Nat Commun.* **2015**, 7340.

(45) Wang, B.; Li, Y.; Ganguly, R.; Hirao, H.; Kinjo, R. *Nat Commun.* **2016**, 11871.

(46) a) Lee, V. Y.; Sekiguchi, A.; Ichinohe, M.; Fukaya, N. *J. Organomet. Chem.* **2000**, *611*, 228 – 235; b) Norihiro, T. *Bull. Chem. Soc. Jpn.* **2004**, *77*, 429 – 441; c) Saito, M.; Yoshioka, M. *Coord. Chem. Rev.* **2005**, *249*, 765 – 780; d) Lee, V. Y.; Sekiguchi, A. *Angew. Chem. Int. Ed.* **2007**, *46*, 6596 – 6620; e) Lee, V. Y.; Sekiguchi, A. *Chem. Soc. Rev.* **2008**, *37*, 1652 – 1665; f) Asay, M.; Jones, C.; Driess, M. *Chem. Rev.* **2011**, *111*, 354 – 396; g) Mizuhata, Y.; Tokitoh, N. *J. Synth. Org. Chem Jpn.* **2011**, *69*, 691 – 704.

(47) a) Krygowski, T. M.; Cyrański, M. K. *Chem. Rev.* **2001**, *101*, 1385 – 1419. b) Haaf, M.; Schmedake, T. A.; West. R. *Acc. Chem. Res*. **2000**, *33*, 704 – 714.

(48) Denk, M.; Lennon, R.; Hayashi, R.; West, R.; Belyakov, A. V.; Verne, H. P.; Haaland, A.; Wagner, M.; Metzler, N. *J. Am. Chem. Soc.* **1994**, *116*, 2691 – 2692.

(49) Haaf, M.; Schmiedl, A.; Schmedake, T. A.; Powell, D. R.; Millevolte, A. J.; Denk, M.; West, R. *J. Am. Chem. Soc.* **1998**, *120*, 12714 – 12719.

(50) Denk, M.; Green, J. C.; Metzler, N.; Wagner, M. *J. Chem. Soc., Dalton Trans.* **1994**, 2405 – 2410.

(51) Ishida, S.; Nishinaga, T.; West, R.; Komatsu, K. *Chem. Commun.* **2005**, 778 – 780.

(52) Herrmann, W. A.; Denk, M.; Behm, J.; Scherer, W.; Klingan, F.-R.; Bock, H.; Solouki, B.; Wagner, M. *Angew. Chem. Int. Ed. Engl.* **1992**, *31*, 1485 – 1488.

(53) Hong, J. H.; Boudjouk, P. *J. Am. Chem. Soc.* **1993**, *115*, 5883 – 5884.

(54) a) Freeman, W. P.; Tilley, T. D.; Yap, G. P. A.; Rheingold, A. L. *Angew. Chem. Int. Ed. Engl.* **1996**, *35*, 882 – 884; b) Freeman, W. P.; Tilley, T. D.; Liable-Sands, L. M.; Rheingold, A. L. *J. Am. Chem. Soc.* **1996**, *118*, 10457 – 10468.

(55) a) Curtis, M. D. *J. Am. Chem. Soc.* **1967**, *89*, 4241 – 4242; b) Jutzi, P.; Karl, A. *J. Organomet. Chem.* **1981**, *215*, 19 – 25.

(56) Dufour, P.; Dubac, J.; Dartiguenave, M.; Dartiguenave, Y. *Organometallics* **1990**, *9*, 3001 – 3003.

(57) Freeman, W. P.; Tilley, T. D.; Arnold, F. P.; Rheingold, A. L.; Gantzel, P. K. *Angew. Chem. Int. Ed. Engl.* **1995**, *34*, 1887 – 1890.

(58) Joo, W.-C.; Hong, J.-H.; Choi, S.-B.; Son, H.-E.; Hwan Kim, C. *J. Organomet. Chem.* **1990**, *391*, 27 – 36.

(59) Hong, J.-H.; Boudjouk, P.; Castellino, S. *Organometallics* **1994**, *13*, 3387 – 3389.

(60) Hong, J-H.; Boudjouk, P. *Bull. Soc. Chim. Fr.* **1995**, *132*, 495 – 498.

(61) West, R.; Sohn, H.; Powell, D. R.; Müller, T.; Apeloig, Y. *Angew. Chem. Int. Ed. Engl.* **1996**, *35*, 1002 – 1004.

(62) Lee, V. Y.; Kato, R.; Ichinohe, M.; Sekiguchi, A. *J. Am. Chem. Soc.* **2005**, *127*, 13142 – 13153.

(63) Yasuda, H.; Lee, V. Y.; Sekiguchi, A. *J. Am. Chem. Soc.* **2009**, *131*, 6352 – 6353.

Chapter 2 Synthesis, characterization and reactivity of 1,4,2-diazaborole†

2.1 Introduction

Since the seminal discovery of the cyclic structure of benzene in 1865, the concept of aromaticity has been of paramount significance in myriad fields of chemistry.[1,2] Indeed, aromatic skeletons are ubiquitous in molecules ranging from naturally occurring compounds to industrial products. In the past decades, the incorporation of the hetero-atoms into the aromatic molecules has been of interest in synthetic chemistry as it greatly enriches their electronic property and reactivity.[3] The replacement of a C=C unit with an isoelectronic and isosteric B-N unit is a commonly applied strategy to approach the various BN aromatic heterocyles, which renders a new class of BN heterocycles featuring unique electronic structures.[4] Among them, several azaborole derivatives which involve a 6π-electrons system over the five-membered ring were synthesized in the 1960s and 70s.[5] Figure 2.1 shows four types of 6π-azaborole derivatives reported to date, namely 1,2-azaborolide **I**,[6] 1,3,2-diazaborole **II**,[5a,7] 1,2,4,3-triazaborole **III**,[5b-c,8] and 1,2,3,4,5-tetrazaborole **IV**,[9] that may formally be regarded as BN heterocyclic counterparts of cyclopentadienide (Cp–), pyrrole, imidazole, and 1,2,3-triazole, respectively. 1,2-Azaborolides were first reported by Schmid et al.,[6m] which have been used as surrogate ligand for Cp in transition metal complexes.[6j,l] The first 1,3,2-diazaborole was prepared by dehydrogenation of 1,3-diaza-2-boracycloalkane.[5a] 1,2,4,3-triazaborole was first reported in

† Portions of this chapter are taken with permission from: Su, B.; Li, Y.; Ganguly, R.; Lim, J.; Kinjo, R. *J. Am. Chem. Soc.* **2015**, *137*, 11274 − 11277. Copyright (2015) American Chemical Society.

1971 by heating a boronic acid derivative (RBX_2, where X = Cl, OCH_3, OC_2H_5, OH, or NMe_3) with the corresponding acid amidrazone in refluxing benzene.[5b] Meanwhile, various synthetic routes of 1,2,3,4,5-tetrazaborole have been developed.[9b-c] In addition, benzo-annulated azaboroles, thus, BN indole derivatives are recognized as feasible candidates for biologically active molecules as well as optoelectonic materials.[10] Although these four types of heterocyclics have been reported over the last few decades, 1,4,2-diazaborole **V**, the skeletal isomer of **II,** has never been prepared probably due to the lack of suitable synthetic methodology.

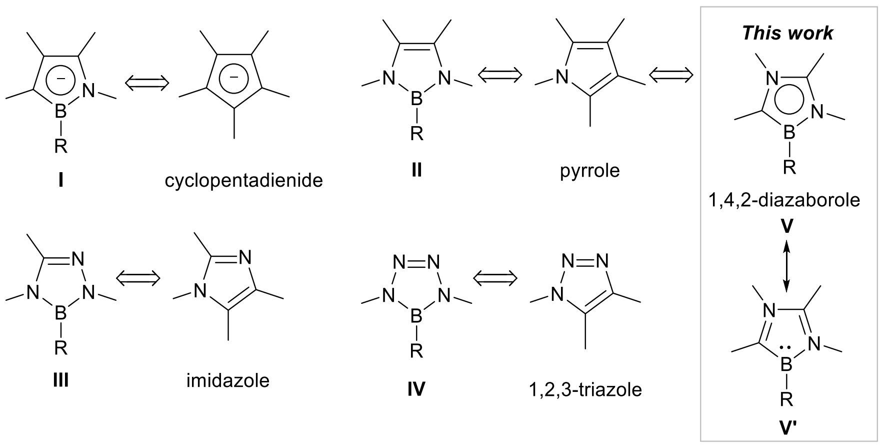

Figure 2.1 Examples of five-membered BN-heterocycles with 6π-system and their isoelectronic organic and N-heterocyclic counterparts.

Synthesis and isolation of nucleophilic boron species have attracted significant attention in organoboron chemistry, because they are expected to exhibit the special reactivity based on their peculiar electronic character.[11] Among them, a series of tricoordinate neutral nucleophilic borylene species have been detailedly investigated (Figure 2.2). The first isolable borylene species **VI** stabilized by two cyclic (alkyl)(amino)carbenes (CAAC) was synthesized by Bertrand et al., in which the strong π-accepting ability of CAACs is critical for the delocalization and stabilization of the lone pair on the HB: fragment.[12] The protonation of **VI** by trifluoromethanesulfonic acid demonstrated the nucleophilicity of the boron center. Later, the same group demonstrated that the HB: fragment **VII** even can be stabilized by replacement of one CAAC with different carbenes.[13] Recently, our group reported a novel tricoordinate nucleophilic boron species **VII** with the PhB: fragment supported by two oxazol-2-ylidene ligands.[14] Its nucleophilic property was demonstrated by the reactions with trifluoromethanesulfonic acid and other transition metals.[15] The Braunschweig group has also prepared various borylene species based on different synthetic routes.[16] In 2015, this group discovered a remarkable approach to the non-carbene stabilized borylenes **IX** by simple treatment of terminal transition borylene complexes with CO or isocyanide.[16f] Among them, the bis-isocyanide borylenes could further react with gallium trihalide to form the boron-gallium adducts.[16e] Later, the first cyanoborylene tetramer **X** was prepared in the same group by the reduction of a CAAC-supported monocyanodihaloborane precursor (CAAC)BBr_2(CN).[16d] Interestingly, addition of a small NHC to **X** resulted in a new borylene **XI**. By contrast, the borylene species **XII** could only be obtained by reduction of the precursor (CAAC)BBr_2(CN) in the presence of excess PEt_3. Recently, the same group reported a new synthetic route to the neutral silylisonitrile borylenes **XIII** by treatment of the isolable boryl anion $[(CAAC)BH(CN)]^-$ with the hard silyl electrophiles $SiClR_3$ (R = Me, Ph), where no reduction process is necessary.[16a] The first isolable CO- and CAAC-stablized arylborylene **XIV** (L = CO) was prepared by the reaction of CAAC with the iron borylene complex $[(PMe_3)(CO)_3Fe{=}BDur)]$.[16b] Interestingly, photolytic reaction of **XIV** (L = CO) in the presence of Lewis bases (pyridine, carbene) resulted in two new borylene species **XIV** (L = IMe, pyridine) via the a reactive dicoordinate boron(I) intermediate [(CAAC)DurB:]. In addition to those acyclic borylene species, the Kato group[17] and the Xie group[18] recently reported the preparation of two new cyclic borylene derivatives **XV** and **XVI**, which are stabilized by NHC as well as an additional phosphine or imino group. These pioneering works show that the strong electron accepting ability of the ligand such as CAAC, NHC, CO, and R-NC is essential to stabilize the nucleophilic boron species by efficient reduction of the electron density on the boron center. Herein, we attempted to utilize the imino-N-heterocyclic carbene as the ligand to stabilize the low-valent boron species. As described in Figure 2.1, the lone pair on the boron in the structure **V'** could be efficiently delocalized over the five-membered ring, expressing a more stable resonance structure **V**. However, it's nucleophilic property could also be demonstrated through the reaction towards the electrophiles.

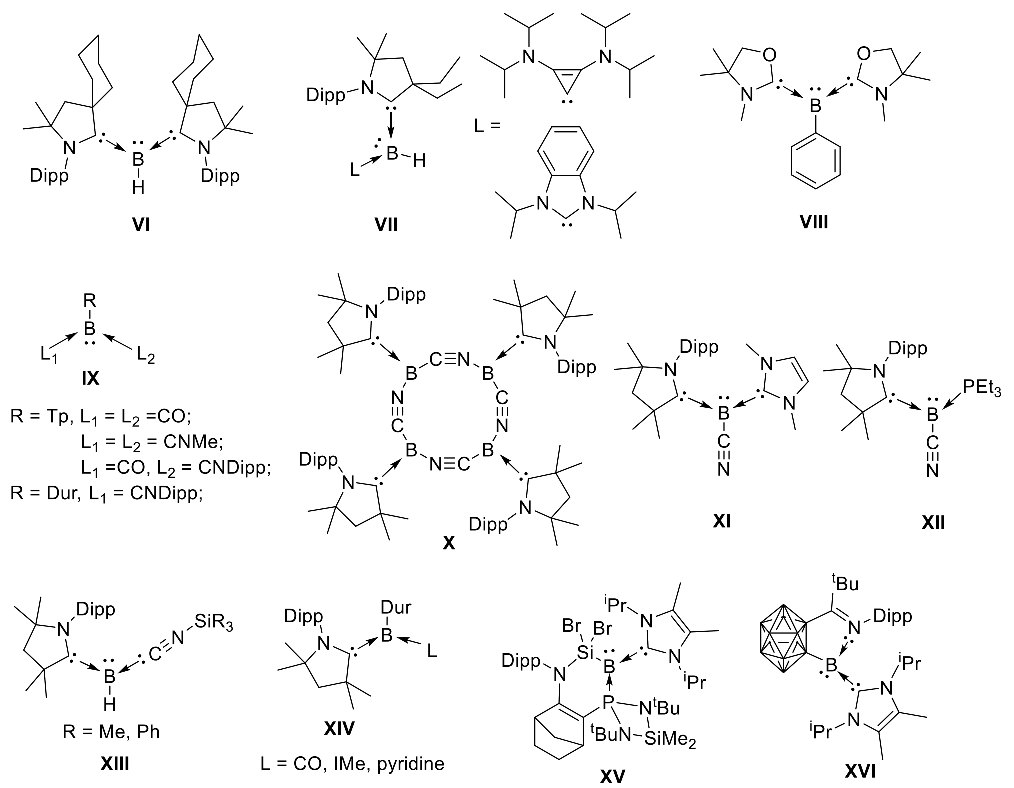

Figure 2.2 Examples of reported tricoordinate neutral borylenes. Dipp = 2,6-diisopropylphenyl, Tp = 2,6-di(2,4,6-triisopropylphenyl)phenyl; Dur = 2,3,5,6-tetramethylphenyl; IMe = 1,3-dimethylimidazol-2-ylidene.

2.2 Results and Discussions

First, the imino-*N*-heterocyclic carbene ligand **3** was synthesized following the reported procedure with slight modification.[19] Treatment of imidoyl chloride **1** with one equivalent of $NaBF_4$ in acetonitrile generated the nitrilium cation $[MesN{\equiv}C^tBu]^+$ which was coupled with N-adamantyl-dihydroimidazole afforded the carbene precursor **2** (Scheme 2.1). Deprotonation of **2** with one equivalent of potassium hexamethyldisilazide (KHMDS) in THF cleanly occurred. After work-up, a free carbene **3** was obtained as white solid in 86% yield. The ^1H NMR signal at δ = 7.07 ppm for NC*H*N in the **2** disappeared and a significantly downfield shifted peak around δ = 242.3 ppm was observed in the ^{13}C NMR spectrum of **3**, indicating the generation of the free carbene. The solid-state structure was decisively confirmed by a single-crystal X-ray diffraction study (Figure 2.3). The imino unit adopts the *E*-conformation and the four atoms (C8, N2, C11, and N3) are coplanar, which are in contrast to the reported unsaturated imino-N-heterocyclic carbene.[19c] The distance of 1.273(2) Å for C11–N3 indicates its double bond character, which is comparable to these reported data.[19c]

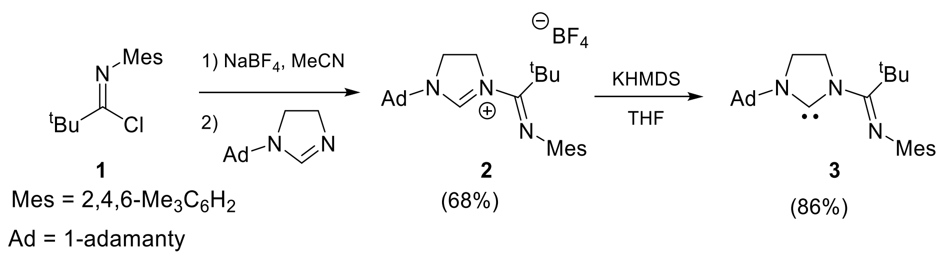

Scheme 2.1 Synthesis of the imino-N-heterocyclic carbene 3.

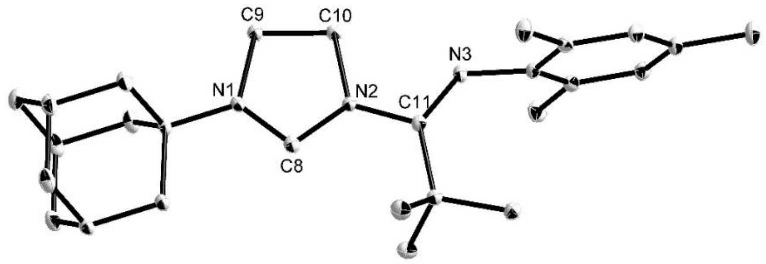

Figure 2.3 Solid-state structure of **3** (hydrogen atoms are omitted for clarity). Thermal ellipsoids are set at the 50% probability level.

Next, we attempted to prepare the NHC-borane adduct. Treatment of **3** with one equivalent dichloromesitylborane in hexane at room temperature afforded a white precipitate (Scheme 2.2). The solid was separated by filtration and washed three times with hexane to give **4** in 72% yield. The ^{11}B NMR spectrum shows a singlet at $\delta = 1.4$ ppm. Compound **4** is thermally stable both in solid state and in solution at ambient temperature but it gradually decomposes upon exposure to air.

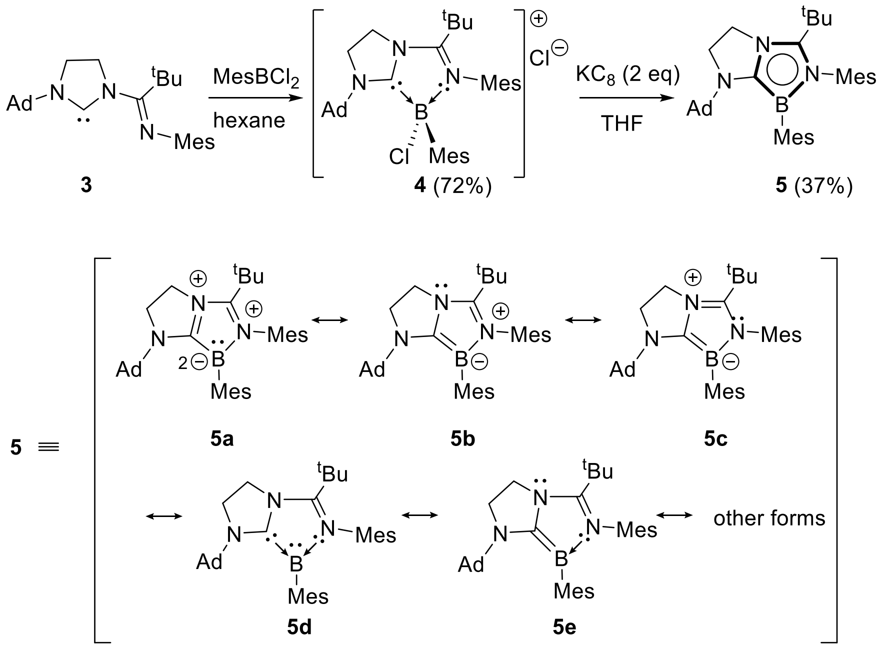

Scheme 2.2 Synthesis of **4** and **5**.

Single crystals suitable for X-ray diffraction studies of **4** were obtained by slow evaporation of an acetonitrile solution at room temperature. In the solid state, the boron atom is coordinated by both carbene carbon atom and imine nitrogen atom and thus involved in the BC_2N_2 five membered ring (Figure 2.4a). All five atoms of the central BC_2N_2 ring are nearly coplanar (the sum of internal pentagon angles = 539.91°). Compound **4** represents the first boronium cationic species supported by an imino-N-heterocyclic carbene.

(a) (b)

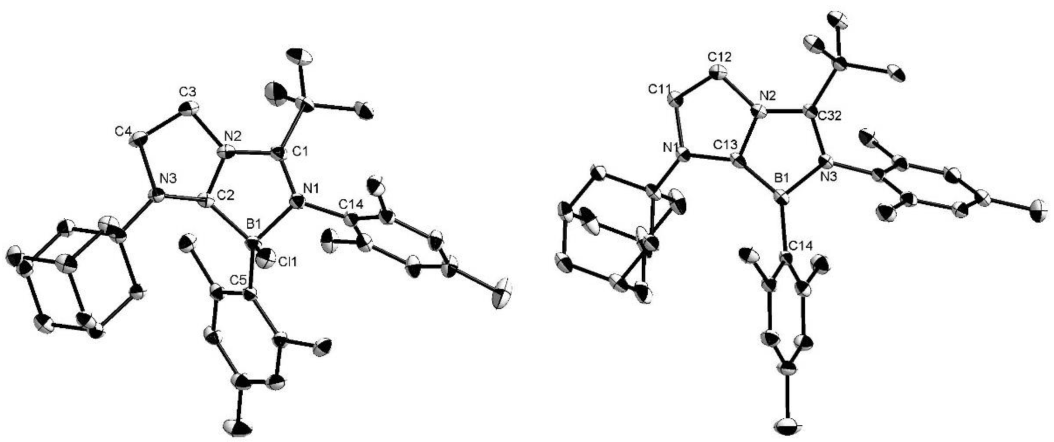

Figure 2.4 Solid-state structures of **4** (a) and **5** (b) (hydrogen atoms, solvent molecules, and counteranion (Cl^-) for **4**, are omitted for clarity). Thermal ellipsoids are set at the 50% probability.

With **4** in hand, we next investigated its reduction. When THF was added to the mixture of **4** with two equivalents of potassium graphite (KC_8) at room temperature, the color changed to light yellow immediately. After work up, **5** was obtained from the toluene solution as a pale yellow crystalline solid in 37% yield. In the ^{11}B NMR spectrum, a sharp singlet at 18.3 ppm was observed, which is significantly downfield shifted compared to that (1.4 ppm) of **4**.

Compound **5** is thermally stable both in the solid state and in solution but rapidly decomposes upon exposure to air. In the solid state, the boron atom is tri-coordinated by the carbene carbon, the imino nitrogen atom and one carbon atom of mesityl group (Figure 2.4b). The sum of the bond angles 359.55° around the B1 atom indicates the trigonal-planar geometry of the boron center, showing a sp^2 hybridization character. All atoms (B1, C13, N2, C32, and N3) in the five-membered ring is nearly coplanar (The sum of internal pentagon angles = 539.94°). The bond lengths of B1–C13 (1.474(3) Å) and B1–N3 (1.501(3) Å) are significantly shorter than the corresponding bonds of **4** (B1−C2: 1.632(3) Å and B1−N1: 1.614(2) Å). These structural features suggest the delocalization of 6π-electrons over the skeletal BC_2N_2 five-membered ring, which can be represented by the average of the several resonance forms involving **5a**–**e** (Scheme 2.2). Note that the boron atom in **5a** (and **5d**) shows the formal oxidation state of +1, presents a rare example of the tricoordinate organoboron isoelectronic with amines.

To get a deeper understanding of the electronic structures of **5**, we performed a molecular orbital analysis and natural bond orbital (NBO) analysis. The optimized geometry is in good agreement with the metric data observed by X-ray analysis. The frontier orbitals are depicted in Figure 2.5. The HOMO of **5** is mainly a B–C π-bonding orbital which exhibits antibonding conjugation with the p orbitals of both the carbon bearing ^{t}Bu group and the nitrogen atom substituted with adamantyl group. The LUMO is the π-type orbital of the mesityl group on the N atom, in addition to relatively small participation of 2p orbitals of the nitrogen and carbon atoms in the BC_2N_2 five-membered ring. Wiberg Bond index (WBI) value of the B1–C13 bond is 1.55, which indicates the partial B=C double bond character. WBI values larger than 1 for the C13–N2 (1.12), N2–C32 (1.25), and N3–C32 (1.23) bonds were also confirmed, which supports the delocalization of the 6π-electrons over the ring. In the UV-vis spectrum of **5**, a strong absorption band at a wavelength of 350 nm was observed, which corresponds to the π–π* transition (Figure 2.6). To evaluate the aromatic nature of **5**, nucleus-independent chemical-shift values NICS(0) and NICS(1) were calculated for **5**, parent 1,4,2-diazaborole **5'**, 1,3,2-diazaborole, 1,2-azaborole, and cyclopentadienide (Cp^{-}) at the B3LYP/6-311+G(d,p) level (Figure 2.7). The negative NICS(0) value (−10.2) and NICS(1) value (−6.7) were obtained, supporting the aromatic property of **5**. Meanwhile, the NICS values of the parent 1,4,2-diazaborole **5'** are comparable to those of 1,3,2-diazaborole and 1,2-azaborole, but slightly less negative than that of Cp^{-}. Thus, it is predicted that the aromaticity of 1,4,2-diazaborole is similar to those of 1,3,2-diazaborole and 1,2-azaborole but smaller than that of Cp^{-}.

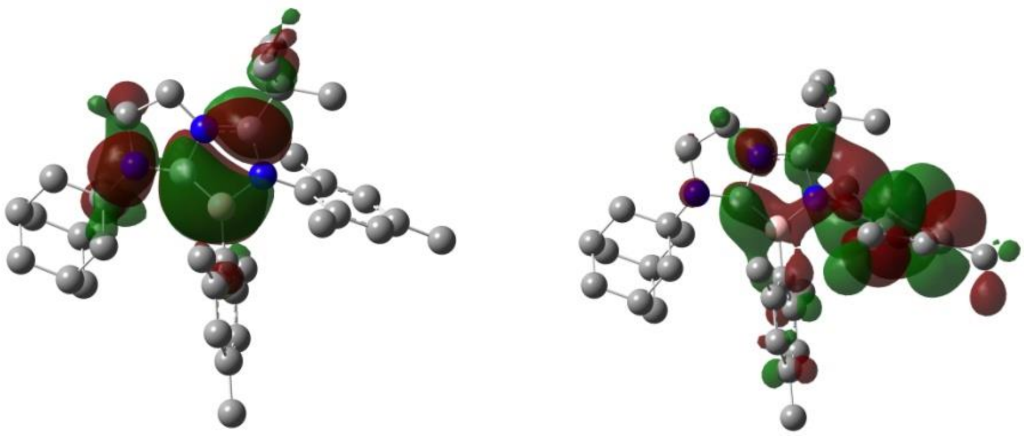

Figure 2.5 Plots of the HOMO (left) and LUMO (right) of **5** calculated at the M05-2X/6-31G(d,p)//B3LYP/6-311G(d,p) level of theory (hydrogen atoms are omitted for clarify).

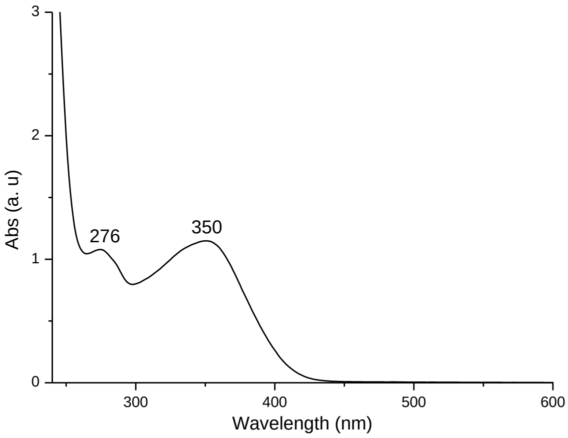

Figure 2.6 UV-vis spectrum of compound **5** in THF.

	5	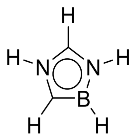 **5'**	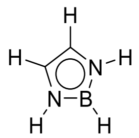	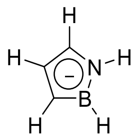	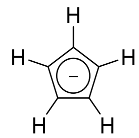
NICS(0)	–10.2	–11.9	–10.5	–10.1	–12.5
NICS(1)	–6.7	–8.5	–7.0	–7.3	–9.5

Figure 2.7 Calculated NICS(0) and NICS(1) values for **5**, **5'**, 1,3,2-diazaborole, 1,2-azaborole, and Cp^{-}, at the B3LYP/6-311+G(d,p) level of theory.

It is well known that cyclopentadienide (Cp^{-}) shows strong nucleophilic property, and can react with various electrophiles to from the σ- or π-complexes, due to its anionic character.[20] In contrast, the neutral molecule 1,3,2-diazaborole **II** rarely expresses the reactivity towards electrophiles, possibly because of the poor π-electron donor ability.[7] Besides the metal-boryl compounds, the boron atom in **II** has never formed a σ-bond with electrophiles.[21,22] Since **5** shows some unique electronic structure based on the DFT calculations, and the B atom is surrounded by eight electrons which is in marked contrast to the electronic state of **II** involving the B atom surrounded by six electrons. Thus, we decided to investigate the reactivity of 1,4,2-

diazaborole **5** towards electrophiles (E^+). Firstly, as the common electrophile agent, trifluoromethanesulfonate (MeOTf) was chosen. Addition of MeOTf to a hexane solution of **5** afforded the insoluble product instantaneously (Scheme 2.3). The white solid **6** was collected by filtration and then washed with hexane. In the ^{11}B NMR spectrum, a new signal appeared at 21.9 ppm which is slightly shifted downfield with respect to that (18.4 ppm) of **5**. Recrystallization by evaporation of a dichloromethane solution of **6** at room temperature afforded single crystals, and the solid-state structure of **6** was confirmed by X-ray diffraction study. (Figure 2.8). The nitrogen atom bearing adamantyl group is methylated, and it is tetracoordinate with a formal charge of +1. The BC_2N_2 ring persists the coplanar geometry (the sum of internal pentagon angles = 539.9). In addition, the bond lengths and angles in the BC_2N_2 ring of **6** are comparable to those of **5**, indicating a delocalization of 6π-electrons over the ring.

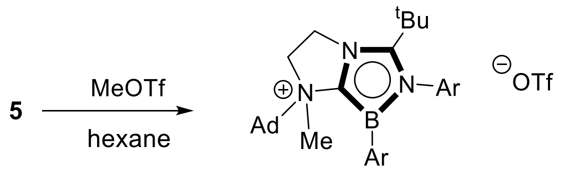

6 (95%)

Scheme 2.3 Reaction of **5** with MeOTf.

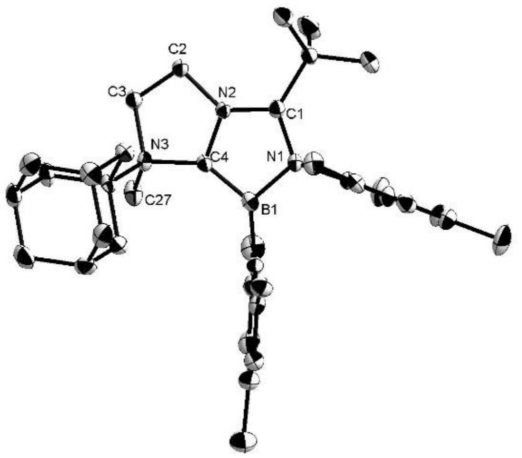

Figure 2.8 Solid-state structures of **6** (hydrogen atoms, solvent molecules, and counteranion (OTf^-) are omitted for clarity). Thermal ellipsoids are set at the 50% probability.

To gain a deeper understanding of the electronic structure of **6**, the DFT calculations were performed. The HOMO and LUMO orbitals consist of the similar orbitals to those in **5** expect for the less contribution of 2p orbital on the nitrogen atom in the HOMO (Figure 2.9). Indeed, the NICS(0) and NICS(1) values of **6** are –9.8 and –6.4, respectively, that are nearly identical to those of **5**, supporting the aromatic property. **6** can be viewed as an analogue of phosphonium cyclopentadienylidene derivative (the Ramirez ylide),[23] which is relevant to the catalytic as the ancillary ligand in metal complexes.

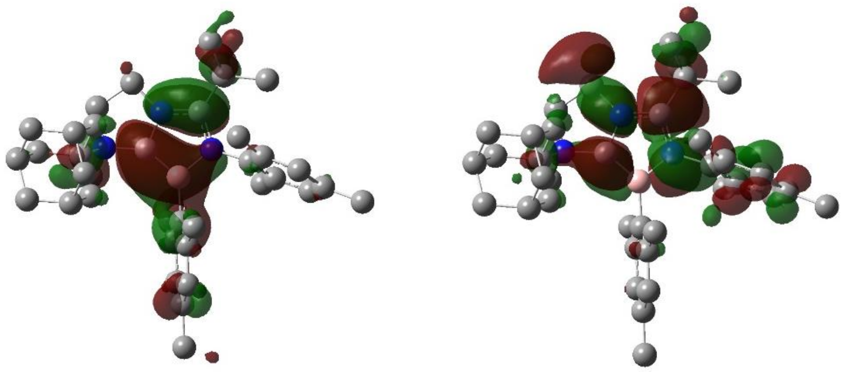

Figure 2.9 Plots of the HOMO (left) and LUMO (right) of **6** (hydrogen atoms are omitted for clarify).

Because the HOMO of **5** mainly consists the π bond orbitals in the B–C bond and the boron center shows the electron rich character rather than the electron deficiency, we proposed that the B–E bond will be possibly formed if the B–E bond is stronger than the N–E bond. Based on this hypothesis, we chose the 1-chloromethyl-4-fluoro-1,4-diazoniabicyclo[2.2.2]octane bis(tetrafluoroborate) (selectfluor) as the electrophilic regent, because normally the B–F bond is stronger than N–F bond. To an acetonitrile suspension of **5** one equivalent of selectfluor was added at room temperature (Scheme 2.4). The reaction proceeded instantaneously. After work-up, recrystallization from a dichloromethane solution under argon afforded **7** as colourless crystals in 63% yield. The ^{19}F NMR spectrum of **7** shows a peak at –173.4 ppm while the ^{11}B NMR spectrum displays a broad peak at 4.9 ppm which is upfield shifted from that (18.3 ppm) of **5**, and near to that (1.4 ppm) of **4**. The structure of **7** was unambiguously confirmed by a single-crystal X-ray diffraction study. In the solid state, the boron atom was tetra-coordinated by the carbene carbon (C1), the imino nitrogen atom (N3), the carbon atom (C28) of mesityl group, and the fluorine atom (Figure 2.10). The generation of the B–F bond in **7** demonstrates the nucleophilic character of boron center, supporting its electron-rich property as shown in resonance structure **5a**. However, it should be noted that electron transfer mechanism involving the radical intermediate cannot be ruled out for the formation of **7**.[24]

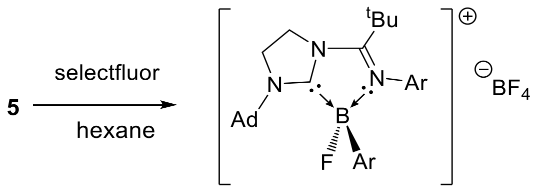

Scheme 2.4 Reactions of **5** with selectfluor.

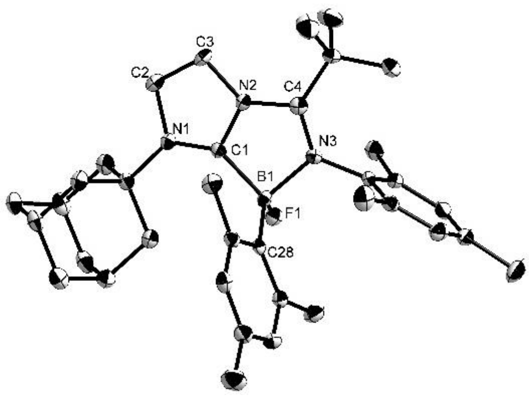

Figure 2.10 Solid-state structures of **7** (hydrogen atoms, solvent molecules, and counteranion BF_4^-) are omitted for clarity). Thermal ellipsoids are set at the 50% probability.

2.3 Summary

In conclusion, we reported the synthesis of a novel aromatic 1,4,2-diazaborole species **5** through reduction of boronium cation which is stabilized by a bidentate imino-N-heterocyclic carbene. X-ray diffraction analysis and computational studies revealed the delocalization of the 6π-electrons over the five-membered BC_2N_2 ring. Reactions of **5** with electrophiles: MeOTf and $FN(SO_2Ph)_2$, afforded the corresponding cationic species **6** and **7**, respectively. Compound **6** represents an analogue of Ramirez ylide. Meanwhile, the formation of B−F bond in **7** shows the electron donating property of the BC_2N_2 five-membered ring and demonstrates the formal nucleophilic nature of the boron center in **5**.

2.4 Experimental Sections

2.4.1 Synthesis of compounds 2–7 and their spectral data

General considerations: All reactions were performed under an atmosphere of argon or nitrogen by using standard Schlenk or dry box techniques; solvents were dried over Na metal, K metal, or CaH_2. Reagents were of analytical grade, obtained from commercial suppliers and used without further purification. ^{1}H and ^{13}C NMR spectra were obtained with a Bruker AVIII 400MHz BBFO1 spectrometer at 298 K unless otherwise stated. NMR multiplicities are abbreviated as follows: s = singlet, d = doublet, t = triplet, m = multiplet, br = broad signal. Coupling constants *J* are given in Hz. Electrospray ionization (ESI) mass spectra were obtained at the Mass Spectrometry Laboratory at the Division of Chemistry and Biological Chemistry, Nanyang Technological University. Melting points were measured with an OpticMelt Stanford Research System. UV−Vis absorption spectroscopic analyses were carried out with a Shimadzu UV-3600 spectrometer. Dichloromesitylborane[25] and 1-admantyl-4, 5-dihydro-1H-imidizole[26] were prepared according to the literature procedures.

Compound 2: CH_3CN (15 mL) was added to a mixture of $NaBF_4$ (0.565 g, 5.15 mmol) and N-mesitylpivalimidoyl chloride **1** (1.22 g, 5.13 mmol) under nitrogen, and then the solution was stirred for 12 h at room temperature. 1-Admantyl-4,5-dihydro-1*H*-imidizole (1.05 g, 5.13 mmol) in CH_3CN (10 mL) was transferred to the suspension, and the light-yellow mixture was stirred for further 12 h at room temperature. After the solvent was removed *in vacuo*, the crude product was dissolved in CH_2Cl_2 (10 mL), and salts were filtered off. After the evaporation of the solvent, the residue was washed with hexane to afford **2** as a white powder (1.73 g, 68 %).

M.p.:171 °C; ^{1}H NMR ($CDCl_3$, 400 MHz, 298 K): δ 7.07 (s, 1H, NC*H*N), 6.89 (s, 2H, *m*-C*H*), 4.39 (t, *J* = 10.0 Hz, 2H, NCH_2), 4.01 (t, *J* = 10.1 Hz, 2H, NCH_2), 2.23 (s, 3H, *p*-CH_3), 2.10 (s, 3H, Ad–C*H*), 2.03 (s, 6H, *o*-CH_3), 1.66–1.63 (m, 3H, Ad–CH_2), 1.54–1.51 (m, 9H, Ad–CH_2), 1.44 (s, 9H, C(CH_3)$_3$); ^{13}C{^{1}H} NMR ($CDCl_3$, 100 MHz, 298 K): 156.9 (*C*=N), 153.7 (N*C*HN), 142.2 (C_{Ar}), 134.0 (C_{Ar}), 129.6 (C_{Ar}), 126.3 (C_{Ar}), 58.5 (Ad-*q*), 49.8 (N*C*H_2), 44.9 (N*C*H_2), 40.1 (*C*(CH_3)$_3$), 39.9 (Ad–*C*H_2), 35.4 (Ad–*C*H_2), 29.1 (Ad–*C*H), 28.7 (C(*C*H_3)$_3$), 20.7 (*p*-*C*H_3), 17.9 (*o*-*C*H_3); HRMS (ESI): *m/z* calcd for $C_{27}H_{40}N_3$: 406.3222 [(M–BF_4)]$^+$; found: 406.3225.

Compound 3: THF (20 mL) was added to a mixture of KN[Si(CH_3)$_3$]$_2$ (525 mg, 2.63 mmol) and compound **2** (1.18 g, 2.39 mmol) at – 78 °C under argon. The mixture was stirred for 30 min at – 78 °C, and then 2 h at room temperature. The solvent was removed under reduced pressure, and the crude product was extracted with hexane (2 ×15 mL), and dried *in vacuo* to give a white solid (0.83 g, 86%). Single crystals suitable for X-ray diffraction studies were grown from a saturated toluene solution at 0 °C. M.p.: 140 °C; ^{1}H NMR (C_6D_6, 400 MHz, 298 K): δ 6.83 (s, 2H, *m*-C*H*), 3.06 (t, *J* = 8.7 Hz, 2H, NCH_2), 2.61 (t, *J* = 8.8 Hz, 2H, NCH_2), 2.24 (s, 3H, *p*-CH_3), 2.20 (s, 6H, o-CH_3), 1.92 (s, 3H, Ad–*H*), 1.82–1.80 (m, 15H, Ad–*H* & C(CH_3)$_3$), 1.54–1.46 (m, 6H, Ad–*H*); ^{13}C{^{1}H} NMR (C_6D_6, 100 MHz, 298 K): 242.3 (N*C*N), 162.8 (*C*=N), 146 (C_{Ar}), 130.2 (C_{Ar}), 128.6 (C_{Ar}), 125.9 (C_{Ar}), 55.3 (Ad-*q*), 47.7 (N*C*H_2), 43.0 (Ad–*C*H_2), 42.8 (N*C*H_2), 36.6 (Ad–*C*H_2), 42.1 (*C*(CH_3)$_3$), 30.4 (Ad–*C*H), 30.0 (C(*C*H_3)$_3$), 20.9 (*p*-*C*H_3), 19.3 (*o*-*C*H_3); HRMS (ESI): *m/z* calcd for $C_{27}H_{40}N_3$: 406.3222 [(M+H)]$^+$; found: 406.3215.

Compound 4: Dichloromesitylborane (0.495 g, 2.46 mmol) was added to a hexane (15 mL) solution of imino-N-heterocyclic carbene (1.00 g, 2.47 mmol) at room temperature. The reaction mixture was stirred overnight. The precipitate was separated by filtration and then washed three times with hexane (3×5 mL) to give **4** as a white solid (1.07 g, 72 %). Single crystals suitable for X-ray diffraction studies were grown from a saturated acetonitrile and dichloromethane solution at −26 °C. M.p.: 136 °C (dec.); ^{1}H NMR ($CDCl_3$, 400 MHz, 298 K): δ 6.90 (s, 1H, *m*-C*H*), 6.64 (s, 1H, *m*-C*H*), 6.60 (s, 1H, *m*-C*H*), 6.57 (s, 1H, *m*-C*H*),5.30–5.22 (m, 1H, NCH_2), 5.05–4.97 (m, 2H, NCH_2), 4.93–4.85 (m, 1H, NCH_2), 2.34 (s, 3H, *o*-CH_3), 2.23 (s, 3H, *o*-CH_3), 2.18–2.11 (m, 9H, *o*-CH_3 & Ad–CH_2), 2.02 (m, 3H, Ad–C*H*), 1.91−1.88 (m, 3H, Ad–CH_2), 1.62 (s, 3H, *p*-CH_3), 1.59−1.52 (m, 6H, Ad–CH_2), 1.36 (s, 9H, C(CH_3)$_3$) 1.20 (s, 3H, *p*-CH_3); ^{13}C{^{1}H} NMR ($CDCl_3$, 100 MHz, 298 K): δ 171.8 (*C*=N), 145.7 (C_{Ar}), 140.7 (C_{Ar}), 138.6 (C_{Ar}), 138.1 (C_{Ar}), 134.8 (C_{Ar}), 134.0 (C_{Ar}), 133.5 (C_{Ar}), 131.3 (C_{Ar}), 129.7 (C_{Ar}), 129.6 (C_{Ar}), 129.3 (C_{Ar}), 64.1 (Ad–*q*), 54.4 (N*C*H_2), 48.4 (N*C*H_2), 39.9 (Ad–*C*H_2), 38.5 (*C*(CH_3)$_3$), 35.4 (Ad–*C*H_2), 29.4 (Ad–*C*H), 28.0 (C(*C*H_3)$_3$), 25.5 (Ar–*C*H_3), 23.9 (Ar–*C*H_3), 21.0 (Ar–*C*H_3), 20.9 (Ar–*C*H_3), 20.9 (Ar–*C*H_3), 18.0 (Ar–*C*H_3); ^{11}B NMR (128.3 MHz, $CDCl_3$): δ 1.42 (s); HRMS (ESI): *m/z* calcd for $C_{40}H_{55}BN_3Cl$: 570.3786 [(*M-Cl*)]$^{+}$; found: 570.3801.

Compound 5: THF (15 mL) was added to the mixture of **4** (0.643 g, 1.06 mmol) and potassium graphite (0.372 g, 2.75 mmol) at room temperature, and the resulting solution was stirred for 30 min. After the solvent was removed under vacuum, pentane (30 mL) was added to the mixture, and then graphite and salts were filtered off. After the solvent was removed under vacuum, the solid residue was dried under vacuum to afford **5** as a pale yellow solid (0.210 g, 37 %). Single crystals suitable for X-ray diffraction studies were grown by evaporation of a toluene solution at room temperature. M.p.: 78 ºC; ^{1}H NMR (C_6D_6, 400 MHz, 298 K): δ 6.82 (s, 2H, *m*-C*H*), 6.58 (s, 2H, *m*-C*H*), 3.65 (t, J = 7.2 Hz, 2H, NCH_2), 3.40 (t, J = 7.2 Hz, 2H, NCH_2), 2.49 (s, 6H, *o*-CH_3), 2.11 (s, 9H, *o*-CH_3 & *p*-CH_3), 2.02 (s, 3H, *p*-CH_3), 1.92 (br, 3H, Ad–C*H*), 1.81 (m, 6H, Ad–CH_2) 1.50 (m, 6H, Ad–CH_2), 0.98 (s, 9H, C(CH_3)$_3$); ^{13}C{^{1}H} NMR (C_6D_6, 100 MHz, 298 K): δ 142.5 (C_{Ar}), 140.9 (C_{Ar}), 135.4 (C_{Ar}), 135.3 (C_{Ar}), 134.9 (C_{Ar}), 128.7 (C_{Ar}), 127.4 (C_{Ar}), 124.7 (*C*–^{t}Bu), 55.6 (Ad–*q*), 49.0 (N*C*H$_2$), 48.4 (N*C*H$_2$), 40.5 (Ad–*C*H$_2$), 37.3 (Ad–*C*H$_2$), 35.7 (*C*(CH$_3$)$_3$), 30.2 (Ad–*C*H), 29.8 (C(*C*H$_3$)$_3$), 23.9 (Ar–*C*H$_3$), 21.3 (Ar–*C*H$_3$), 20.9 (Ar–*C*H$_3$), 19.0 (Ar–*C*H$_3$); ^{11}B NMR (128.3 MHz, C_6D_6): δ 18.44 (s); HRMS (ESI): *m/z* calcd for $C_{36}H_{51}BN_3$: 536.4176 [(*M*+*H*)]$^+$; found: 536.4185.

Compound 6: MeOTf (43.1 uL, 0.393 mmol) was added to a hexane solution (10 mL) of **5** (0.210 g, 0.392 mmol) dropwise at room temperature. The white precipitate was generated immediately. The mixture was stirred for 2 hrs, and then the residue was collected by filtration and washed three times with hexane (3×5 mL). After the solvent was removed under vacuum, **6** was obtained as a white solid (0.261 g, 95%). M.p.: 162 ºC (dec.); ^{1}H NMR (CDCl$_3$, 400 MHz, 298 K): δ 6.74 (s, 2H, *m*-C*H*), 6.64 (s, 1H, *m*-C*H*), 6.54 (s, 1H, *m*-C*H*), 4.94–4.79 (m, 2H, NCH_2), 4.72–4.62 (m, 1H, NCH_2), 4.41–4.31 (m, 1H, NCH_2), 3.27 (s, 3H, NCH_3), 2.28 (s, 3H, *o*-CH_3), 2.19–2.16 (m, 9H, *o*-CH_3), 2.02–1.85 (m, 15H, *p*-CH$_3$, Ad–C*H* & Ad–CH_2), 1.64–1.51(m, 6H, Ad–CH_2), 1.18 (s, 9H, C(CH_3)$_3$); ^{13}C{^{1}H} NMR (CDCl$_3$, 100 MHz, 298 K): δ 141.7 (C_{Ar}), 141.1 (C_{Ar}), 137.9 (C_{Ar}), 137.2 (C_{Ar}), 136.9 (C_{Ar}), 136.3 (*C*–^{t}Bu), 134.4 (C_{Ar}), 134.0 (C_{Ar}), 129.3 (C_{Ar}), 128.4 (C_{Ar}), 127.8 (C_{Ar}), 127.5 (C_{Ar}), 78.2 (Ad–*q*), 62.2 (N*C*H$_2$), 48.7 (N*C*H$_3$), 46.9 (N*C*H$_2$), 36.3 (*C*(CH$_3$)$_3$), 35.3 (Ad–*C*H$_2$), 35.2 (Ad–*C*H$_2$), 30.3 (Ad–*C*H), 29.4

($C(CH_3)_3$), 24.7 (Ar–CH_3), 23.8 (Ar–CH_3), 21.2 (Ar–CH_3), 21.0 (Ar–CH_3), 19.1 (Ar–CH_3), 18.9 (Ar–CH_3), The signal for CF_3 could not be detected, presumably due to an overlap with other peaks; ^{11}B NMR (128.3 MHz, $CDCl_3$): δ 21.94 (s); ^{19}F NMR (376 MHz, $CDCl_3$): δ −78.3 (s, OTf); HRMS (ESI): *m/z* calcd for $C_{37}H_{53}BN_3$: 550.4333 [(*M-OTf*)]$^+$; found: 550.4338.

Compound 7: Selectfluor (0.119 mg, 0.336 mmol) was added to an acetonitrile suspension (15 mL) of **5** (0.180 mg, 0.336 mmol) at room temperature. The mixture was stirred overnight. All the solvent was removed under vacuum, and the residue was washed three times with toluene (3×5 mL) to give the white crude product. Recrystallization from a dichloromethane solution to afford **7** as colourless crystals (0.136g, 63%). M.p.: 145 ºC (dec.); ^{1}H NMR ($CDCl_3$, 400 MHz, 298 K): δ 6.89 (s, 1H, *m*-C*H*), 6.66 (s, 1H, *m*-C*H*), 6.61 (s, 1H, *m*-C*H*), 6.58 (s, 1H, *m*-C*H*), 4.91–4.84 (m, 1H, NCH_2), 4.75–4.62 (m, 3H, NCH_2), 2.27 (s, 3H, *o*-CH_3), 2.24 (s, 3H, *o*-CH_3), 2.19 (s, 3H, *o*-CH_3), 2.08 (s, 3H, *o*-CH_3), 2.05 (m, 3H, Ad–C*H*), 2.01–1.98 (m, 3H, Ad–CH_2), 1.90–1.87 (m, 3H, Ad–CH_2), 1.62–1.56 (m, 6H, *p*-CH_3 & Ad–CH_2), 1.48–1.46 (m, 3H, Ad–CH_2), 1.33 (s, 9H, C(CH_3)$_3$), 1.30 (s, 3H, *p*-CH_3); ^{13}C{^{1}H} NMR (C_6D_6, 100 MHz, 298 K): δ 171.9 (*C*=N), 144.7 (d, C_{Ar}), 139.5 (d, C_{Ar}), 138.3 (C_{Ar}), 137.9 (C_{Ar}), 134.6 (C_{Ar}), 133.8 (C_{Ar}), 133.3 (C_{Ar}), 130.8 (C_{Ar}), 129.6 (C_{Ar}), 129.3 (C_{Ar}), 129.3 (C_{Ar}), 63.1 (Ad–*q*), 53.1 (NCH_2), 47.5 (NCH_2), 40.3 (d, Ad–CH_2), 38.2 (*C*(CH_3)$_3$), 35.4 (Ad–CH_2), 29.3 (Ad–*C*H), 27.7 (C(CH_3)$_3$), 23.8 (Ar–CH_3), 22.4 (d, Ar–CH_3), 21.0 (Ar–CH_3), 20.9 (Ar–CH_3), 19.5 (d, Ar–CH_3), 17.7 (Ar–CH_3); ^{11}B NMR (128.3 MHz, $CDCl_3$): δ 4.91 (br, *B*–F), –0.90 (s, BF_4); ^{19}F NMR (376 MHz, $CDCl_3$): δ −152.8 (s, BF_4), −173.4 (br, B–*F*); HRMS (ESI): *m/z* calcd for $C_{36}H_{51}BN_3$: 554.4082 [(*M-BF₄*)]$^+$; found: 554.4094.

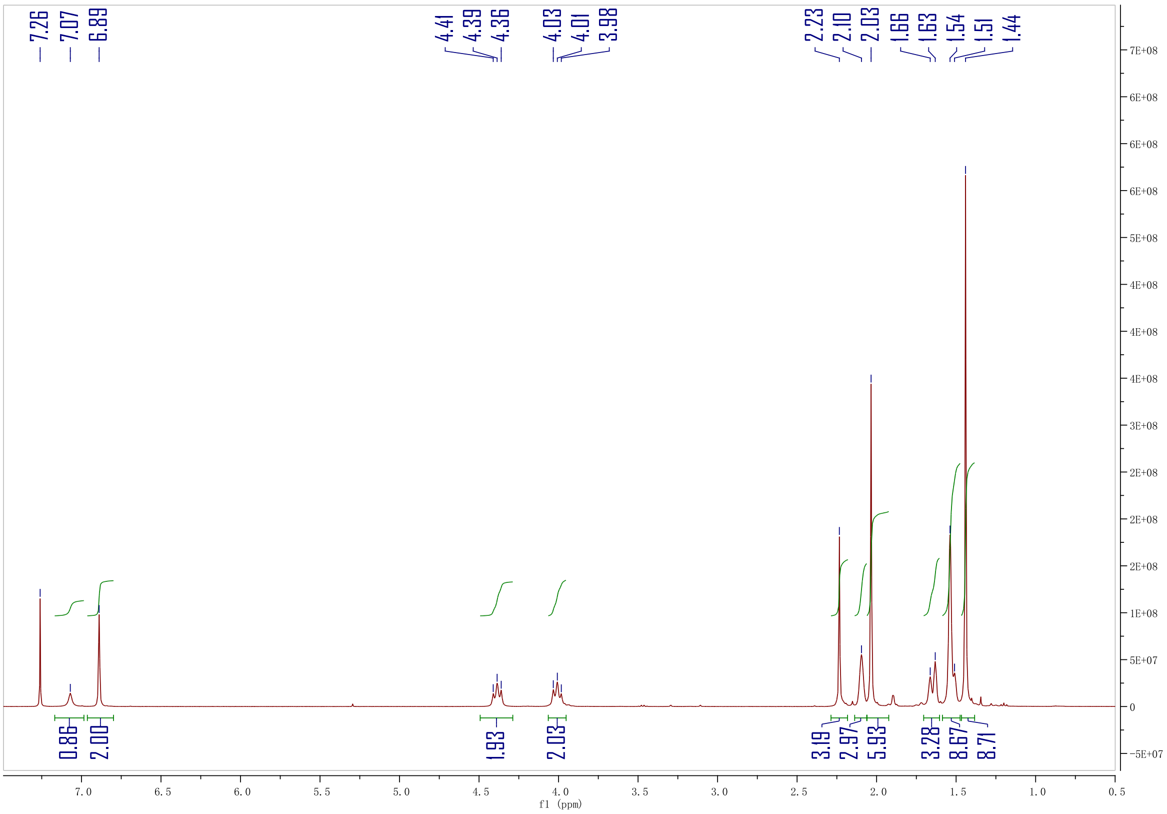

Figure 2.11 ^{1}H NMR spectrum of **2**.

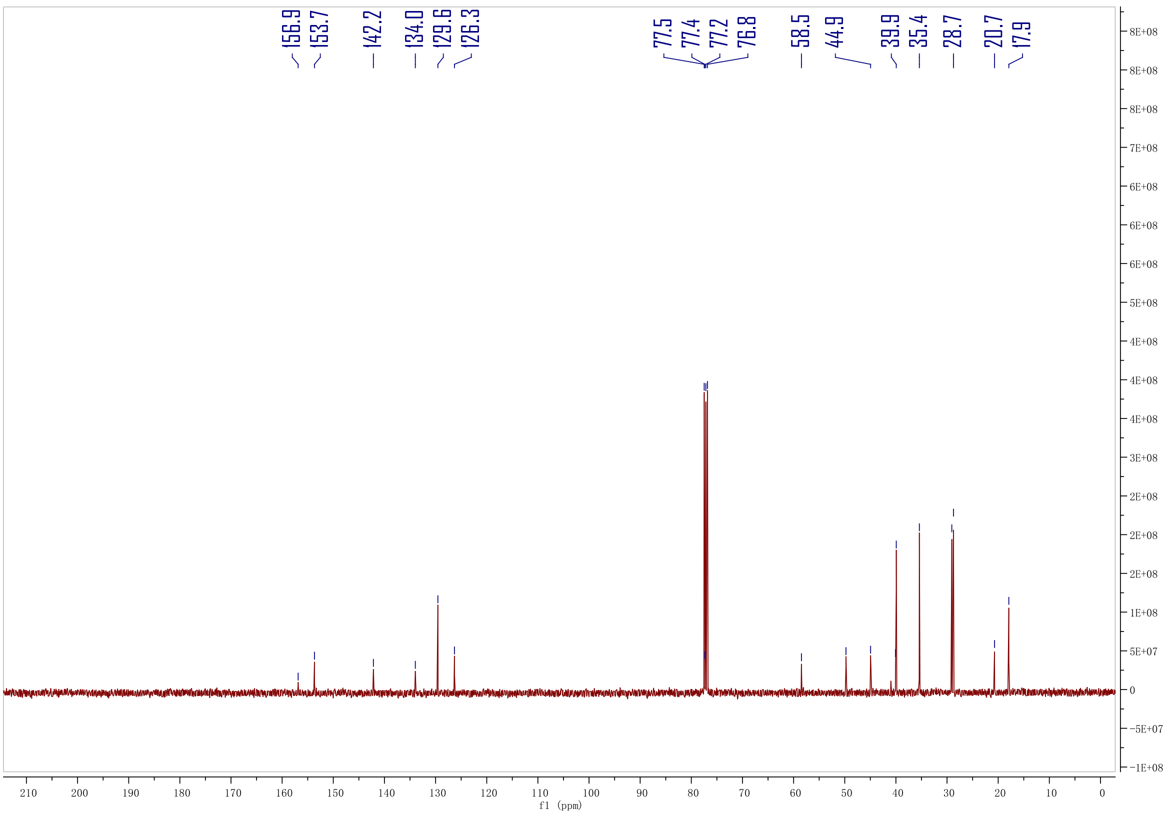

Figure 2.12 $^{13}C\{^{1}H\}$ NMR spectrum of **2**.

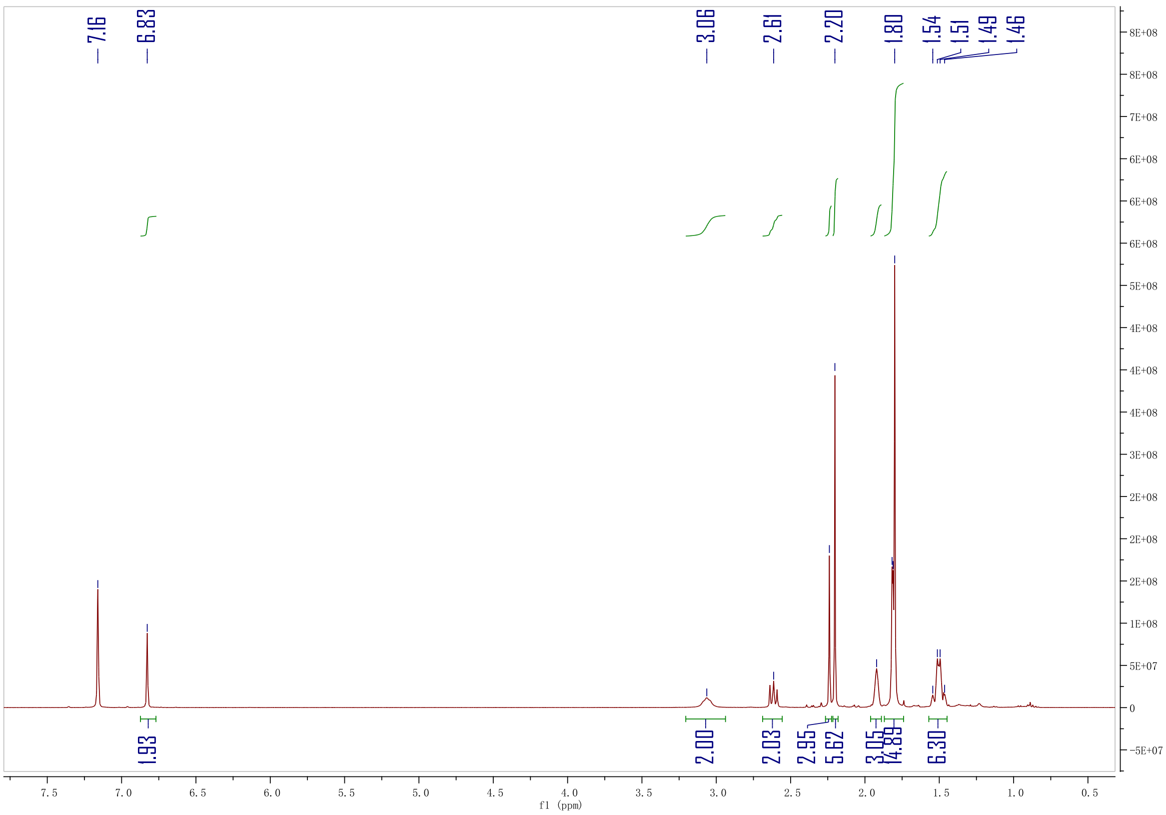

Figure 2.13 ^{1}H NMR spectrum of **3**.

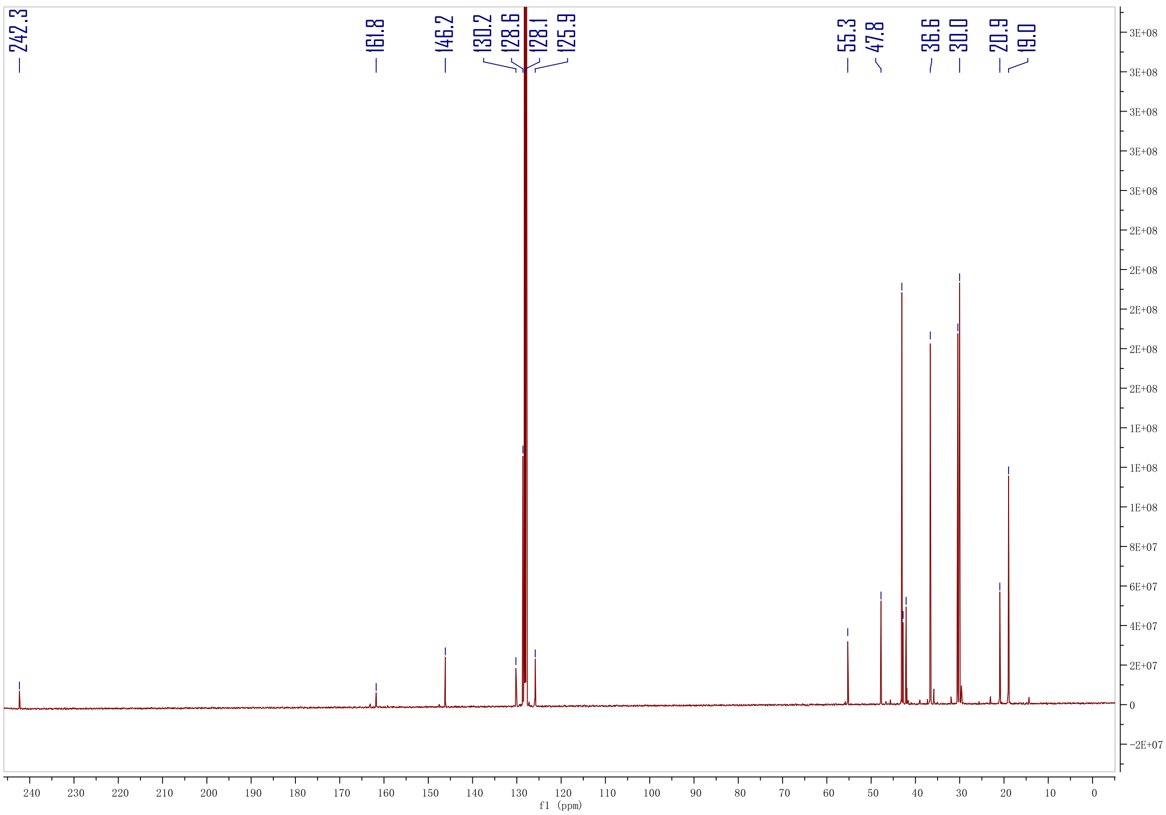

Figure 2.14 ^{13}C{^{1}H} NMR spectrum of **3**.

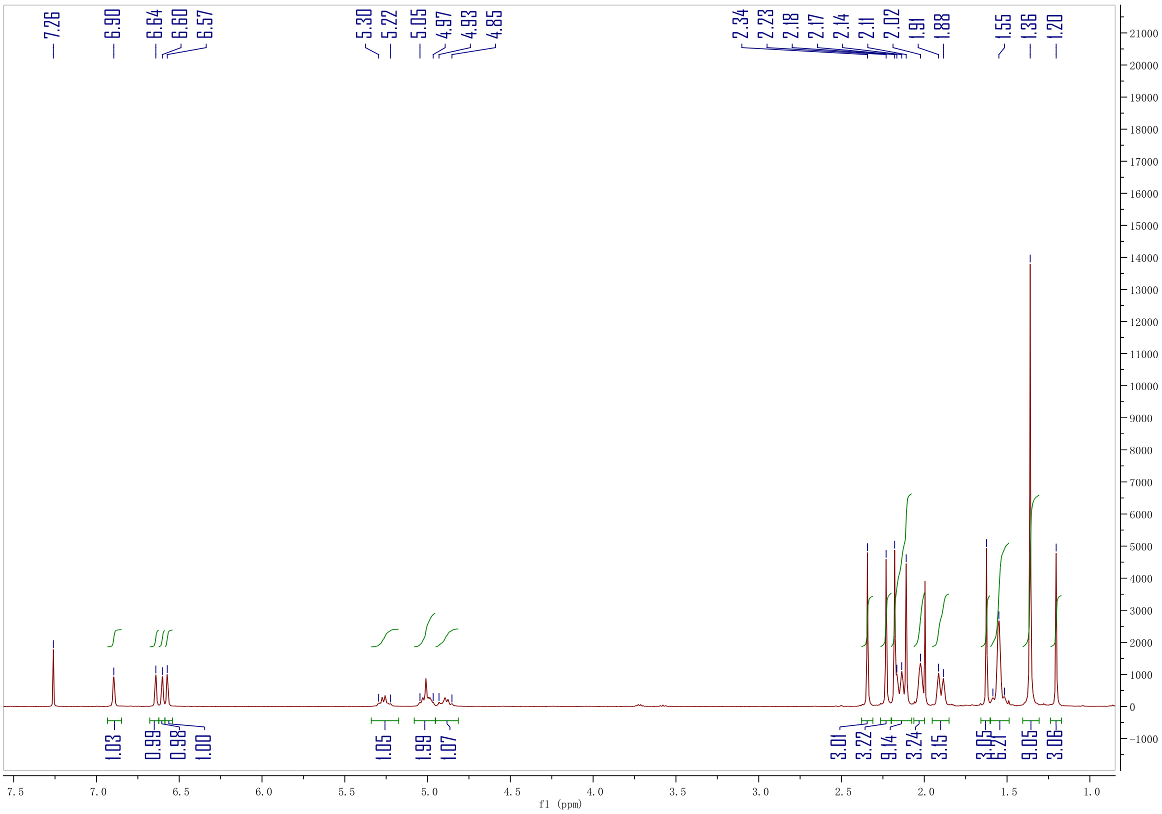

Figure 2.15 [1]H NMR spectrum of **4**.

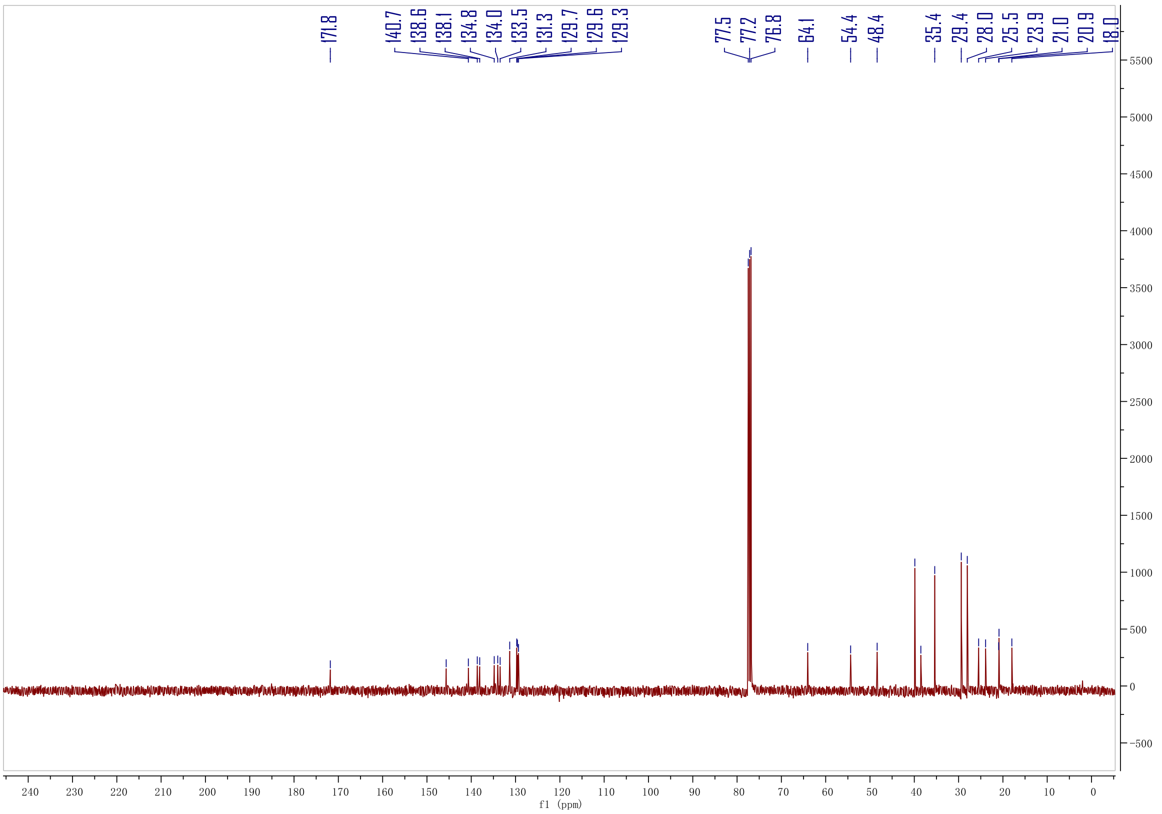

Figure 2.16 [13]C{[1]H} NMR spectrum of **4**.

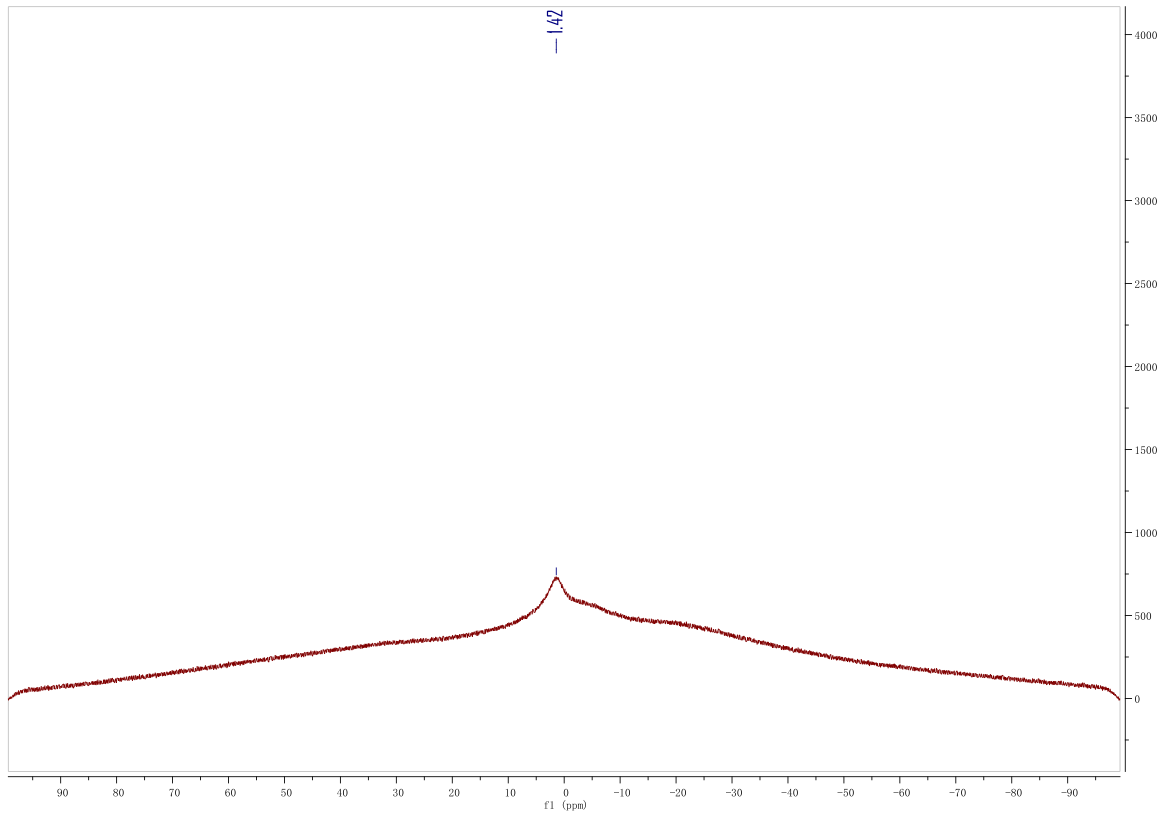

Figure 2.17 ^{11}B NMR spectrum of **4**.

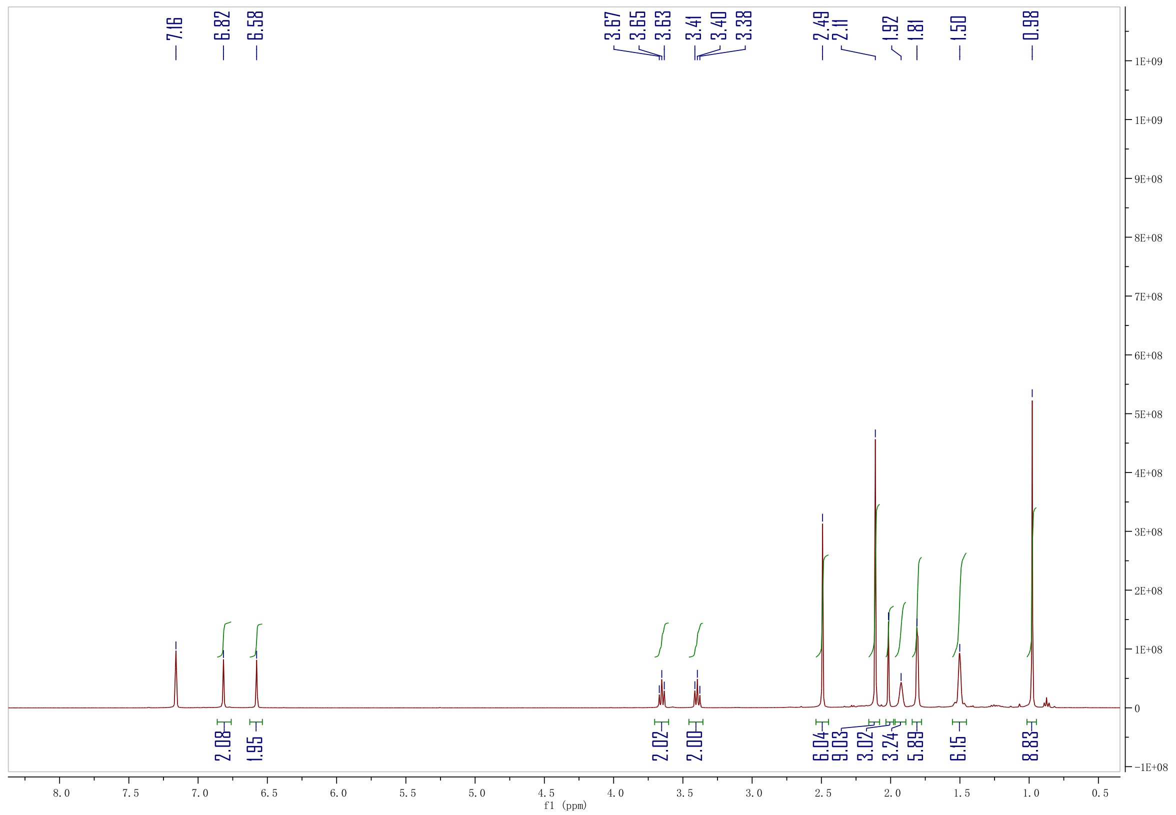

Figure 2.18 ^{1}H NMR spectrum of **5**.

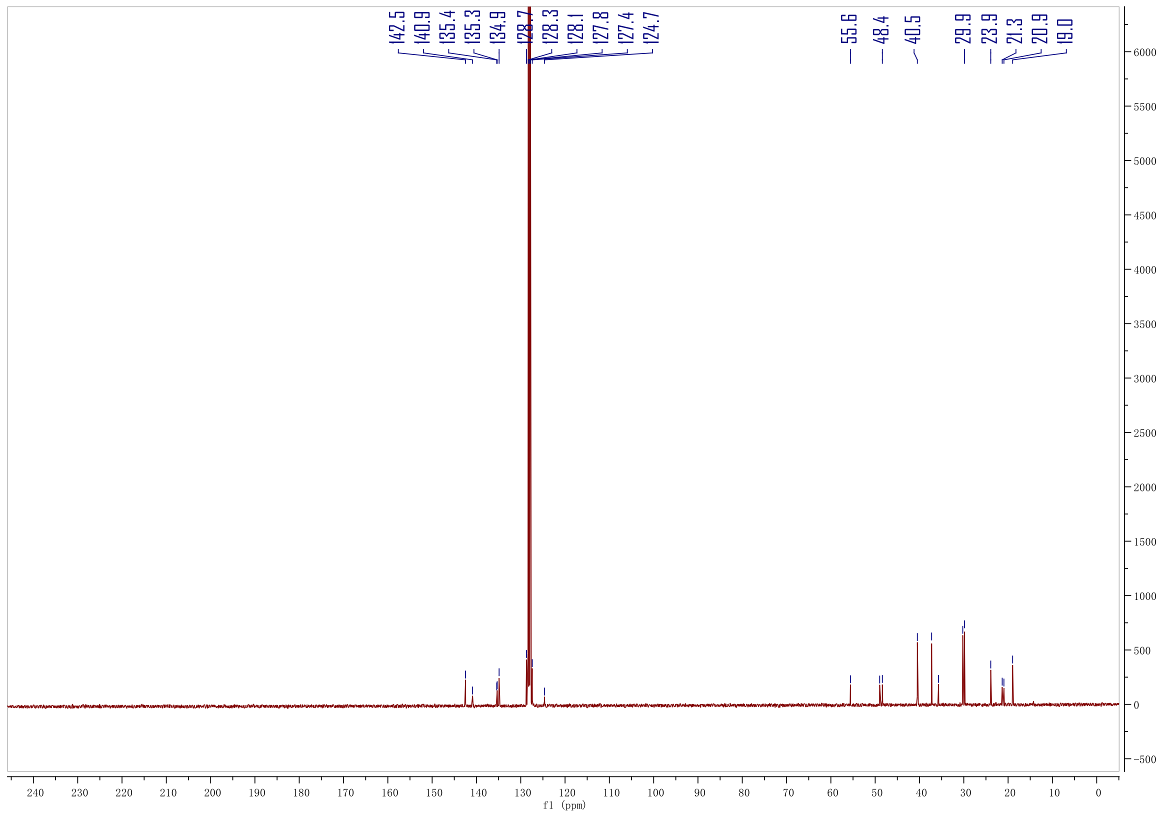

Figure 2.19 $^{13}C\{^1H\}$ NMR spectrum of **5**.

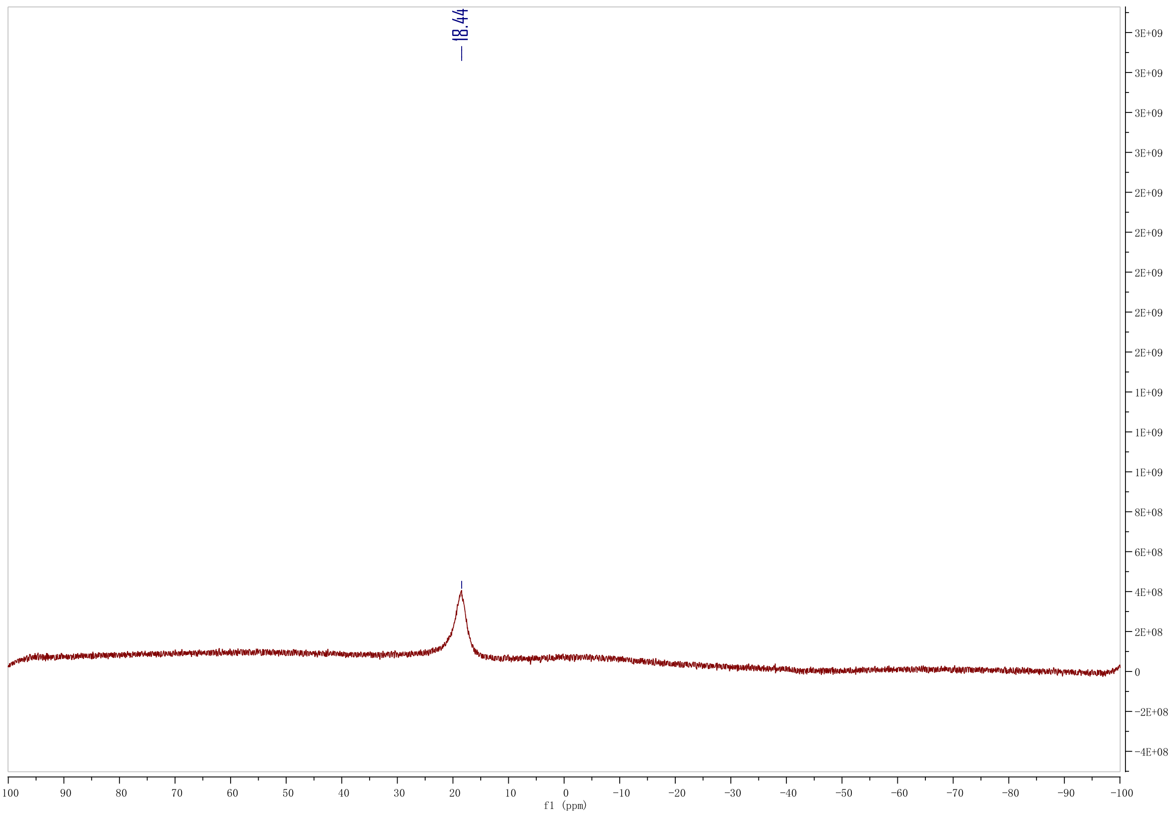

Figure 2.20 ^{11}B NMR spectrum of **5**.

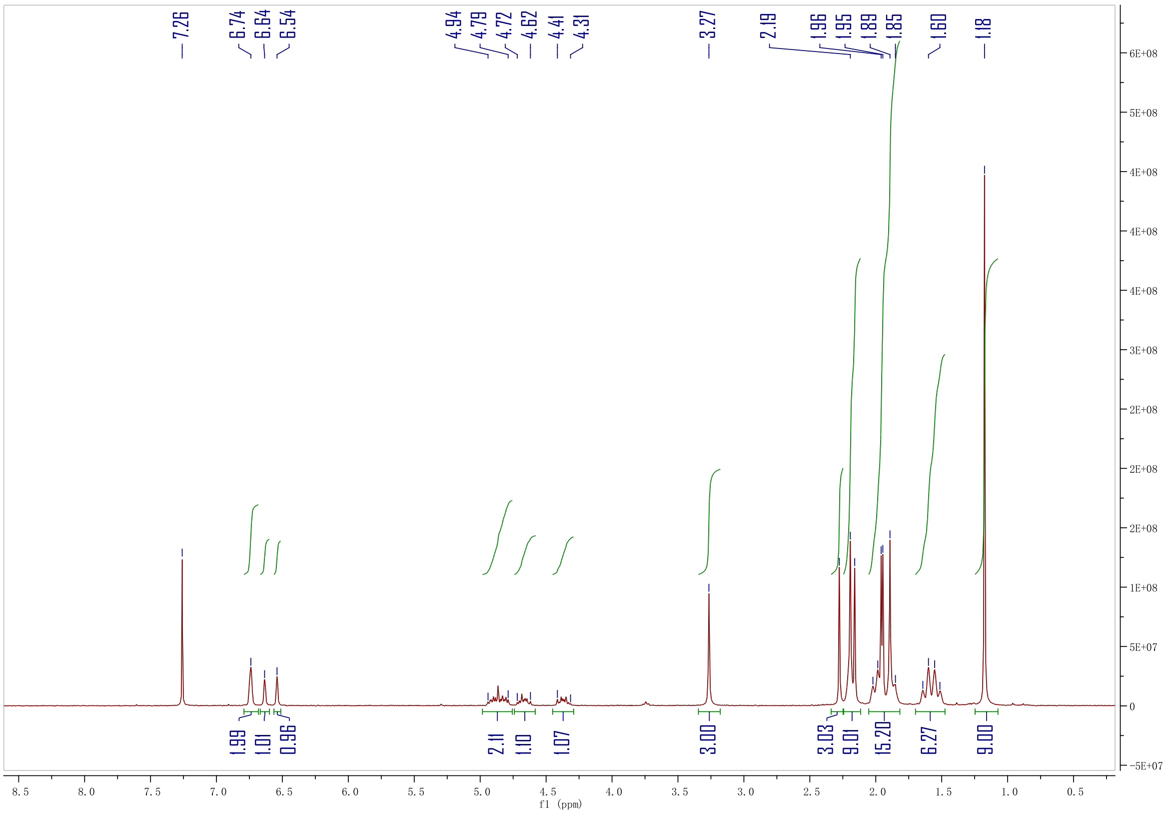

Figure 2.21 ^{1}H NMR spectrum of **6**.

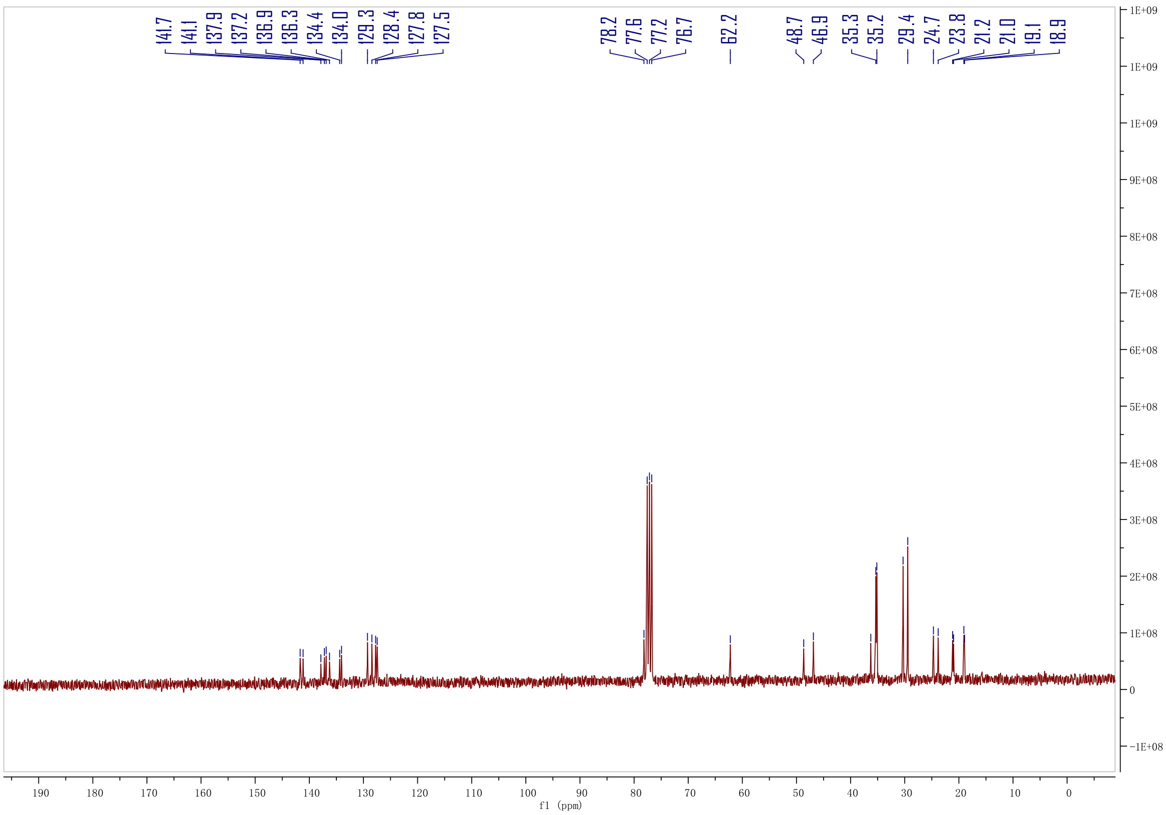

Figure 2.22 $^{13}C\{^{1}H\}$ NMR spectrum of **6**.

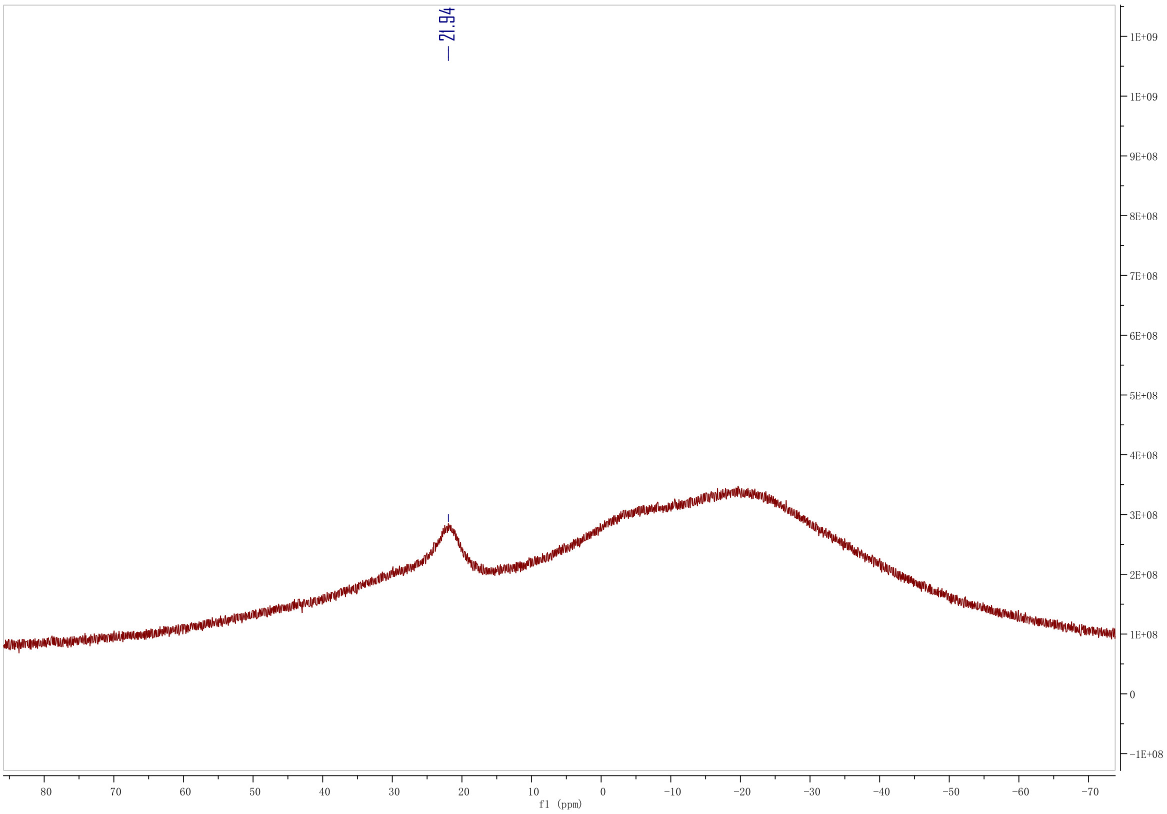

Figure 2.23 ^{11}B NMR spectrum of **6**.

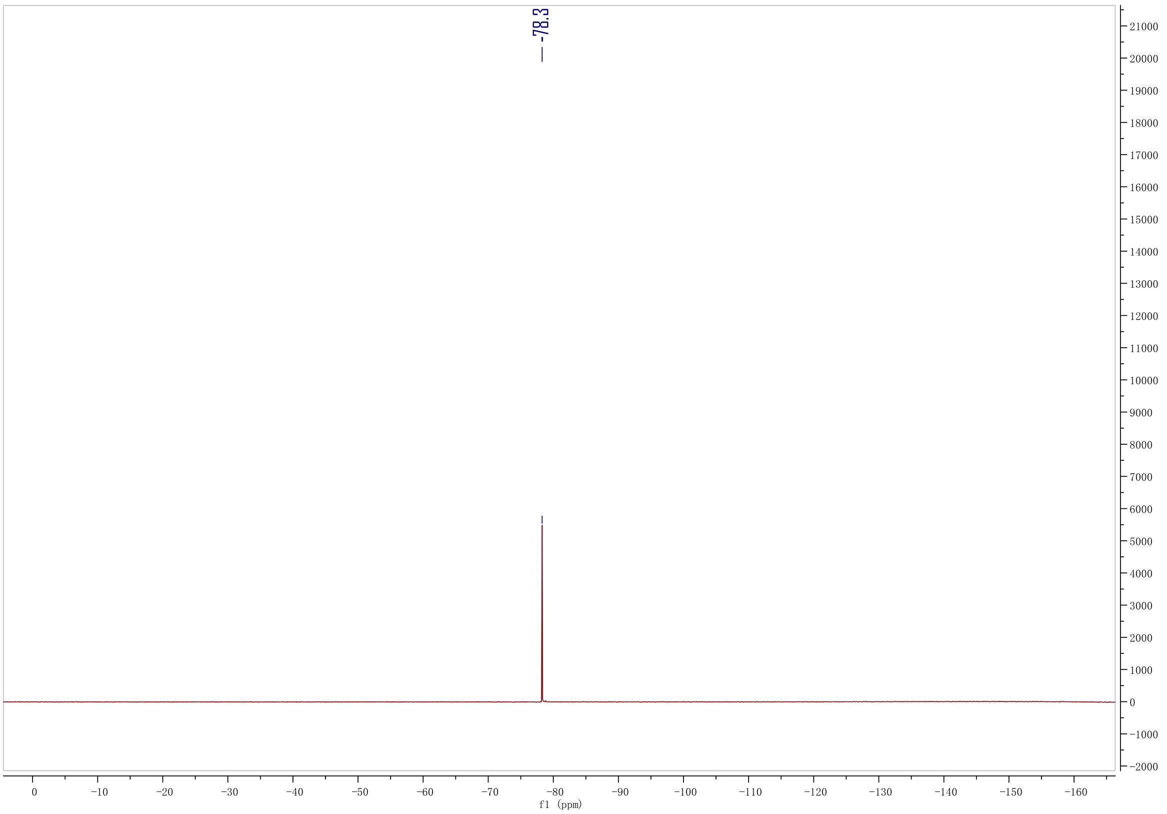

Figure 2.24 ^{19}F NMR spectrum of **6**.

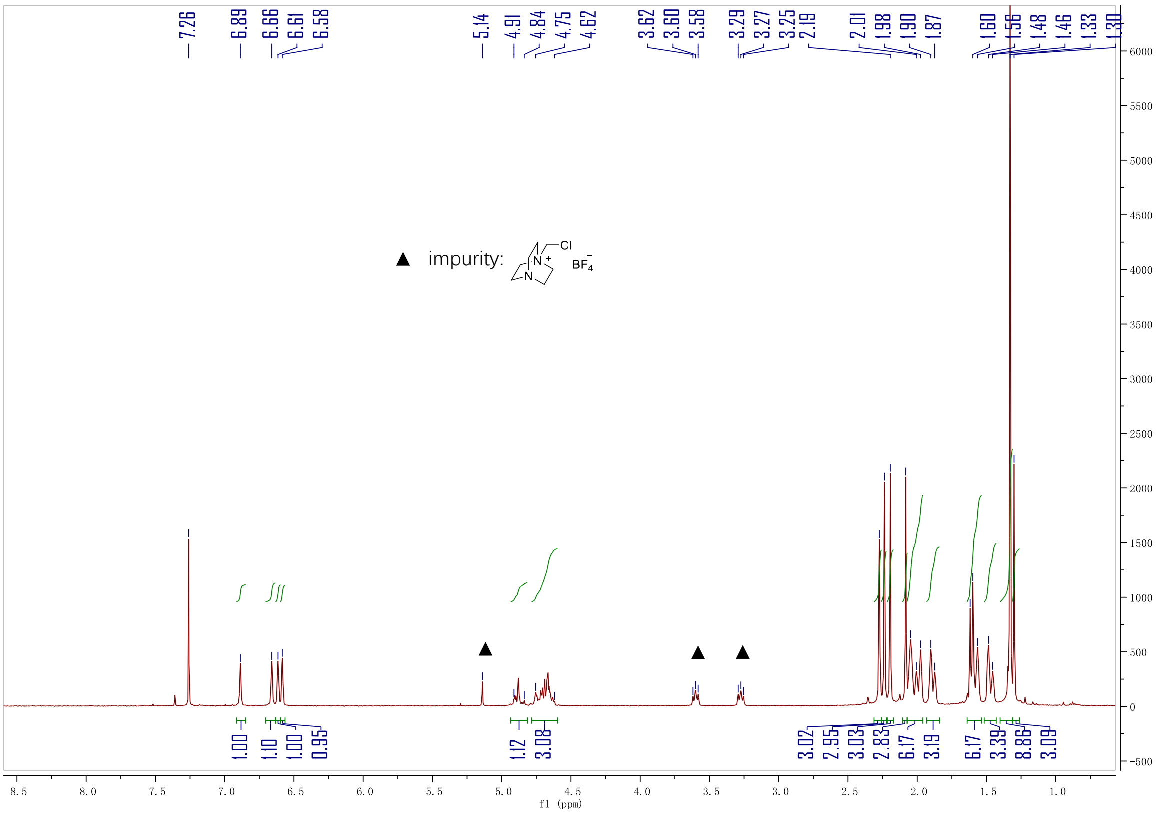

Figure 2.25 ^{1}H NMR spectrum of **7**.

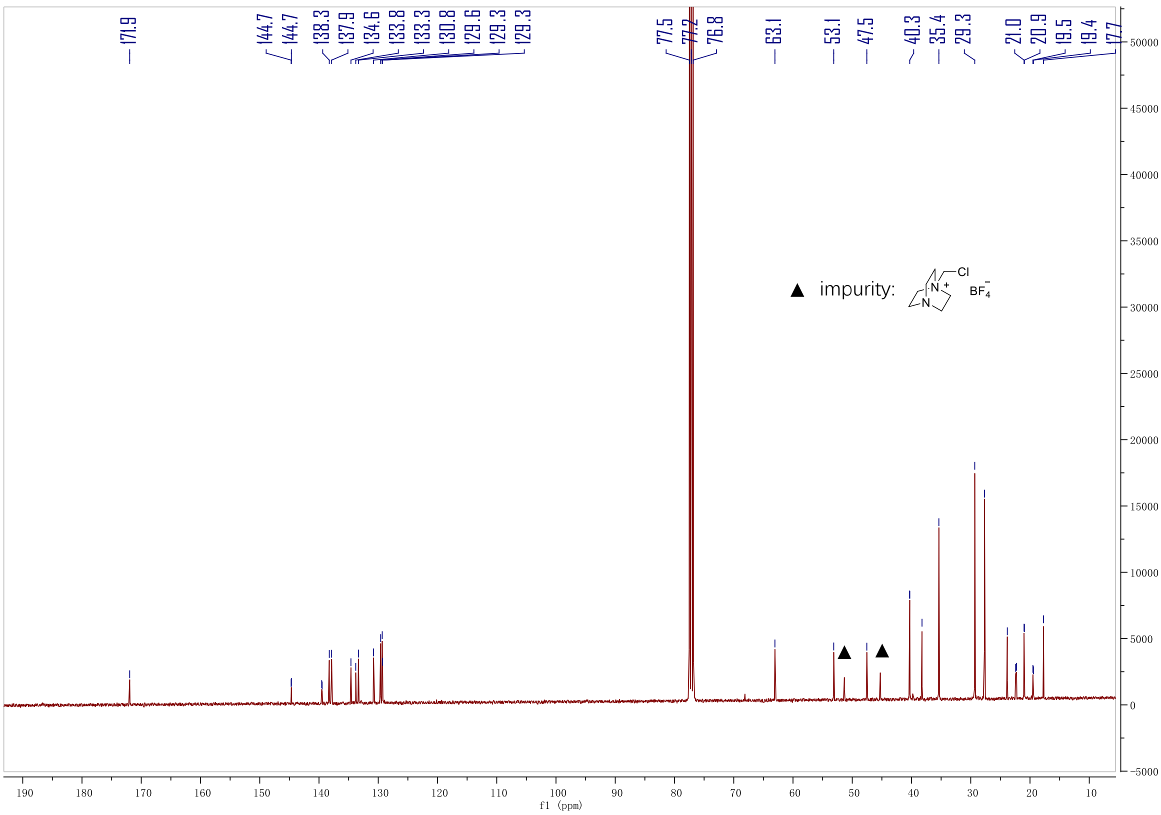

Figure 2.26 $^{13}C\{^{1}H\}$ NMR spectrum of **7**.

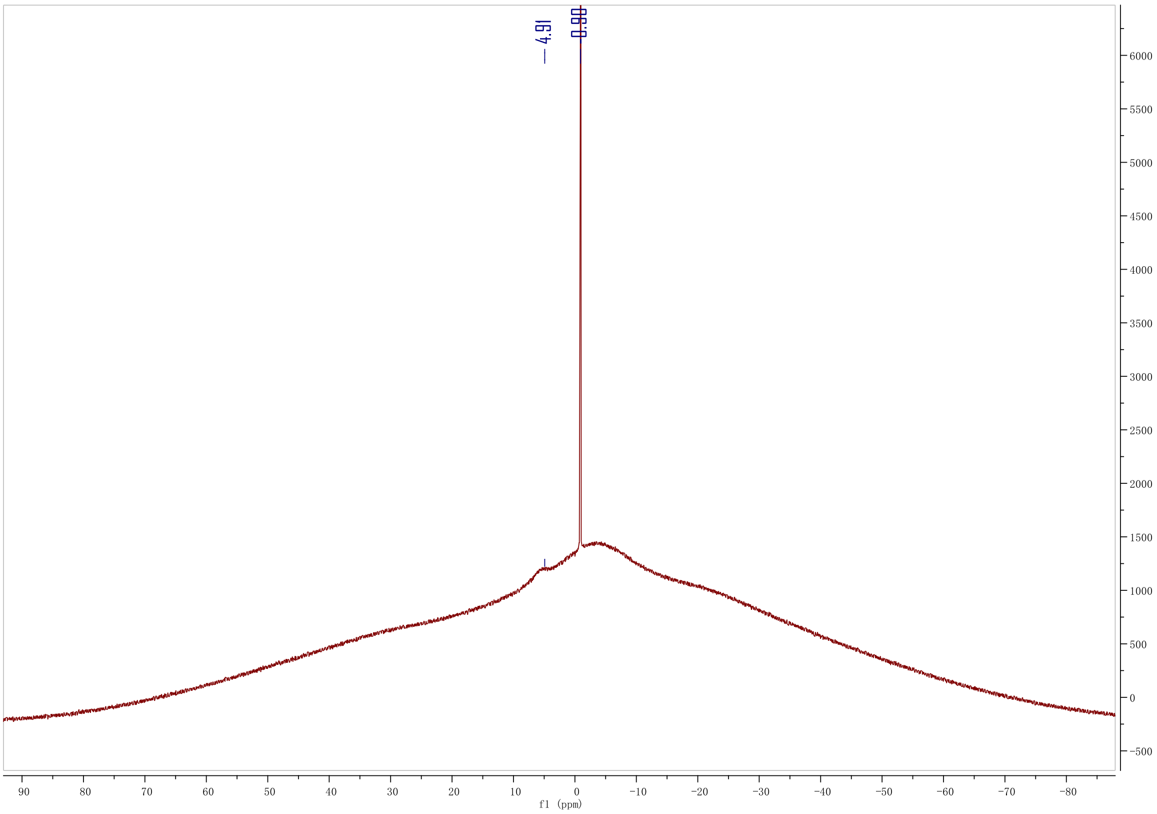

Figure 2.27 ^{11}B NMR spectrum of **7**.

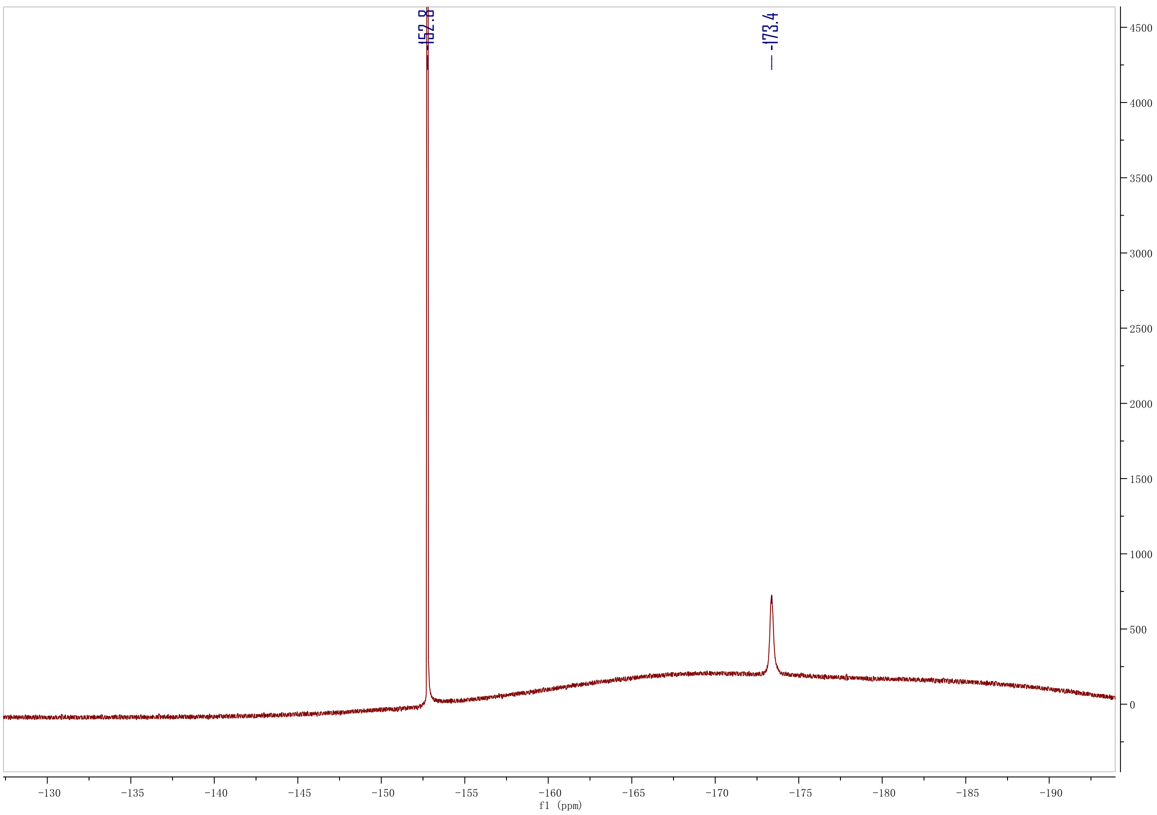

Figure 2.28 ^{19}F NMR spectrum of **7**.

2.4.2 Crystal structural parameters

X-ray data collection and structural refinement were performed. Intensity data for compounds **3–7** was collected using a Bruker APEX II diffractometer. The crystals of **3–7** were measured at 103(2) K. The structure was solved by direct phase determination (SHELX-2013) and refined for all data by full-matrix least squares methods on F^2.[27] All non-hydrogen atoms were subjected to anisotropic refinement. The hydrogen atoms were generated geometrically and allowed to ride in their respective parent atoms; they were assigned appropriate isotropic thermal parameters and included in the structure-factor calculations.

Table 1 Crystallographic data for compounds **3–5**.

Compounds	**3**	**4**•$(CH_3CN)_{1.7}(CH_2Cl_2)_{0.15}$	**5**
Formula	$C_{27}H_{39}N_3$	$C_{39.55}H_{55.40}BCl_{2.30}N_{4.70}$	$C_{36}H_{50}BN_3$
Fw	405.61	689.03	535.60
Cryst syst	monoclinic	monoclinic	monoclinic
Space group	*P*2$_1$/*m*	*P*2$_1$/*c*	*C*2/*c*
Size (mm^3)	0.340 x 0.400 x 0.420	0.120 x 0.160 x 0.220	0.220 x 0.300 x 0.340
T, K	103(2)	153(2)	103(2)
a, Å	6.8926(7)	10.0389(4)	27.818(4)
b, Å	10.0715(10)	31.4758(13)	15.0843(18)
c, Å	16.3279(16)	12.8082(5)	17.152(2)
β, deg	90.221(4)	111.7249(15)	120.030(4)
V, Å^3	1133.5(2)	3759.7(3)	6231.1(14)
Z	2	4	8
d_{calcd} g·cm^{-3}	1.188	1.215	1.142
μ, mm^{-1}	0.069	0.225	0.066
Refl collected	24971	60363	36021

T_{max}/T_{min}	0.9770/0.9710	0.9740/0.9520	0.9860/0.9780
N_{measd}	3823	12017	8054
[R_{int}]	0.0441	0.0468	0.1294
R [I>2sigma(I)]	0.0449	0.0605	0.0703
R_w[I>2sigma(I)]	0.1133	0.1447	0.1503
GOF	1.090	1.103	0.993
Largest diff. peak/hole[e·Å^{-3}]	0.393/-0.277	0.465/-0.456	0.336 / -0.340

Table 2 Crystallographic data for compounds **6** and **7**.

Compounds	**6**•$(CH_2Cl_2)_1$	**7**•$(CH_2Cl_2)_1$
Formula	$C_{39}H_{55}BCl_2F_3N_3O_3S$	$C_{37}H_{52}B_2Cl_2F_5N_3$
Fw	784.63	726.33
Cryst syst	monoclinic	monoclinic
Space group	*C*2/*c*	$P2_1/n$
Size (mm^3)	0.080 x 0.120 x 0.160	0.060 x 0.100 x 0.120
T, K	153(2)	153(2)
a, Å	40.4055(15)	10.3443(6)
b, Å	13.0469(4)	29.9302(15)
c, Å	34.7282(14)	12.7246(7)
β, deg	118.6046(17)	111.635(3)
V, Å^3	16073.0(10)	3662.1(4)
Z	16	4
d_{calcd} g·cm^{-3}	1.297	1.317
μ, mm^{-1}	0.268	0.234
Refl collected	106994	31299
T_{max}/T_{min}	0.9790/ 0.9580	0.9860/0.9720
N_{measd}	16598	7253

[R_{int}]	0.1160	0.0808
R [I>2sigma(I)]	0.0590	0.0551
R_w[I>2sigma(I)]	0.1507	0.1474
GOF	1.060	1.030
Largest diff. peak/hole[e·Å^{-3}]	0.660/-0.574	0.534/-0.582

2.4.3 Theoretical calculation

Gaussian 09 was used for all density functional theory (DFT) calculations.[28] Geometry optimization and frequency calculations on compound **5** and **6** were performed at the B3LYP/6-311G(d,p)//M05-2X/6-31G(d,p) level of theory. Natural bond order (NBO) analysis of compound **5** and **6** were performed at M05-2X/6-311+G(d,p) level of theory.

Figure 2.29. Calculated optimized structures for **5** and **6** at B3LYP/6-311G(d,p) level of theory.

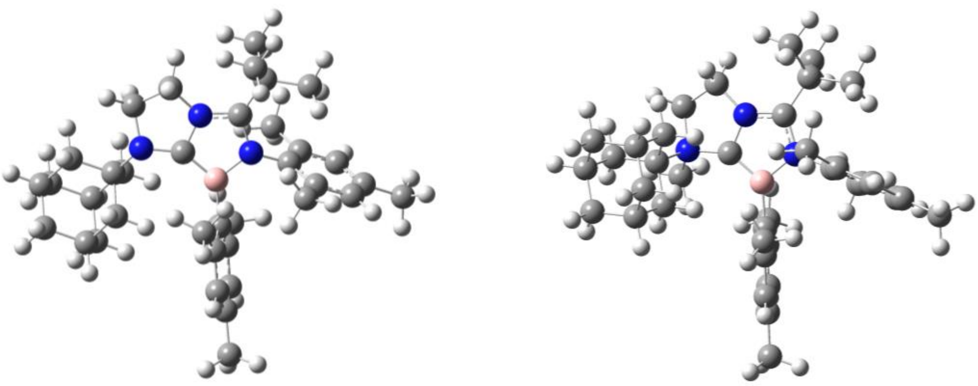

5 **6**

Table 3. Optimized structures of **5** and **6** (atom, x-, y-, z- positions in Å)

5

B	0.262753	-0.078441	-0.330527
C	-3.108383	-0.980161	-0.009918
C	-4.409263	-1.803334	-0.179800
C	-5.622976	-1.028443	0.372735
C	-5.786251	0.299338	-0.387595
C	-4.505430	1.135183	-0.215208
C	-3.300368	0.350251	-0.769707
C	-2.916932	-0.677355	1.497794
C	-4.128759	0.103489	2.048477
C	-5.406354	-0.739422	1.871138
C	-4.278660	1.431129	1.280147
C	-1.928019	-3.174891	-0.339226
C	-0.538343	-3.580720	-0.814539
C	-0.621172	-1.267070	-0.439694
C	0.040808	1.486686	-0.460205
C	-0.227466	2.022209	-1.750831
C	-0.358512	1.123976	-2.963774
C	-0.416733	3.393222	-1.923456
C	-0.363501	4.286794	-0.850672
C	-0.547618	5.770121	-1.065794
C	-0.129253	3.760677	0.414463
C	0.072032	2.389926	0.623133
C	0.312579	1.928983	2.042926
C	2.783997	-0.015225	0.214237
C	3.549183	0.759936	-0.674876
C	3.221497	0.852269	-2.143445
C	4.651777	1.456455	-0.179018
C	5.014115	1.416165	1.167577
C	6.195014	2.206913	1.677240
C	4.235979	0.643445	2.026111
C	3.123037	-0.073553	1.577383
C	2.346757	-0.905222	2.571254
C	1.542918	-2.091077	-0.378728
C	2.639198	-3.152318	-0.535407
C	2.491034	-3.849811	-1.915719
C	2.543133	-4.217004	0.586862
C	4.073567	-2.585190	-0.498083
N	-1.968421	-1.728361	-0.609791
N	0.222879	-2.378387	-0.471524
N	1.616707	-0.723620	-0.252509

H	-4.335351	-2.755954	0.353654
H	-4.553634	-2.033437	-1.241887
H	-6.520914	-1.642597	0.242437
H	-6.655723	0.847331	-0.006004
H	-5.970332	0.105447	-1.450707
H	-4.598510	2.076936	-0.766024
H	-3.447711	0.125466	-1.831408
H	-2.399988	0.958041	-0.685105
H	-2.000660	-0.098855	1.634318
H	-2.792899	-1.613215	2.055956
H	-3.969469	0.310210	3.112748
H	-5.318915	-1.679847	2.428516
H	-6.272695	-0.205900	2.279127
H	-5.121043	2.005426	1.683813
H	-3.380517	2.044481	1.407361
H	-2.706226	-3.712223	-0.879766
H	-2.026629	-3.400255	0.735820
H	-0.166145	-4.475989	-0.322802
H	-0.526001	-3.728815	-1.898810
H	-0.490339	1.716555	-3.872649
H	-1.216223	0.452720	-2.869676
H	0.517400	0.485940	-3.097641
H	-0.620648	3.775518	-2.920377
H	0.346143	6.218643	-1.513737
H	-0.738309	6.288422	-0.123321
H	-1.383997	5.975748	-1.740035
H	-0.105341	4.430706	1.270175
H	1.366201	2.035795	2.319048
H	0.044593	0.879999	2.172282
H	-0.272517	2.523127	2.750667
H	2.461303	1.617386	-2.321567
H	2.831312	-0.089179	-2.533504
H	4.110267	1.123113	-2.717634
H	5.246249	2.046247	-0.870782
H	5.934112	3.262794	1.807506
H	7.034736	2.164507	0.978504
H	6.539598	1.831681	2.643314
H	4.494916	0.594386	3.080023
H	1.336992	-1.121968	2.224539
H	2.276608	-0.385472	3.529725

H	2.848944	-1.859913	2.760779
H	1.553782	-4.395814	-2.018781
H	3.303553	-4.569682	-2.053051
H	2.547580	-3.118556	-2.725989
H	2.697942	-3.763949	1.567383
H	3.313492	-4.980724	0.441699
H	1.579038	-4.726480	0.606398
H	4.243380	-1.841219	-1.276531
H	4.766199	-3.413156	-0.673831
H	4.328690	-2.136889	0.460528

6

B	-0.398189	0.203216	-0.576370
C	-0.984739	-2.112699	-0.522445
C	1.343127	-2.947907	-1.284702
C	2.376203	-2.028450	-1.940802
C	0.743130	-0.670912	-0.914547
C	-0.613691	1.768823	-0.588746
C	-0.777532	2.448151	-1.821708
C	-0.816582	1.738861	-3.162660
C	-0.921050	3.839587	-1.849502
C	-0.909344	4.607533	-0.689392
C	-1.088729	6.104767	-0.733720
C	-0.749592	3.937764	0.524166
C	-0.611192	2.551827	0.593606
C	-0.488070	1.934580	1.968597
C	-2.696137	-0.523566	0.368095
C	-3.770430	-0.005087	-0.372948
C	-3.715906	0.177009	-1.869267
C	-4.937977	0.342671	0.306753
C	-5.067024	0.200582	1.689170
C	-6.337480	0.609075	2.392589
C	-3.983675	-0.322281	2.392510
C	-2.794167	-0.692084	1.759581
C	-1.690305	-1.301328	2.592616
C	-1.747558	-3.448049	-0.605436
C	-1.868281	-3.836721	-2.104765
C	-0.995537	-4.554966	0.173841
C	-3.186105	-3.409327	-0.050007
C	2.279547	0.375213	-2.487922
C	3.222066	-0.283959	-0.189240
C	2.908133	1.110606	0.375904
C	4.667175	-0.291742	-0.729052
C	5.643057	0.027463	0.435491
C	5.499770	-1.030339	1.543300
C	4.056732	-1.007931	2.078390
C	3.728369	0.382206	2.649287
C	3.880821	1.431570	1.535125
C	5.325198	1.421817	1.004338
C	3.083035	-1.337236	0.923049
N	-1.441181	-0.841694	-0.289065
N	0.307242	-2.001292	-0.882183
N	2.149886	-0.626423	-1.366275
H	0.978656	-3.683284	-1.998257
H	1.744217	-3.471778	-0.417490
H	2.198999	-1.960072	-3.011994
H	3.400274	-2.345947	-1.775073
H	-1.721135	2.005250	-3.716038
H	-0.797764	0.653966	-3.061951
H	0.027852	2.038133	-3.793039
H	-1.046599	4.333928	-2.808967
H	-2.121313	6.380386	-0.494835
H	-0.861785	6.506296	-1.723174
H	-0.444424	6.605225	-0.006732
H	-0.734874	4.512471	1.446009
H	0.017979	2.613260	2.659343
H	0.063877	0.993344	1.954450
H	-1.476062	1.721306	2.386655
H	-4.706243	0.035437	-2.306368
H	-3.028428	-0.521190	-2.347870
H	-3.386149	1.187430	-2.123053
H	-5.772537	0.735748	-0.265752
H	-6.339604	0.285700	3.434751
H	-7.216262	0.180649	1.903368
H	-6.458241	1.696760	2.380491
H	-4.061556	-0.451277	3.467529
H	-1.836512	-2.380619	2.712102
H	-1.685025	-0.869784	3.595186
H	-0.704291	-1.150422	2.153850
H	-2.447616	-3.090404	-2.652770

H	-2.388523	-4.793740	-2.191850
H	-0.903702	-3.944333	-2.603433
H	-0.023782	-4.804515	-0.251476
H	-1.590936	-5.470481	0.157103
H	-0.850233	-4.272226	1.219005
H	-3.222822	-3.196323	1.016706
H	-3.622550	-4.399124	-0.203566
H	-3.817952	-2.688039	-0.564228
H	1.572644	0.095051	-3.262659
H	3.293442	0.363508	-2.880059
H	2.020533	1.360161	-2.114583
H	1.877804	1.150844	0.725774
H	3.023718	1.877811	-0.392840

H	4.803193	0.463435	-1.506055
H	4.940089	-1.260665	-1.157317
H	6.659725	0.011044	0.033086
H	6.204932	-0.820621	2.353033
H	5.749018	-2.025622	1.157855
H	3.934840	-1.769258	2.854170
H	2.709438	0.397798	3.050240
H	4.400896	0.614327	3.480624
H	3.630865	2.424003	1.919597
H	5.452600	2.187492	0.231361
H	6.026106	1.664703	1.808662
H	3.328199	-2.334142	0.545175
H	2.054787	-1.354945	1.292538

Figure 2.30 Plots of the frontier orbitals of compounds **5** and **6**.

Compound 5:

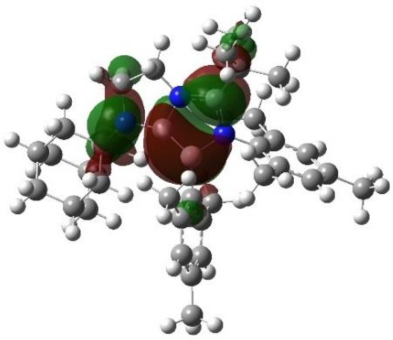

LUMO (–0.2185 eV)

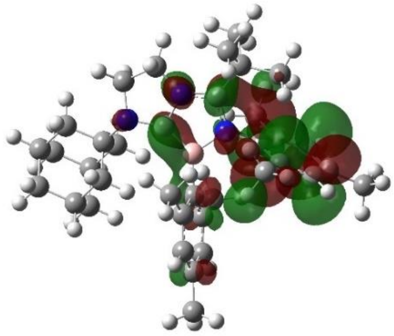

HOMO (–3.8418 eV)

Compound 6:

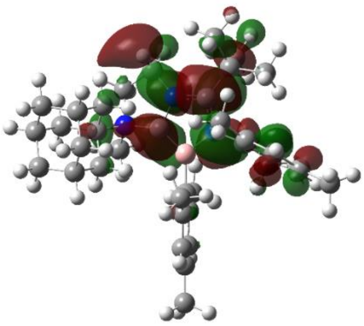

LUMO (–3.1797 eV)

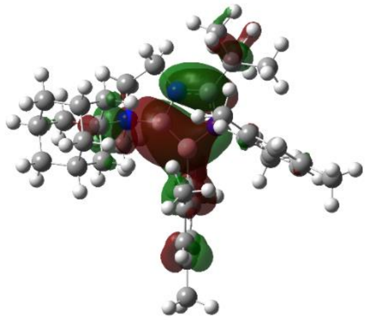

HOMO (–8.1283 eV)

Table 4. Optimized structures of **5'**, 1,3,2-diazaborole, 1,2-azaborole, and Cp⁻ (atom, x-, y-, z-positions in Å)

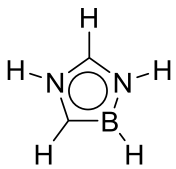

C	0.335316	-1.068926	-0.000021	H	2.163464	-0.162867	0.000341
H	0.610253	-2.109269	0.000470	H	0.940229	2.314756	0.000111
H	-1.705599	-1.240269	0.000039	N	1.169670	-0.016745	-0.000098
C	-0.984713	0.768642	0.000062	B	0.414283	1.248944	-0.000023
H	-1.968321	1.206836	0.000165	N	-0.914678	-0.619284	-0.000081

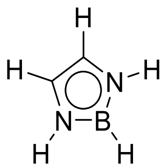

C	-0.675418	-0.951258	0.000392	H	1.347702	-1.792506	-0.000578
C	0.675416	-0.951259	-0.000350	H	2.102366	0.588868	0.000292
H	0.000002	2.434505	-0.000161	N	1.124924	0.367789	0.000163
H	-2.102365	0.588872	-0.000186	N	-1.124923	0.367790	-0.000135
H	-1.347706	-1.792503	0.000717	B	0.000001	1.247762	-0.000106

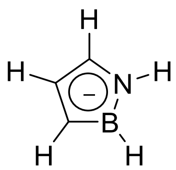

C	0.517724	-1.035053	0.000000	H	-2.177400	0.922535	0.000001
C	-0.844587	-0.833678	-0.000001	H	0.496472	2.441670	0.000000
C	-1.151805	0.564848	0.000000	N	1.154383	0.202893	0.000000
H	1.076966	-1.962310	0.000001	H	2.155625	0.261134	0.000000
H	-1.559460	-1.654162	-0.000001	B	0.159825	1.278836	0.000000

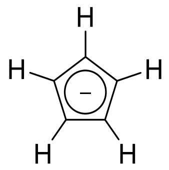

C	0.000000	0.704608	-0.969972
H	0.000128	1.342336	-1.848393
C	0.000003	1.140239	0.370458
H	0.000012	2.172480	0.706269
C	0.000000	0.000000	1.198999

H	0.000000	0.000000	2.284417
C	0.000000	-0.704608	-0.969972
H	-0.000128	-1.342336	-1.848393
C	-0.000003	-1.140239	0.370458
H	-0.000012	-2.172480	0.706269

2.5 References

(1) a) Kekulé, A. *Bull, A. Soc. Chim. Fr.* **1865**, *3*, 98 – 110; b) Faraday, M. *Phil. Trans. R. Soc. Lond.* **1825**, *115*, 440 – 466.

(2) For selected recent articles, see (references are therein): a) Suzuki, S.; Segawa, Y.; Itami, K.; Yamaguchi, J. *Nat. Chem.* **2015**, *7*, 227 – 233; b) Taylor, R. D.; MacCoss, M.; Lawson, A. D. G. *J. Med. Chem.* **2014**, *57*, 5845 – 5859; c) Hoye, T. R.; Baire, B.; Niu, D.; Willoughby, P. H.; Woods, B. P. *Nature* **2012**, *490*, 208 – 212; d) Domínguez, G.; Pérez-Castells, J. *Chem. Soc. Rev.* **2011**, *40*, 3430 – 3444; e) Otterlo, W. A. L. v.; de Koning, C. B. *Chem. Rev.* **2009**, *109*, 3743 – 3782.

(3) a) Chen, J.-R.; Hu, X.-Q.; Lu, L.-Q.; Xiao, W.-J. *Chem. Rev.* **2015**, *115*, 5301 – 5365; b) Gulevich, A. V.; Dudnik, A. S.; Chernyak, N.; Gevorgyan, V. *Chem. Rev.* **2013**, *113*, 3084 – 3213; c) Quin, L. D.; Tyrell, J. *Fundamentals of Heterocyclic Chemistry: Importance in Nature and in the Synthesis of Pharmaceuticals*, John Wiley & Sons Inc.: New York, **2010**;

d) Katritzky,;A. R.; Scriven,;E. F. V.; Rees, C. W. *Comprehensive Heterocyclic Chemistry III*, Elsevier: Oxford, U.K., **2008**.

(4) For review, see: a) Campbell, P. G.; Marwitz, A. J. V.; Liu, S.-Y. *Angew. Chem. Int. Ed.* **2012**, *51*, 6074 – 6092; b) Bosdet, M. J. D.; Piers, W. E. *Can. J. Chem.* **2009**, *87*, 8 – 29; c) Liu, Z.; Marder, T. B. *Angew. Chem. Int. Ed.* **2008**, *47*, 242 – 244.

(5) a) Merriam, J. S.; Niedenzu, K. *J. Organomet. Chem.* **1973**, *51*, C1-C2; b) Dewar, M. J. S.; Golden, R.; Spanninger, P. A. *J. Am. Chem. Soc.* **1971**, *93*, 3298 – 3299; c) Paetzold, P. I. *Z. Anorg. Allg. Chem.* **1963**, *326*, 64 – 69.

(6) a) Xie, L.; Zhang, J.; Cui, C. *Chem. Eur. J.* **2014**, *20*, 9500 – 9503; b) Liu, Z.; Xu, J.; Ruan, W.; Fu, C.; Zhang, H.-J.; Wen, T.-B. *Dalton Trans.* **2013**, *42*, 11976 – 11980; c) Fang, X.; Li, X.; Hou, Z.; Assoud, J.; Zhao, R. *Organometallics* **2009**, *28*, 517 – 522; d) Fang, X.; Deng, Y.; Xie, Q.; Moingeon, F. *Organometallics* **2008**, *27*, 2892 – 2895; e) Fang, X.; Assoud, J. *Organometallics* **2008**, *27*, 2408 – 2410; f) Liu, S.-Y.; Lo, M. M.-C.; Fu, G. C. *Angew. Chem. Int. Ed.* **2002**, *41*, 174 – 176; g) Liu, S.-Y.; Hills, I. D.; Fu, G. C. *Organometallics* **2002**, *21*, 4323 – 4325; h) Ashe, A. J., III; Fang, X.; Kampf, J. W. *Organometallics* **2001**, *20*, 5413 – 5418; i) Ashe, A. J., III; Fang, X. *Org. Lett.* **2000**, *2*, 2089 – 2091; j) Schmid, G.; Schütz, M. *J. Organomet. Chem.* **1995**, *492*, 185 – 189; k) Schmid, G. *Comments Inorg. Chem.* **1985**, *4*, 17 – 32; l) Amirkhalili, S.; Boese, R.; Höhner, U.; Kampmann, D.; Schmid, G.; Rademacher, P. *Chem. Ber.* **1982**, *115*, 732 – 737; m) Schulze, J.; Schmid, G. *Angew. Chem. Int. Ed.* **1980**, *19*, 54 – 55.

(7) a) Weber, L. *Coord. Chem. Rev.* **2008**, *252*, 1 – 31; b) Weber, L.; Dobbert, E.; Stammler, H.-G.; Neumann, B.; Boese, R.; Bläser, D. *Eur. J. Inorg. Chem.* **1999**, 491 – 497; c) Weber, L.;

Dobbert, E.; Boese, R.; Kirchner, M. T.; Bläser, D. *Eur. J. Inorg. Chem.* **1998**, 1145 – 1152; d) Schmid, G.; Lehr, J.; Polk, M.; Boese, R.; *Angew. Chem. Int. Ed.* **1991**, *30*, 1015 – 1016; e) Schmid, G.; Polk, M.; Boese, R. *Inorg. Chem.* **1990**, *29*, 4421 – 4429.

(8) a) Loh, Y.-K.; Chong, C.-C.; Ganguly, R.; Li, Y.; Vidovic, D.; Kinjo, R. *Chem. Commun.* **2014**, *50*, 8561 – 8564; b) Weber, L.; Schnieder, M.; Stammler, H.-G.; Neumann, B.; Shoeller, W. W. *Eur. J. Inorg. Chem.* **1999**, 1193 – 1198.

(9) a) Leach, J. B.; Morris, J. H. *J. Organomet. Chem.* **1968**, *13*, 313 – 321; b) Paetzold, P.; Plotho, C. V.; Schmid, G.; Boese, R.; Schrader, B.; Bougeard, D.; Pfeiffer, U.; Gleiter, R.; Schüfer, W. *Chem. Ber.* **1984**, *117*, 1089 – 1102; c) Paetzold, P.; Plotho, C. V. ; *Chem. Ber.* **1982**, *115*, 2819 – 2825.

(10) a) Chrostowska, A.; Xu, S.; Maziere, A.; Boknevitz, K.; Li, B.; Abbey, E. R.; Dargelos, A.; Graciaa, A.; Liu, S.-Y. *J. Am. Chem. Soc.* **2014**, *136*, 11813 – 11820; b) Abbey, E. R.; Liu, S.-Y. *Org. Biomol. Chem.* **2013**, *11*, 2060 – 2069; c) Abbey, E. R.; Zakharov, L. N.; Liu, S.-Y. *J. Am. Chem. Soc.* **2011**, *133*, 11508 – 11511; d) Abbey, E. R.; Zakharov, L. N.; Liu, S.-Y. *J. Am. Chem. Soc.* **2010**, *132*, 16340 – 16342; e) Chrostowska, A.; Maciejczyk, M.; Dargelos, A.; Baylere, P.; Weber, L.; Werner, V.; Eickhooff, D.; Stammler, H. G.; Neumann, B. *Organometallics* **2010**, *29*, 5192 – 5198; f) Kubo, Y.; Tsuruzoe, K.; Okuyama, S.; Nishiyabu, R.; Fujihara, T. *Chem. Commun.* **2010**, *46*, 3604 – 3606; g) Weber, L.; Werner, V.; Fox, M. A.; Marder, T. B.; Scwedler, S.; Brockhinke, A.; Stammler, H.-G.; Neumann, B. *Dalton Trans.* **2009**, 1339 – 1351; h) Weber, L.; Werner, V.; Fox, M. A.; Marder, T. B.; Scwedler, S.; Brockhinke, A.; Stammler, H.-G.; Neumann, B. *Dalton Trans.* **2009**, 2823 – 2831; i) Maruyama, S.; Kawanishi, Y. *J. Mater. Chem.* **2002**, *12*, 2245 – 2249.

(11) a) Stephan, D. R. *Angew. Chem. Int. Ed.* **2017**, *56*, 5984 – 5992; b) Soleilhavoup, M.; Bertrand, G. *Angew. Chem. Int. Ed.* **2017**, *56*, 10282 – 10292.

(12) Kinjo, R.; Donnadieu, B.; Celik, M. A.; Frenking, G.; Bertrand, G. *Science* **2011**, *333*, 10 – 613.

(13) Ruiz, D. A.; Melaimi, M.; Bertrand, G. *Chem. Commun.* **2014**, *50*, 7837 – 7839.

(14) Kong, L. B.; Li, Y. X.; Ganguly, R.; Vidovic, D.; Kinjo, R. *Angew. Chem. Int. Ed.* **2014**, *53*, 9280 – 9283.

(15) Kong, L. B.; Ganguly. R.; Li, Y. X.; Kinjo, R. *Chem. Sci*. **2015**, *6*, 2893 – 2902.

(16) a) Arrowsmith, M.; Auerhammer, D.; Bertermann, R.; Braunschweig, H.; Celik, M. A.; Erdmannsdörfer, J.; Krummenacher, I.; Kupfer, T. *Angew. Chem. Int. Ed.* **2017**, *56*, 11263 – 11267; b) Braunschweig, H.; Krummenacher, I.; Légaré, M.-A.; Matler, A.; Radacki, K.; Ye, Q. *J. Am. Chem. Soc.* **2017**, *139*, 1802 – 1805; c) Braunschweig, H.; Celik, M. A.; Dewhurst, R. D.; Ferkinghoff, K.; Hermann, A.; Jimenez-Halla, J. O. C.; Kramer, T.; Radacki, K.; Shang, R.; Siedler, E.; Weißenberger, F.; Werner, C. *Chem. Eur. J.* **2016**, *22*, 11736 – 11744; d) Arrowsmith, M.; Auerhammer, D.; Bertermann, R.; Braunschweig, H.; Bringmann, G.; Celik, M. A.; Dewhurst, R. D.; Finze, M.; Grüne, M.; Hailmann, M.; Hertle, T.; Krummenacher, I. *Angew. Chem. Int. Ed.* **2016**, *55*, 14464 – 14468; e) Braunschweig, H.; Dewhurst, R. D.; Pentecost, L.; Radacki, K.; Vargas, A.; Ye, Q. *Angew. Chem. Int. Ed.* **2016**, *55*, 436-440; f) Braunschweig, H.; Dewhurst, R. D.; Hupp, F.; Nutz, M.; Radacki, K.; Tate, C. W.; Vargas, A.; Ye, Q. *Nature* **2015**, *522*, 327 – 330.

(17) Rosas-Sánchez, A.; Alvarado-Beltran, I.; Baceiredo, A.; Hashizume, D.; Saffon-Merceron, N.; Branchadell, V.; Kato, T. *Angew. Chem. Int. Ed.* **2017**, *56*, 4814 – 4818.

(18) Wang, H.; Zhang, J.; Lin, Z.; Xie, Z. *Chem. Commun.* **2015**, *51*, 16817 – 16820.

(19) a) Liu, P.; Wesolek, M.; Danopoulos, A. A.; Braunstein, P. *Organometallics* **2013**, *32*, 6286 – 6297; b) Thagfi, J. A.; Lavoie, G. G. *Organometallics* **2012**, *31*, 7351 – 7358; c) Larocque, T. G.; Badaj, A. C.; Dastgir, S.; Lavoie, G. G. *Dalton Trans.* **2011**, *40*, 12705 – 12712; d) Thagfi, J. A.; Dastgir, S.; Lough, A. J.; Lavoie, G. G. *Organometallics* **2010**, *29*, 3133 – 3138.

(20) a) Siemeling, U. *Chem. Rev.* **2000**, *100*, 1495 – 1526; b) Jutzi, P. *Chem. Rev.* **1999**, *99*, 969 – 990; c) Janiak, C.; Schumann, H. *Adv. Organomet. Chem.* **1991**, *33*, 291 – 393.

(21) a) Cid, J.; Gulyás, H.; Carbó, J. J.; Fernández, E. *Chem. Soc. Rev.* **2012**, *41*, 3558 – 3570; b) Weber, L. *Eur. J. Inorg. Chem.* **2012**, 5595 – 5609; c) Gulyás, H.; Bonet, A.; Pubill-Ulldemolins, C.; Solé, C.; Cid, J.; Fernández, E. *Pure Appl. Chem.* **2012**, *84*, 2219 – 2231; d) Yamashita, M. *Bull. Chem. Soc. Jpn.* **2011**, *84*, 983 – 999; e) Yamashita, M.; Nozaki, K. J. *Synth. Org. Chem. Jpn.* **2010**, *68*, 359 – 369; f) Segawa, Y.; Suzuki, Y.; Yamashita, M.; Nozaki, K. *J. Am. Chem. Soc.* **2008**, *130*, 16069 – 16079; g) Yamashita, M.; Nozaki, K. *Bull. Chem. Soc. Jpn.* **2008**, *81*, 1377 – 1392; h) Segawa, Y.; Yamashita, M.; Nozaki, K. *Science* **2006**, *314*, 113 – 115.

(22) For selected examples of relevant anionic borole derivatives, see: a) Braunschweig, H.; Chiu, C.-W.; Kupfer, T.; Radacki, K. *Inorg. Chem.* **2011**, *50*, 4247 – 4249; b) Braunschweig, H.; Chiu, C.-W.; Radacki, K.; Kupfer, T. *Angew. Chem. Int. Ed.* **2010**, *49*, 2041 – 2044; c) Braunschweig, H.; Chiu, C.-W.; Wahler, J.; Radacki, K.; Kupfer, T. *Chem. Eur. J.* **2010**, *16*, 12229 – 12233; d) So, C.-W.; Watanabe, D.; Wakamiya, A.; Yamaguchi, S. *Organometallics* **2008**, *27*, 3496 – 3501; e) Herberich, G. E.; Wagner, T.; Marx, H.-W. *J. Organomet. Chem.*

1995, *502*, 67– 74; f) Herberich, G. E.; Hostalek, M.; Laven, R.; Boese, R. *Angew. Chem. Int. Ed.* **1990**, *29*, 317 – 318.

(23) For review, see: a) Brownie, J. H.; Baird, M. C. *Coord. Chem. Rev.* **2008**, *252*, 1734 – 1754. For recent examples, see: b) Kübler, P.; Oelkers, B.; Sudermeyer, J. *J. Organomet. Chem.* **2014**, *767*, 165 – 176; c) Gong, W.-T.; Na, D.; Mehdi, H.; Ye, J.-W.; Ning, G.-L. *J. Organomet. Chem.* **2014**, *772*, 314 – 319.

(24) Bertermann, R.; Braunschweig, H.; Dewhurst, R. D.; Hörl, C.; Kramer, T.; Krummenacher, I. *Angew. Chem. Int. Ed.* **2014**, *53*, 5453 – 5457.

(25) Sundararaman, A.; Jakle, F. *J. Organomet. Chem.*, **2003**, *681*, 134–142.

(26) Paczal, A.; Benyei, A. C.; Kotschy, A. *J. Org. Chem.* **2006**, *71*, 5969–5979.

(27) Bruker AXS SHELXTL, Madison, WI; *SHELX-97G*. M. Sheldrick, Acta Crystallogr. A, **2008**, *64*, 112–122, *SHELX-2013*, http://shelx.uni-ac. gwdg.de/SHELX/index.php.

(28) Gaussian 09, Revision B.01, Frisch, M. J.; Trucks, G. W.; Schlegel, H. B.; Scuseria, G. E.; Robb, M. A.; Cheeseman, J. R.; Scalmani, G.; Barone, V.; Mennucci, B.; Petersson, G. A.; Nakatsuji, H.; Caricato, M.; Li, X.; Hratchian, H. P.; Izmaylov, A. F.; Bloino, J.; Zheng, G.; Sonnenberg, J. L.; Hada, M.; Ehara, M.; Toyota, K.; Fukuda, R.; Hasegawa, J.; Ishida, M.; Nakajima, T.; Honda, Y.; Kitao, O.; Nakai, H.; Vreven, T.; Montgomery, J. A. Jr.,; Peralta, J. E.; Ogliaro, F.; Bearpark, M.; Heyd, J. J.; Brothers, E.; Kudin, K. N.; Staroverov, V. N.; Keith, T.; Kobayashi, R.; Normand, J.; Raghavachari, K.; Rendell, A.; Burant, J. C.; Iyengar, S. S.; Tomasi, J.; Cossi, M.; Rega, N.; Millam, J. M.; Klene, M.; Knox, J. E.; Cross, J. B.; Bakken, V.; Adamo, C.; Jaramillo, J.; Gomperts, R.; Stratmann, R. E.; Yazyev, O.; Austin, A. J.; Cammi, R.; Pomelli, C.; Ochterski, J. W.; Martin, R. L.; Morokuma, K.; Zakrzewski,

V. G.; Voth, G. A.; Salvador, P.; Dannenberg, J. J.; Dapprich, S.; Daniels, A. D.; Farkas, O.; Foresman, J. B.; Ortiz, J. V.;Cioslowski, J.; Fox, D. J. Gaussian, Inc., Wallingford CT, **2010**.

Chapter 3 Investigation on the ring-expansion of 1,4,2-diazaborole and its further functionalization†

3.1 Introduction

Isoelectronic and isosteric relationships between C=C and B−N units is one of the most significant concepts in modern boron-nitrogen chemistry arsenal.[1] Accordingly, the replacement of a C=C unit with a B-N unit is a commonly applied strategy to approach the various BN aromatic heterocycles, which renders two classes of well-known small heterocyclic aromatic molecules, namely, six-membered azaborinines and five-membered azaboroles.[2] Since the landmark work by Dewar et al. in 1958,[3] Azaborinines have been widely investigated in various research fields such as coordination chemistry,[4] materials science[5] and biomedical chemistry.[6] Moreover, the recent demonstration that azaborinines can be employed as a chemical hydrogen storage,[7] a synthon in organic molecular synthesis,[8] a small molecule activator,[9] as well as, a pre-catalyst,[10] explicitly indicates its diverse utility in various application. Likewise, several azaborole derivatives bearing an aromatic BN five-membered ring framework have also reported since the 1960s.[11] In contrast to azaborinines, however, the reported application of azaboroles is still limited mainly to the use as ligands for metal complexes, while it has been shown that some of them exhibit the unique biological activity and optoelectronic nature,[12] indicating its feasible application usability.

Since the first isolation and characterization of a "bottleable" N-heterocyclic carbene

† Portions of this chapter are taken with permission from: Su, B.; Li, Y.; Ganguly, R.; Kinjo, R. *Angew. Chem. Int. Ed.* **2017**, *56*, 14572 – 14576. Copyright (2017) WILEY-VCH Verlag GmbH & Co. KGaA, Weinheim.

(NHC) was reported by Arduengo et al.,[13] NHCs have been intensively applied to transition-metal chemistry,[14] organocatalysis[15] and main group chemistry[16] due to their robust two-electrons σ-donor ability and easy preparation and modification.[17] Recent studies show that NHCs can be activated by main group elements leading to the modification of the heterocyclic framework.[18] Very recently, it has been demonstrated that ring expansion reactions (RER) by insertion of main group elements such as Si,[19] Be,[20], Al,[21] B, [22] into the C-N bond of NHC with the five-membered ring result in the formation of six-membered framework. The first RER involving the insertion of boron atom into the C-N bond of NHC was reported by Rivard et al. by heating of NHC-borane adduct **I** (Figure 3.1).[22a] Shortly afterwards, Inoue et al. reported a detailed study on the reaction of NHC with imino-boranes to afford the RER product **II**.[22b] Stephan et al. discovered that the reaction of NHCs of the form $C_3H_2(NPR_2)_2$ with 9-BBN could undergo RERs to form the ring expansion products **III**.[22c] Beyond the RERs based on the carbene boron hydride adducts, the reactions of NHCs with diboranes such as B_2cat_2 (cat = 1,2-$O_2C_6H_4$), B_2neop_2 (neop = $OCH_2CMe_2CH_2O$) and B_2eg_2 (eg = 1,2-$O_2C_2H_4$) could also undergo rearrangements to afford the ring expansion products **IV**–**VII**.[22d,22f]

Free borylenes (R–B:) possessing two vacant orbitals and only one substituent are extremely electron-deficient and highly reactive, so they are only spectroscopically characterized in the gas phase or in matrices at very low temperatures. Recently, more attentions have been paid on the borylene chemistry and rapid progress has been achieved.[23] With the suitable ligands to adjust the electronic structures, several borylene species have been successfully isolated.[24] However, most of the in situ generated borylenes are extremely reactive and undergo further reaction through insertion into C–H,[25] C–C,[26] C=C,[25c,27] C–O[25c] as well as

C–N bonds.[28] The only reported example of C–N bond insertion of borylene was observed during reduction of N-heterocyclic olefins (NHOs) borane adduct with potassium graphite, where the boron atom was inserted into the σ-bond of the carbon atom (Dipp group) and the nitrogen atom to furnish **VIII**. To the best of our knowledge, the ring expansion reaction of NHC via borylene insertion into the C–N bond is rarely reported until now.

In chapter 2, we have presented the first isolation of the 1,4,2-diazaborole. On the course of our continuous study of 1,4,2-diazaborole chemistry, we discovered the unique skeletal transformation of 1,4,2-diazaboroles. In this chapter, we report the first example of the ring expansion via borylene insertion into C–N bond of the 1,4,2-diazaboroles and the detailed reaction mechanism is also proposed.

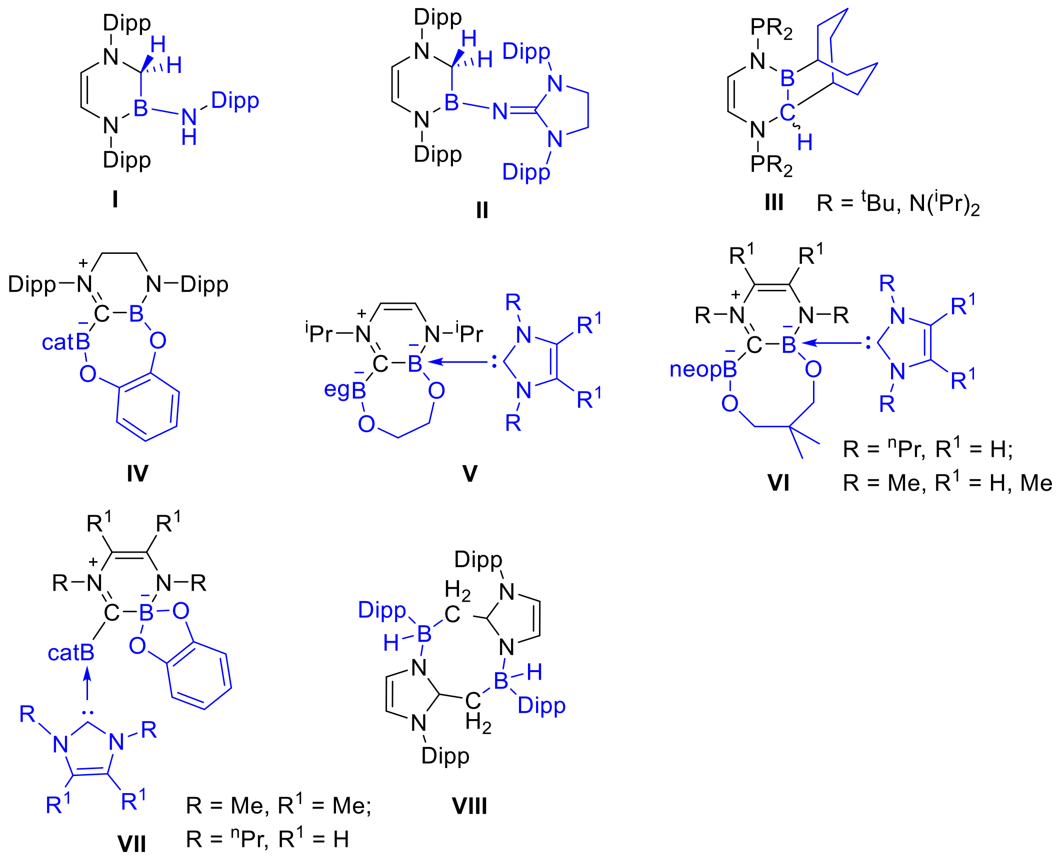

Figure 3.1 Reported ring expansion reactions (RER) by insertion of boron (**I–VII**) and the first example of borylene insertion into C–N bond (**VIII**).

3.2 Results and Discussions

To begin a reactivity study of 1,4,2-diazaborole, we attempted to synthesize a new 1,4,2-diazaborole by the reported synthetic procedure in chapter 2. Treatment of an imino-N-heterocyclic carbene **1** with two equivalents of boron tribromide in hexane at room temperature readily afforded compound **2** in 92% yield (Scheme 3.1a). Compound **2** was fully characterized by multiple NMR spectroscopy and X-ray diffraction analysis. In the ^{11}B NMR spectrum, one broad peak at −7.28 ppm and a sharp peak at −24.14 ppm are observed. In the solid-state molecular structure, the boron atom in the cationic part is coordinated by both of carbene carbon atoms and the imino nitrogen atom, along with BBr_4 as the counteranion (Figure 3.2a). Next, we performed the reduction of **2** with five equivalents of potassium graphite (KC_8) in toluene. After work-up, a BN-dihydroindole derivative **3** involving two boron atoms was obtained as a white solid in 72% yield. Compound **3** is thermally stable both in solid state and in solution at room temperature, but rapidly decomposed upon exposure to air or moisture. Compound **3** was fully characterized by standard spectroscopic means and X-ray diffraction analysis. In the ^{11}B NMR spectrum of **3**, a broad signal due to the overlap of two peaks appears at 29 ppm, which is significantly shifted downfield compared with that (−7.28 ppm) of the cationic part of **2**. The solid-state molecular structure of **3** reveals the formation of a six-membered ring by incorporating one additional boron atom into the carbene ring of **2** (Figure 3.2b). The BC_2N_2 five-membered ring moiety is nearly coplanar, and both B1 and B2 atoms show the trigonal-planar geometry, indicative of characteristic for sp^2 hybridization. The B2–C1 bond distance (1.523(9) Å) is longer than the B1–C1 bond (1.449(9) Å), and both B1–C1 and B1–N1 (1.449(8) Å) bond distances are significantly shorter than those (1.617(14) Å and 1.573(13) Å, respectively) of **2**. In addition, the lengthening of the bonds of C1–N2 (1.421(8) Å) and C2–N1 (1.376(8) Å) and the shortening of C2–N2 (1.337(8) Å) are observed with respect to those of **2**. These metric parameters suggest the delocalization of π-electrons over the BC_2N_2 five-membered ring (Scheme 3.1b).

(a)

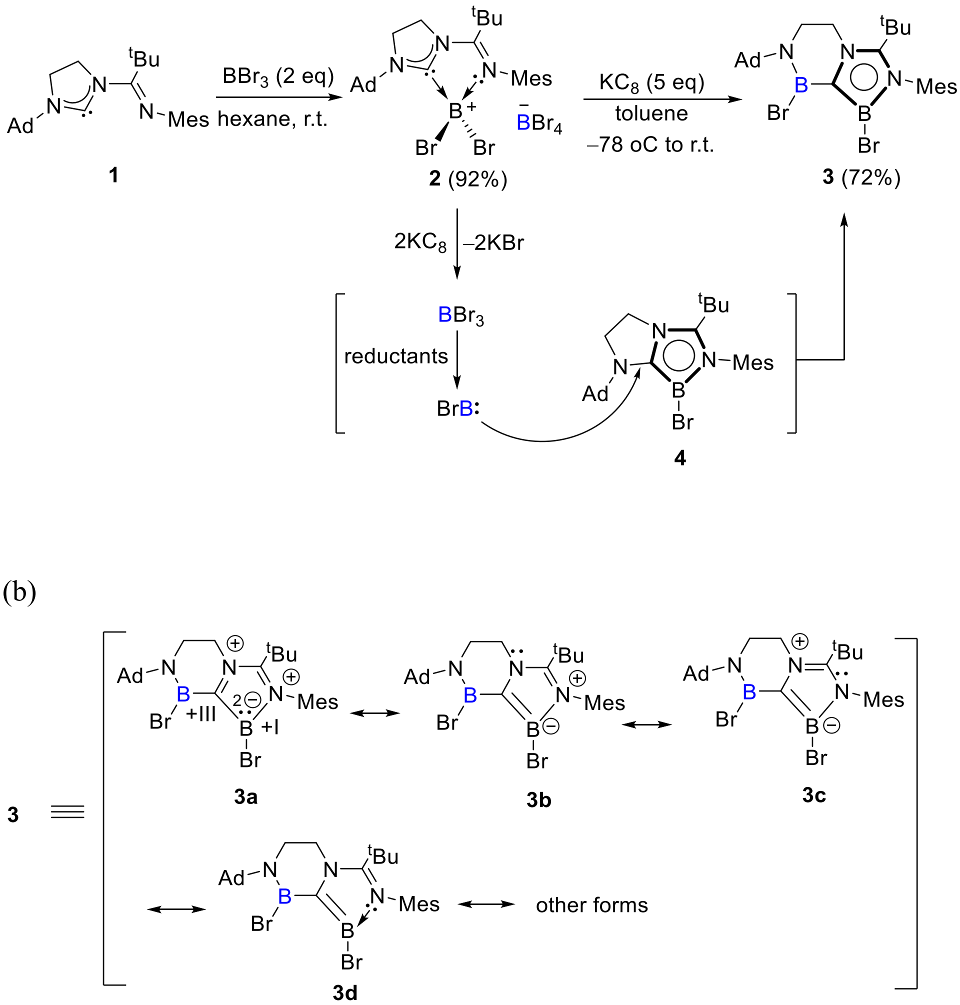

Scheme 3.1 (a) Synthesis of **3** and proposed mechanism; (b) 3a-d present the selected resonance forms for **3**.

(a) (b)

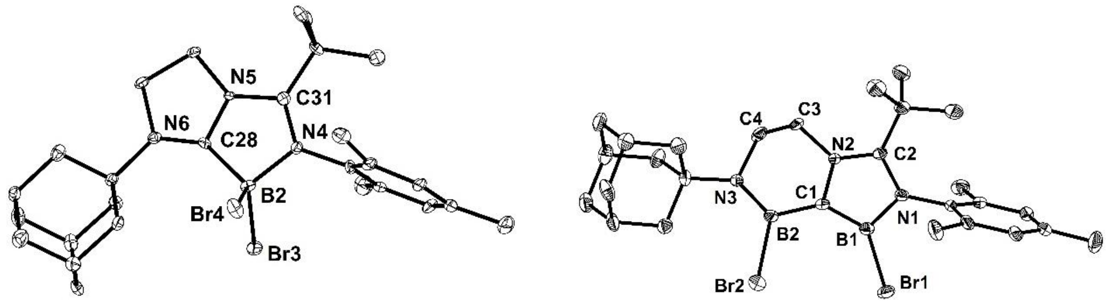

Figure 3.2 Solid-state structures of **2** (a) and **3** (b) (hydrogen atoms and solvent molecules, and counteranion (BBr_4^-) for **2**, are omitted for clarity). Thermal ellipsoids are set at the 50% probability.

To further investigate the electronic structures of **3**, we performed a molecular orbital analysis and natural bond orbital (NBO) analysis. The optimized geometry is in good agreement with the metric data observed by X-ray analysis. DFT calculation reveals that the HOMO of **3** is mainly the B1–C1 and C2–N2 π-bonding orbitals with some contribution from the p orbitals of the B2, N1, N3, Br1, Br2 atoms (Figure 3.3a). Wiberg bond index (WBI) values larger than 1 for B1–C1 (1.21), C1–N2 (1.04), N2–C2 (1.32) and C2–N1 (1.20) supports the delocalization of π-electrons over the BC_2N_2 five-membered ring. Meanwhile, the LUMO consists of the π* orbitals of the C_2N_2B ring as well as the boron in the six-membered ring (Figure 3.3b). Indeed, the negative nucleus independent chemical-shift values NICS(0) = –8.77 and NICS(1) = –6.36 for the BC_2N_2 ring confirms the aromatic property of **3**. Note that the formal oxidation state of the boron atoms in **3** can be deemed +I for B1 and +III for B2, respectively, indicating the unique mixed valence nature of **3**.

(a) (b)

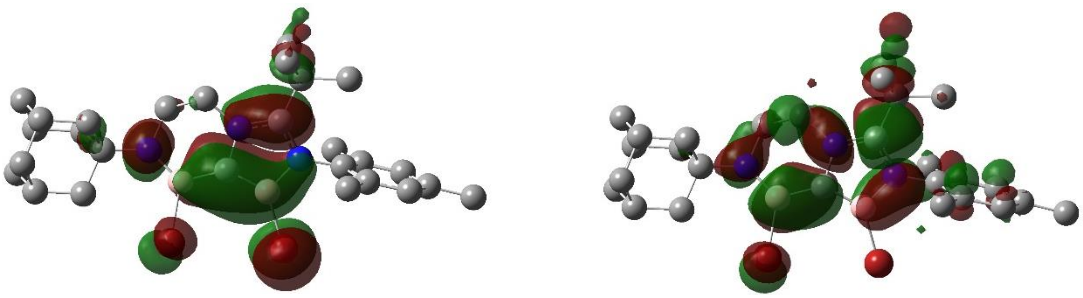

HOMO (−5.0181 eV) LUMO (−0.5687 eV)

Figure 3.3 Plots of the HOMO (a) and LUMO (b) of **3** calculated at the B3LYP/6-311G(d,p) level of theory (hydrogen atoms are omitted for clarity).

Detailed investigations on the formation of **3** were also performed. We envisaged that **3** was formed via 1,4,2-diazaborole **4** (Scheme 3.1a) Thus, an initial reduction of **2** may generate **4** in situ concomitant with BBr_3, which can be reduced by either KC_8 or **4** to yield bromoborylene (**BrB:**).[23] Subsequent insertion of **BrB:** into the C–N(Ad) bond of **4** furnishes **3** via the ring expansion.[28] To bear out the hypothesis, we decided to isolate **4** by modification of the counterion of **2** (Scheme 3.2). Reacting **2** with three equivalents of silver triflate afforded the boronium **5** with $BBr(OTf)_3$ in 63% yield, which was decisively confirmed by X-ray diffraction analysis (Figure 3.4). In the ^{11}B NMR spectrum of **5**, a sharp singlet peak assigned to the boron atom in the conteranion appeared at −2.87 ppm, which is significantly shifted down field with respect to that (−24.14 ppm) of **2**. Meanwhile, a broad peak for the cation part appears around −7.28 ppm is same to that of **2**. The solid-state structure of **5** reveals that the geometry of the cation part is almost identical to that of **2**, however the boron atom in the counter anion is coordinated by one bromine atom and three oxygen atoms of triflate anion.

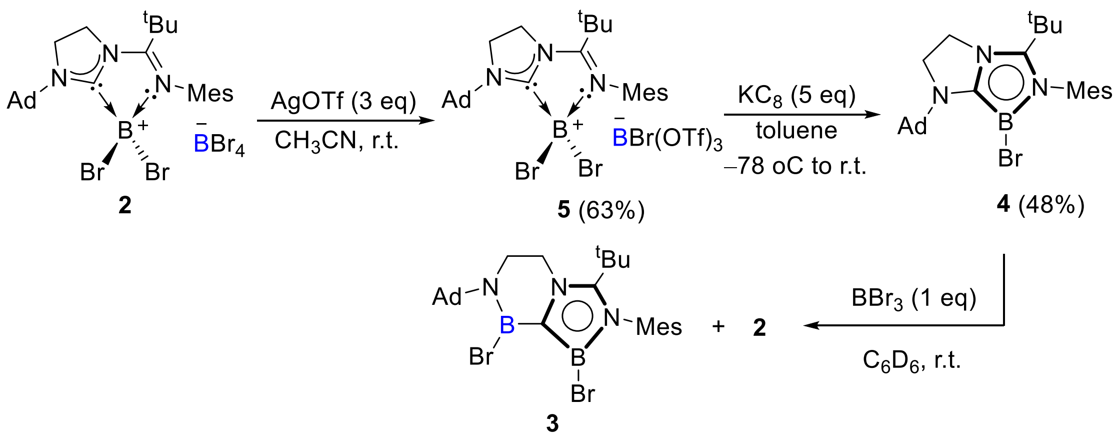

Scheme 3.2 Synthesis of **4** and its reactivity toward BBr_3. Ad = 1-adamantyl, ^{t}Bu = tert-butyl.

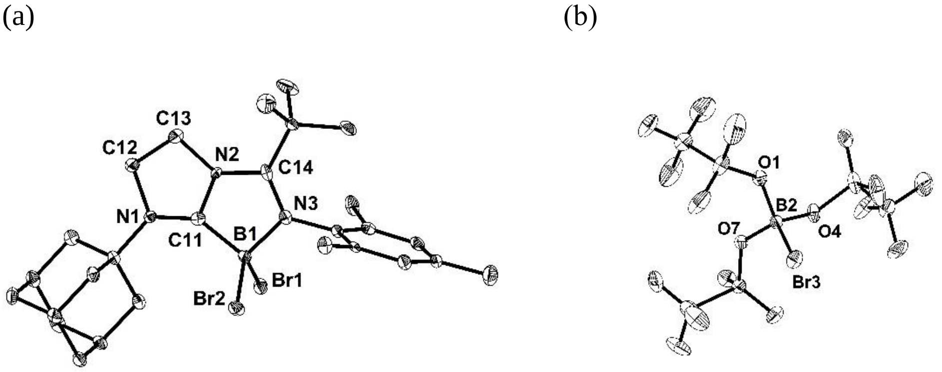

Figure 3.4 Solid-state structure of **5**: the cation part (a), the anion part (b) (solvent molecules, hydrogen atoms are omitted for clarity). Thermal ellipsoids are set at the 50% probability.

Next, we performed reduction of **5** with five equivalents of KC_8. After work-up, 1,4,2-diazaborole **4** was obtained as a colourless solid in 48% yield. The ^{11}B NMR spectrum of **4** displays a singlet at 9.60 ppm. Single crystals of **4** were obtained by slow evaporation of a toluene solution and the solid-state structure was confirmed by X-ray diffraction analysis (Figure 3.5a). The structural features and the electronic property of **4** are identical to those of the previously reported 1,4,2-diazaborole in chapter 2. The HOMO of **4** is dominated by π orbital of B−C bond which exhibits antibonding conjugation with p orbital of the bromine atom and the π orbital of N–C–N bond (Figure 3.5b). In addition, the more negative NICS values (NICS(0) = −11.54 and NICS(1) = −7.12) in comparison with those of **3** indicates a more efficient delocalization of the 6π-electrons over the BC_2N_2 ring.

(a)

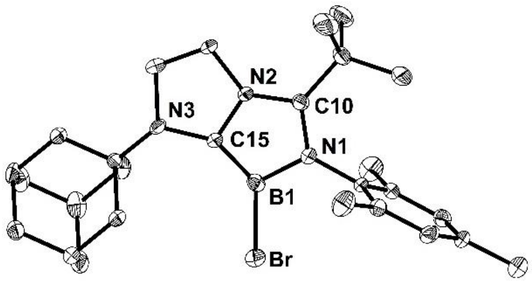

(b)

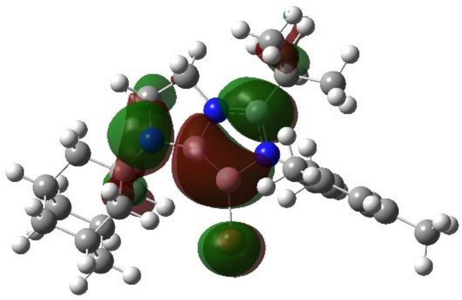

HOMO (−3.9897 eV)

Figure 3.5 (a) Solid-state structure of **4** (solvent molecules, hydrogen atoms are omitted for clarity). Thermal ellipsoids are set at the 50% probability. (b) The plot of the HOMO of **4** calculated at the B3LYP/6-311G(d,p) level of theory (hydrogen atoms are omitted for clarity).

To examine the proposed mechanism of the formation of **3**, we investigate the reaction of **4** towards BBr_3 followed by addition of KC_8 (Scheme 3.2). When **4** was treated with one equivalent of BBr_3, the mixture of **2** and **3** was formed, probably via the disproportionation reaction (Figure 3.6, 3.7). The addition of excess KC_8 to the mixture yielded **3** as the sole product. These results indicate that BBr_3 can be reduced by **4** in addition to KC_8, as well as, **4** is the key compound for the formation of **3** from **2**. Note that while several reports on ring expansion of N-heterocyclic carbene ring by the insertion of boron into the $C_{carbene}$-N bond have been reported, the mechanism is most likely confined to the activation of either B-H bond or B-B bond.[22] To the best of our knowledge, the ring expansion via the regioselctive insertion of borylene into the C-N bond of the C_3N_2 five-membered ring has never been described until now.[28] However, the proposed bromoborylene (**BrB:**) was not directly observed, and hence, a radical process cannot be ruled out. We have also tried the reactions with $AlCl_3$, $GaCl_3$, $GeCl_2$ and isonitriles, $(PPh)_5$, none of which afforded the analogous CN-bond insertion products.

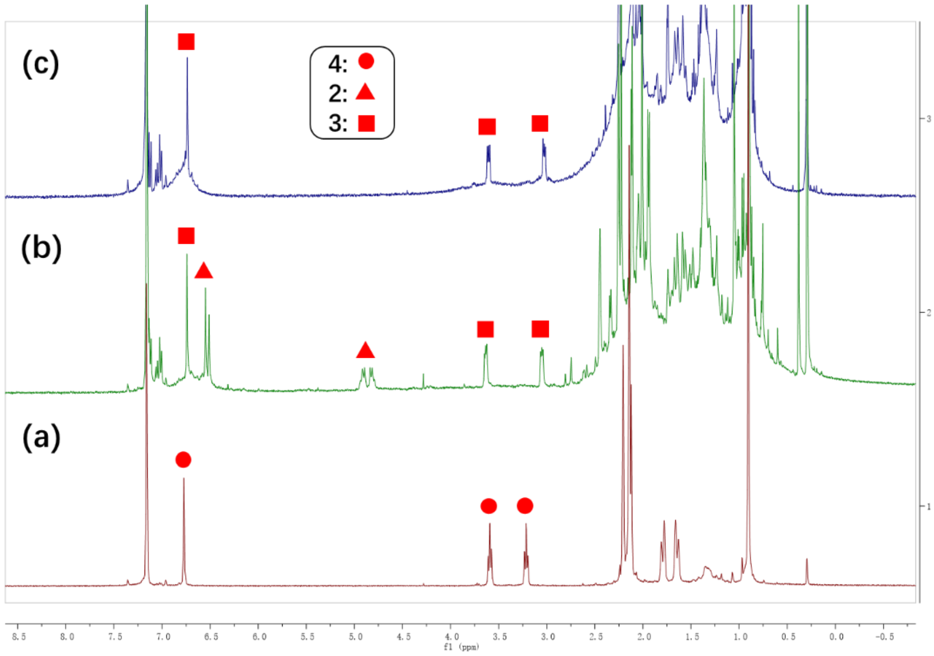

Figure 3.6 Stacked ^{1}H NMR spectra from the reactions of **4** with BBr_3 followed by reduction with KC_8. (a) The ^{1}H NMR spectrum for **4**. (b) The crude ^{1}H NMR spectrum after addition of one equivalent of BBr_3 to **4**. (c) The crude ^{1}H NMR spectrum after reduction of the mixture with excess KC_8.

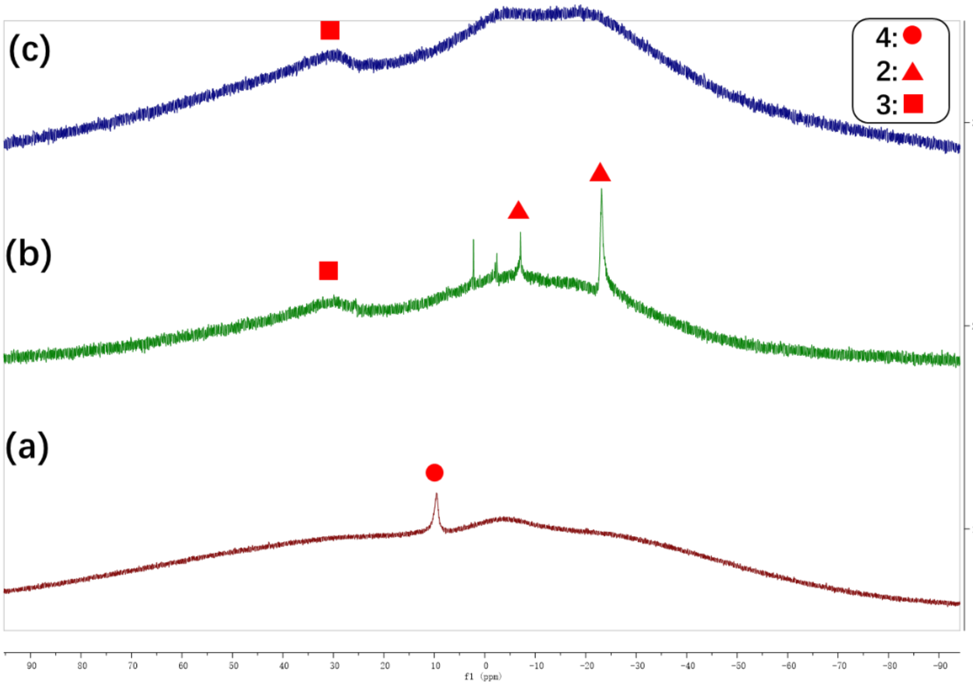

Figure 3.7 Stacked [11]B NMR spectra from the reactions of **4** with BBr_3 followed by reduction with KC_8. (a) The [11]BNMR spectrum for **4**. (b) Crude [11]B NMR spectrum after addition of one equivalent of BBr_3 to **4**. (c) Crude [11]B NMR spectrum after reduction of the mixture with excess KC_8.

Nucleophilic substitution reactions of boron halide compounds have been widely investigated, which are demonstrated an elegant strategy to modify the substitutes on the boron center.[29] We briefly examined the reactivity of **3** towards several nucleophiles (Scheme 3.3). Treatment of **3** with one equivalent of methyllithium (sp^3-C), phenyllithium (sp^2-C) and lithium phenylacetylide (sp-C) yielded compounds **6**–**8**, respectively. Compounds **6**–**8** were confirmed by multiple NMR spectroscopy and X-ray diffraction analysis. X-ray diffraction analysis (Figure 3.8) discloses that the substitution reactions selectively occurred at the B2 atom of **3**. Even with excess lithium species were applied, no functionalization of the B1 atom was observed, possibly due to the electron-richness of the boron atom.

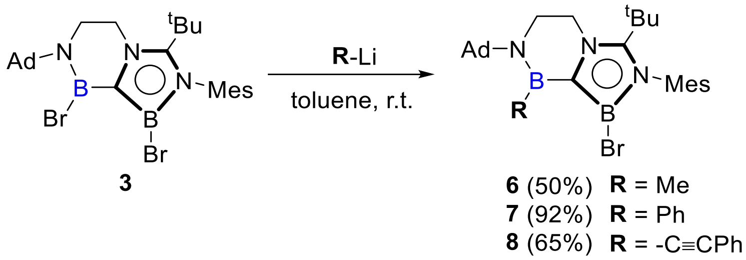

Scheme 3.3 Nucleophilic substitution of **3**.

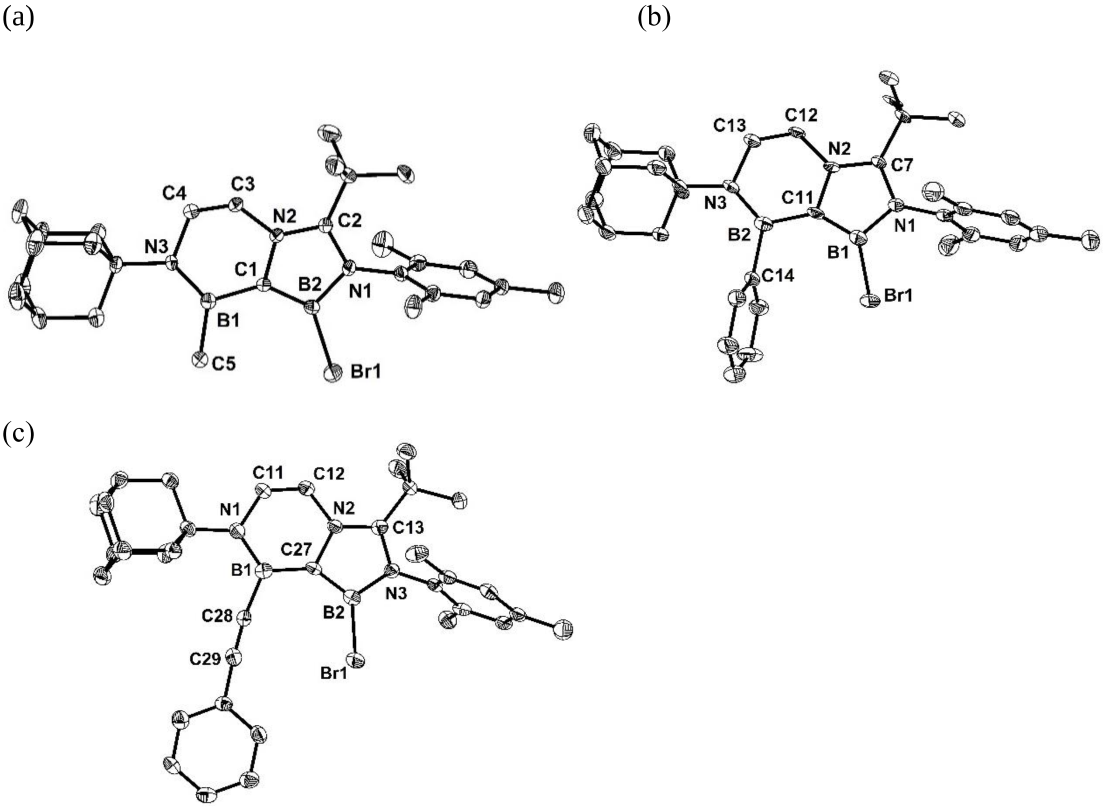

Figure 3.8 Solid-state structure of **6** (a), **7** (b) and **8** (c) (solvent molecules, hydrogen atoms are omitted for clarity). Thermal ellipsoids are set at the 50% probability.

3.3 Summary

In conclusion, we have demonstrated the skeletal transformation of the B,N-heterocyclic skeleton of 1,4,2-diazaborole derivatives advantageously having the annulated C_3N_2 five-membered ring. Ring expansion via the regioselective insertion of a BrB unit into **4** affords a

B,N-dihydroindole derivative **3** bearing two B-Br bonds. In addition, the reactions of **3** with nucleophiles undergo regiospecific substitution to afford the functionalized B,N-dihydroindole derivatives **6-8**.

3.4 Experimental Sections

3.4.1 Synthesis of compounds 2–8 and their spectral data

General considerations: All reactions were performed under an atmosphere of argon or nitrogen by using standard Schlenk or dry box techniques; solvents were dried over Na metal, K metal, or CaH_2. Reagents were of analytical grade, obtained from commercial suppliers and used without further purification. ^{1}H, ^{13}C, ^{11}B and ^{19}F NMR spectra were obtained with a Bruker AVIII 400MHz BBFO1 spectrometer at 298 K unless otherwise stated. NMR multiplicities are abbreviated as follows: s = singlet, d = doublet, t = triplet, m = multiplet, br = broad signal. Coupling constants *J* are given in Hz. Electrospray ionization (ESI) mass spectra were obtained at the Mass Spectrometry Laboratory at the Division of Chemistry and Biological Chemistry, Nanyang Technological University. Melting points were measured with an OpticMelt Stanford Research System. Phenyllithium and lithium phenylacetylide were prepared following the literature procedures.[30]

Compound 2: Boron tribromide (5.00 mL, 52.69 mmol) was added dropwise to a hexane (400 mL) solution of imino-*N*-heterocyclic carbene (10.70 g, 26.37 mmmol) at room temperature. The reaction mixture was stirred overnight. The precipitate was separated by filtration and then washed three times with hexane (3×100 mL) and dried in vacuum to afford **2** as a white solid (20.25 g, 85%). Single crystals suitable for X-ray diffraction studies were grown from a saturated toluene solution at room temperature. M.p.: 110 ºC (dec.); ^{1}H NMR (CD_3Cl, 400 MHz, 298 K): δ 6.94 (s, 2H, Mes), 5.03–4.95 (m, 4H, NCH_2), 2.45 (m, 6H, Ad–CH_2), 2.31 (m, 12H, Ad–CH&Ar-CH_3), 1.74–1.70 (m, 6H, Ad–CH_2), 1.36 (s, 9H, $(CH_3)_3$); $^{13}C\{^{1}H\}$ NMR ($CDCl_3$, 100 MHz, 298 K): 173.9 (C=N), 139.5 (C_{Ar}), 135.2 (C_{Ar}), 132.6 (C_{Ar}), 130.0 (C_{Ar}), 66.4 (Ad-*q*), 55.2 (NCH$_2$), 46.9 (NCH$_2$), 41.2 (Ad-CH$_2$), 38.6 (C(CH$_3$)$_3$, 35.3 (Ad-CH$_2$), 29.7 (Ad-CH), 28.1 (C(CH$_3$)$_3$), 21.9 (*o*-CH$_3$), 21.1 (*p*-CH$_3$); ^{11}B NMR (128.3 MHz, $CDCl_3$): δ –7.28 (BBr_2), –24.14 (s, BBr_4); HRMS (ESI): *m/z* calcd for $C_{27}H_{39}BBr_2N_3$: 574.1604. [(*M-BBr$_4$*)]$^+$; found: 574.1607.

Compound 3: Toluene (35 mL) was added to the mixture of **2** (3.50 g, 3.86 mmol) and potassium graphite (2.60 g, 19.23 mmol) at −78 ºC, and the resulting solution was stirred for four hours at room temperature. The solvent was removed under vacuum after the graphite and salts were filtered off. The residue was washed three times with Et_2O (3×10 mL) and dried in vacuum to afford a white solid (1.62 g, 72%). Colorless single crystals suitable for X-ray diffraction studies were grown by evaporation of a toluene solution at room temperature. M.p.: 216 ºC (dec.); ^{1}H NMR (C_6D_6, 400 MHz, 298 K): δ 6.74 (s, 2H, *m*-CH), 3.63–3.61 (m, 2H, NCH_2), 3.05–3.03 (m, 2H, NCH_2), 2.26–2.25 (m, 6H, Ad–CH_2), 2.12 (s, 3H, *p*-CH_3), 2.04 (m, 3H, Ad–CH), 2.01 (s, 6H, *o*-CH_3), 1.65 (d, J = 11.6 Hz, 3H, Ad–CH_2), 1.57 (d, J = 12.2 Hz, 3H, Ad–CH_2), 0.98 (s, 9H, (CH_3)$_3$); ^{13}C{^{1}H} NMR (C_6D_6, 100 MHz, 298 K): 141.9 (C-^{t}Bu), 138.8 (C_{Ar}), 136.9 (C_{Ar}), 135.2 (C_{Ar}), 129.1 (C_{Ar}), 57.7 (Ad-*q*), 51.2 (NCH$_2$), 43.6 (NCH$_2$), 43.4 (Ad-CH$_2$), 36.7 (Ad-CH$_2$), 35.2 (C(CH$_3$)$_3$), 30.8 (Ad-CH), 30.1 (C(CH$_3$)$_3$), 21.1 (Ar-CH$_3$), 18.7 (Ar-CH$_3$); ^{11}B NMR (128.3 MHz, C_6D_6): δ 28.96 (br, *B*–Br & *B*–Br); HRMS (ESI): *m/z* calcd for $C_{27}H_{40}B_2Br_2N_3$: 586.1775. [(*M*+*H*)]$^+$; found: 586.1770.

Compound 4: Toluene (15 mL) was added to the mixture of **5** (1.00 g, 0.90 mmol) and potassium graphite (0.73 g, 5.4 mmol) at –78 ºC, and the resulting solution was slowly allowed to warm up to room temperature and stirred overnight. After the graphite and salts were filtered off, the solvent was removed under vacuum. The residue was extracted with hexane twice (2×20 mL), and then the solvent was removed to afford a light brown solid (0.21 mg, 48%). Colorless single crystals suitable for X-ray diffraction studies were grown by evaporation of a toluene solution at room temperature. M.p.: 127 ºC (dec.); ^{1}H NMR (C_6D_6, 400 MHz, 298 K): δ 6.77 (s, 2H, Mes), 3.59 (t, J = 7.0 Hz, 2H, NCH_2), 3.21 (t, J = 7.0 Hz, 2H, NCH_2), 2.20 (m, 6H, Ad–C*H*&*o*-CH_3), 2.14 (s, 6H, *p*-CH_3), 2.12 (br, 6H, Ad–CH_2), 1.78 (d, J = 11.8 Hz, 3H, Ad–CH_2), 1.61 (d, J = 12.0 Hz, 3H, Ad–CH_2), 0.90 (s, 9H, (CH_3)$_3$); ^{13}C{^{1}H} NMR (C_6D_6, 100 MHz, 298 K): δ 139.6 (C_{Ar}), 136.5 (C_{Ar}), 135.4 (C_{Ar}), 128.9 (C_{Ar}), 124.6 (*C*-^{t}Bu), 54.2 (Ad–*q*), 49.3 (N*C*H$_2$), 48.5 (N*C*H$_2$), 40.5 (Ad–*C*H$_2$), 37.2 (Ad–*C*H$_2$), 35.2 (*C*(CH$_3$)$_3$), 30.3 (Ad–*C*H), 29.7 (C(*C*H$_3$)$_3$), 21.1 (Ar–*C*H$_3$), 18.5 (Ar–*C*H$_3$); ^{11}B NMR (128.3 MHz, C_6D_6): δ 9.60 (s, *B*Br); HRMS (ESI): *m/z* calcd for $C_{27}H_{40}BBrN_3$: 496.2499. [(*M*+*H*)]$^{+}$; found: 496.2503.

Compound 5: CH_3CN (50 mL) was added to a mixture of silver trifluoromethanesulfonate (4.26 g, 16.6 mmol) and **2** (5.00 g, 5.52 mmol) at 0 ºC. The suspension was stirred overnight at room temperature in the dark. After the precipitate was filtered off, all the solvent was removed under vacuum. The residue was washed with small amount of toluene (5 mL), and then dried in vacuum to afford light brown solid (3.87 g, 63%). Colourless single crystals were obtained by the evaporation of a saturated toluene solution at room temperature. M.p.: 82 ºC (dec.); ^{1}H NMR ($CDCl_3$, 400 MHz, 298 K): δ 6.95 (s, 2H, Mes), 4.78–4.74 (m, 2H, NCH_2), 4.71–4.66 (m, 2H, NCH_2), 2.39 (m, 6H, Ad–CH_2), 2.31 (m, 12H, Ad–C*H*&Ar-CH_3), 1.74 (m, 6H, Ad–CH_2), 1.31 (s, 9H, (CH_3)$_3$); ^{13}C{^{1}H} NMR (CDCl$_3$, 100 MHz, 298 K): 173.9 (*C*=N), 139.6 (C_{Ar}), 135.1 (C_{Ar}), 132.6 (C_{Ar}), 130.1 (C_{Ar}), 66.4 (Ad-*q*), 54.6 (NCH$_2$), 46.8 (NCH$_2$), 41.0 (Ad-CH$_2$), 38.6 (C(CH$_3$)$_3$, 35.2 (Ad-CH$_2$), 29.7 (Ad-CH), 27.7 (C(CH$_3$)$_3$), 21.5 (*o*-CH$_3$), 21.1 (*p*-CH$_3$); ^{11}B NMR (128.3 MHz, CDCl$_3$): δ -2.87 (s, *B*Br(OTf)$_3$), -7.28 (*B*Br$_2$); ^{19}F NMR (376 MHz, CDCl$_3$): δ −76.64 (s, BBr(OTf)$_3$); HRMS (ESI): *m/z* calcd for $C_{27}H_{39}BBr_2N_3$: 574.1604. [(*M–BBr(OTf)$_3$*)]$^+$; found: 574.1602.

Compound 6: A methyllithium solution (0.32 mL, 3.0 M in diethoxymethane, 0.96 mmol) was added dropwise to a toluene solution (15 mL) of **3** (0.56 g, 0.95 mmol) at room temperature over 15 min. The resulting solution was stirred overnight, and then all the solvents were removed under vacuum after the solid was filtered off. The residue was dissolved in a minimum amount of toluene and kept at −26 ºC to get a colorless crystalline solid (0.25 g, 50%). Single crystals suitable for X-ray diffraction studies were grown by evaporation of a benzene solution at room temperature. M.p.: 127 ºC (dec.); ^{1}H NMR (C_6D_6, 400 MHz, 298 K): δ 6.76 (s, 2H, Mes), 3.75–3.73 (m, 2H, NCH_2), 3.07–3.04 (m, 2H, NCH_2), 2.13 (s, 3H, *p*-CH_3), 2.07 (s, 6H, *o*-CH_3), 2.02 (m, 3H, Ad–C*H*), 1.98 (m, 6H, Ad–CH_2), 1.60 (m, 6H, Ad–CH_2), 1.47 (s, 3H, B–CH_3), 0.94 (s, 9H, (CH_3)$_3$); ^{13}C{^{1}H} NMR (C_6D_6, 100 MHz, 298 K): 139.9 (C-^{t}Bu), 139.3 (C_{Ar}), 136.6 (C_{Ar}), 135.3 (C_{Ar}), 129.0 (C_{Ar}), 57.2 (Ad-*q*), 51.6 (NCH$_2$), 43.6 (Ad-CH$_2$), 43.0 (NCH$_2$), 37.0 (Ad-CH$_2$), 35.1 (C(CH$_3$)$_3$), 30.6 (Ad-CH), 30.3 (C(CH$_3$)$_3$), 21.1 (Ar-CH$_3$), 18.7 (Ar-CH$_3$); ^{11}B NMR (128.3 MHz, C_6D_6): δ 39.78 (br, *B*–Me), 26.98 (br, *B*–Br); HRMS (ESI): *m/z* calcd for $C_{28}H_{43}B_2BrN_3$: 522.2826. [(*M*+*H*)]$^+$; found: 522.2842.

Compound 7: Toluene (25 mL) was added dropwise to the mixture of phenyllithium (0.086 g, 1.02 mmol) and **3** (0.50 g, 0.85 mmol) at –78 °C. The resulting suspension was stirred overnight, and then the solvent was removed under vacuum after the solid was filtered off. The residue was washed three times with Et_2O (3×5 mL) and dried in vacuum to afford compound **7** as a white solid (0.46 g, 92%). Colorless single crystals suitable for X-ray diffraction studies were grown by evaporation of a toluene solution at room temperature. M.p.: 154 °C (dec.); ^{1}H NMR (C_6D_6, 400 MHz, 298 K): δ 7.80 (d, J = 6.9 Hz, 2H, Ph), 7.37 (t, J = 7.5 Hz, 2H, Ph), 7.24 (t, J = 7.4 Hz, 1H, Ph), 6.69 (s, 2H, Mes), 3.88–3.85 (m, 2H, NCH_2), 3.20–3.17 (m, 2H, NCH_2), 2.06 (s, 3H, p-CH_3), 2.03 (s, 6H, o-CH_3), 1.91 (m, 3H, Ad–C*H*), 1.86 (m, 6H, Ad–CH_2), 1.48 (m, 6H, Ad–CH_2), 0.94 (s, 9H, $(CH_3)_3$); $^{13}C\{^{1}H\}$ NMR (C_6D_6, 100 MHz, 298 K): 141.4 (C-^{t}Bu), 139.1 (C_{Mes}), 136.6 (C_{Mes}), 135.1 (C_{Mes}), 132.5 (C_{Ph}), 129.0 (C_{Mes}), 127.1 (C_{Ph}), 126.2 (C_{Ph}), 57.8 (Ad-*q*), 51.7 (NCH_2), 44.3 (Ad-CH_2), 43.0 (NCH_2), 36.8 (Ad-CH_2), 35.2 ($C(CH_3)_3$), 30.4 (Ad-*C*H), 30.2 ($C(CH_3)_3$), 21.0 (Ar-CH_3), 18.7 (Ar-CH_3); ^{11}B NMR (128.3 MHz, C_6D_6): δ 38.16 (br, *B*–Ph), 28.74 (br, *B*–Br); HRMS (ESI): *m/z* calcd for $C_{33}H_{45}B_2BrN_3$: 584.2983. $[(M+H)]^+$; found: 584.3003.

Compound 8: A lithium phenylacetylide solution (1.5 mL, 0.30 M in THF, 0.45 mmol) was added dropwise to a toluene solution (10 mL) of **3** (0.22 g, 0.37 mmol) at room temperature. The resulting solution was stirred overnight, and then all the solvents were removed under vacuum after the solid was filtered off. The residue was washed three times with Et_2O (3×5 mL) and dried in vacuum to afford compound **8** as a white solid (0.15 g, 65%). Colourless single crystals were obtained by the evaporation of a saturated Et_2O solution at room temperature.

M.p.: 151 °C (dec.); ^{1}H NMR (C_6D_6, 400 MHz, 298 K): δ 7.85–7.83 (m, 2H, Ph), 6.99–6.91 (m, 3H, Ph), 6.74 (s, 2H, Mes), 3.73–3.70 (m, 2H, NCH_2), 3.07–3.05 (m, 2H, NCH_2), 2.33 (m, 6H, Ad–CH_2), 2.14 (m, 3H, Ad–CH), 2.10 (s, 3H, *p*-CH_3), 2.06 (s, 6H, *o*-CH_3), 1.75 (d, J = 11.5 Hz, 3H, Ad–CH_2), 1.66 (d, J = 12.2 Hz, 3H, Ad–CH_2), 0.93 (s, 9H, (CH_3)$_3$); ^{13}C{^{1}H} NMR (C_6D_6, 100 MHz, 298 K): 141.0 (*C*-^{t}Bu), 139.1 (C_{Mes}), 136.8 (C_{Mes}), 135.2 (C_{Mes}), 132.1 (C_{Ph}), 129.1 (C_{Mes}), 128.4 (C_{Ph}), 127.7 (C_{Ph}), 126.4 (C_{Ph}), 108.2 (Ph-*C*≡C), 56.5 (Ad–*q*), 51.2 (N*C*H$_2$), 43.7 (Ad–*C*H$_2$), 42.6 (N*C*H$_2$), 37.1 (Ad–*C*H$_2$), 35.2 (*C*(CH$_3$)$_3$), 30.8 (Ad–*C*H), 30.2 (C(*C*H$_3$)$_3$), 21.0 (Ar–*C*H$_3$), 18.7 (Ar–*C*H$_3$); ^{11}B NMR (128.3 MHz, C_6D_6): δ 28.60 (br, *B*–C≡CPh & *B*–Br); HRMS (ESI): *m/z* calcd for $C_{35}H_{45}B_2BrN_3$: 608.2983. [(*M*+*H*)]$^{+}$; found: 608.2999.

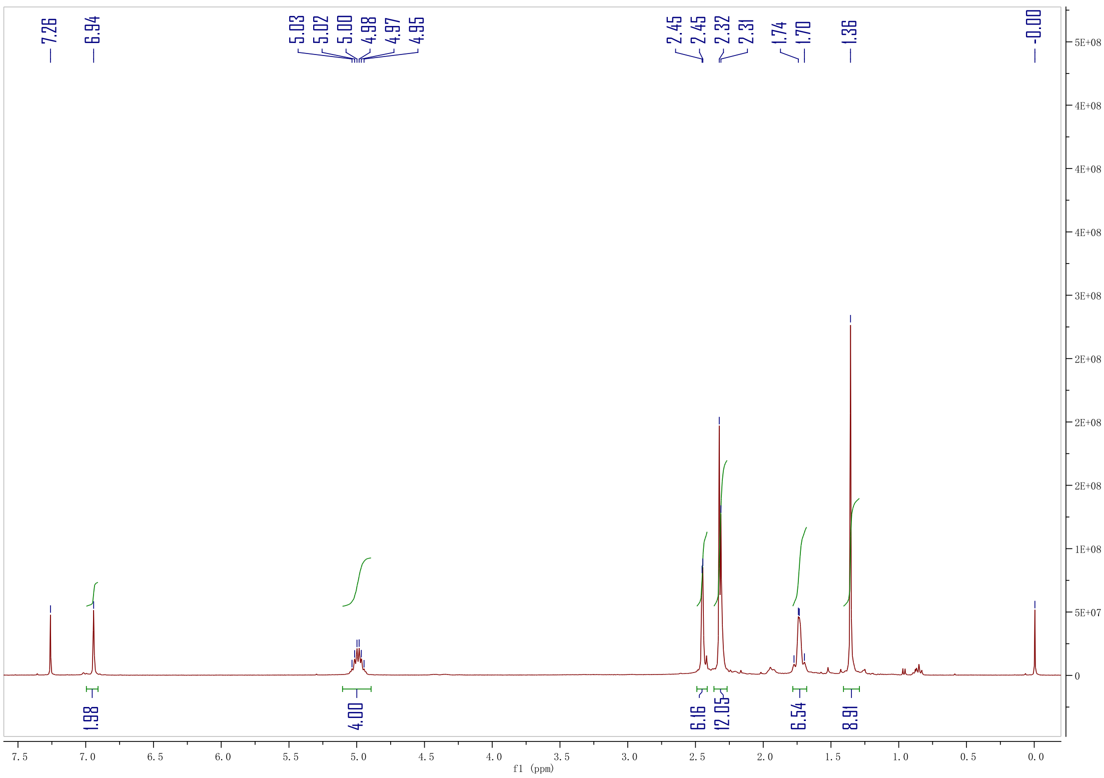

Figure 3.9 ^{1}H NMR spectrum of **2**.

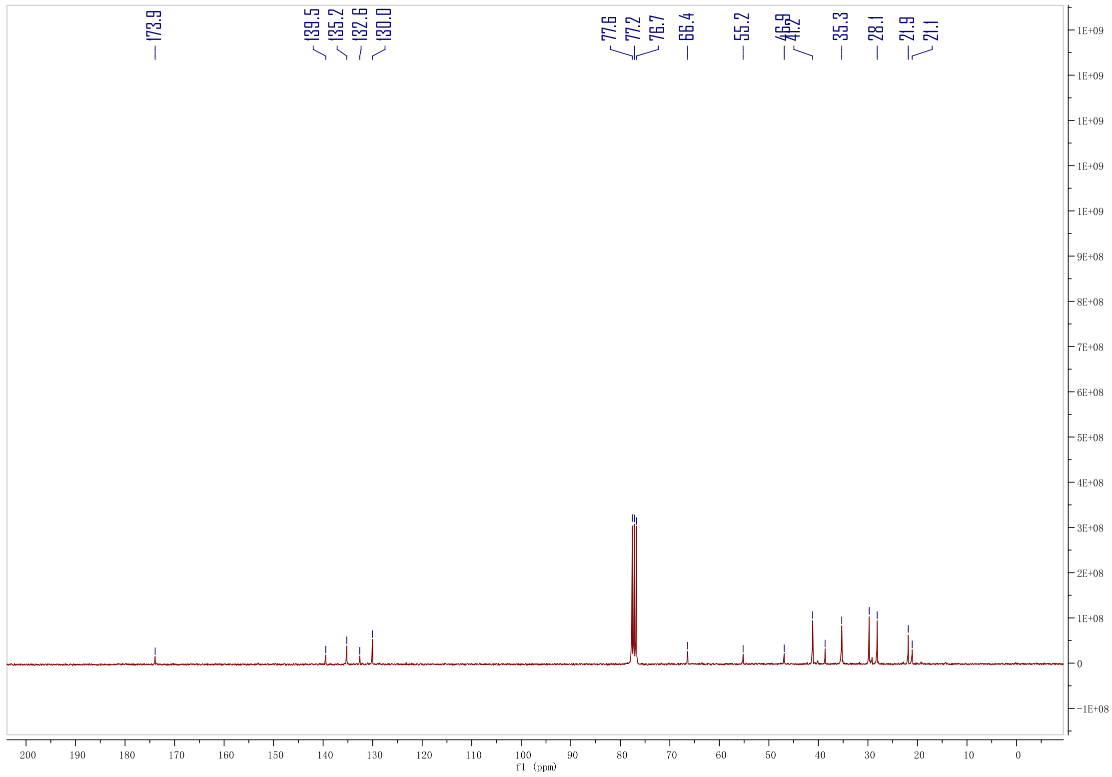

Figure 3.10 $^{13}C\{^{1}H\}$ NMR spectrum of **2**.

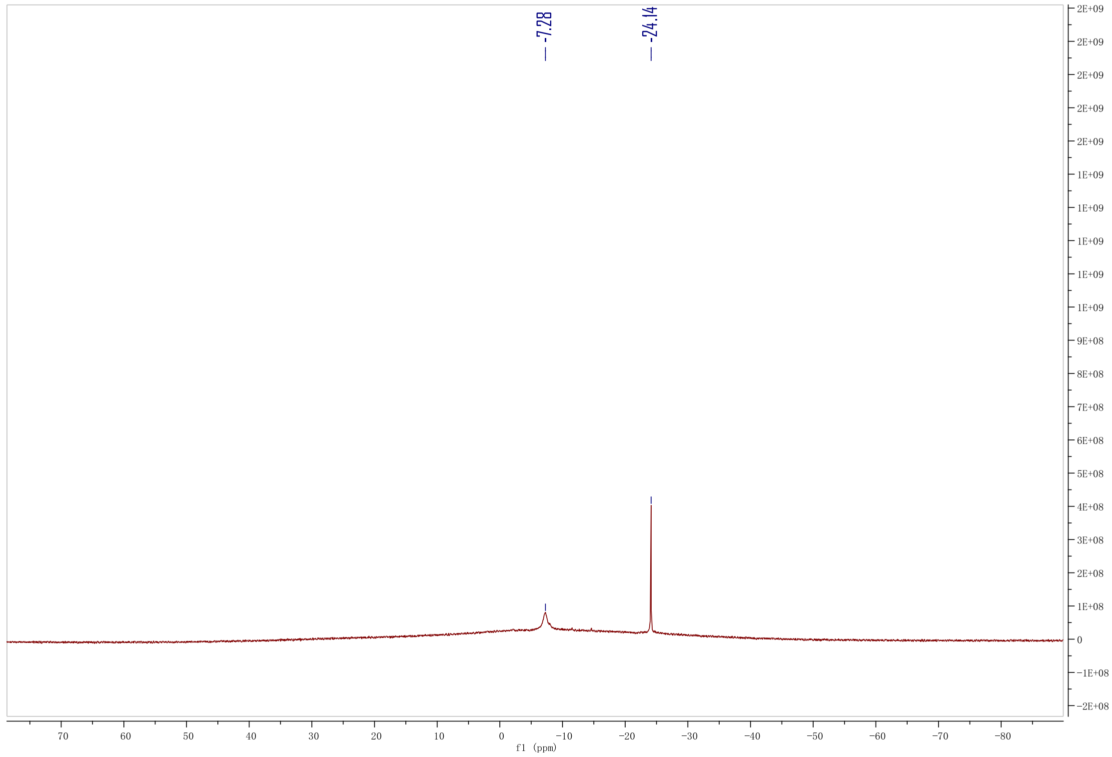

Figure 3.11 ^{11}B NMR spectrum of **2**.

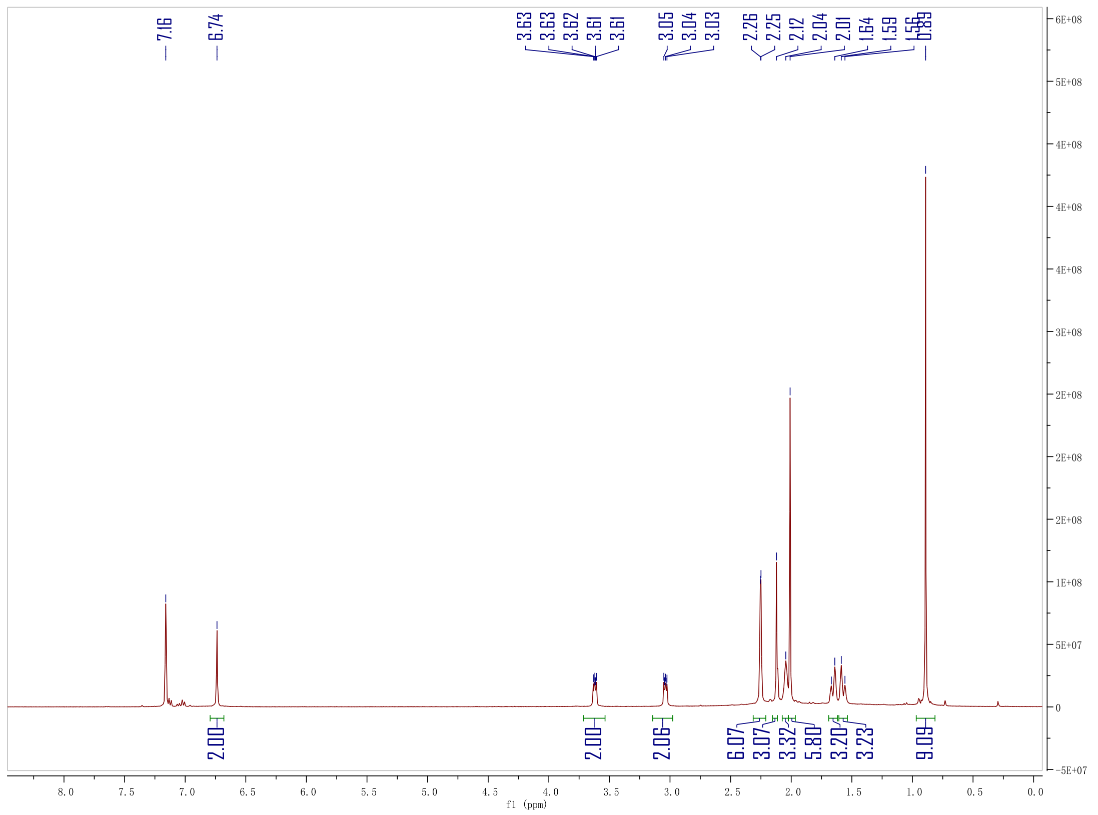

Figure 3.12 ^{1}H NMR spectrum of **3**.

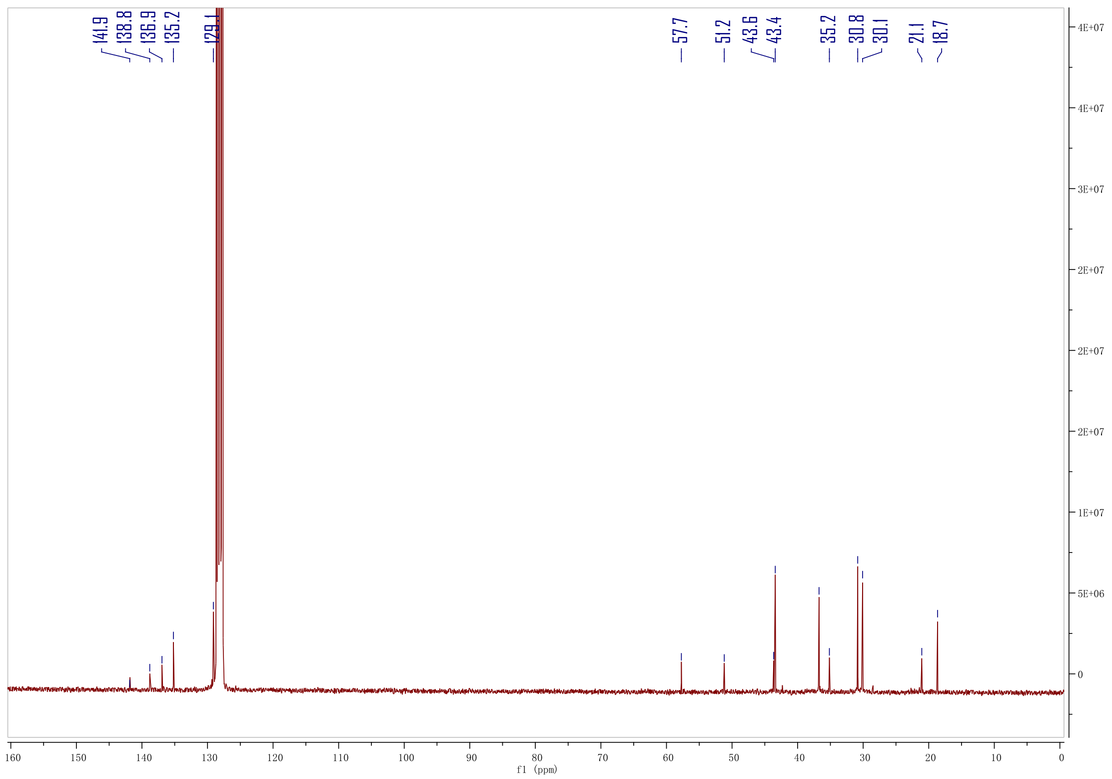

Figure 3.13 $^{13}C\{^{1}H\}$ NMR spectrum of **3**.

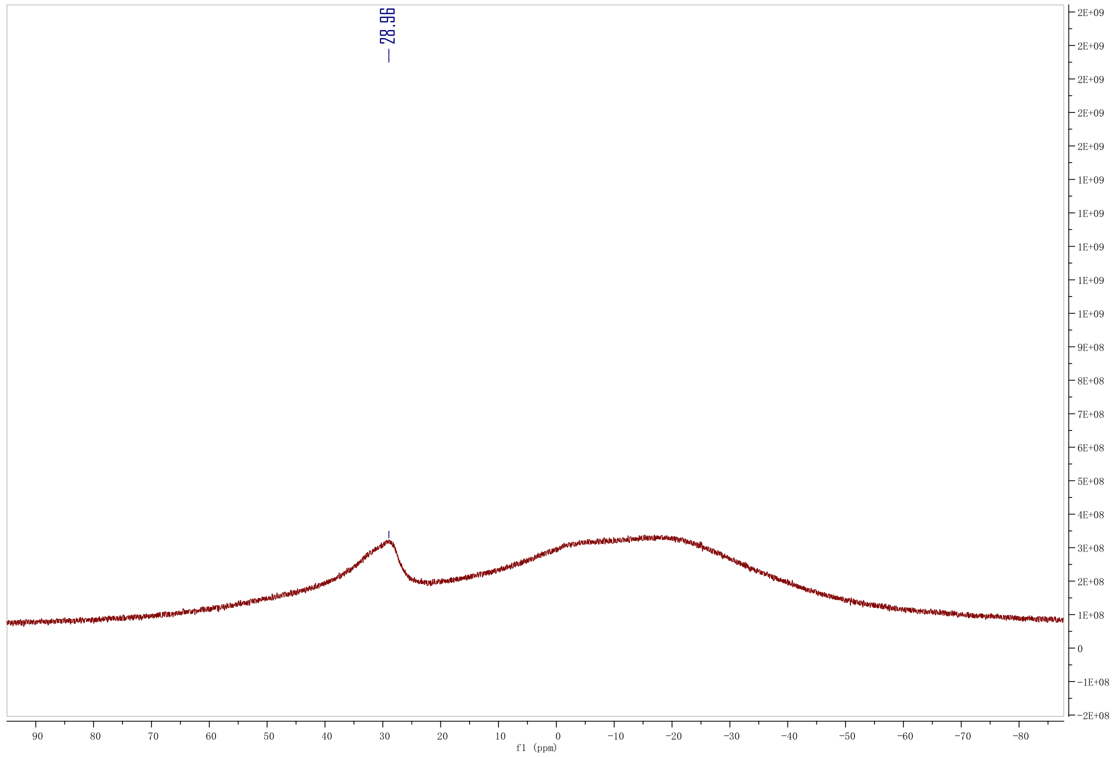

Figure 3.14 ^{11}B NMR spectrum of **3**.

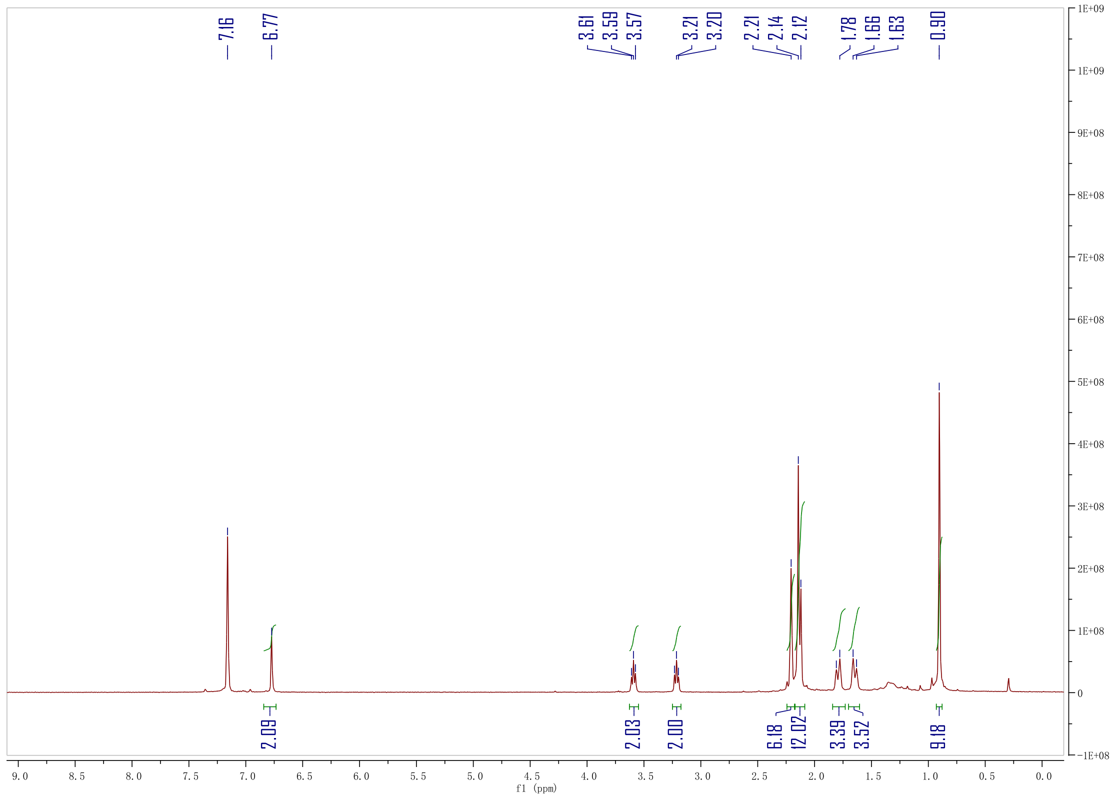

Figure 3.15 ^{1}H NMR spectrum of **4**.

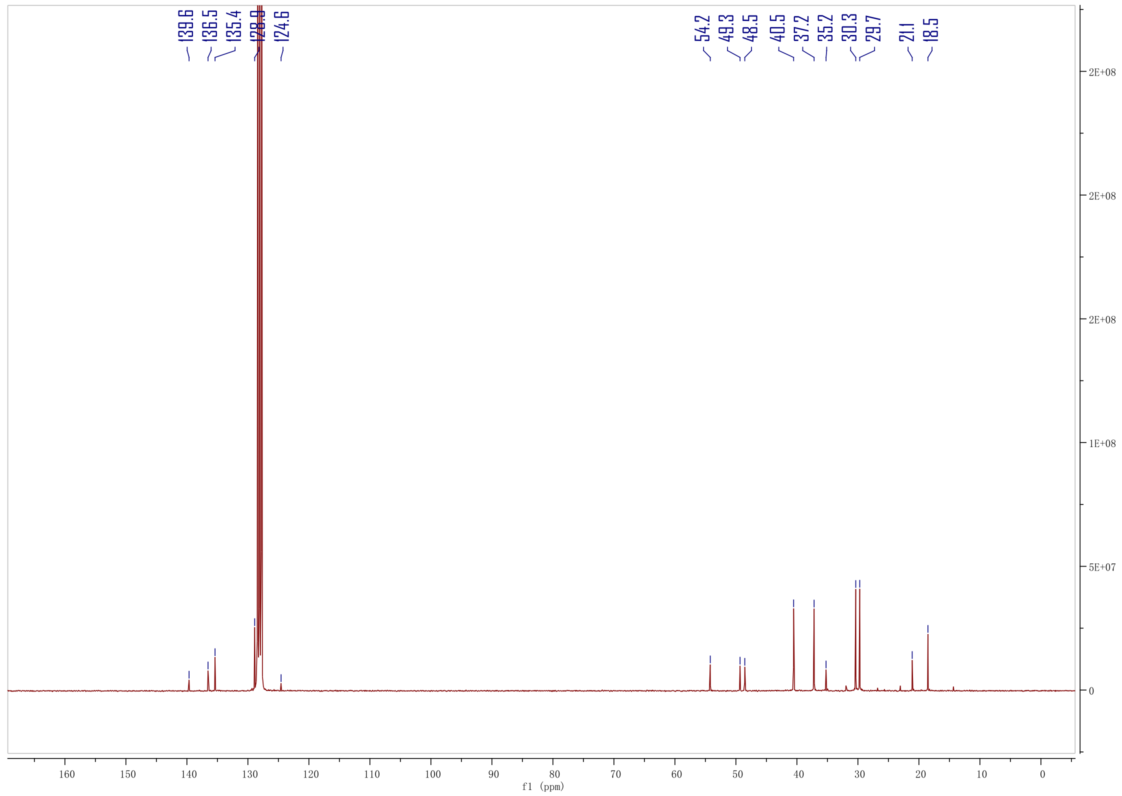

Figure 3.16 $^{13}C\{^{1}H\}$ NMR spectrum of **4**.

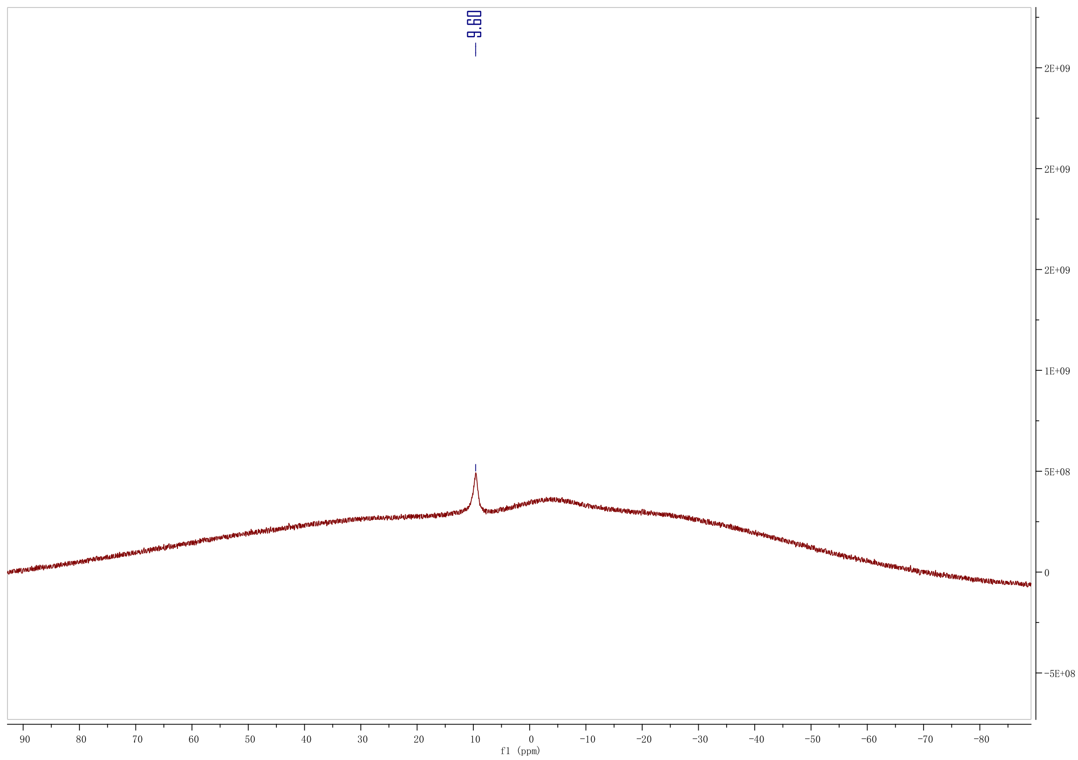

Figure 3.17 ^{11}B NMR spectrum of **4**.

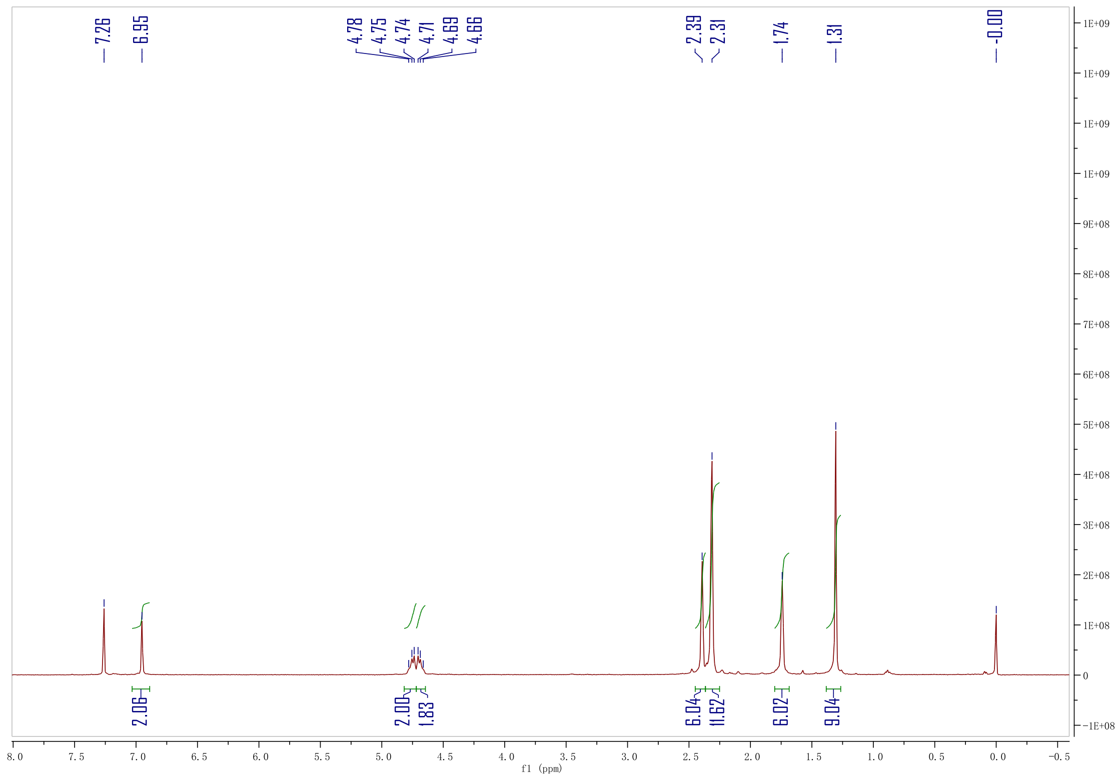

Figure 3.18 ^{1}H NMR spectrum of **5**.

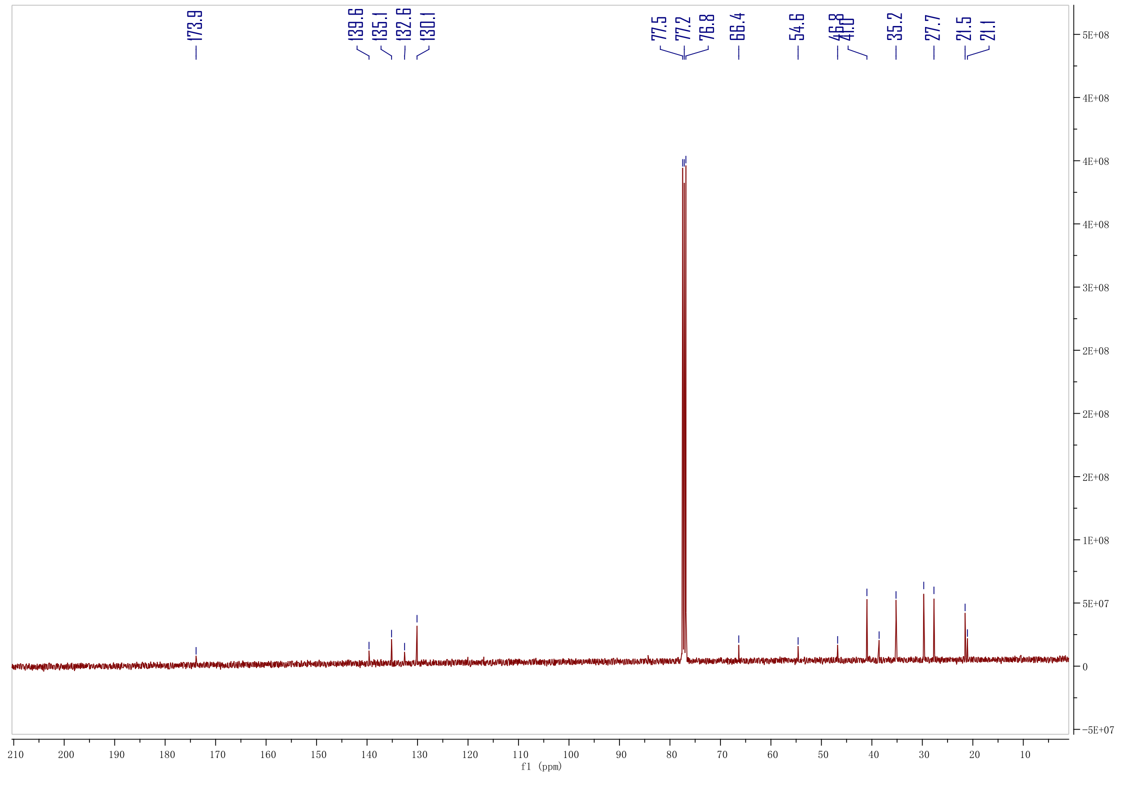

Figure 3.19 ^{13}C{^{1}H} NMR spectrum of **5**.

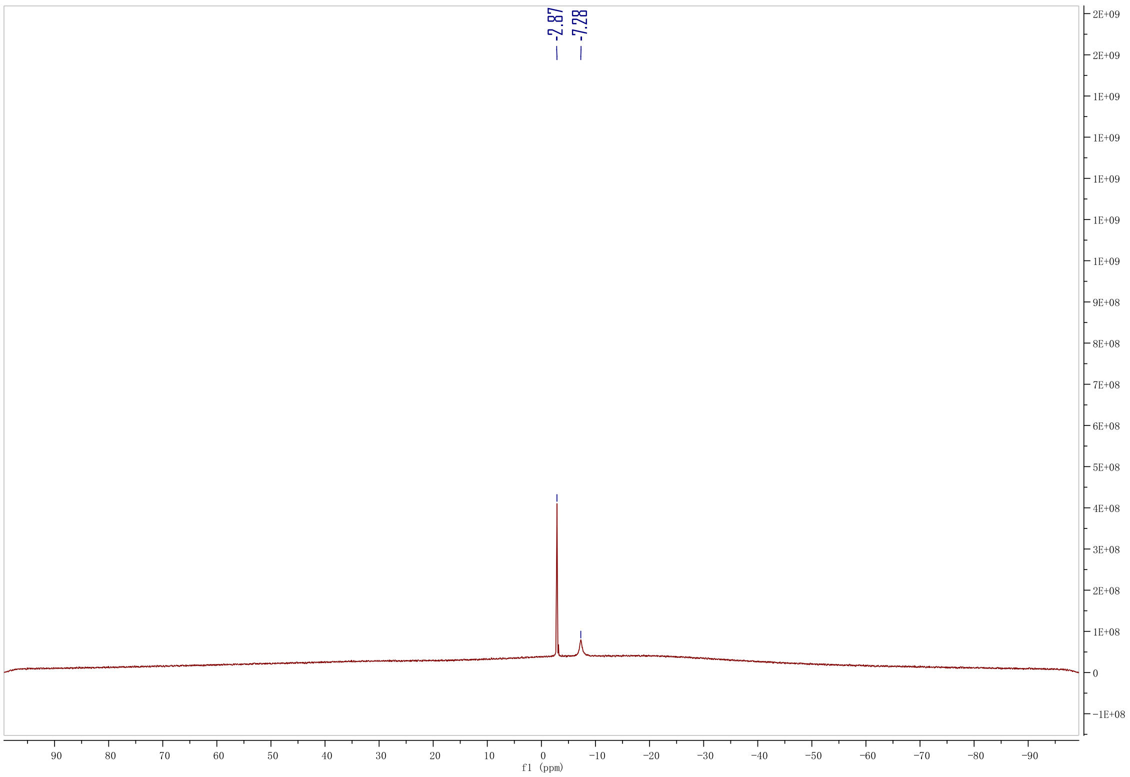

Figure 3.20 ^{11}B NMR spectrum of **5**.

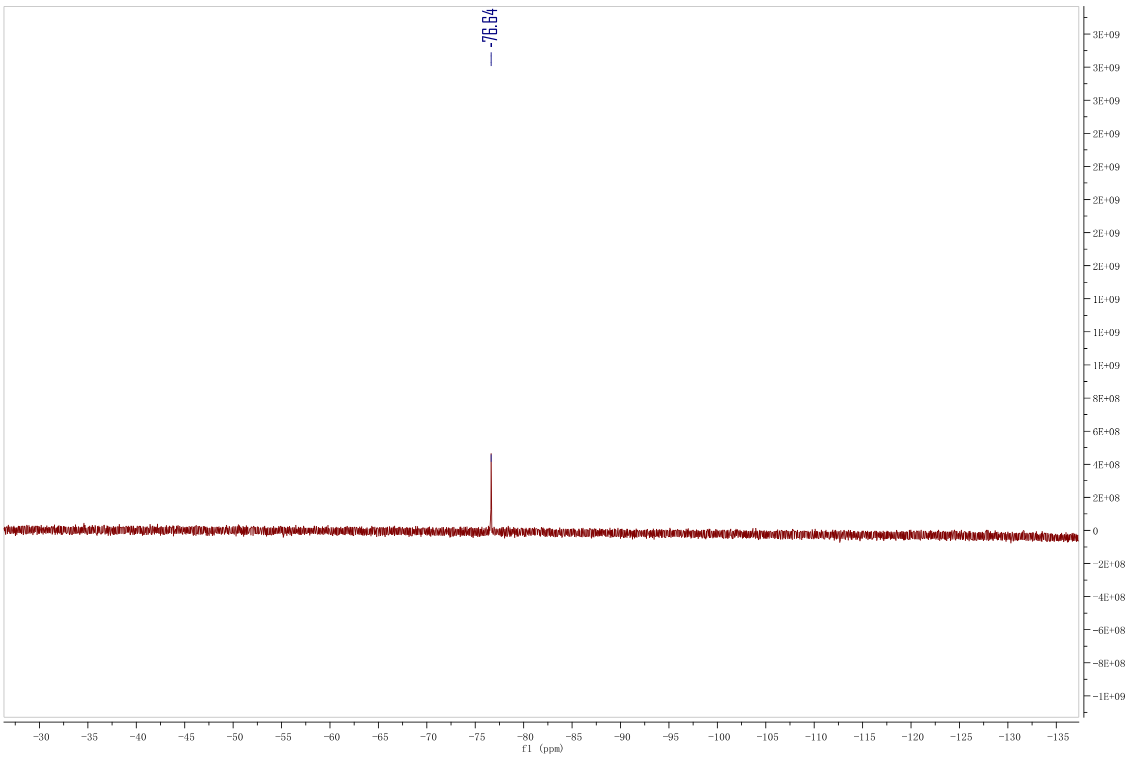

Figure 3.21 ^{19}F NMR spectrum of **5**.

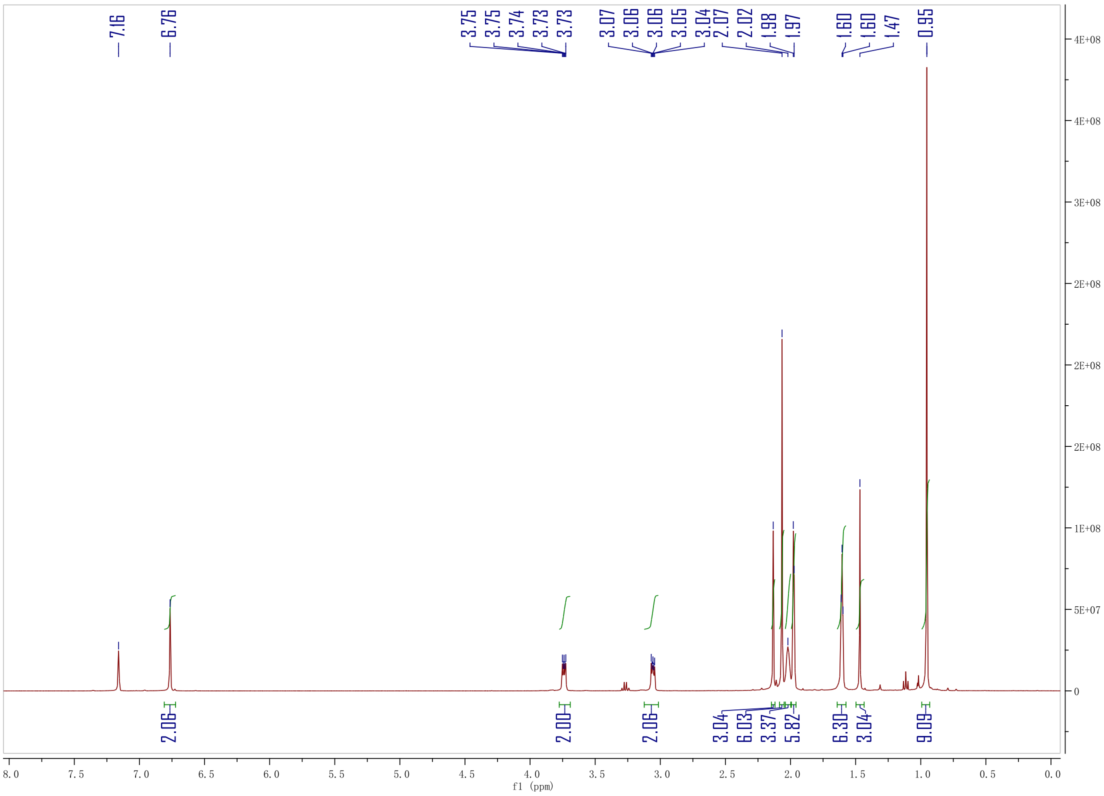

Figure 3.22 ^{1}H NMR spectrum of **6**.

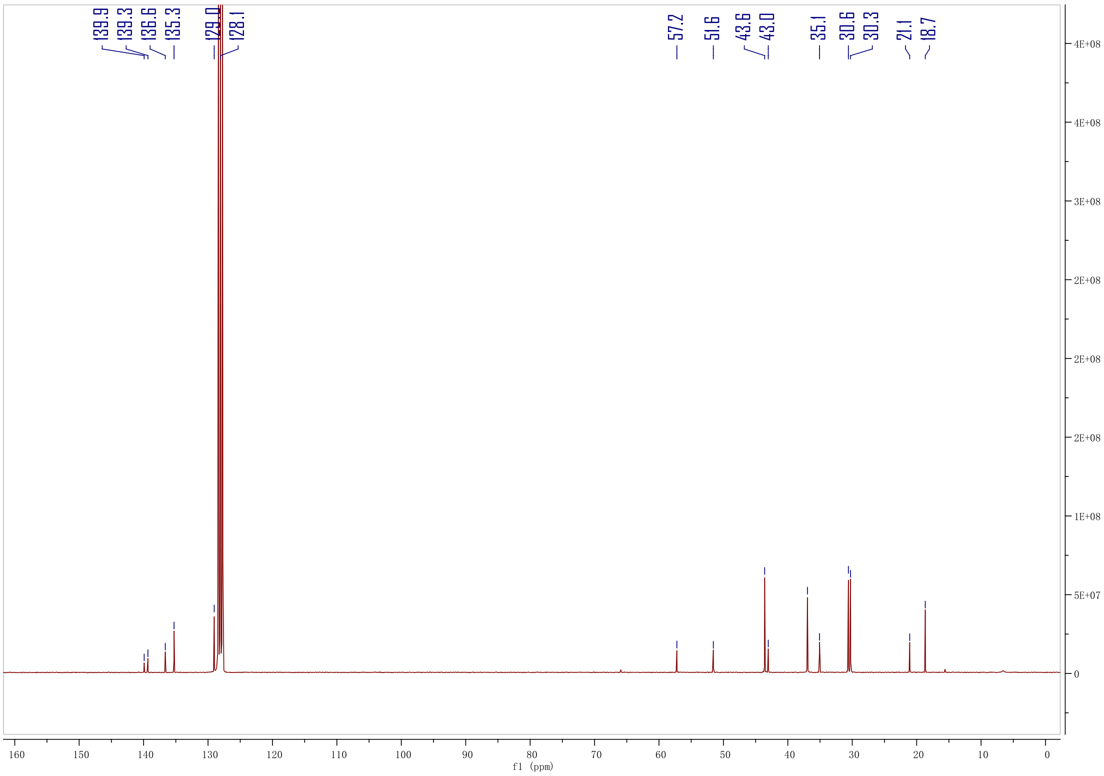

Figure 3.23 $^{13}C\{^{1}H\}$ NMR spectrum of **6**.

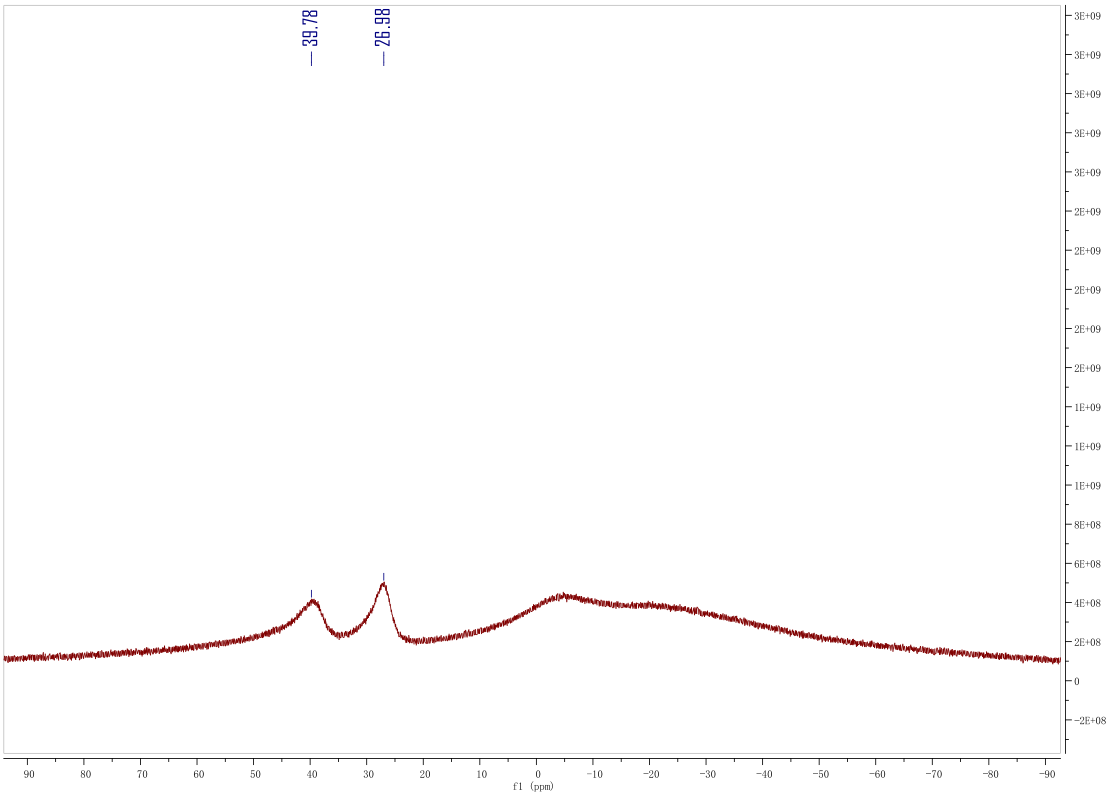

Figure 3.24 ^{11}B NMR spectrum of **6**.

Figure 3.25 ^{1}H NMR spectrum of **7**.

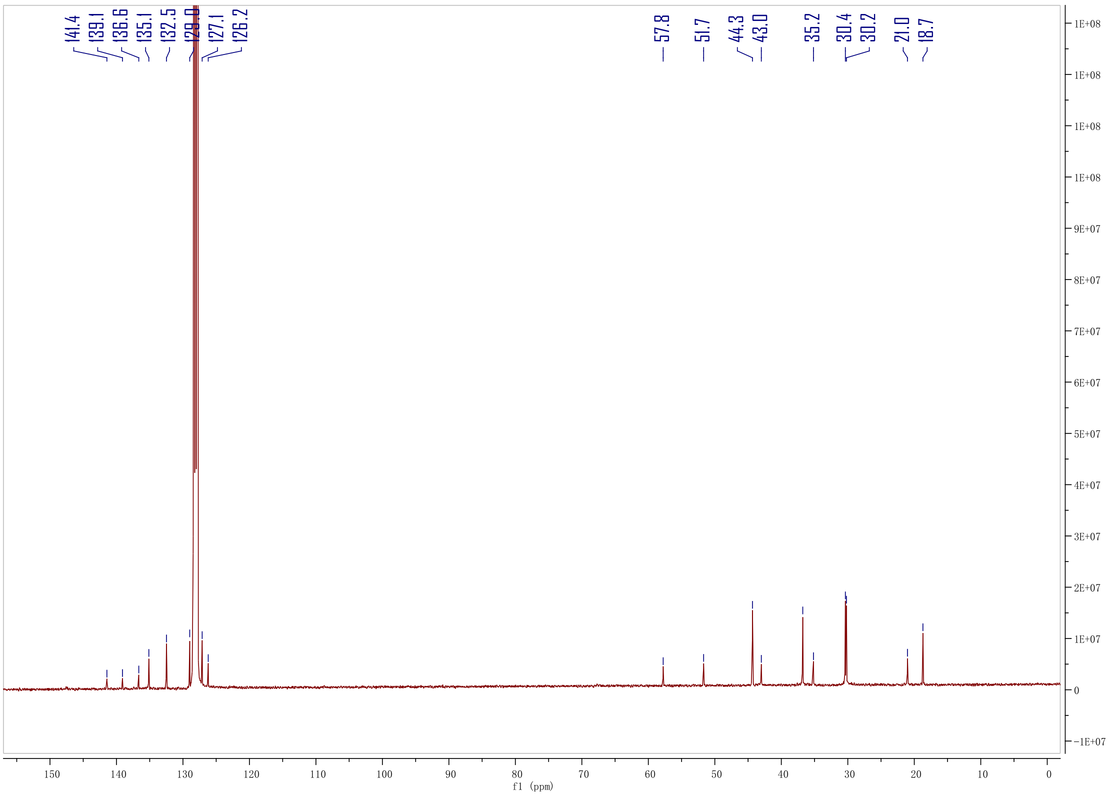

Figure 3.26 $^{13}C\{^{1}H\}$ NMR spectrum of **7**.

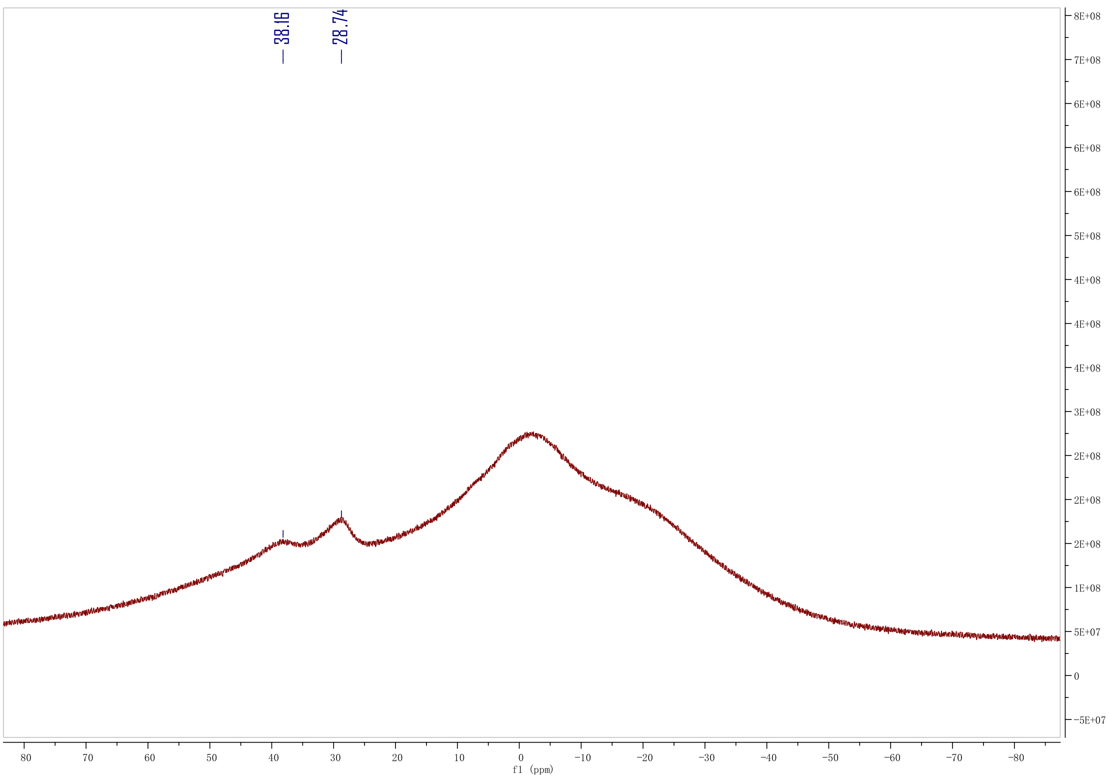

Figure 3.27 ^{11}B NMR spectrum of **7**.

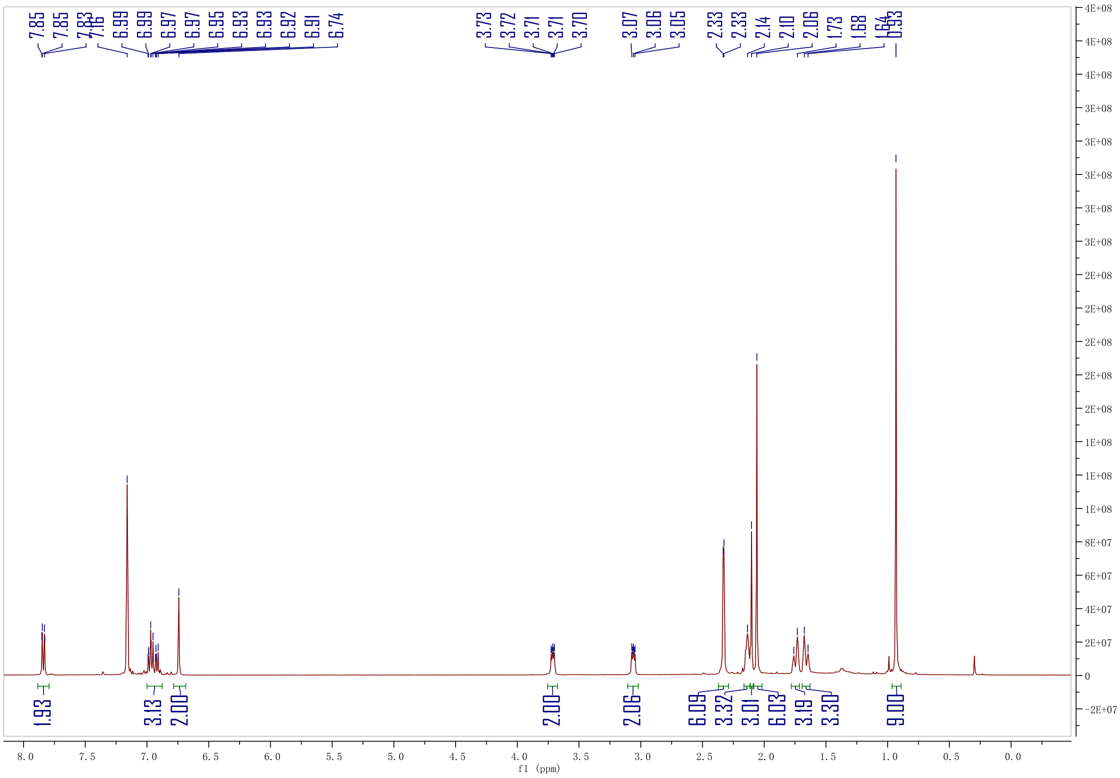

Figure 3.28 ^{1}H NMR spectrum of **8**.

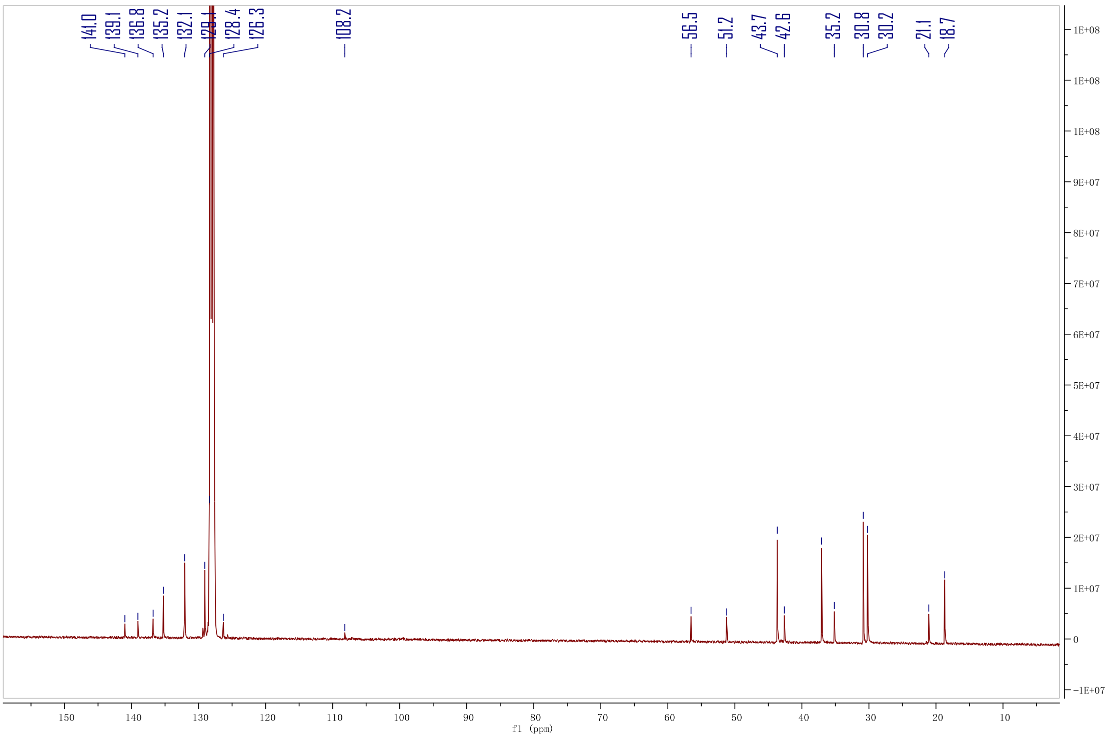

Figure 3.29 $^{13}C\{^{1}H\}$ NMR spectrum of **8**.

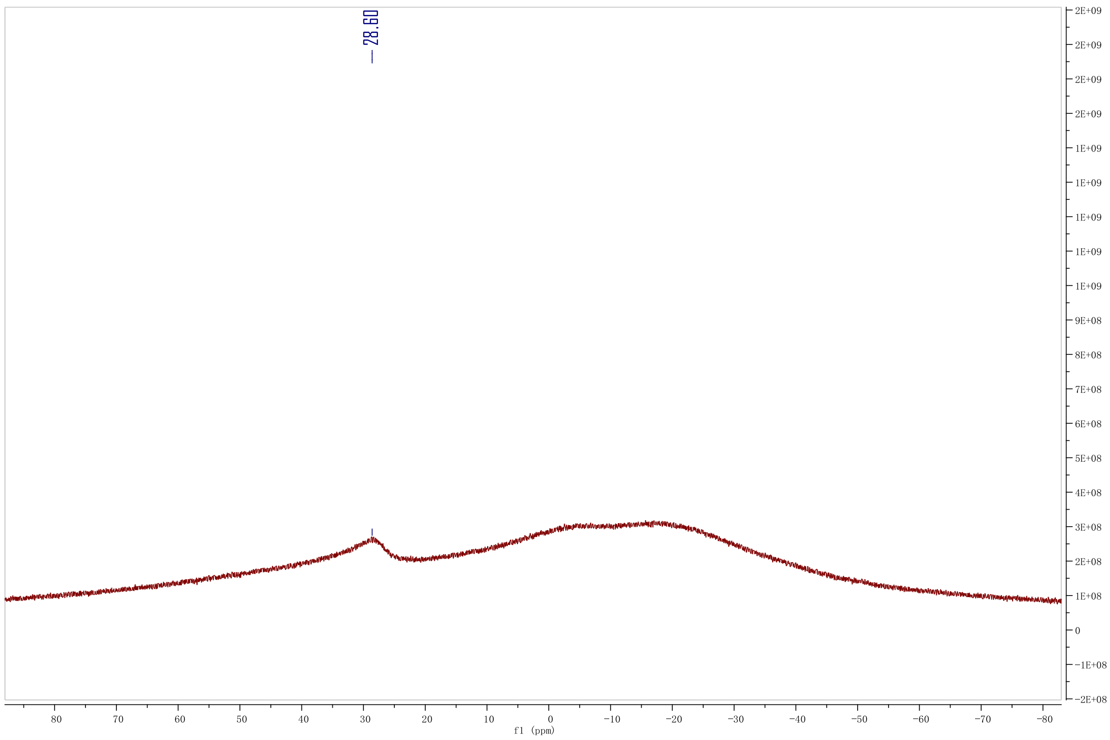

Figure 3.30 ^{11}B NMR spectrum of **8**.

3.4.2 Crystal structure parameters

X-ray data collection and structural refinement. Intensity data for compounds **2–8** was collected using a Bruker APEX II diffractometer. The structure was solved by direct phase determination (SHELX-2013) and refined for all data by full-matrix least squares methods on *F2*.[31] All non-hydrogen atoms were subjected to anisotropic refinement. The hydrogen atoms were generated geometrically and allowed to ride in their respective parent atoms; they were assigned appropriate isotropic thermal parameters and included in the structure-factor calculations. CCDC; 1570545-1570551 contains the supplementary crystallographic data for this paper. The data can be obtained free of charge from the Cambridge Crystallography Data Center via www.ccdc.cam.ac.uk/data_request/cif.

Table 3.1 Crystallographic data for **2–5.**

Compounds	**2**•$(C_6H_6)_{1.5}$	**3**	**4**	**5**
Formula	$C_{36}H_{48}B_2Br_6N_3$	$C_{27}H_{39}B_2Br_2N_3$	$C_{27}H_{39}BBrN_3$	$C_{30}H_{39}B_2Br_3F_9N_3O_9S_3$
Fw	1023.85	587.05	496.33	1114.17
Cryst syst	monoclinic	orthorhombic	monoclinic	orthorhombic
Space group	*P c*	$P2_12_12_1$	$P2_1/c$	*Pbca*
Size (mm^3)	0.140 x 0.220 x 0.320	0.180 x 0.200 x 0.320	0.080 x 0.140 x 0.180	0.040 x 0.120 x 0.230
T, K	103(2)	103(2)	153(2)	103(2)
a, Å	18.0580(10)	8.6123(8)	14.3740(8)	11.4237(9)
b, Å	13.7872(8)	14.1310(13)	11.9575(6)	21.6317(18)
c, Å	17.7455(9)	21.9529(19)	14.5487(7)	33.603(2)
β, deg	116.6655(13)	90	90.123(3)	90
V, $Å^3$	3948.2(4)	2671.7(4)	2500.6(2)	8303.8(11)
Z	4	4	4	8
d_{calcd} $g\cdot cm^{-3}$	1.722	1.459	1.318	1.782
μ, mm^{-1}	6.131	3.055	1.664	3.159
Refl collected	91664	50676	35163	69338
T_{max}/T_{min}	0.4810/0.2440	0.6090/ 0.4410	0.8780/ 0.7540	0.8840/ 0.5300
N_{measd}	23786	6669	4475	12728
[R_{int}]	0.1597	0.1046	0.1573	0.1557
R [I>2sigma(I)]	0.0676	0.0452	0.0492	0.0587
R_w[I>2sigma(I)]	0.0877	0.1152	0.1052	0.1008
GOF	0.991	0.863	1.005	1.030
Largest diff. peak/hole[$e\cdot Å^{-3}$]	1.680/-1.681	0.542/-0.699	0.595/-0.561	1.203 /-1.448

Table 3.2 Crystallographic data for **6–8**.

Compounds	**6**•$(C_6D_6)_{0.5}$	**7**	**8**
Formula	$C_{31}H_{42}B_2BrD_3N_3$	$C_{33}H_{44}B_2BrN_3$	$C_{35}H_{44}B_2BrN_3$
Fw	564.25	584.24	608.26
Cryst syst	triclinic	monoclinic	monoclinic
Space group	*P*-1	$P2_1/m$	$P2_1/c$
Size (mm^3)	0.140 x 0.240 x 0.420	0.080 x 0.120 x 0.180	0.010 x 0.080 x 0.320
T, K	153(2)	153(2)	133(2)
a, Å	8.8273(4)	10.004(3)	18.6970(7)
b, Å	11.3571(6)	10.717(3)	13.0692(5)
c, Å	14.8183(7)	14.614(4)	13.3176(5)
α, deg	91.737(2)	90	90
β, deg	96.385(2)	106.934(11)	108.508(2)
γ, deg	96.924(2)	90	90
V, $Å^3$	1464.15(12)	1498.9(7)	3085.9(2)
Z	2	2	4
d_{calcd} $g{\cdot}cm^{-3}$	1.280	1.294	1.309
μ, mm^{-1}	1.428	1.398	2.019
Refl collected	27132	18470	17695
T_{max}/T_{min}	0.8250/ 0.5850	0.8960/0.7870	0.9800/0.5640
N_{measd}	7291	3053	5430
[R_{int}]	0.0659	0.1662	0.1002
R [I>2sigma(I)]	0.0434	0.0723	0.0667
R_w[I>2sigma(I)]	0.0893	0.1678	0.1696
GOF	1.032	1.033	0.995
Largest diff. peak/hole[$e{\cdot}Å^{-3}$]	0.465/-0.604	1.848/-1.791	0.912/-0.721

3.4.3 Theoretical calculation

Gaussian 09 was used for all density functional theory (DFT) calculations.[32] Geometry optimization, frequency calculations, and Natural bond orbital (NBO) analysis on compound **3** and **4** were performed at the B3LYP/6-311G(d,p) level of theory.

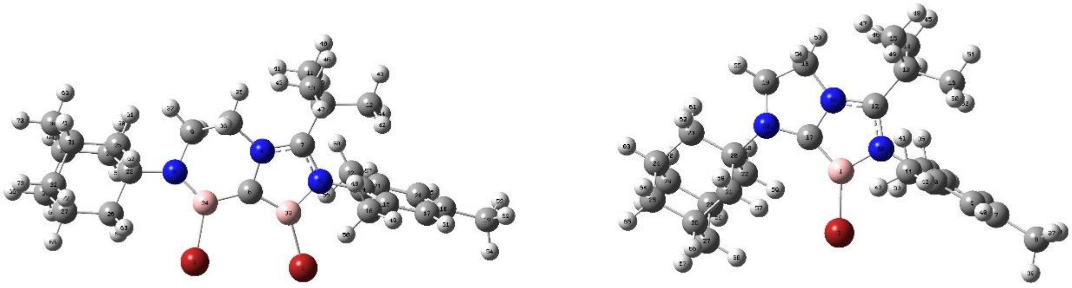

3 **4**

Figure 3.31 Calculated optimized structures for **3** and **4** at the B3LYP/6-311G(d,p) level of theory.

Table 3.3 Optimized structures of **3** and **4** (atom, x-, y-, z- positions in Å)

3

Br	-2.009900	-2.581890	0.237459
Br	1.656585	-2.495117	-0.433174
N	-2.348869	0.365331	-0.042792
N	-0.354280	1.272510	-0.146421
N	2.460395	0.380286	0.147343
C	-0.052362	-0.113381	-0.058094
C	-1.668893	1.557759	-0.157381
C	0.784994	2.180836	-0.289240
C	1.933595	1.690383	0.579392
C	-2.237176	2.985957	-0.285936
C	-1.868261	3.823484	0.968347
C	-3.776622	3.052844	-0.398402
C	-1.699893	3.660281	-1.577124
C	-3.774694	0.163986	0.037524
C	-4.492416	-0.123155	-1.131828
C	-3.808405	-0.196663	-2.474154
C	-5.863580	-0.362253	-1.025452

C	-6.523029	-0.347511	0.203680
C	-8.000625	-0.643649	0.296431
C	-5.769235	-0.096751	1.350753
C	-4.396154	0.147363	1.294340
C	-3.608429	0.358395	2.563206
C	3.960087	0.317508	0.127244
C	4.524474	0.690665	1.526195
C	4.515290	1.310951	-0.933266
C	4.515260	-1.077442	-0.230629
C	6.059305	-1.078306	-0.240753
C	6.589513	-0.696254	1.151846
C	6.066615	0.704353	1.514548
C	6.564593	1.725992	0.472924
C	6.057920	1.326367	-0.926910
C	6.581800	-0.075312	-1.283103
B	-1.386994	-0.746729	0.023894
B	1.411693	-0.560812	-0.079803

H	0.517930	3.187467	0.014043
H	1.096820	2.203034	-1.338674
H	2.714172	2.446203	0.529255
H	1.593415	1.645356	1.621628
H	-2.340450	3.403563	1.859175
H	-2.239145	4.844879	0.844882
H	-0.798205	3.884280	1.163804
H	-4.155841	2.526808	-1.273401
H	-4.052216	4.106011	-0.500704
H	-4.285217	2.663037	0.480918
H	-0.619457	3.783528	-1.595930
H	-2.144803	4.654364	-1.675104
H	-1.984492	3.079851	-2.458373
H	-3.248559	0.714622	-2.703069
H	-4.537932	-0.354493	-3.270161
H	-3.092736	-1.023110	-2.500104
H	-6.427304	-0.574846	-1.928713
H	-8.523258	-0.358393	-0.619427
H	-8.462847	-0.111283	1.131073
H	-8.175495	-1.713512	0.453894
H	-6.258370	-0.102404	2.320128
H	-2.857176	-0.426317	2.688740
H	-4.267615	0.339794	3.432592
H	-3.074703	1.312789	2.565265
H	4.153478	-0.035559	2.257438
H	4.166344	1.673975	1.844672
H	4.154974	2.327687	-0.750100
H	4.140005	1.013411	-1.918346
H	4.143830	-1.386267	-1.209204
H	4.159307	-1.814085	0.489606
H	6.395790	-2.087715	-0.499036
H	7.685541	-0.706625	1.158574
H	6.256855	-1.427451	1.896970
H	6.425355	0.989218	2.509601
H	6.211287	2.731791	0.730517
H	7.659733	1.763650	0.478060
H	6.408191	2.054177	-1.667023
H	6.244783	-0.360765	-2.285961
H	7.677804	-0.079277	-1.299762

4

B	-0.236557	-0.263279	-0.163320
Br	-0.057750	-2.221884	-0.180479
C	-2.786864	-0.388954	-0.000699
C	-3.254420	-0.840680	1.241765
C	-2.513623	-0.533375	2.519102
C	-4.422604	-1.604494	1.272202
C	-5.114130	-1.944699	0.109174
C	-6.356882	-2.800520	0.167199
C	-4.600081	-1.508086	-1.111929
C	-3.435032	-0.743269	-1.192444
C	-2.885116	-0.330954	-2.535082
C	-1.456053	1.743908	-0.069004
C	-2.508675	2.843547	0.105030
C	-2.315439	3.543328	1.476847
C	-2.377761	3.890274	-1.032124
C	-3.964991	2.337193	0.060012
C	0.692674	0.877020	-0.225815
C	0.675004	3.224781	-0.263866
C	2.056680	2.696112	0.118398
C	3.183509	0.436326	-0.139450
C	3.213874	-0.675853	-1.213864
C	3.144545	-0.205205	1.271083
C	4.499478	1.241344	-0.269991
C	5.722255	0.322487	-0.068362
C	5.722029	-0.792595	-1.129678
C	4.422754	-1.607512	-0.999966
C	4.347374	-2.239512	0.404582
C	4.364755	-1.127503	1.472461
C	5.660927	-0.306149	1.337507
N	-1.565798	0.373338	-0.065636
N	-0.127829	2.002943	-0.141577
N	2.031270	1.326059	-0.409272
H	-1.517671	-0.984192	2.507831
H	-3.055876	-0.924410	3.381704
H	-2.373432	0.540922	2.664807
H	-4.795648	-1.948705	2.232192
H	-7.021177	-2.596715	-0.675720
H	-6.916881	-2.629780	1.089716

H	-6.100750	-3.865136	0.132574
H	-5.112879	-1.775945	-2.030829
H	-2.763515	0.753057	-2.613530
H	-3.546396	-0.657777	-3.339306
H	-1.898678	-0.772194	-2.702373
H	-2.479462	2.839913	2.296123
H	-3.036408	4.359586	1.584521
H	-1.317236	3.966728	1.598417
H	-1.421381	4.411469	-1.026582
H	-3.160183	4.647195	-0.924393
H	-2.498686	3.417354	-2.009783
H	-4.208751	1.858766	-0.888507
H	-4.624183	3.202103	0.175412
H	-4.194597	1.636503	0.860808
H	0.330999	4.021912	0.390796
H	0.661393	3.571616	-1.301482
H	2.848600	3.292318	-0.332195

H	2.171095	2.723548	1.215660
H	2.290758	-1.254236	-1.181371
H	3.263452	-0.201085	-2.199827
H	2.219181	-0.773534	1.390512
H	3.140574	0.582242	2.034807
H	4.536260	2.039260	0.478735
H	4.537151	1.714762	-1.257936
H	6.633023	0.923976	-0.163710
H	5.796517	-0.358773	-2.133663
H	6.596032	-1.440366	-0.994344
H	4.402794	-2.396568	-1.759160
H	5.194222	-2.919079	0.556863
H	3.433743	-2.835124	0.499072
H	4.315254	-1.576361	2.470606
H	5.693025	0.478051	2.103464
H	6.535126	-0.947112	1.500330

Figure 3.32 Plots of the frontier orbitals of **3** and **4**.

3:

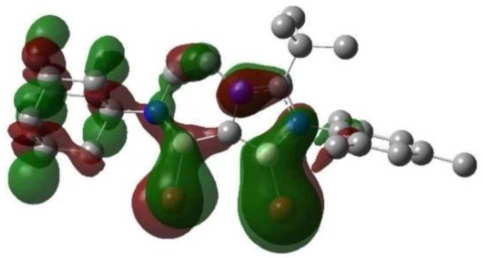

HOMO-8 (–7.7642 eV)

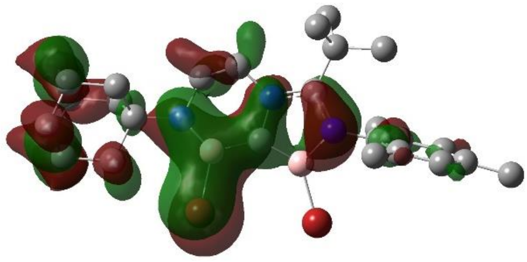

HOMO-10 (–8.0548 eV)

4:

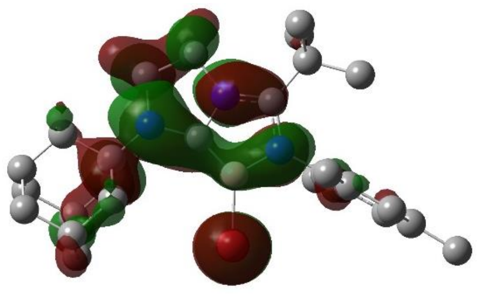

HOMO-2 (–6.4564 eV)

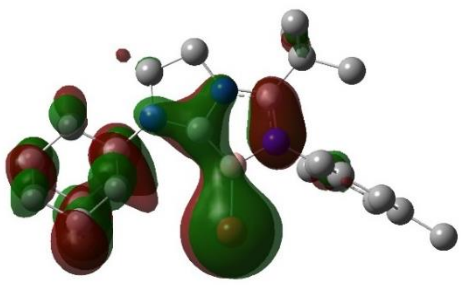

HOMO-5 (–7.4026 eV)

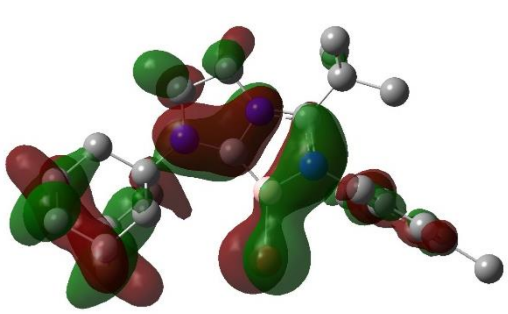

HOMO-8 (–7.9327 eV)

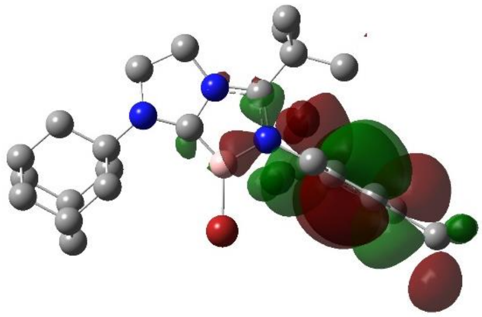

LUMO (–0.2561 eV)

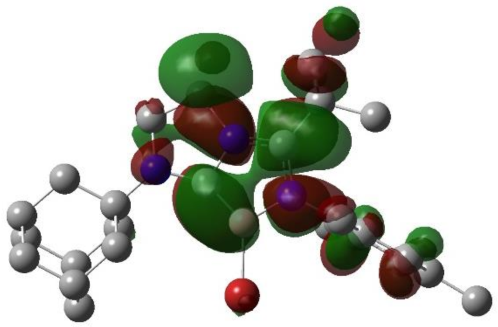

LUMO+2 (0.0996 eV)

Table 3.4 The NPA charges of **3** and **4** calculated at B3LYP/6-311G(d,p) level of theory.

3:

Atom	No	Charge	Core	Valence	Rydberg	Total
Br	1	-0.14630	27.99914	7.13531	0.01185	35.14630
Br	2	-0.16897	27.99921	7.15888	0.01088	35.16897
N	3	-0.66456	1.99910	5.65349	0.01198	7.66456
N	4	-0.34789	1.99912	5.33697	0.01180	7.34789
N	5	-0.76128	1.99911	5.74872	0.01345	7.76128
C	6	-0.65538	1.99845	4.64014	0.01679	6.65538
C	7	0.47360	1.99890	3.49410	0.03340	5.52640
C	8	-0.17139	1.99915	4.15584	0.01640	6.17139
C	9	-0.16406	1.99915	4.14824	0.01667	6.16406
C	10	-0.07641	1.99914	4.06434	0.01294	6.07641
C	11	-0.56001	1.99922	4.54819	0.01259	6.56001
C	12	-0.57187	1.99924	4.55857	0.01407	6.57187
C	13	-0.56375	1.99923	4.55212	0.01240	6.56375
C	14	0.14907	1.99867	3.83081	0.02145	5.85093
C	15	0.00319	1.99885	3.98340	0.01455	5.99681

C	16	-0.58596	1.99923	4.57752	0.00922	6.58596
C	17	-0.21192	1.99890	4.19716	0.01585	6.21192
C	18	0.00415	1.99896	3.98269	0.01420	5.99585
C	19	-0.58159	1.99923	4.57275	0.00961	6.58159
C	20	-0.21280	1.99890	4.19805	0.01585	6.21280
C	21	-0.00039	1.99885	3.98696	0.01457	6.00039
C	22	-0.58466	1.99922	4.57614	0.00929	6.58466
C	23	0.20322	1.99902	3.77547	0.02228	5.79678
C	24	-0.40398	1.99912	4.38642	0.01844	6.40398
C	25	-0.40246	1.99912	4.38405	0.01930	6.40246
C	26	-0.41152	1.99911	4.39173	0.02067	6.41152
C	27	-0.19226	1.99917	4.17468	0.01841	6.19226
C	28	-0.38526	1.99919	4.36838	0.01770	6.38526
C	29	-0.19434	1.99917	4.17677	0.01840	6.19434
C	30	-0.38521	1.99919	4.36836	0.01765	6.38521
C	31	-0.19490	1.99917	4.17725	0.01848	6.19490
C	32	-0.38516	1.99919	4.36833	0.01765	6.38516
B	33	0.58123	1.99828	2.39203	0.02846	4.41877
B	34	0.70557	1.99847	2.26907	0.02689	4.29443
H	35	0.20008	0.00000	0.79621	0.00372	0.79992
H	36	0.20231	0.00000	0.79392	0.00377	0.79769
H	37	0.19952	0.00000	0.79770	0.00278	0.80048
H	38	0.19023	0.00000	0.80607	0.00370	0.80977
H	39	0.20215	0.00000	0.79542	0.00243	0.79785
H	40	0.20000	0.00000	0.79756	0.00244	0.80000
H	41	0.18963	0.00000	0.80868	0.00169	0.81037
H	42	0.20883	0.00000	0.78845	0.00272	0.79117
H	43	0.19831	0.00000	0.79916	0.00253	0.80169
H	44	0.21260	0.00000	0.78466	0.00273	0.78740
H	45	0.19545	0.00000	0.80295	0.00159	0.80455
H	46	0.19962	0.00000	0.79789	0.00249	0.80038
H	47	0.20329	0.00000	0.79431	0.00240	0.79671
H	48	0.19992	0.00000	0.79749	0.00259	0.80008
H	49	0.20174	0.00000	0.79655	0.00171	0.79826
H	50	0.22743	0.00000	0.77053	0.00204	0.77257
H	51	0.19722	0.00000	0.79894	0.00384	0.80278
H	52	0.20196	0.00000	0.79620	0.00184	0.79804
H	53	0.20216	0.00000	0.79598	0.00186	0.79784
H	54	0.21042	0.00000	0.78750	0.00208	0.78958
H	55	0.19704	0.00000	0.79913	0.00383	0.80296
H	56	0.22607	0.00000	0.77192	0.00200	0.77393
H	57	0.20190	0.00000	0.79640	0.00169	0.79810
H	58	0.19860	0.00000	0.79882	0.00258	0.80140
H	59	0.20564	0.00000	0.79115	0.00321	0.79436

H	60	0.19164	0.00000	0.80529	0.00307	0.80836
H	61	0.18635	0.00000	0.81028	0.00337	0.81365
H	62	0.20340	0.00000	0.79310	0.00350	0.79660
H	63	0.21393	0.00000	0.78259	0.00349	0.78607
H	64	0.21758	0.00000	0.77873	0.00369	0.78242
H	65	0.20615	0.00000	0.79119	0.00266	0.79385
H	66	0.19363	0.00000	0.80332	0.00305	0.80637
H	67	0.19697	0.00000	0.80047	0.00256	0.80303
H	68	0.20296	0.00000	0.79429	0.00276	0.79704
H	69	0.19090	0.00000	0.80645	0.00266	0.80910
H	70	0.19637	0.00000	0.80064	0.00299	0.80363
H	71	0.20235	0.00000	0.79488	0.00277	0.79765
H	72	0.19608	0.00000	0.80133	0.00258	0.80392
H	73	0.19379	0.00000	0.80314	0.00307	0.80621
* Total *		0.00000	119.96716	181.36223	0.67060	302.00000

4:

Atom	No	Charge	Core	Valence	Rydberg	Total
B	1	0.41488	1.99818	2.56361	0.02334	4.58512
Br	2	-0.18168	27.99922	7.16941	0.01305	35.18168
C	3	0.15218	1.99867	3.82835	0.02080	5.84782
C	4	0.00129	1.99886	3.98538	0.01448	5.99871
C	5	-0.58443	1.99922	4.57593	0.00927	6.58443
C	6	-0.21383	1.99891	4.19908	0.01584	6.21383
C	7	0.00244	1.99896	3.98439	0.01420	5.99756
C	8	-0.58115	1.99923	4.57234	0.00958	6.58115
C	9	-0.21348	1.99890	4.19876	0.01581	6.21348
C	10	0.00373	1.99886	3.98302	0.01439	5.99627
C	11	-0.58530	1.99923	4.57688	0.00919	6.58530
C	12	0.40844	1.99892	3.55764	0.03500	5.59156
C	13	-0.07101	1.99914	4.05863	0.01324	6.07101
C	14	-0.56022	1.99923	4.54824	0.01275	6.56022
C	15	-0.56390	1.99923	4.55205	0.01261	6.56390
C	16	-0.57188	1.99924	4.55887	0.01378	6.57188
C	17	-0.01998	1.99855	3.99335	0.02808	6.01998
C	18	-0.16850	1.99921	4.15275	0.01654	6.16850
C	19	-0.16646	1.99922	4.15043	0.01681	6.16646
C	20	0.19985	1.99905	3.77849	0.02261	5.80015
C	21	-0.40537	1.99911	4.38646	0.01980	6.40537

C	22	-0.41537	1.99912	4.39795	0.01831	6.41537
C	23	-0.40296	1.99913	4.38534	0.01849	6.40296
C	24	-0.19122	1.99917	4.17355	0.01850	6.19122
C	25	-0.38440	1.99919	4.36766	0.01755	6.38440
C	26	-0.19520	1.99917	4.17762	0.01840	6.19520
C	27	-0.38654	1.99919	4.36999	0.01736	6.38654
C	28	-0.19338	1.99918	4.17590	0.01830	6.19338
C	29	-0.38482	1.99919	4.36804	0.01759	6.38482
N	30	-0.63295	1.99912	5.62193	0.01190	7.63295
N	31	-0.37521	1.99911	5.36480	0.01130	7.37521
N	32	-0.53159	1.99925	5.51159	0.02075	7.53159
H	33	0.22545	0.00000	0.77251	0.00203	0.77455
H	34	0.19959	0.00000	0.79869	0.00172	0.80041
H	35	0.20120	0.00000	0.79618	0.00262	0.79880
H	36	0.19613	0.00000	0.80001	0.00385	0.80387
H	37	0.20146	0.00000	0.79669	0.00185	0.79854
H	38	0.20178	0.00000	0.79635	0.00187	0.79822
H	39	0.20919	0.00000	0.78872	0.00209	0.79081
H	40	0.19609	0.00000	0.80004	0.00387	0.80391
H	41	0.20240	0.00000	0.79488	0.00272	0.79760
H	42	0.19983	0.00000	0.79845	0.00172	0.80017
H	43	0.22503	0.00000	0.77301	0.00196	0.77497
H	44	0.19968	0.00000	0.79787	0.00246	0.80032
H	45	0.19613	0.00000	0.80129	0.00258	0.80387
H	46	0.18879	0.00000	0.80949	0.00172	0.81121
H	47	0.19240	0.00000	0.80590	0.00170	0.80760
H	48	0.19700	0.00000	0.80037	0.00263	0.80300
H	49	0.20119	0.00000	0.79624	0.00257	0.79881
H	50	0.20656	0.00000	0.79067	0.00277	0.79344
H	51	0.19650	0.00000	0.80094	0.00256	0.80350
H	52	0.21098	0.00000	0.78623	0.00279	0.78902
H	53	0.20055	0.00000	0.79594	0.00351	0.79945
H	54	0.19421	0.00000	0.80117	0.00461	0.80579
H	55	0.20021	0.00000	0.79742	0.00237	0.79979
H	56	0.16483	0.00000	0.82901	0.00616	0.83517
H	57	0.22104	0.00000	0.77490	0.00406	0.77896
H	58	0.19754	0.00000	0.79837	0.00409	0.80246
H	59	0.21766	0.00000	0.77890	0.00343	0.78234
H	60	0.18995	0.00000	0.80660	0.00345	0.81005
H	61	0.19328	0.00000	0.80344	0.00328	0.80672
H	62	0.19983	0.00000	0.79600	0.00417	0.80017
H	63	0.20062	0.00000	0.79665	0.00273	0.79938
H	64	0.19287	0.00000	0.80445	0.00268	0.80713
H	65	0.19256	0.00000	0.80435	0.00309	0.80744

H	66	0.20335	0.00000	0.79391	0.00273	0.79665
H	67	0.19098	0.00000	0.80594	0.00308	0.80902
H	68	0.20462	0.00000	0.79298	0.00240	0.79538
H	69	0.20149	0.00000	0.79565	0.00287	0.79851
H	70	0.19117	0.00000	0.80614	0.00269	0.80883
H	71	0.19387	0.00000	0.80305	0.00307	0.80613
* Total *		0.00000	89.96994	171.37786	0.65220	262.00000

3.5 References

(1) a) Wang, X.-Y.; Wang, J.-Y.; Pei, J. *Chem. Eur. J.* **2015**, *21*, 3528 – 3539; b) Campbell, P. G.; Marwitz, A. J. V.; Liu, S.-Y. *Angew. Chem. Int. Ed.* **2012**, *51*, 6074 – 6092; c) Bosdet, M. J. D.; Piers, W. E. *Can. J. Chem.* **2009**, *87*, 8 – 29; d) Z. Liu, T. B. Marder, *Angew. Chem. Int. Ed.* **2008**, *47*, 242 – 244.

(2) For recent reviews, see: a) Su, B.; Kinjo, R. *Synthesis*, **2017**, *49*, 2985 – 3034; b) Bélanger-Chabot, G.; Braunschweig, H.; Roy, D. K. *Eur. J. Inorg. Chem.* **2017**, *25*, DOI: 10.1002/ejic.201700562.

(3) Dewar, M. J. S.; Kubba, V. P.; Pettit, R. *J. Chem. Soc.* **1958**, 3073 – 3076.

(4) a) McConnell, C. R.; Campbell, P. G.; Fristoe, C. R.; Memmel, P.; Zakharov, L. N.; Li, B.; Darrigan, C.; Chrostowska, A.; Liu, S.-Y. *Eur. J. Inorg. Chem.* **2017**, 2207 – 2210; b) Xu, S.; Zhang, Y.; Li, B.; Liu, S.-Y. *J. Am. Chem. Soc.* **2016**, *138*, 14566 – 14569; c) Ashe, A. J. III. *Organometallics* **2009**, *28*, 4236 – 4248.

(5) a) See ref 1a. For recent examples, see: b) Wan, W.-M.; Baggett, A. W.; Cheng, F.; Lin, H.; Liu, S.-Y.; Jäkle, F. *Chem. Commun.* **2016**, *52*, 13616 – 13619; c) Murphy, C. J.; Miller, D. P.; Simpson, S.; Baggett, A. W.; Pronschinske, A.; Liriano, M. L.; Therrien, A. J.; Enders, A.; Liu, S.-Y.; Zurek, E.; Sykes, E. C. H. *J. Phys. Chem. C* **2016**, *120*, 6020 – 6030;

d) Sun, F.; Lv, L.; Huang, M.; Zhou, Z.; Fang, X. *Org. Lett.* **2014**, *16*, 5024 – 5027; e) Hashimoto, S.; Ikuta, T.; Shiren, K.; Nakatsuka, S.; Ni, J.; Nakamura, M.; Hatakeyama, T. *Chem. Mater*. **2014**, *26*, 6265 – 6271.

(6) a) Zhao, P.; Nettleton, D. O.; Karki, R.; Zecri, F. J.; Liu, S.-Y. *ChemMedChem* **2017**, *12*, 358 – 361; b) Lee, H; Fischer, M.; Shoichet, B. K.; Liu, S.-Y. *J. Am. Chem. Soc*. **2016**, *138*, 12021 – 12024; c) Knack, D. H.; Marshall, J. L.; Harlow, G. P.; Dudzik, A.; Szaleniec, M.; Liu, S.-Y.; Heider, J. *Angew. Chem. Int. Ed.* **2013**, *52*, 2599 – 2601; d) Liu, L.; Marwitz, A. J. V.; Matthews, B. W.; Liu, S.-Y. *Angew. Chem. Int. Ed*. **2009**, *48*, 6817 – 6819.

(7) Campbell, P. G.; Zakharov, L. N.; Grant, D.; Dixon, D. A.; Liu, S.-Y. *J. Am. Chem. Soc.* **2010**, *132*, 3289 – 3291.

(8) Burford, R. J.; Li, B.; Vasiliu, M.; Dixon, D. A.; Liu, S.-Y. *Angew. Chem. Int. Ed.* **2015**, *54*, 7823 – 7827.

(9) a) Wang, B.; Li, Y.; Ganguly, R.; Hirao, H.; Kinjo, R. *Nat. Commun.* **2016**, *7*, 11871; b) Wu, D.; Kong, L.; Li, Y.; Ganguly, R.; Kinjo, R. *Nat. Commun.* **2015**, *6*, 7340; c) Wu, D.; Ganguly, R.; Li, Y.; Hoo, S.-N.; Hirao, H.; Kinjo, R. *Chem. Sci.* **2015**, *6*, 7150 – 7155.

(10) a) Wu, D.; Wang, R.; Li, Y.; Ganguly, R.; Hirao, H.; Kinjo, R. *Chem* **2017**, *3*, 134 – 151; See also: b) Geri, J. B.; Szymczak, N. K. *J. Am. Chem. Soc.* **2017**, *139*, 9811 – 9820.

(11) a) Weber, L.; Böhling, L. *Coord. Chem. Rev.* **2015**, *284*, 236 – 275; b) Weber, L. *Eur. J. Inorg. Chem.* **2012**, 2012, 5595 – 5609; c) Weber, L. *Coord. Chem. Rev.* **2008**, *252*, 1 – 31; d) Ashe, A. J. III. *Comprehensive Heterocyclic Chemistry III*, Elsevier, Oxford, **2008**, pp. 1189 – 1224; e) Weber, L. *Coord. Chem. Rev.* **2001**, *215*, 39-77; f) Schmid, G.; Schulze, J. *Angew. Chem. Int. Ed. Engl.* **1977**, *16*, 249 – 250; g) See also ref 2a.

(12) a) Chrostowska, A.; Xu, S.; Maziere, A.; Boknevitz, K.; Li, B.; Abbey, E. R.; Dargelos, A.; Graciaa, A.; Liu, S.-Y. *J. Am. Chem. Soc.* **2014**, *136*, 11813 – 11820; b) Abbey, E. R.; Liu, S.-Y. *Org. Biomol. Chem*. **2013**, *11*, 2060 – 2069; c) Abbey, E. R.; Zakharov, L. N.; Liu, S.-Y. *J. Am. Chem. Soc.* **2011**, *133*, 11508 – 11511; d) Abbey, E. R.; Zakharov, L. N.; Liu, S.-Y. *J. Am. Chem. Soc.* **2010**, *132*, 16340 – 16342; e) Chrostowska, A.; Maciejczyk, M.; Dargelos, A.; Baylere, P.; Weber, L.; Werner, V.; Eickhoff, D.; Stammler, H. G.; Neumann, B. *Organometallics* **2010**, *29*, 5192 – 5198; f) Kubo, Y.; Tsuruzoe, K.; Okuyama, S.; Nishiyabu, R.; Fujihara, T. *Chem. Commun.* **2010**, *46*, 3604 – 3606; g) Weber, L.; Werner, V.; Fox, M. A.; Marder, T. B.; Scwedler, S.; Brockhinke, A.; Stammler, H.-G.; Neumann, B. *Dalton Trans.* **2009**, 1339 – 1351; h) Weber, L.; Werner, V.; Fox, M. A.; Marder, T. B.; Schwedler, S.; Brockhinke, A.; Stammler, H.-G.; Neumann, B. *Dalton Trans.* **2009**, 2823 – 2831; i) Maruyama, S.; Kawanishi, Y. *J. Mater. Chem.* **2002**, *12*, 2245 2249.

(13) a) Arduengo, A. J.; Harlow, R. L.; Kline, M. *J. Am. Chem. Soc.* **1991**, *113*, 361− 363; b) Arduengo, A. J. *Acc. Chem. Res.* **1999**, *32*, 913 − 921.

(14) a) Díez-González, S.; Marion, N.; Nolan, S. P. *Chem. Rev.* **2009**, *109*, 3612 − 3676; b) Arnold, P. L.; Casely, I. J. *Chem. Rev.* **2009**, *109*, 3599 − 3611; c) de Frémont, P.; Marion, N.; Nolan, S. P. *Coord. Chem. Rev.* **2009**, *253*, 862 − 892; d) Jacobsen, H.; Correa, A.; Poater, A.; Costabile, C.; Cavallo, L. *Coord. Chem. Rev.* **2009**, *253*, 687 − 703; e) Poyatos, M.; Mata, J. A.; Peris, E. *Chem. Rev.* **2009**, *109*, 3677 − 3707; f) Hindi, K. M.; Panzner, M. J.; Tessier, C. A.; Cannon, C. L.; Youngs, W. J. *Chem. Rev.* **2009**, *109*, 3859 − 3884; g) Hahn, F. E.; Jahnke, M. C. *Angew. Chem. Int. Ed.* **2008**, *47*, 3122 − 3172.

(15) a) Naumann, S.; Dove, A. P. *Polym. Chem.* **2015**, *6*, 3185 − 3200; b) Fevre, M.; Pinaud, J.; Gnanou, Y.; Vignolle, J.; Taton, D. *Chem. Soc. Rev.* **2013**, *42*, 2142 − 2172; c) X. Bugaut, F. Glorius, *Chem. Soc. Rev.* **2012**, *41*, 3511 − 3522; d) Nair, V.; Menon, R. S.; Biju, A. T.; Sinu, C. R.; Paul, R. R.; Jose, A.; Sreekumar, V. *Chem. Soc. Rev.* **2011**, *40*, 5336 − 5346.

(16) a) Martin, C. D.; Soleilhavoup, M.; Bertrand, G. *Chem. Sci.* **2013**, *4*, 3020 − 3030; b) Fuchter, M. J. *Chem. Eur. J.* **2010**, *16*, 12286 − 12294; c) Curran, D. P.; Solovyev, A.; Makhlouf Brahmi, M.; Fensterbank, L.; Malacria, M.; Lacôte, E. *Angew. Chem. Int. Ed.* **2011**, *50*, 10294 − 10317; d) Martin, D.; Soleilhavoup, M.; Bertrand, G. *Chem. Sci.* **2011**, *2*, 389 − 399; e) Murphy, L. J.; Robertson, K. N.; Masuda, J. D.; Clyburne, J. A. C. In *N-Heterocyclic Carbenes*; Wiley-VCH Verlag GmbH & Co. KGaA: 2014, p 427 − 498; f) Kuhn, N.; Al-Sheikh, A. *Coord. Chem. Rev.* **2005**, *249*, 829 − 857.

(17) a) Hopkinson, M. N.; Richter, C.; Schedler, M.; Glorius, F. *Nature* **2014**, *510*, 485 − 496; b) Nelson, D. J.; Nolan, S. P. *Chem. Soc. Rev.* **2013**, *42*, 6723 − 6753; c) Benhamou, L.; Chardon, E.; Lavigne, G.; Bellemin-Laponnaz, S.; César, V. *Chem. Rev.* **2011**, *111*, 2705 − 2733; d) Díez-González, S.; Nolan, S. P. *Coord. Chem. Rev.* **2007**, *251*, 874 − 883.

(18) a) Wurtemberger-Pietsch, S.; Radius, U.; Marder, T. B. *Dalton Trans.* **2016**, *45*, 5880 − 5895; b) Iversen, K. J.; Wilson, D. J. D.; Dutton, J. L. *Dalton Trans.* **2014**, *43*, 12820 − 12823.

(19) Schmidt, D.; Berthel, J. H. J.; Pietsch, S.; Radius, U. *Angew. Chem. Int. Ed.* **2012**, *51*, 8881 − 8885.

(20) a) Arrowsmith, M.; Hill, M. S.; Kociok-Köhn, G.; MacDougall, D. J.; Mahon, M. F. *Angew. Chem. Int. Ed.* **2012**, *51*, 2098 − 2100; b) Arrowsmith, M.; Hill, M. S.; Kociok-Köhn, G.

Organometallics **2015**, *34*, 653 − 662.

(21) Anker, M. D.; Colebatch, A. L.; Iversen, K. J.; Wilson, D. J. D.; Dutton, J. L.; García, L.; Hill, M. S.; Liptrot, D. J.; Mahon, M. F. *Organometallics* **2017**, *36*, 1173 − 1178.

(22) a) Al-Rafia, S. M. I.; McDonald, R.; Ferguson, M. J.; Rivard, E. *Chem. Eur. J.* **2012**, *18*, 13810 − 13820; b) Franz, D.; Inoue, S. *Chem. Asian, J.* **2014**, *9*, 2083 − 2087; c) Wang, T.; Stephan, D. W. *Chem. Eur. J.* **2014**, *20*, 3036 − 3039; d) Pietsch, S.; Paul, U.; Cade, I. A.; Ingleson, M. J.; Radius, U.; Marder, T. B. *Chem. Eur. J.* **2015**, *21*, 9018 − 9021; e) Würtemberger-Pietsch, S.; Schneider, H.; Marder, T. B.; Radius, U. *Chem. Eur. J.* **2016**, *22*, 13032 − 13036; f) Eck, M.; Wurtemberger-Pietsch, S.; Eichhorn, A.; Berthel, J. H. J.; Bertermann, R.; Paul, U. S. D.; Schneider, H.; Friedrich, A.; Kleeberg, C.; Radius, U.; Marder, T. B. *Dalton Trans.* **2017**, *46*, 3661 − 3680.

(23) a) Bertrand, G.; Soleilhavoup, M. *Angew. Chem. Int. Ed.* **2017**, *56*, 10282 − 10292; b) Braunschweig, H.; Dewhurst, R. D.; Schneider, A. *Chem. Rev.* **2010**, *110*, 3924 − 3957; c) Braunschweig, H.; Dewhurst, R. D.; Gessner, V. H. *Chem. Soc. Rev.* **2013**, *42*, 3197 − 3208.

(24) a) Dahcheh, F.; Martin, D.; Stephan, D. W.; Bertrand, G. *Angew. Chem. Int. Ed.* **2014**, *53*, 13159 − 13163; b) Ledet, A. D.; Hudnall, T. W. *Dalton Trans.* **2016**, *45*, 9820 − 9826; c) Kinjo, R.; Donnadieu, B.; Celik, M. A.; Frenking, G.; Bertrand, G. *Science* **2011**, *333*, 610 − 613; d) Arrowsmith, M.; Auerhammer, D.; Bertermann, R.; Braunschweig, H.; Bringmann, G.; Celik, M. A.; Dewhurst, R. D.; Finze, M.; Grüne, M.; Hailmann, M.; Hertle, T.; Krummenacher, I. *Angew. Chem. Int. Ed.* **2016**, *55*, 14464 − 14468; e) Kong, L.; Li, Y.; Ganguly, R.; Vidovic, D.; Kinjo, R. *Angew. Chem. Int. Ed.* **2014**, *53*, 9280 − 9283; f) Ruiz, D. A.; Melaimi, M.; Bertrand, G. *Chem. Commun.* **2014**, *50*, 7837 − 7839; g) Braunschweig,

H.; Dewhurst, R. D.; Hupp, F.; Nutz, M.; Radacki, K.; Tate, C. W.; Vargas, A.; Ye, Q. *Nature* **2015**, *522*, 327 − 330.

(25) a) Wang, Y.; Robinson, G. H. *Inorg. Chem.* **2011**, *50*, 12326 − 12337; b) Bissinger, P.; Braunschweig, H.; Damme, A.; Dewhurst, R. D.; Kupfer, T.; Radacki, K.; Wagner, K. *J. Am. Chem. Soc.* **2011**, *133*, 19044 − 19047; c) Pachaly, B.; West, R. *Angew. Chem. Int. Ed. Engl.* **1984**, *23*, 454 − 455.

(26) Grigsby, W. J.; Power, P. P. *J. Am. Chem. Soc.* **1996**, *118*, 7981 − 7988.

(27) Bissinger, P.; Braunschweig, H.; Kraft, K.; Kupfer, T. *Angew. Chem. Int. Ed.* **2011**, *50*, 4704 − 4707.

(28) Ghadwal, R. S.; Schürmann, C. J.; Engelhardt, F.; Steinmetzger, C. *Eur. J. Inorg. Chem.* **2014**, *29*, 4921 − 4926.

(29) a) Weber, L. *Coord. Chem. Rev.* **2001**, *215*, 39 − 77; b) Lamm, A. N.; Garner, E. B.; Dixon, D. A.; Liu, S.-Y. *Angew. Chem. Int. Ed.* **2011**, *50*, 8157 − 8160; c) Xu, S.; Mikulas, T. C.; Zakharov, L. N.; Dixon, D. A.; Liu, S.-Y. *Angew. Chem. Int. Ed.* **2013**, *52*, 7527 − 7531.

(30) J. J. Eisch, K. Yu, A. L. Rheingold, *Eur. J. Org. Chem.* **2014**, 818 − 832.

(31) Bruker AXS SHELXTL, Madison, WI; *SHELX-97G*. M. Sheldrick, Acta. Crystallogr. A, **2008**, *64*, 112 – 122, *SHELX-2013*, http://shelx.uni-ac. gwdg.de/SHELX/index.php.

(32) Gaussian 09, Revision B.01, Frisch, M. J.; Trucks, G. W.; Schlegel, H. B.; Scuseria, G. E.; Robb, M. A.; Cheeseman, J. R.; Scalmani, G.; Barone, V.; Mennucci, B.; Petersson, G. A.; Nakatsuji, H.; Caricato, M.; Li, X.; Hratchian, H. P.; Izmaylov, A. F.; Bloino, J.; Zheng, G.; Sonnenberg, J. L.; Hada, M.; Ehara, M.; Toyota, K.; Fukuda, R.; Hasegawa, J.; Ishida, M.; Nakajima, T.; Honda, Y.; Kitao, O.; Nakai, H.; Vreven, T.; Montgomery, J. A. Jr.,;

Peralta, J. E.; Ogliaro, F.; Bearpark, M.; Heyd, J. J.; Brothers, E.; Kudin, K. N.; Staroverov, V. N.; Keith, T.; Kobayashi, R.; Normand, J.; Raghavachari, K.; Rendell, A.; Burant, J. C.; Iyengar, S. S.; Tomasi, J.; Cossi, M.; Rega, N.; Millam, J. M.; Klene, M.; Knox, J. E.; Cross, J. B.; Bakken, V.; Adamo, C.; Jaramillo, J.; Gomperts, R.; Stratmann, R. E.; Yazyev, O.; Austin, A. J.; Cammi, R.; Pomelli, C.; Ochterski, J. W.; Martin, R. L.; Morokuma, K.; Zakrzewski, V. G.; Voth, G. A.; Salvador, P.; Dannenberg, J. J.; Dapprich, S.; Daniels, A. D.; Farkas, O.; Foresman, J. B.; Ortiz, J. V.;Cioslowski, J.; Fox, D. J. Gaussian, Inc., Wallingford CT, **2010**.

Chapter 4 Photo-isomerization, and retro-cyclization of 1,4,2-diazaboroles†

4.1 Introduction

Organoboron compounds have been widely utilized as building blocks in the synthesis of optoelectronic materials, as well as the fabrication of optoelectronic devices, which is mainly due to the electron-deficient properties of the boron atom serving as an excellent π-acceptor in the conjugated molecules.[1] Although many studies have been focused on their applications in the π systems, the photo-isomerization of organoboron compounds are rarely explored (Scheme 4.1). Among them, detailed investigations on the photo-isomerization of the N,C-, C,C-chelate boron compounds have been carried out by Wang group.[2] In 2008, they discovered that the colorless four-coordinate organoboron **I** underwent a photo-isomerization process to generate the dark blue compound **II** via intramolecular C–C bond formation. Interestingly, **II** can be fully converted back to the starting material **I**. which represents the first example of reversible photo-thermal color switching of organoboron (Scheme 4.1a).[2a] Moreover, it was found that the reversible conversion properties of organoboranes could be affected by replacement of the pyridyl moiety with other donors such as carbenes[2c] and azoles,[2d,e] or modification of the aryl groups with various substitutes.[2b,f,g] These different results mainly due to the change of their electronic structures and the steric congestion around the boron center. In 2012, Piers et al. reported the synthesis of the first ladder diborole **IV** by photo-isomerization of the boracylo-

† Portions of this chapter are taken with permission from: Su, B.; Li, Y.; Ganguly, R.; Kinjo, R. *Angew. Chem. Int. Ed.* **2017**, *56*, 14572 – 14576.

butylidene **III**, where the photo-induced hemolytic cleavage of B–C bond is the key step (Scheme 4.1b).[3] In 2013, Yamaguchi et al. discovered the first bora-Nazarov cyclization product **VI** in the photoreaction of the borylated dibenzoborepin **V**, along with a color change from colorless to navy blue (Scheme 4.1c).[4] Interestingly, the photoproduct **VI** could be thermally converted to the starting borepin **V**. Later, the same group discovered a different photoisomerization mode of dimesitylboryl-substituted (hetero)arenes (Scheme 4.1d).[5] Under irradiation of UV light, the boron species **VII** underwent a formal intramolecular C–H bond addition to afford the unprecedented spirocyclic boraindanes **VIII**. Most likely, this process involves a [1,6]-sigmatropic hydrogen rearrangement, which may result from a significant contribution of the vacant p orbital of the boron atom. Very recently, Xie et al. reported a reversible photothermal isomerization between carborane-fused azaborole **IX** and borirane **X**, which provided a new strategy to prepare carborane-fused three-membered-ring containing the main group elements (Scheme 4.1e).[6] In 2017, Braunschweig et al. described a photo-induced ring-contraction of (*cis*)1,2-dihydrodiborane(4)s **XI** and **XIV** (Scheme 4.1f).[7] Under irradiation of UV light, both diboranes **XI** and **XIV** formed the corresponding *1H*-1,3,2-diazaboroles **XII** and **XV**. Furthermore, in contrast to **XIV** the irradiation of **XI** in the presence of PEt_3 led to the formation of the first unsymmetrical 1,1-dihydrodiborane(5) **XIII**. Although several types of photoreactions of boron-containing compounds have been reported until now, the photo-controlled structural transformation of the organoboron compounds remains extremely rare. In this chapter, we show a variety of transformation of the BN-heterocycle framework of 1,4,2-diazaborole derivatives via photo-isomerization and retro-cyclization reactions.

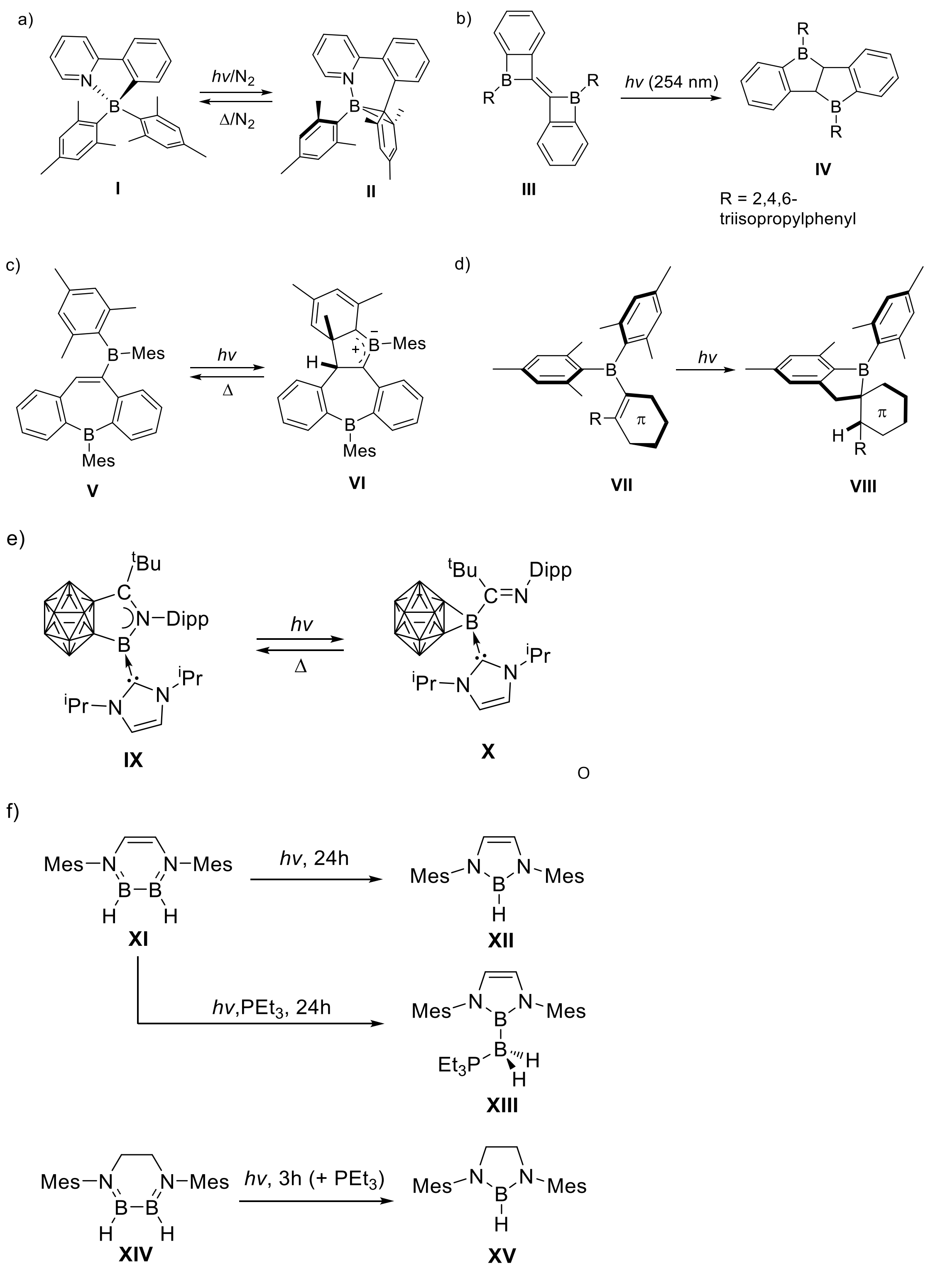

Scheme 4.1 Photo-induced reactions of the organoboranes.

4.2 Results and Discussions

Compound **1** and **3** were prepared following the procedure described in chapter 3. Upon irradiation of a benzene solution of **1** with the Hg(Xe) light, the reaction process was monitored by ^{11}B NMR spectroscopy, which showed that two new signals gradually appeared at 32.4 ppm and 19.7 ppm (Scheme 4.2). After work-up, single crystals of **2** were obtained in 30% yield by slow evaporation of a diethyl ether solution at room temperature, and the solid-state structure was confirmed by X-ray analysis (Figure 4.1). While the BN_2C_3 six-membered ring retains the origin geometry, the skeletal rearrangement of the BN_2C_2 five-membered ring is confirmed. All the five atoms in the BN_2C_2 ring are coplanar with the sum of the internal angles of 539.9°. The bond lengths of B1–N1 (1.415(4) Å) and B1–N2 (1.397(4) Å) are comparable to those (1.41–1.43 Å) of the reported 1,3,2-diazaboroles.[8] The C1–C2 bond distance of 1.376(4) Å falls in the range of typical C=C double bond distances. DFT calculation on **2** shows that the HOMO is mainly π orbital of the N1–B1–N2 moiety, which exhibits an antibonding conjugation with the π orbital of the C1–C2 unit (Figure 4.2a). The LUMO consists of the π^* orbital of the C_2N_2B ring with the combination of the π-bonding orbitals of B-N unit in the six-membered ring (Figure 4.2b). NICS values (NICS(0) = – 8.42 and NICS(1) = – 5.49) for the BN_2C_2 five-membered ring of **2** are slightly less negative than those (NICS(0) = – 8.77 and NICS(1) = – 6.36) of **1**, suggesting its partial aromatic property. Although the photo-induced ring contraction of BN-aromatic has been described,[7] the ring rearrangement has never been documented to date. The detailed mechanism of the photo-isomerization of **1** to **2** is still unclear.

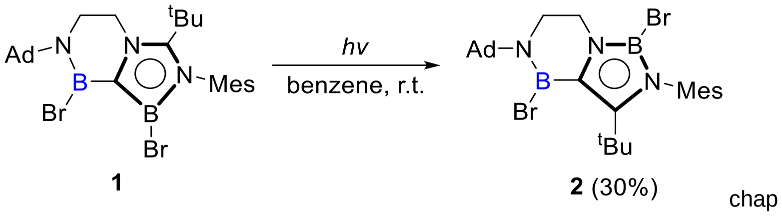

Scheme 4.2 Photo-isomerization reactions of **1**.

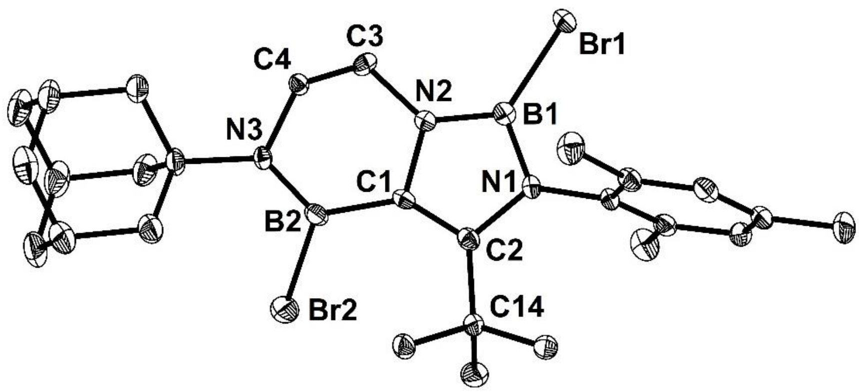

Figure 4.1 The solid-state structure of **2** (hydrogen atoms are omitted for clarity). Thermal ellipsoids are set at the 50% probability.

a)

b)

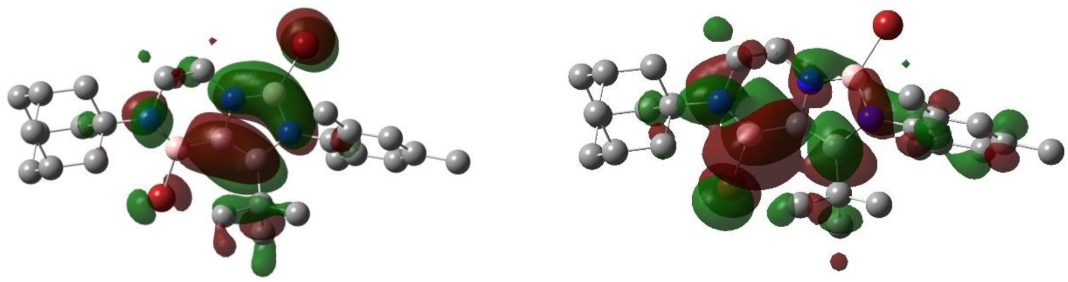

HOMO (–5.3503 eV)

LUMO (–0.7124 eV)

Figure 4.2 The plots of the HOMO (a) and LUMO (b) of **2**

Inspired with the photo-isomerization of **1**, we investigated the photoreaction of **3** as well. Irradiation of a benzene solution of **3** with Hg(Xe) light led to the formation of new species **4** in 52% yield (Scheme 4.3), which was confirmed by multiple NMR spectroscopy and X-ray diffraction analysis. In the ^{11}B NMR spectrum, a singlet appears at 2.25 ppm, which is slightly shifted upfield compared with that (9.60 ppm) of **3**. The solid-state molecular structure confirms the formation of the new bicyclic framework via migration of the CH_2-CH_2 unit in the C_3N_2 ring of **4**, which is in sharp contrast to the result from the photo-isomerization of **1** (Scheme 4.2). The solid-state molecular structure is depicted in Figure 4.4a, the B1–N1 bond distance of 1.541 Å is much longer than that (1.460(6) Å) of **3** and comparable with those (1.573(13) Å, 1.580(6) Å) of $NHCBBr_2^+[BBr_4]^-$ and $NHCBBr_2^+[BBr(OTf)_3]^-$ reported in chapter 2, indicating a typical dative bonding character. The bond lengths for N3–C2 (1.309(4) Å), C2–N2 (1.353(4) Å), N2–C1 (1.357(4) Å), C1–N1 (1.350(4) Å) are intermediate between those of a single and a double bond, indicating the partial double bound character. The sum angles of 359.5° around the N3 atom support its nearly planar geometry, thus indicating the delocalization of the lone pair of the N3 atom on the N3-C2-N2-C1-N1 π-system. To get a deeper understanding of the electronic structure of **10**, the computational studies were performed (Figure 4.4b). The HOMO is mainly the π-type orbitals on the N3-C2-N2-C1-N1 unit with some combination of π orbitals of the Mes group. WBI values (1.36, 1.32, 1.33, 1.35) larger than 1 for N3–C2, C2–N2, N2–C1, C1–N1 also support their partial double bond character. **4** is a rare example of 1,3-azaborolidin-2-imine derivative involving the intramolecular N→B coordination.

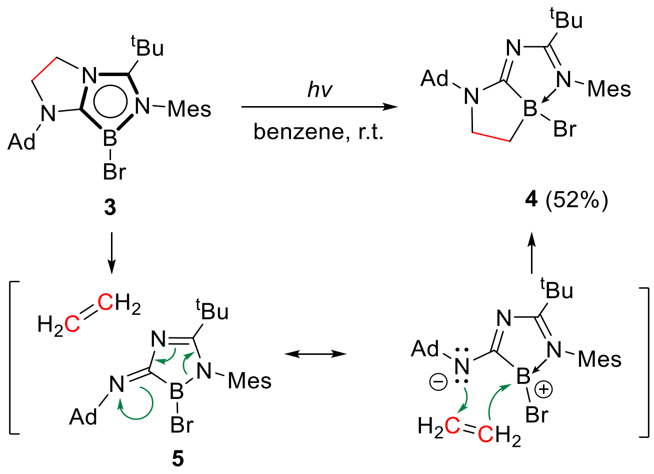

Scheme 4.3 Photo-isomerization of **3**

a)

b)

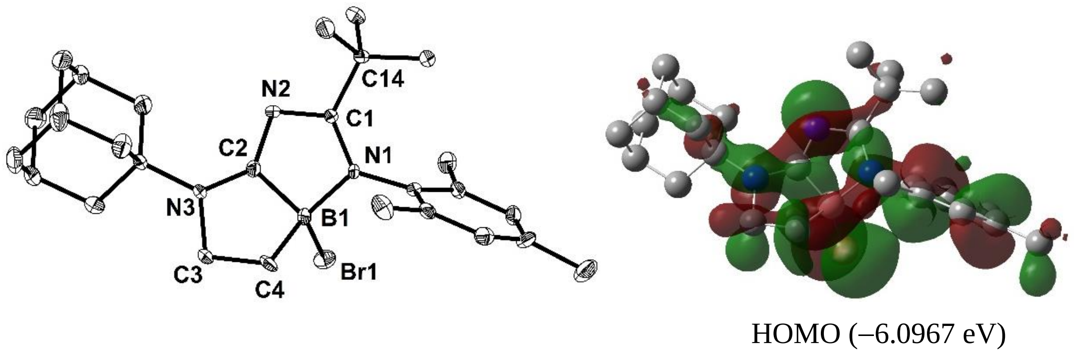

Figure 4.4 a) Solid-state structure of **4** (hydrogen atoms are omitted for clarity). Thermal ellipsoids are set at the 50% probability. b) The plot of the HOMO of **4**.

The proposed mechanism for the formation of **4** is as follows (Scheme 4.3): (i) Initially, **4** undergoes the photo-induced retro-[2+3]-cycloaddition to generate 1,4,2-diazaborol-3-imine intermediate **5** and ethylene. (ii) Subsequent 1,3-dipolar cycloaddition between **5** and ethylene occurs to form **4**. We postulated that the 1,3-dipolar cycloaddition step could possibly be prevented by installing a bulkier group on the boron, which would allow detection of intermediate **5**. To test the hypothesis, we carried out the photo-reaction employing **6** bearing a bulky Mes group on the B atom, which was prepared in chapter 2. Upon the irradiation of a benzene solution of **6**, the color turned to greenish yellow from pale yellow (Scheme 4.4). In the ^{1}H NMR spectrum, a singlet corresponding to ethylene was observed at 5.25 ppm whereas the ^{11}B NMR showed a new broad peak for the product **7** around 48.6 ppm, which is significantly shifted downfield in comparison with that (18.4 ppm) of **6**.

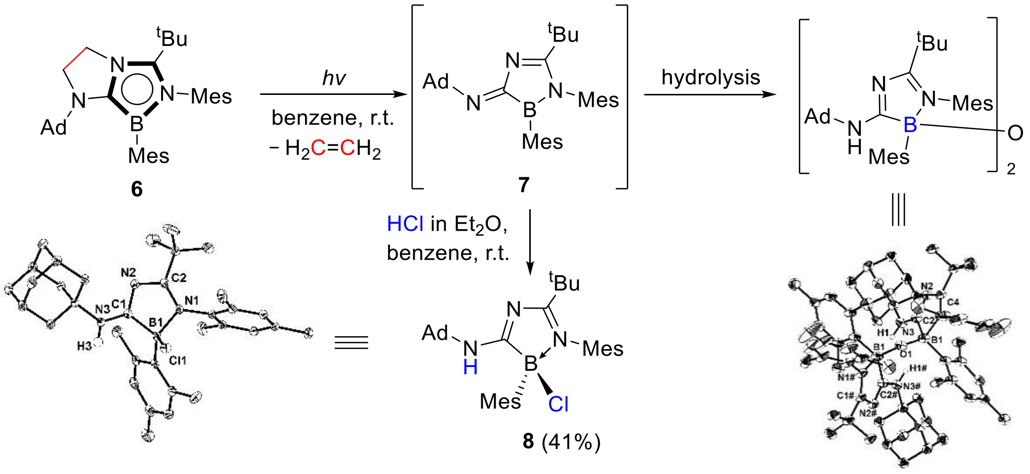

Scheme 4.4 Retro-cyclization of **6**, hydrolysis and the trapping reaction of **7** with HCl

The product **7**, which is an isoelectronic with fulvene,[9] is thermally highly stable with no signs of decomposition even heating to 100 °C, but extremely moisture sensitive, which has impeded its isolation. After the hydrolysis of **7**, a diboron species with a bridging oxygen atom was observed. Meanwhile, the chemical trapping of **7** with HCl proceeded cleanly, and the corresponding adduct **8** was obtained in 41% yield. An X-ray diffraction study confirms the loss of -CH_2-CH_2- unit on the N2 and N3 atoms, as well as, the addition of a proton and chloride to the N3 atom and B1 atom, respectively, supporting the formation of **7** by the photo-reaction of **6**.

4.3 Summary

In conclusion, we have demonstrated the photo-induced skeletal transformation of the B,N-heterocyclic 1,4,2-diazaborole derivative. The photo-reactions of **1** and **3** lead to the formation of the corresponding skeletal isomer **2** and **4**. The former is formed via the rearrangement of the BN_2C_2 five-membered ring of **1**. By contrast, the latter results from retro-cyclization of the N_2C_3 five-membered ring of **3** followed by 1,3-dipolar cycloaddition, in line with the generation of **7** by photolysis of **6**.

4.4 Experimental Sections

4.4.1 Synthesis of compounds 2, 4, 7, and 8 and their spectral data

General considerations: All reactions were performed under an atmosphere of argon or nitrogen by using standard Schlenk or dry box techniques; solvents were dried over Na metal, K metal, or CaH_2. Reagents were of analytical grade, obtained from commercial suppliers and used without further purification. ^{1}H, ^{13}C and ^{11}B NMR spectra were obtained with a Bruker AVIII 400MHz BBFO1 spectrometer at 298 K unless otherwise stated. NMR multiplicities are abbreviated as follows: s = singlet, d = doublet, t = triplet, m = multiplet, br = broad signal. Coupling constants J are given in Hz. Electrospray ionization (ESI) mass spectra were obtained at the Mass Spectrometry Laboratory at the Division of Chemistry and Biological Chemistry, Nanyang Technological University. Melting points were measured with an OpticMelt Stanford Research System. Compound 1 and 3 was prepared following the procedures reported in chapter 2 and 3.

Compound 2: Compound **1** (0.30 g, 0.51 mmol) was dissolved in benzene and placed under Hg (Xe) light. The reaction was monitored by means of ^{11}B NMR spectroscopy. After compound **1** was fully consumed, all the volatiles were removed under vacuum. The residue was extracted with Et_2O, and then slow evaporation of the Et_2O solution at room temperature afforded the isomerized product as the colorless crystals (0.09 g, 30%). M.p.: 113 °C (dec.); ^{1}H NMR (C_6D_6, 400 MHz, 298 K): δ 6.78 (s, 2H, *m*-C*H*), 3.33 (m, 2H, NCH_2), 2.85–2.83 (m, 2H, NCH_2), 2.21 (s, 6H, *o*-CH_3), 2.12 (s, 3H, *p*-CH_3), 2.07 (m, 6H, Ad–CH_2), 1.93 (m, 3H, Ad–C*H*), 1.51 (m, 15H, Ad–CH_2 &(CH_3)$_3$); $^{13}C\{^{1}H\}$ NMR (C_6D_6, 100 MHz, 298 K): 146.2 (*C*-^{t}Bu), 139.1 (C_{Ar}), 136.4 (C_{Ar}), 136.3 (C_{Ar}), 129.4 (C_{Ar}), 59.1 (Ad–*q*), 46.2 (NCH$_2$), 46.1 (NCH$_2$), 42.2 (Ad–CH$_2$), 36.5 (Ad–CH$_2$), 34.9 (C(CH$_3$)$_3$), 32.8 (C(CH$_3$)$_3$), 30.6 (Ad–CH), 21.0 (*p*-CH$_3$), 19.0 (*o*-CH$_3$); ^{11}B NMR (128.3 MHz, C_6D_6): δ 32.36 (br, NB(Br)C), 19.74 (NB(Br)N); HRMS (ESI): *m/z* calcd for $C_{27}H_{40}B_2Br_2N_3$: 586.1775. [(*M*+*H*)]$^+$; found: 586.1763.

Compound 4: Compound **3** (0.45 g, 0.91 mmol) was dissolved in benzene and placed under Hg (Xe) light. The reaction was monitored by means of ^{11}B NMR spectroscopy. After compound **3** was fully consumed, all the volatiles were removed under vacuum. The residue was extracted with hexane, and then the solvent was removed to afford a slightly brown solid (0.23 g, 52%). Colorless single crystals suitable for X-ray diffraction studies were grown by slow evaporation of a toluene solution at –26 ºC. M.p.: 147 ºC (dec.); ^{1}H NMR (C_6D_6, 400 MHz, 298 K): δ 6.72 (s, 1H, Mes), 6.71 (s, 1H, Mes), 4.18–4.12 (m, 1H, NCH_2), 3.49–3.45 (m, 1H, NCH_2), 2.63 (s, 3H, *o*-CH_3), 2.19–2.16 (m, 6H, Ad–CH_2&*o*-CH_3), 2.08 (s, 3H, *p*-CH_3), 1.90–1.87 (m, 6H, Ad–CH_2&Ad–CH), 1.57–1.44 (m, 8H, B–CH_2&Ad–CH_2), 1.18 (s, 9H, (CH_3)$_3$); ^{13}C{^{1}H} NMR (C_6D_6, 100 MHz, 298 K): δ 192.3 (C=N-Mes), 138.5 (C_{Ar}), 136.1 (C_{Ar}), 136.0 (C_{Ar}), 134.6 (C_{Ar}), 130.0 (C_{Ar}), 129.0 (C_{Ar}), 58.7 (Ad–*q*), 56.8 (NCH$_2$), 40.3 (Ad–CH$_2$), 39.8 (C(CH$_3$)$_3$), 36.3 (Ad–CH$_2$), 29.8 (Ad–CH&(C(CH$_3$)$_3$, overlapped), 21.6 (Ar–CH$_3$), 20.9 (Ar–CH$_3$), 19.8 (Ar–CH$_3$); ^{11}B NMR (128.3 MHz, C_6D_6): δ 2.25 (s, BBr); HRMS (ESI): *m/z* calcd for $C_{27}H_{40}BBrN_3$: 496.2499. [(*M*+*H*)]$^+$; found: 496.2493.

Compound 7: Compound **6** (11 mg, 0.02 mmol) was dissolved in C_6D_6 in a J-Young NMR tube and then placed under Hg (Xe) light. The reaction was monitored by means of ^{1}H NMR spectroscopy. Under the irradiation, the solution changed from pale yellow to deeper green-yellow. After compound **7** was fully consumed, compound **7** was generated nearly quantitatively. However, **7** is extremely air- and moisture sensitive, which impeded its purification and isolation. ^{1}H NMR (C_6D_6, 400 MHz, 298 K): δ 6.56 (s, 2H, Mes), 6.50 (s, 2H, Mes), 2.61 (s, 6H, Ad–CH_2), 2.19 (m, 9H, *o*-CH_3&Ad–C*H*), 2.03 (s, 6H, *o*-CH_3), 2.01 (s, 3H, *p*-CH_3), 1.94 (s, 3H, *p*-CH_3), 1.89–1.85 (m, 3H, Ad–CH_2), 1.73–1.70 (m, 3H, Ad–CH_2), 1.19 (s, 9H, (CH_3)$_3$); ^{13}C{^{1}H} NMR (C_6D_6, 100 MHz, 298 K): δ 180.9 (*C*-^{t}Bu), 140.4 (C_{Ar}), 138.1 (C_{Ar}), 137.8 (C_{Ar}), 136.6 (C_{Ar}), 135.2 (C_{Ar}), 129.5 (C_{Ar}), 127.9 (C_{Ar}), 60.3 (Ad–*q*), 44.4 (Ad–*C*H_2), 38.2 (*C*(CH_3)$_3$), 37.4 (Ad–*C*H_2), 30.7 (Ad–*C*H), 29.8 (C(*C*H_3)$_3$), 23.8 (*o*-*C*H_3), 21.1 (*p*-*C*H_3), 20.8 (*p*-*C*H_3) 19.7 (*o*-*C*H_3); ^{11}B NMR (128.3 MHz, C_6D_6): δ 48.55 (s, *B*Mes)*. (*the calculated ^{11}B NMR chemical shift for the computationally optimized molecule **7** is 48.05 ppm at the B3LYP/6-311G(d,p) level of theory, in line with the experimental observation).

Compound 8: A diethyl ether solution of hydrogen chloride (2.0 M, 327 uL) was added at room temperature to a benzene solution of compound **7** which was directly obtained from compound **6** (350 mg, 0.65 mmol) by irradiation of UV light. The mixture was stirred overnight, and then all the solvents were removed under vacuum. The resulting solid was extracted with pentane (2 x 10 mL) and the filtrate was dried under vacuum to yield the targeted product (145 mg, 41%). Single crystals suitable for X-ray analysis were obtained by slow evaporation of a mixture of pentane and hexane solution of **8** at –26°C. M.p.: 119 °C; ^{1}H NMR (C_6D_6, 400 MHz, 298 K): δ 6.88 (s, 1H, Mes), 6.80 (s, 1H, Mes), 6.77 (s, 1H, Mes), 6.48 (s, 1H, Mes), 5.92 (s, 1H, N*H*), 2.64 (s, 3H, Ar–CH_3), 2.48 (s, 3H, Ar–CH_3), 2.33 (s, 3H, Ar–CH_3), 2.18 (s, 3H, Ar–CH_3), 2.06–2.05 (m, 6H, Ad–CH_2& Ar–CH_3), 1.91 (s, 3H, Ad–CH), 1.61 (s, 3H, Ar–CH_3), 1.57–1.48 (m, 6H, Ad–CH_2), 1.20 (s, 9H, (CH_3)$_3$); ^{13}C{^{1}H} NMR (C_6D_6, 100 MHz, 298 K): δ 188.5 (C-^{t}Bu), 146.7 (C_{Ar}), 141.3 (C_{Ar}), 137.7 (C_{Ar}), 136.5 (C_{Ar}), 136.4 (C_{Ar}), 136.3 (C_{Ar}), 135.0 (C_{Ar}), 131.0 (C_{Ar}), 129.5 (C_{Ar}), 128.9 (C_{Ar}),55.0 (Ad–q), 41.2 (Ad–CH$_2$), 39.3 (C(CH$_3$)$_3$), 36.3 (Ad–CH$_2$), 29.9 (C(CH$_3$)$_3$), 29.4 (Ad–CH), 25.7 (Ar–CH$_3$), 24.9 (Ar–CH$_3$), 21.1 (Ar–CH$_3$), 20.9 (Ar–CH$_3$), 20.8 (Ar–CH$_3$), 18.6(Ar–CH$_3$); ^{11}B NMR (128.3 MHz, C_6D_6): δ 3.49 (s, BMes); HRMS (ESI): m/z calcd for $C_{34}H_{48}BClN_3$: 544.3630. [(M+H)]$^+$; found: 544.3620.

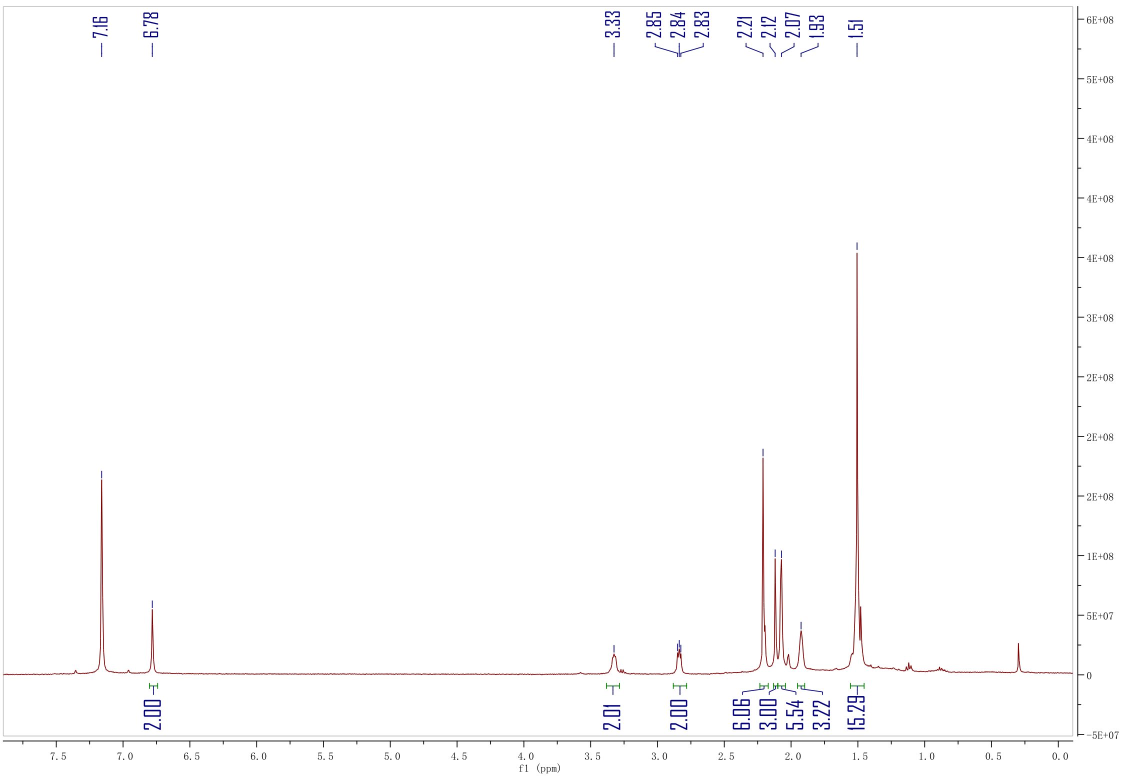

Figure 4.5 ^{1}H NMR spectrum of **2**.

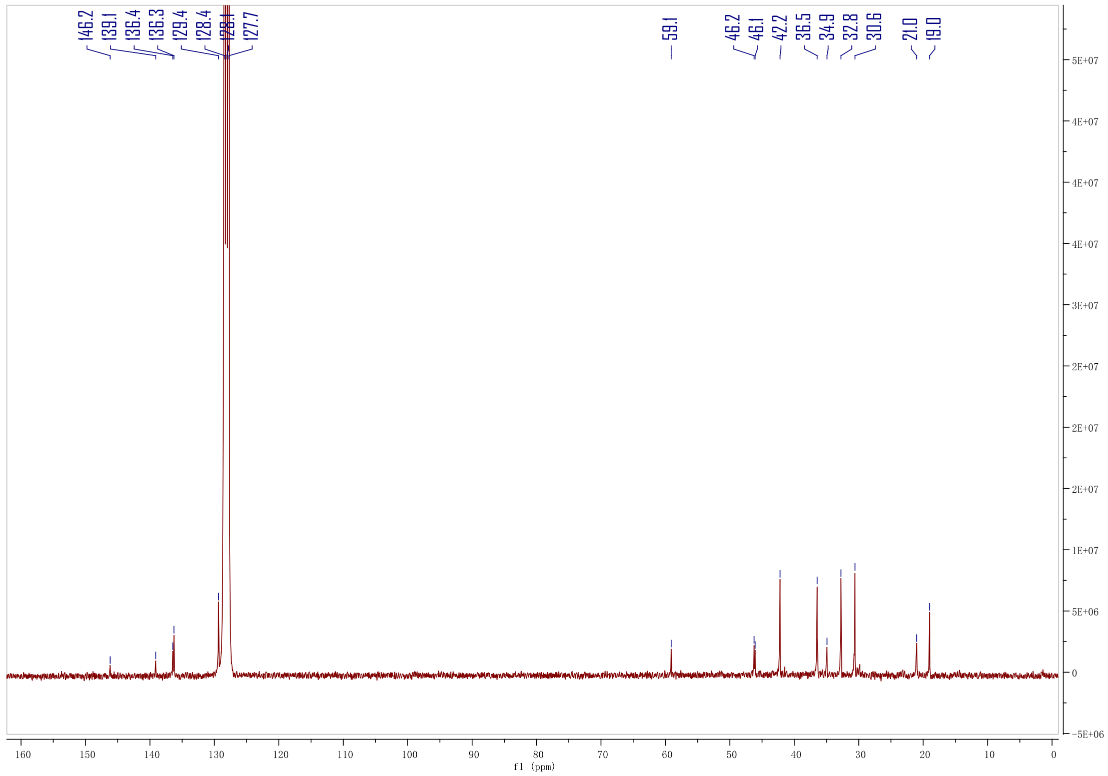

Figure 4.6 $^{13}C\{^{1}H\}$ NMR spectrum of **2**.

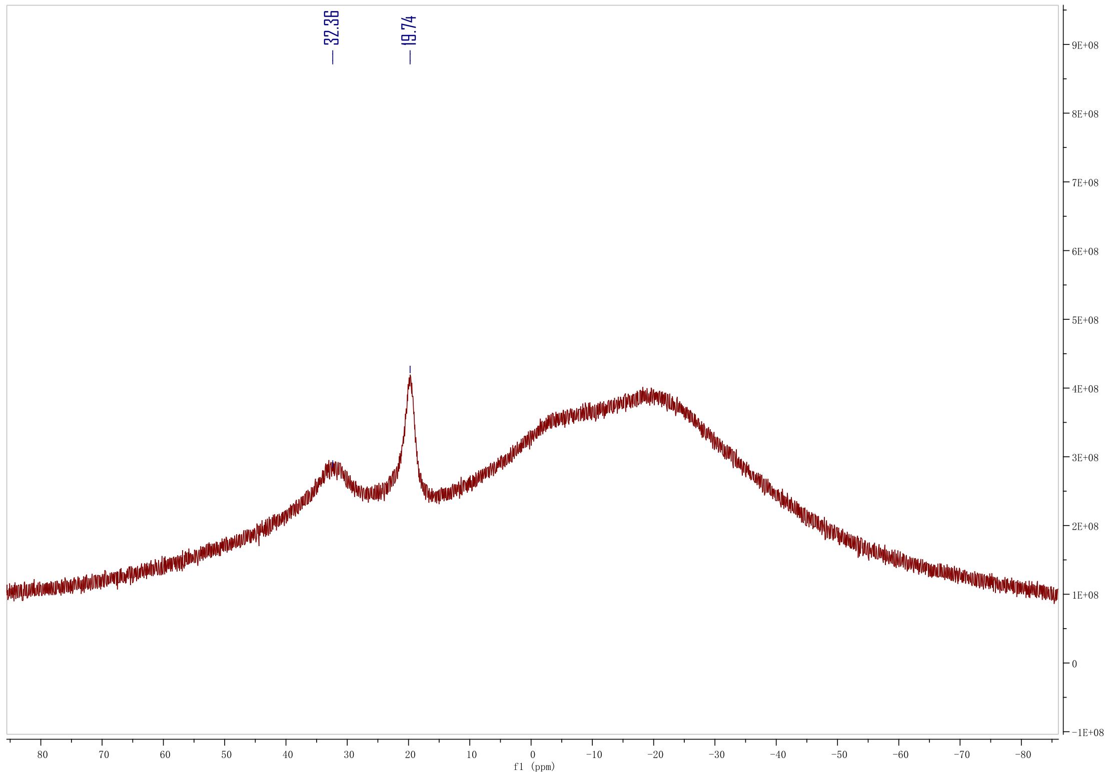

Figure 4.7 ^{11}B NMR spectrum of **2**.

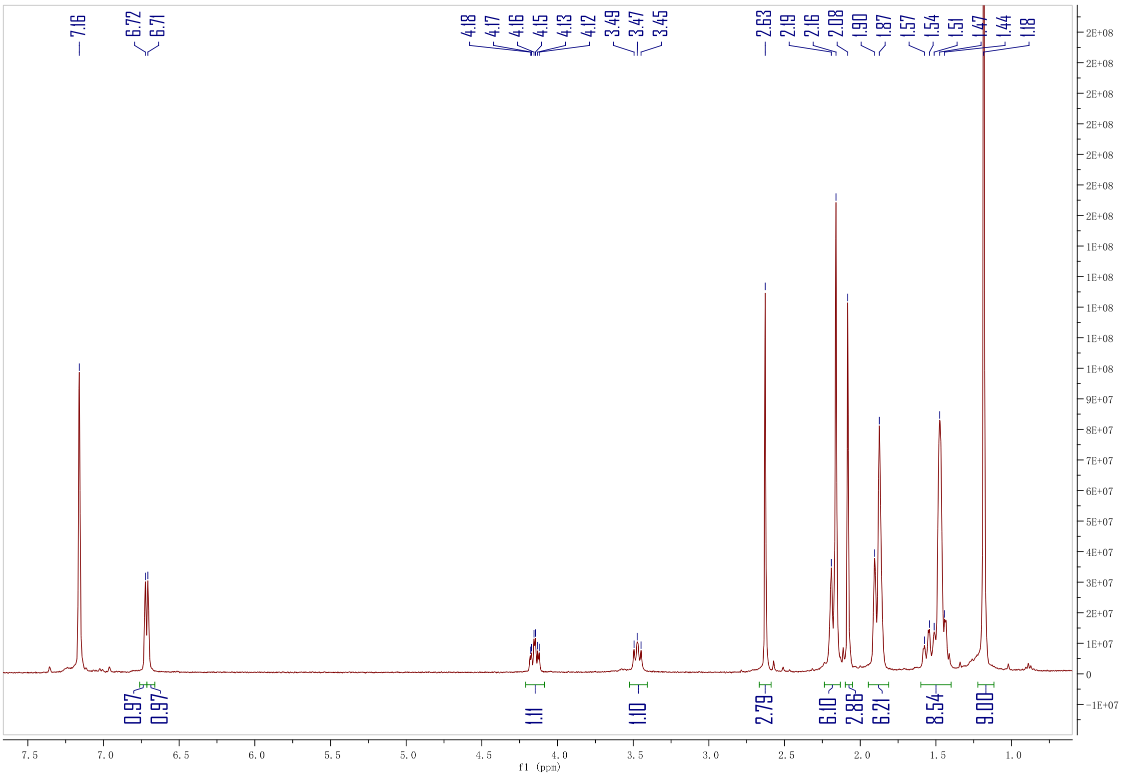

Figure 4.8 ^{1}H NMR spectrum of **4**.

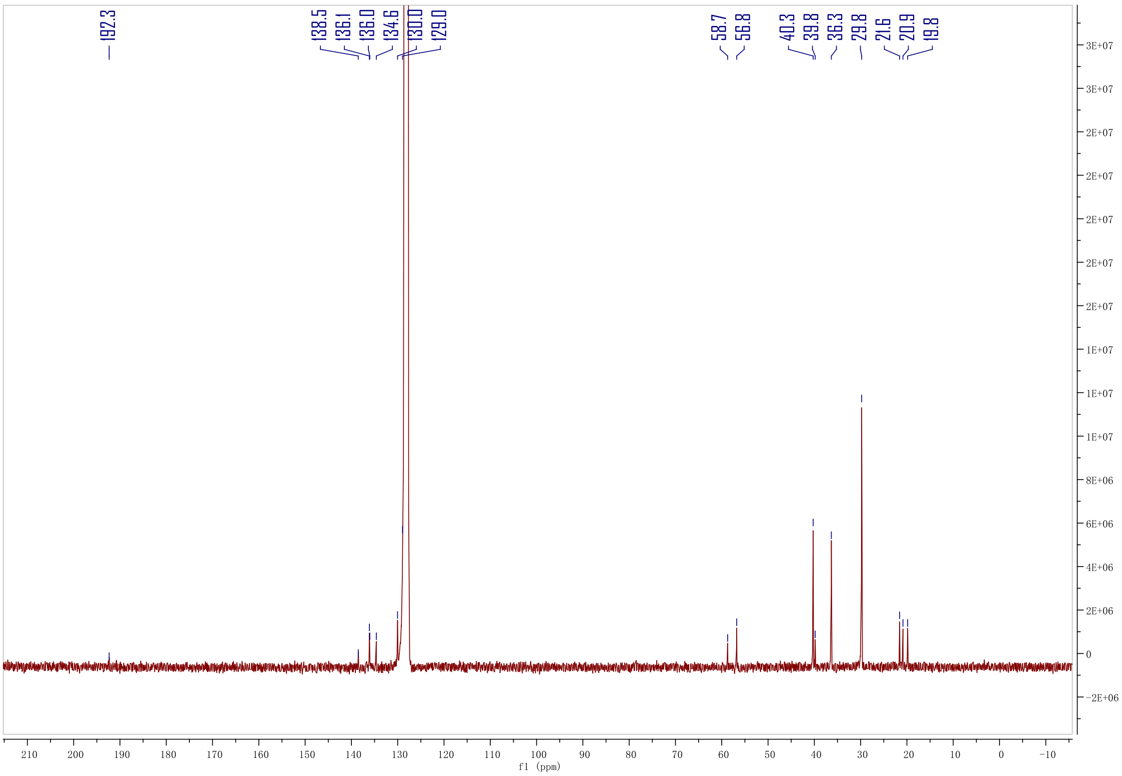

Figure 4.9 $^{13}C\{^{1}H\}$ NMR spectrum of **4**.

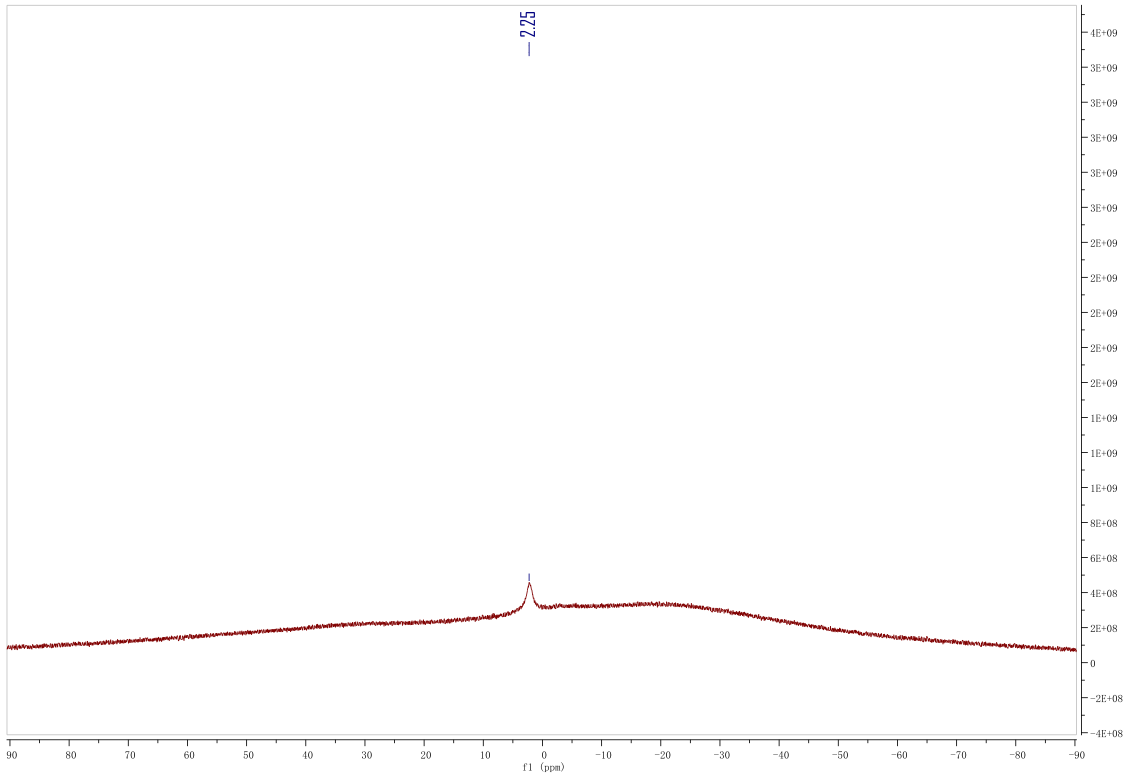

Figure 4.10 [11]B NMR spectrum of **4**.

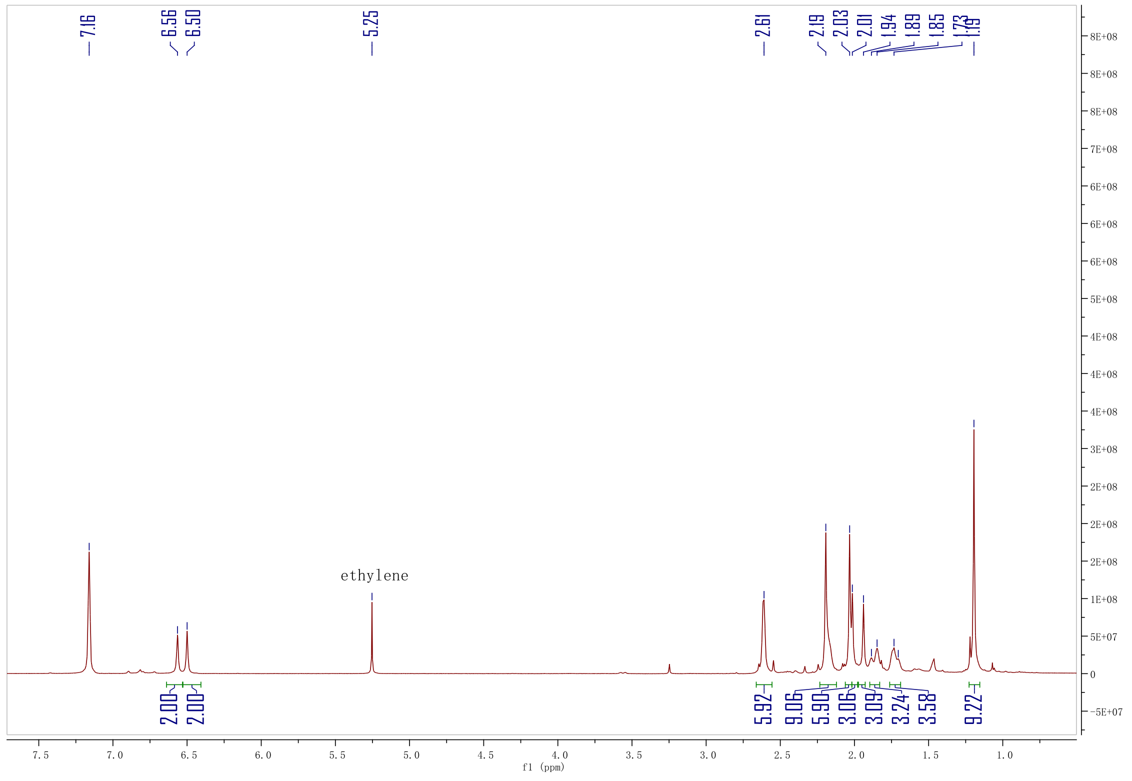

Figure 4.11 [1]H NMR spectrum of **7**.

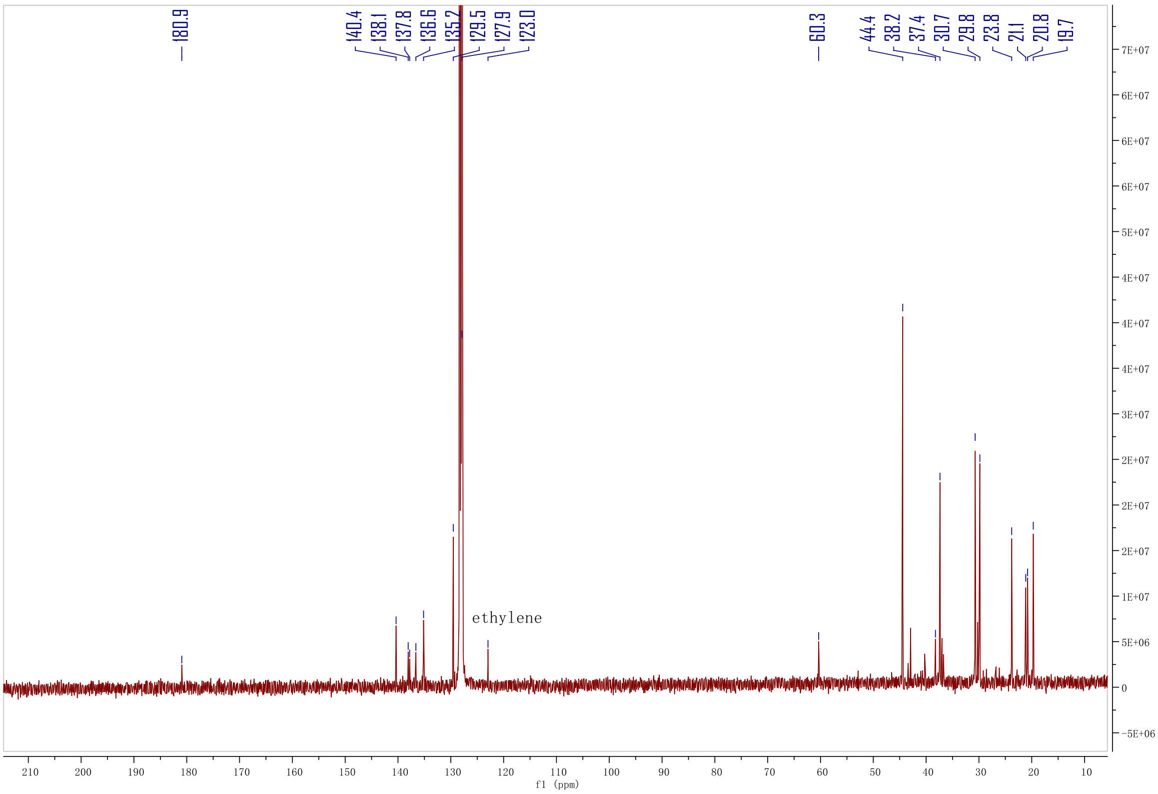

Figure 4.12 $^{13}C\{^{1}H\}$ NMR spectrum of **7**.

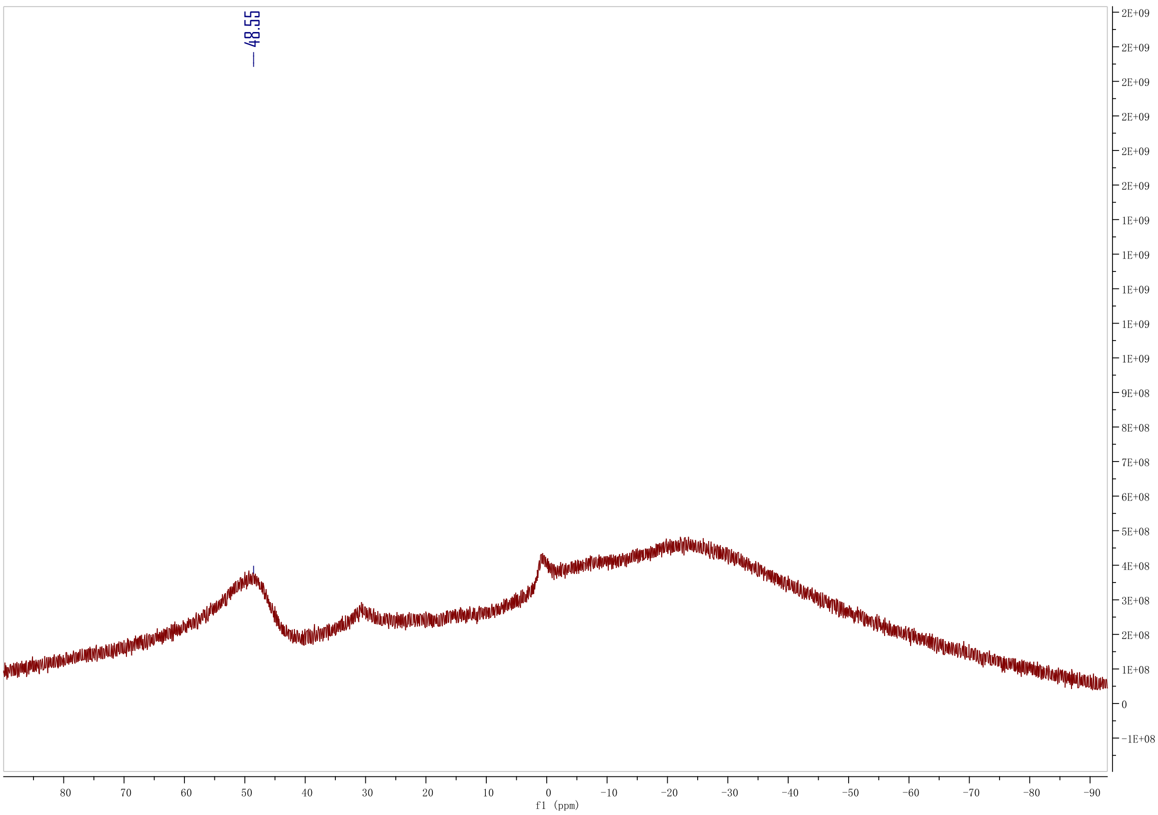

Figure 4.13 ^{11}B NMR spectrum of **7**.

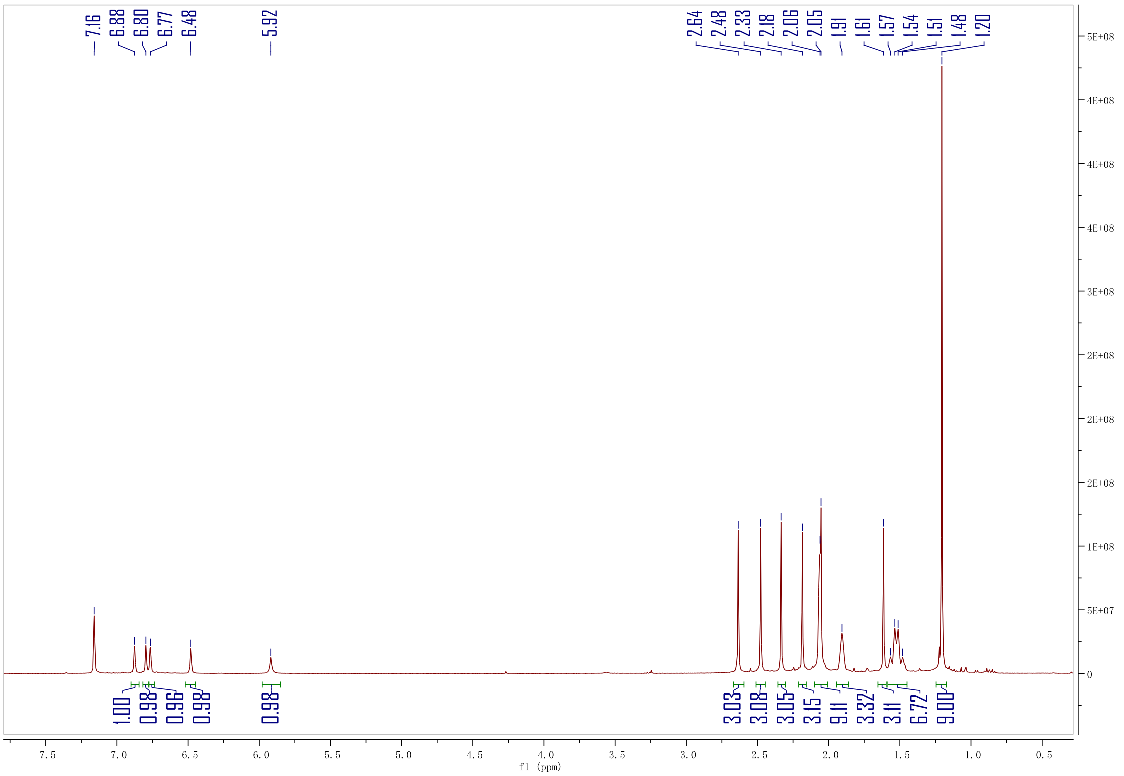

Figure 4.14 ^{1}H NMR spectrum of **8**.

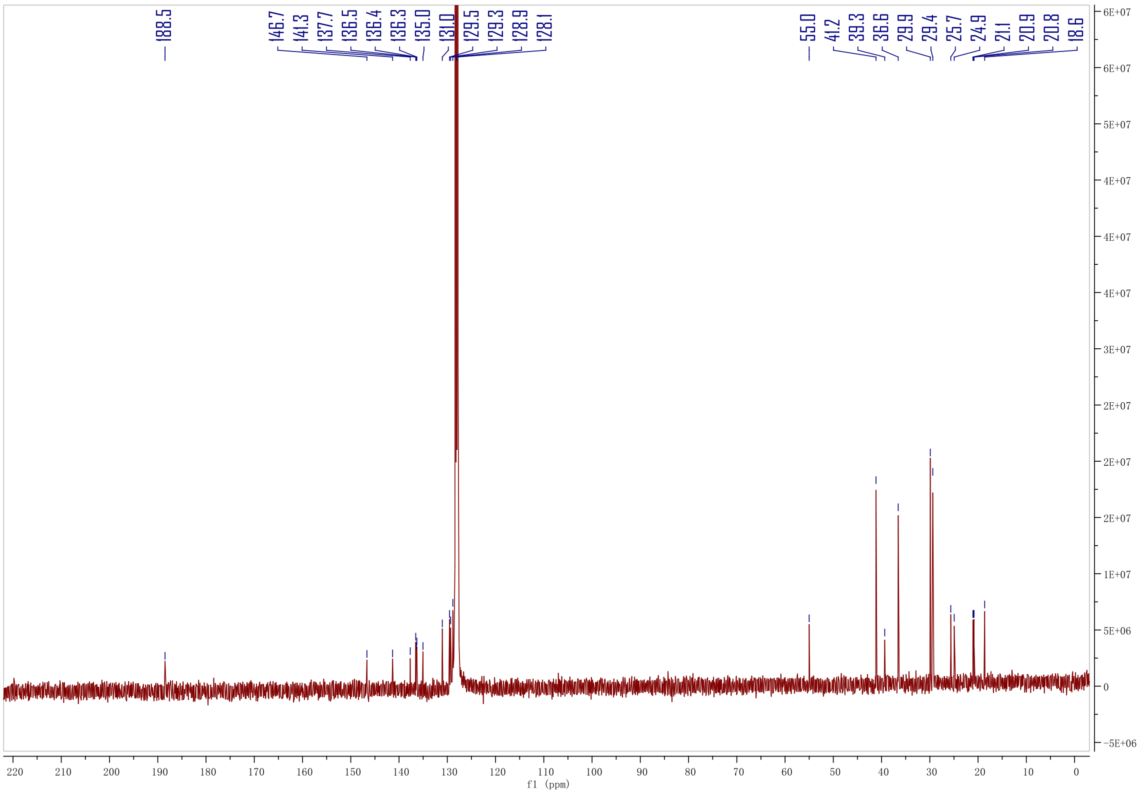

Figure 4.15 $^{13}C\{^{1}H\}$ NMR spectrum of **8**.

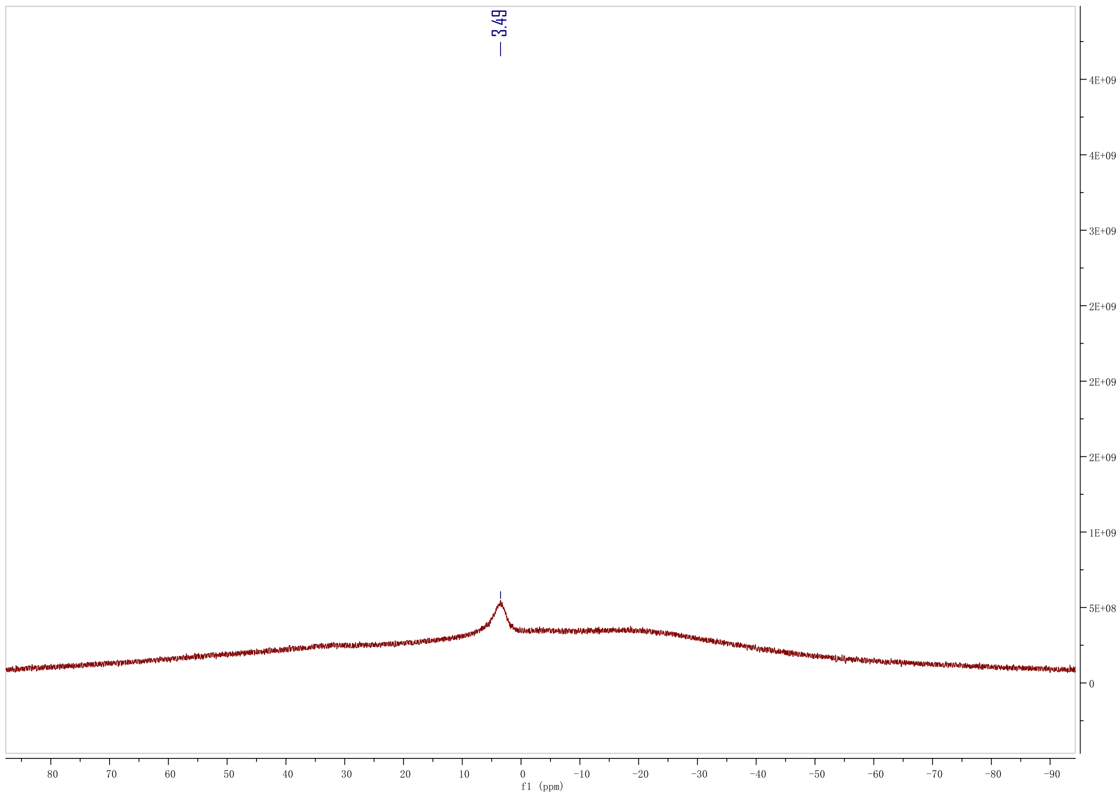

Figure 4.16 ^{11}B NMR spectrum of **8**.

4.4.2 Crystal structure parameters

X-ray data collection and structural refinement. Intensity data for compounds **2**, **4** and **8** was collected using a Bruker APEX II diffractometer. The structure was solved by direct phase determination (SHELX-2013) and refined for all data by full-matrix least squares methods on *F2*.[10] All non-hydrogen atoms were subjected to anisotropic refinement. The hydrogen atoms were generated geometrically and allowed to ride in their respective parent atoms; they were assigned appropriate isotropic thermal parameters and included in the structure-factor calculations. CCDC; 1570552-1570554 contains the supplementary crystallographic data. The data can be obtained free of charge from the Cambridge Crystallography Data Center via www.ccdc.cam.ac.uk/data_request/cif.

Table 4.1 Crystallographic data for **2**, **4** and **8**.

Compounds	**2**	**4**	**8**
Formula	$C_{27}H_{39}BBrN_3$	$C_{27}H_{39}BBrN_3$	$C_{34}H_{47}BClN_3$
Fw	496.33	496.33	544.00
Cryst syst	monoclinic	monoclinic	monoclinic
Space group	*C*2/*c*	*C*2/*c*	$P2_1/n$
Size (mm^3)	0.140 x 0.180 x 0.200	0.140 x 0.180 x 0.200	0.204 x 0.326 x 0.535
T, K	103(2)	103(2)	100(2)
a, Å	21.8149(16)	21.8149(16)	9.2439(2)
b, Å	16.4503(10)	16.4503(10)	18.8273(4)
c, Å	13.9374(9)	13.9374(9)	18.3925(4)
β, deg	92.191(2)	92.191(2)	104.4806(7)
V, Å^3	4997.9(6)	4997.9(6)	3099.30(12)
Z	8	8	4
d_{calcd} g·cm^{-3}	1.319	1.319	1.166
, mm^{-1}	1.665	1.665	0.150
Refl collected	12659	12659	83688
T_{max}/T_{min}	0.8000/0.7320	0.8000/0.7320	0.9700/0.9240
N_{measd}	6630	6630	7085
[R_{int}]	0.0929	0.0929	0.0426
R [I>2sigma(I)]	0.0671	0.0671	0.0424
R_w[I>2sigma(I)]	0.1747	0.1747	0.1078
GOF	1.095	1.095	1.046
Largest diff. peak/hole[e·Å^{-3}]	1.310/-1.063	1.310/-1.063	0.396/-0.391

4.4.3 Theoretical calculation

Gaussian 09 was used for all density functional theory (DFT) calculations.[11] Geometry optimization, frequency calculations, and Natural bond orbital (NBO) analysis on compound **2** and **4** were performed at the B3LYP/6-311G(d,p) level of theory.

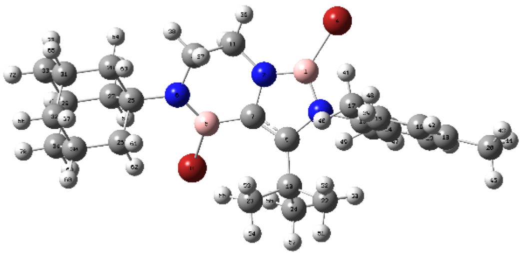

2

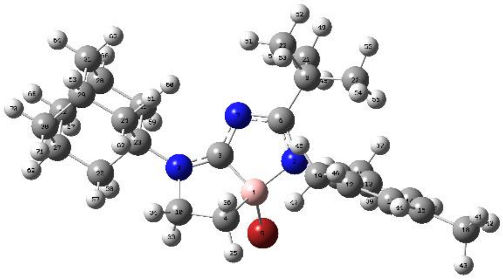

4

Figure 4.17 Calculated optimized structures for **2** and **4** at the B3LYP/6-311G(d,p) level of theory.

Table 4.2 Optimized structures of **2** and **4** (atom, x-, y-, z- positions in Å)

2

B	1.854270	1.409406	-0.340812
N	0.465796	1.271335	-0.471640
N	2.354019	0.122356	0.031958
Br	2.881667	3.037119	-0.622117
B	-1.425472	-0.352587	-0.379336
N	-2.353030	0.657070	-0.032586
C	0.106638	-0.081349	-0.225839
Br	-2.013643	-1.997937	-1.345702
C	1.254552	-0.781850	0.113226
C	1.358024	-2.248983	0.586704
C	-0.574425	2.234809	-0.752963
C	-1.761279	2.001760	0.170473
C	3.759217	-0.143970	0.194008
C	4.504231	-0.603756	-0.903121
C	4.385977	0.159356	1.413746
C	5.752664	-0.090807	1.540037

C	3.624099	0.774777	2.561709
C	6.509787	-0.610915	0.489416
C	5.868976	-0.844941	-0.726854
C	7.977636	-0.916275	0.667618
C	3.883352	-0.766450	-2.269524
C	2.605273	-2.567397	1.444567
C	0.150502	-2.580709	1.498105
C	1.387158	-3.211926	-0.625415
C	-3.845964	0.515027	0.190877
C	-4.125101	-0.733750	1.067934
C	-4.612735	0.411388	-1.150345
C	-4.431260	1.729680	0.965970
C	-6.123333	0.218392	-0.895592
C	-5.636554	-0.925876	1.297076
C	-5.943864	1.548376	1.223256
C	-6.196356	0.284444	2.060215

C	-6.678141	1.430029	-0.125341
C	-6.347677	-1.061186	-0.064326
H	-0.906292	2.156383	-1.796545
H	-0.176519	3.239603	-0.601325
H	-1.450687	2.146611	1.212297
H	-2.502445	2.761095	-0.064101
H	4.194843	0.697270	3.489064
H	2.652148	0.302247	2.714592
H	3.436144	1.836669	2.372878
H	6.238426	0.131186	2.485560
H	8.444912	-0.227568	1.375491
H	8.517247	-0.846781	-0.279620
H	8.123792	-1.931033	1.054048
H	6.446750	-1.210281	-1.570581
H	4.529943	-1.358836	-2.919674
H	3.745737	0.212688	-2.741113
H	2.902542	-1.240712	-2.234795
H	3.537068	-2.508267	0.887214
H	2.505385	-3.594632	1.806462
H	2.681773	-1.920778	2.320245
H	0.136653	-1.922963	2.371279

H	0.236839	-3.611999	1.853018
H	-0.804764	-2.496053	0.988127
H	0.541490	-3.052835	-1.291823
H	1.357361	-4.248715	-0.275263
H	2.308877	-3.085364	-1.197509
H	-4.440612	1.325494	-1.731186
H	-4.223844	-0.420062	-1.737947
H	-3.607013	-0.609967	2.025787
H	-3.721490	-1.627070	0.595873
H	-3.903866	1.859372	1.916879
H	-4.311572	2.653307	0.395341
H	-6.304952	2.430037	1.763631
H	-7.269710	0.162208	2.244824
H	-5.710514	0.371944	3.038876
H	-5.788729	-1.838705	1.882624
H	-5.962720	-1.933076	-0.604039
H	-7.420538	-1.225757	0.087345
H	-6.635060	0.125957	-1.859356
H	-7.755015	1.315016	0.041878
H	-6.542293	2.346187	-0.711872

4

B	0.593191	-1.000646	0.246574
N	1.575376	0.211244	0.127173
C	-0.711720	-0.176524	-0.073566
C	0.051005	-1.786277	1.550059
Br	0.955528	-2.407898	-1.270391
C	0.858925	1.269725	-0.313783
N	-0.478462	1.081309	-0.473834
C	1.331991	2.706607	-0.584544
N	-1.816420	-0.772350	0.348550
C	-1.436989	-1.987322	1.149467
C	3.003559	0.106544	0.295225
C	3.529896	0.124818	1.602303
C	3.850031	-0.091510	-0.808463
C	5.216549	-0.279651	-0.574131
C	3.376172	-0.060823	-2.242594
C	5.763863	-0.272636	0.704529
C	4.900099	-0.057361	1.779958
C	7.237408	-0.512329	0.927987

C	2.655614	0.350192	2.812538
C	2.811146	3.023091	-0.304113
C	1.017786	3.024077	-2.066768
C	0.476508	3.636955	0.315447
C	-3.228352	-0.315329	0.253734
C	-3.625809	0.449006	1.539965
C	-4.156147	-1.543940	0.081517
C	-3.427993	0.610006	-0.967734
C	-5.627493	-1.090772	-0.001134
C	-4.899249	1.064815	-1.051511
C	-5.099444	0.897287	1.451270
C	-6.005300	-0.340439	1.290857
C	-5.278396	1.825462	0.234313
C	-5.816410	-0.161197	-1.213119
H	-1.561033	-2.885224	0.539160
H	-2.105400	-2.059601	2.009293
H	0.528078	-2.740240	1.782431
H	0.080654	-1.158920	2.448206

H	3.729198	0.848806	-2.742029
H	2.294658	-0.110287	-2.331767
H	3.783375	-0.911809	-2.792954
H	5.868280	-0.434476	-1.429235
H	7.620821	0.097316	1.750178
H	7.819340	-0.280254	0.033423
H	7.429571	-1.560390	1.182430
H	5.302609	-0.029502	2.788296
H	1.879935	1.095546	2.626002
H	3.257164	0.687032	3.659019
H	2.149346	-0.571142	3.112723
H	1.616879	2.407227	-2.740595
H	1.253421	4.072682	-2.269263
H	-0.035778	2.850832	-2.285125
H	-0.585600	3.504640	0.118378
H	0.751173	4.676941	0.118588
H	0.659996	3.436552	1.375266
H	3.094326	2.814092	0.728386

H	2.963976	4.092128	-0.477652
H	3.494204	2.484134	-0.957722
H	-4.040195	-2.233860	0.921909
H	-3.870641	-2.087178	-0.825500
H	-3.144107	0.069320	-1.877040
H	-2.765524	1.471588	-0.891670
H	-2.967926	1.315683	1.657240
H	-3.480874	-0.191987	2.416631
H	-5.364861	1.433518	2.368498
H	-6.316317	2.172079	0.175257
H	-4.649297	2.715816	0.344099
H	-5.010499	1.727093	-1.916214
H	-5.575274	-0.694680	-2.139402
H	-6.863645	0.153141	-1.287869
H	-6.261850	-1.976534	-0.110757
H	-7.056542	-0.033949	1.252835
H	-5.898014	-1.002738	2.157876

Figure 4.18 Plots of the frontier orbitals of compounds **2** and **4**.

2:

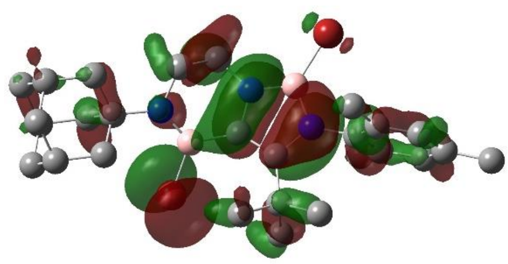

HOMO-5 (−7.3659 eV)

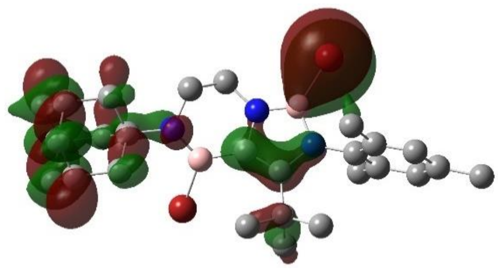

HOMO-9 (−8.0176 eV)

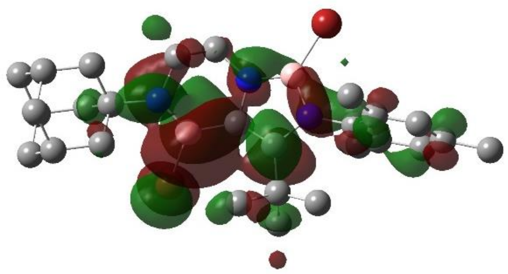

LUMO (−0.7124 eV)

4:

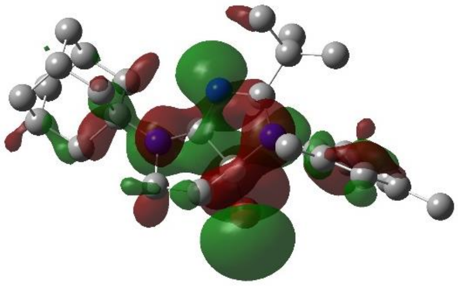

HOMO-1 (−6.2866 eV)

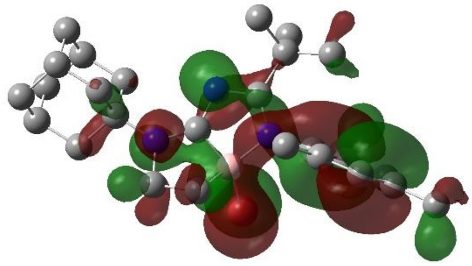

HOMO-2 (−6.4635 eV)

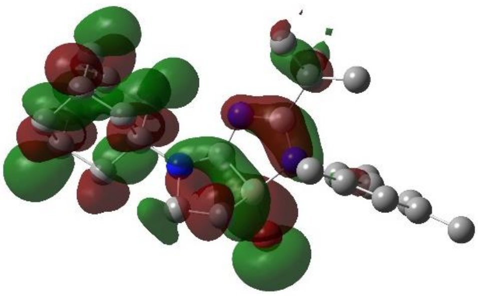

OMO-6 (−7.8510 eV)

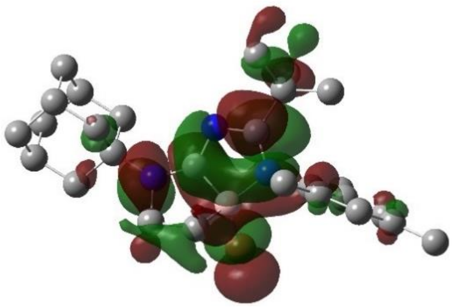

LUMO (−1.4476 eV)

Table 4.3 The NPA charges of **2** and **4** calculated at B3LYP/6-311G(d,p) level of theory.

2:

Atom	No	Charge	Core	Valence	Rydberg	Total
B	1	0.75522	1.99830	2.21214	0.03434	4.24478
N	2	-0.67039	1.99903	5.66003	0.01132	7.67039
N	3	-0.69230	1.99905	5.68224	0.01100	7.69230
Br	4	-0.15247	27.99914	7.14333	0.01000	35.15247
B	5	0.75758	1.99864	2.21453	0.02925	4.24242
N	6	-0.77322	1.99907	5.76122	0.01293	7.77322
C	7	-0.25303	1.99864	4.23389	0.02050	6.25303
Br	8	-0.17549	27.99919	7.16440	0.01191	35.17549
C	9	0.21702	1.99878	3.75760	0.02660	5.78298
C	10	-0.05804	1.99910	4.04536	0.01358	6.05804
C	11	-0.16114	1.99918	4.14367	0.01829	6.16114
C	12	-0.16031	1.99915	4.14498	0.01619	6.16031
C	13	0.14610	1.99869	3.83409	0.02112	5.85390
C	14	0.00041	1.99886	3.98650	0.01423	5.99959
C	15	0.00711	1.99886	3.97980	0.01423	5.99289

C	16	-0.21410	1.99890	4.19925	0.01595	6.21410
C	17	-0.58829	1.99923	4.57991	0.00915	6.58829
C	18	0.00240	1.99896	3.98444	0.01420	5.99760
C	19	-0.21500	1.99891	4.20027	0.01583	6.21500
C	20	-0.58077	1.99923	4.57195	0.00959	6.58077
C	21	-0.58806	1.99923	4.57948	0.00936	6.58806
C	22	-0.57403	1.99924	4.56096	0.01383	6.57403
C	23	-0.56287	1.99924	4.55118	0.01245	6.56287
C	24	-0.56854	1.99921	4.55653	0.01279	6.56854
C	25	0.20305	1.99902	3.77515	0.02279	5.79695
C	26	-0.41132	1.99911	4.39349	0.01871	6.41132
C	27	-0.40804	1.99910	4.38981	0.01912	6.40804
C	28	-0.40686	1.99913	4.38942	0.01831	6.40686
C	29	-0.19557	1.99917	4.17805	0.01835	6.19557
C	30	-0.19394	1.99917	4.17639	0.01838	6.19394
C	31	-0.18881	1.99917	4.17119	0.01846	6.18881
C	32	-0.38551	1.99918	4.36867	0.01766	6.38551
C	33	-0.38553	1.99919	4.36863	0.01771	6.38553
C	34	-0.38569	1.99919	4.36902	0.01748	6.38569
H	35	0.18917	0.00000	0.80778	0.00306	0.81083
H	36	0.21257	0.00000	0.78491	0.00252	0.78743
H	37	0.18874	0.00000	0.80771	0.00354	0.81126
H	38	0.19908	0.00000	0.79798	0.00294	0.80092
H	39	0.20105	0.00000	0.79714	0.00181	0.79895
H	40	0.20828	0.00000	0.78960	0.00213	0.79172
H	41	0.21808	0.00000	0.77961	0.00232	0.78192
H	42	0.19610	0.00000	0.80005	0.00384	0.80390
H	43	0.20268	0.00000	0.79545	0.00187	0.79732
H	44	0.20219	0.00000	0.79596	0.00185	0.79781
H	45	0.20739	0.00000	0.79055	0.00205	0.79261
H	46	0.19651	0.00000	0.79963	0.00386	0.80349
H	47	0.20115	0.00000	0.79706	0.00180	0.79885
H	48	0.21615	0.00000	0.78173	0.00213	0.78385
H	49	0.21318	0.00000	0.78479	0.00202	0.78682
H	50	0.20971	0.00000	0.78733	0.00296	0.79029
H	51	0.19624	0.00000	0.80116	0.00260	0.80376
H	52	0.19608	0.00000	0.80094	0.00297	0.80392
H	53	0.19555	0.00000	0.80222	0.00223	0.80445
H	54	0.19351	0.00000	0.80392	0.00257	0.80649
H	55	0.20429	0.00000	0.79254	0.00318	0.79571
H	56	0.21348	0.00000	0.78432	0.00220	0.78652
H	57	0.19221	0.00000	0.80537	0.00241	0.80779
H	58	0.19256	0.00000	0.80533	0.00211	0.80744
H	59	0.19344	0.00000	0.80305	0.00352	0.80656

H	60	0.22015	0.00000	0.77691	0.00294	0.77985
H	61	0.19893	0.00000	0.79770	0.00337	0.80107
H	62	0.21776	0.00000	0.77810	0.00414	0.78224
H	63	0.20313	0.00000	0.79369	0.00318	0.79687
H	64	0.19310	0.00000	0.80320	0.00369	0.80690
H	65	0.20388	0.00000	0.79344	0.00268	0.79612
H	66	0.19543	0.00000	0.80154	0.00303	0.80457
H	67	0.19443	0.00000	0.80295	0.00262	0.80557
H	68	0.20516	0.00000	0.79213	0.00271	0.79484
H	69	0.19993	0.00000	0.79755	0.00251	0.80007
H	70	0.19466	0.00000	0.80235	0.00298	0.80534
H	71	0.20504	0.00000	0.79226	0.00270	0.79496
H	72	0.19605	0.00000	0.80094	0.00301	0.80395
H	73	0.19337	0.00000	0.80398	0.00264	0.80663
* Total *		0.00000	119.96726	181.36043	0.67230	302.00000

4:

Atom	No	Charge	Core	Valence	Rydberg	Total
B	1	0.56709	1.99860	2.40249	0.03182	4.43291
N	2	-0.65759	1.99908	5.64410	0.01441	7.65759
C	3	0.29874	1.99853	3.66408	0.03865	5.70126
C	4	-0.70265	1.99898	4.68987	0.01379	6.70265
Br	5	-0.26363	27.99938	7.25543	0.00882	35.26363
C	6	0.59739	1.99891	3.36651	0.03719	5.40261
N	7	-0.64509	1.99928	5.62841	0.01740	7.64509
C	8	-0.07730	1.99908	4.06251	0.01572	6.07730
N	9	-0.41142	1.99908	5.39322	0.01912	7.41142
C	10	-0.14688	1.99920	4.13183	0.01585	6.14688
C	11	0.14338	1.99866	3.83736	0.02060	5.85662
C	12	-0.00122	1.99887	3.98842	0.01392	6.00122
C	13	0.00548	1.99887	3.98144	0.01421	5.99452
C	14	-0.21024	1.99890	4.19524	0.01610	6.21024
C	15	-0.59513	1.99922	4.58585	0.01006	6.59513
C	16	0.00220	1.99896	3.98480	0.01404	5.99780
C	17	-0.21446	1.99891	4.19968	0.01587	6.21446
C	18	-0.58101	1.99923	4.57222	0.00956	6.58101
C	19	-0.58441	1.99923	4.57578	0.00940	6.58441
C	20	-0.57785	1.99923	4.56488	0.01373	6.57785
C	21	-0.56299	1.99923	4.55075	0.01301	6.56299
C	22	-0.55879	1.99923	4.54650	0.01306	6.55879

C	23	0.19008	1.99904	3.78814	0.02275	5.80992
C	24	-0.39978	1.99911	4.38211	0.01856	6.39978
C	25	-0.40176	1.99913	4.38423	0.01840	6.40176
C	26	-0.41460	1.99912	4.39505	0.02042	6.41460
C	27	-0.19317	1.99917	4.17561	0.01839	6.19317
C	28	-0.19310	1.99917	4.17579	0.01814	6.19310
C	29	-0.19556	1.99917	4.17806	0.01833	6.19556
C	30	-0.38581	1.99919	4.36905	0.01757	6.38581
C	31	-0.38531	1.99919	4.36865	0.01748	6.38531
C	32	-0.38568	1.99919	4.36886	0.01763	6.38568
H	33	0.20121	0.00000	0.79564	0.00315	0.79879
H	34	0.18582	0.00000	0.81170	0.00247	0.81418
H	35	0.22176	0.00000	0.77530	0.00294	0.77824
H	36	0.20338	0.00000	0.79356	0.00306	0.79662
H	37	0.19862	0.00000	0.79900	0.00238	0.80138
H	38	0.22323	0.00000	0.77455	0.00222	0.77677
H	39	0.21629	0.00000	0.78181	0.00190	0.78371
H	40	0.19652	0.00000	0.79972	0.00375	0.80348
H	41	0.20222	0.00000	0.79587	0.00191	0.79778
H	42	0.20147	0.00000	0.79669	0.00183	0.79853
H	43	0.20886	0.00000	0.78907	0.00208	0.79114
H	44	0.19530	0.00000	0.80088	0.00382	0.80470
H	45	0.20372	0.00000	0.79367	0.00261	0.79628
H	46	0.20153	0.00000	0.79669	0.00178	0.79847
H	47	0.21409	0.00000	0.78357	0.00234	0.78591
H	48	0.19937	0.00000	0.79843	0.00221	0.80063
H	49	0.19574	0.00000	0.80198	0.00228	0.80426
H	50	0.21612	0.00000	0.78160	0.00228	0.78388
H	51	0.21709	0.00000	0.78060	0.00231	0.78291
H	52	0.19476	0.00000	0.80286	0.00238	0.80524
H	53	0.19338	0.00000	0.80421	0.00242	0.80662
H	54	0.20561	0.00000	0.79171	0.00268	0.79439
H	55	0.19847	0.00000	0.79898	0.00255	0.80153
H	56	0.20757	0.00000	0.78944	0.00299	0.79243
H	57	0.19970	0.00000	0.79705	0.00326	0.80030
H	58	0.20734	0.00000	0.78935	0.00331	0.79266
H	59	0.20574	0.00000	0.79107	0.00320	0.79426
H	60	0.23268	0.00000	0.76290	0.00442	0.76732
H	61	0.20670	0.00000	0.78980	0.00350	0.79330
H	62	0.19563	0.00000	0.80086	0.00351	0.80437
H	63	0.20489	0.00000	0.79240	0.00271	0.79511
H	64	0.19530	0.00000	0.80169	0.00301	0.80470
H	65	0.19677	0.00000	0.80064	0.00259	0.80323
H	66	0.20610	0.00000	0.79128	0.00263	0.79390

H	67	0.19682	0.00000	0.80061	0.00257	0.80318
H	68	0.19488	0.00000	0.80210	0.00301	0.80512
H	69	0.20543	0.00000	0.79190	0.00267	0.79457
H	70	0.19692	0.00000	0.80012	0.00297	0.80308
H	71	0.19405	0.00000	0.80333	0.00262	0.80595
* Total *		-0.00000	89.97016	171.35955	0.67029	262.00000

4.5 References

(1) a) Ji, L.; Griesbeck, S.; Marder, T. B. *Chem. Sci.* **2017**, *8*, 846 – 863; b) Escande, A.; Ingleson, M. J. *Chem. Commun.* **2015**, *51*, 6257 – 6274; c)Hudson, Z. M.; Wang, S. *Acc. Chem. Res.* **2009**, *42*, 1584 – 1596; d) Entwistle, C. D.; Marder, T. B. *Angew. Chem. Int. Ed.* **2002**, *41*, 2927 – 2931; e) Entwistle, C. D.; Marder, T. B. *Chem. Mater.* **2004**, *16*, 4574 – 4585.

(2) a) Rao, Y.-L.; Amarne, H.; Zhao, S.-B.; McCormick, T. M.; Martić, S.; Sun, Y.; Wang, R.-Y.; Wang, S. *J. Am. Chem. Soc.* **2008**, *130*, 12898 – 12900; b) Amarne, H.; Baik, C.; Murphy, S. K.; Wang, S. *Chem. Eur. J.* **2010**, *16*, 4750 – 4761; c) Rao, Y.-L.; Chen, L. D.; Mosey, N. J.; Wang, S. *J. Am. Chem. Soc.* **2012**, *134*, 11026 – 11034; d) Rao, Y.-L.; Amarne, H.; Chen, L. D.; Brown, M. L.; Mosey, N. J.; Wang, S. *J. Am. Chem. Soc.* **2013**, *135*, 3407 – 3410; e) Rao, Y.-L.; Hörl, C.; Braunschweig, H.; Wang, S. *Angew. Chem. Int. Ed.* **2014**, *53*, 9086 – 9089; f) Mellerup, S. K.; Yuan, K.; Nguyen, C.; Lu, Z.-H.; Wang, S. *Chem. Eur. J.* **2016**, *22*, 12464 – 12472; g) Mellerup, S. K.; Li, C.; Peng, T.; Wang, S. *Angew. Chem. Int. Ed.* **2017**, *56*, 6093 – 6097; h) Rao, Y.-L.; Amarne, H.; Wang, S. *Coord. Chem. Rev.* **2012**, *256*, 759 – 770.

(3) Araneda, J. F.; Neue, B.; Piers, W. E.; Parvez, M. *Angew. Chem. Int. Ed.* **2012**, *51*, 8546 – 8550.

(4) Iida, A.; Saito,S.; Sasamori, T.; Yamaguchi, S. *Angew. Chem. Int. Ed.* **2013**, *52*, 3760 – 3764.

(5) Ando, N.; Fukazawa, A.; Kushida, T.; Shiota, Y.; Itoyama, S.; Yoshizawa, K.; Matsui, Y.; Kuramoto, Y.; Ikeda, H.; Yamaguchi, S. *Angew. Chem. Int. Ed.* **2017**, *56*, 12210 – 1221410.

(6) Wang, H.; Zhang, J.; Xie, Z. *Angew. Chem. Int. Ed.* **2017**, *56*, 9198 – 9201.

(7) Arrowsmith, M.; Braunschweig, H.; Radacki, K.; Thiess, T.; Turkin, A. *Chem. Eur. J.* **2017**, *23*, 2179 – 2184.

(8) a) Su, B.; Kinjo, R. *Synthesis* **2017**, *49*, 2985 – 3034; b) Weber, L.; Böhling, L. *Coord. Chem. Rev.* **2015**, *284*, 236 – 275. c) Weber, L. *Eur. J. Inorg. Chem.* **2012**, 2012, 5595 – 5609. d) Weber, L. *Coord. Chem. Rev.* **2008**, *252*, 1 – 31. e) Ashe, A. J. III *Comprehensive Heterocyclic Chemistry III*, Elsevier, Oxford, **2008**, pp. 1189 – 1224. f) Weber, L. *Coord. Chem. Rev.* **2001**, *215*, 39 – 77. g) Schmid, G.; Schulze, J.*Angew. Chem. Int. Ed. Engl.* **1977**, *16*, 249 – 250.

(9) Preethalayam, P.; Krishnan, K. S.; Thulasi, S.; Chand, S. S.; Joseph, J.; Nair, V.; Jaroschik, F.; Radhakrishnan, K. V. *Chem. Rev.* **2017**, *117*, 3930 – 3989.

(10) Bruker AXS SHELXTL, Madison, WI; *SHELX-97G*. M. Sheldrick, Acta. Crystallogr. A, **2008**, *64*, 112–122, *SHELX-2013*, http://shelx.uni-ac. gwdg.de/SHELX/index.php.

(11) Gaussian 09, Revision B.01, Frisch, M. J.; Trucks, G. W.; Schlegel, H. B.; Scuseria, G. E.; Robb, M. A.; Cheeseman, J. R.; Scalmani, G.; Barone, V.; Mennucci, B.; Petersson, G. A.; Nakatsuji, H.; Caricato, M.; Li, X.; Hratchian, H. P.; Izmaylov, A. F.; Bloino, J.; Zheng,

G.; Sonnenberg, J. L.; Hada, M.; Ehara, M.; Toyota, K.; Fukuda, R.; Hasegawa, J.; Ishida, M.; Nakajima, T.; Honda, Y.; Kitao, O.; Nakai, H.; Vreven, T.; Montgomery, J. A. Jr.,; Peralta, J. E.; Ogliaro, F.; Bearpark, M.; Heyd, J. J.; Brothers, E.; Kudin, K. N.; Staroverov, V. N.; Keith, T.; Kobayashi, R.; Normand, J.; Raghavachari, K.; Rendell, A.; Burant, J. C.; Iyengar, S. S.; Tomasi, J.; Cossi, M.; Rega, N.; Millam, J. M.; Klene, M.; Knox, J. E.; Cross, J. B.; Bakken, V.; Adamo, C.; Jaramillo, J.; Gomperts, R.; Stratmann, R. E.; Yazyev, O.; Austin, A. J.; Cammi, R.; Pomelli, C.; Ochterski, J. W.; Martin, R. L.; Morokuma, K.; Zakrzewski, V. G.; Voth, G. A.; Salvador, P.; Dannenberg, J. J.; Dapprich, S.; Daniels, A. D.; Farkas, O.; Foresman, J. B.; Ortiz, J. V.;Cioslowski, J.; Fox, D. J. Gaussian, Inc., Wallingford CT, **2010**.

Chapter 5 Synthesis and Characterization of an Isolable Imino-N-heterocyclic Carbene/Germanium(0) Adduct: A Mesoionic Germylene Equivalent†

5.1 Introduction

Since the first isolation of the carbenes was reported two decades ago, the chemistry of stable singlet carbenes has been greatly developed.[1] As the most widely studied carbenes, the N-heterocyclic carbenes (NHCs) have been intensively applied to transition-metal chemistry,[2] organocatalysis[3] and main group chemistry.[4] Besides, various types of carbenes other than NHCs have been prepared and enriched this field.[5] Among them, Bertrand et al. successfully isolated the free imidazole-5-ylidene **I** (Figure 5.1a), termed an abnormal N-heterocyclic carbene (*a*NHC) or mesoionic carbene (MIC),[6] which is more basic than its normal NHC isomer based on the calculations. Since then, *a*NHCs have led the further diversity in the application of singlet carbenes for catalysis due to their peculiar electronic property.[7] Meanwhile, the corresponding heavier group 14 analogues **IIa** (E = Si, Ge, Sn, Pb; Figure 5.1b) have not been described before despite the long history of tetrylene chemistry,[8] probably because of the lack of the suitable synthetic methodology.

Recently, the chemistry of low-valent main group species has attracted considerable interest due to their diverse reactivity.[8] Among them, a series of molecules featuring heavier group 14 elements in the zero-oxidation state have been reported (Figure 5.2). Their unusual

† Portions of this chapter are taken with permission from: Su, B.; Ganguly, R.; Li, Y.; Kinjo, R. *Angew. Chem. Int. Ed.* **2014**, *53*, 13106 – 130109. Copyright (2014) WILEY-VCH Verlag GmbH & Co. KGaA, Weinheim.

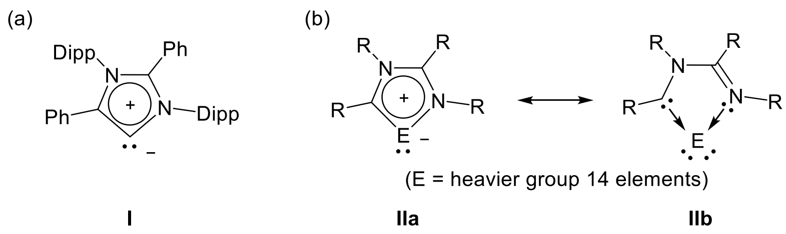

Figure 5.1 (a) The first isolable abnormal-N-heterocyclic carbene **I** (b) Two canonical forms of **II**

group 14 elements in the zero-oxidation state have been reported (Figure 5.2). Their unusual reactivity owing to the peculiar electronic structures have been detailedly investigated by the theoretical calculations by the research groups of Frenking and Apeloig.[9] In 1999, Wiberg et al. synthesized the tristanaallene **III** bearing a tin(0) atom.[10] Later, Kira et al. isolated the trisilaallene, 1,3-digermasilaallene and trigermaallene **IV** with the centered silicon(0) and germanium(0) atom, respectively.[11] In contrast to the allenes which have the rigid linear C=C=C structure, the geometries of these heavier analogues are not linear but bent with angles of 122º–137º. Meanwhile, Sekiguchi et al. reported another trisilaallene **V** which possesses the distinctive electronic property and striking reactivity toward alcohols.[12] The carbene ligands, due to their strong electron-donating ability, have shown a great advantage in stabilizing low-valent main group sepecies, including the heavier group 14 species.[4] The groups of Robinson and Jones isolated several diatomic silicon, germanium and tin species **VI** supported by two NHC ligands (L:→E=E←:L, L = NHC).[13] The electron donation from carbene to the empty orbitals of heavier atoms is one of the key factors to stabilize these reactive species. Interestingly, several group 14 compounds featuring only one E^0 atom (E = Si, Ge) have also been isolated, which could be represented as ylidones (L:→E←:L, L = carbene), possessing two lone pairs.[14] In 2013, Roesky group reported the isolation of E^0 (E = Si, Ge) species **VII** which were supported by two strong σ-donating cyclic alkyl(amino) carbenes (CAACs).[14a,b] Experimental results and DFT calculations revealed that these molecules show a diradicaloid character, which is due to the stronger π-accepting ability of CAACs. At the same time, by the employment of the bidentate NHC as the σ-donating ligand, The Driess group successfully isolated the E^0 (E = Si, Ge) speices **VIII**. [14c,d] DFT calculations showed that both species **VIII** exhibit the similar electronic features. The HOMO mainly consists of the π-type orbital at the E atom center (E = Si, Ge), including E–C π bonding. The HOMO–1 represents a σ lone-pair orbital at E atom. In addition, the calculations revealed that bis-NHC silylones possess a larger nucleophilicity at the Si^0 atom compared with two CAAC stabilized analogues, due to the weaker π-accepting character of the NHC ligand. Remarkably, Nikonov *et al*. demonstrated that germanium(0) can be prepared even in the absence of carbene ligands.[15] Thus, they synthesized the first tricoordinate compound (**IX**) of germanium(0) stabilized by a bis(imino)pyridine, wherein partial delocalization of one of the germanium lone pairs onto the π*(C=N) orbitals was observed, and contributes to the strong interaction between germanium(0) and the ligand. The same ligand was also applicable to isolate the tricoordinate Sn(0) compound.[16] These pioneering works demonstrated that the heavier group 14 atoms in zero oxidation state can be stabilized by carbene- or imino-based ligands, which inspired us to study whether the combination of one singlet carbene and one imino group can stabilize such species. Since the imino-N-heterocyclic carbene **1** has been successfully applied to generate the unusual aromatic 1,4,2-diazaborole mentioned in chapter 2, we were interested in employing the same carbene as the ligand because the resulting E^0 species **IIb** may correspond to an equivalent of the synthetically challenging **IIa** (Figure 5.1). Herein, we report the synthesis, single-crystal X-ray diffraction analysis, and computational studies of a novel germanium(0) derivative supported by an imino-N-heterocyclic carbene.

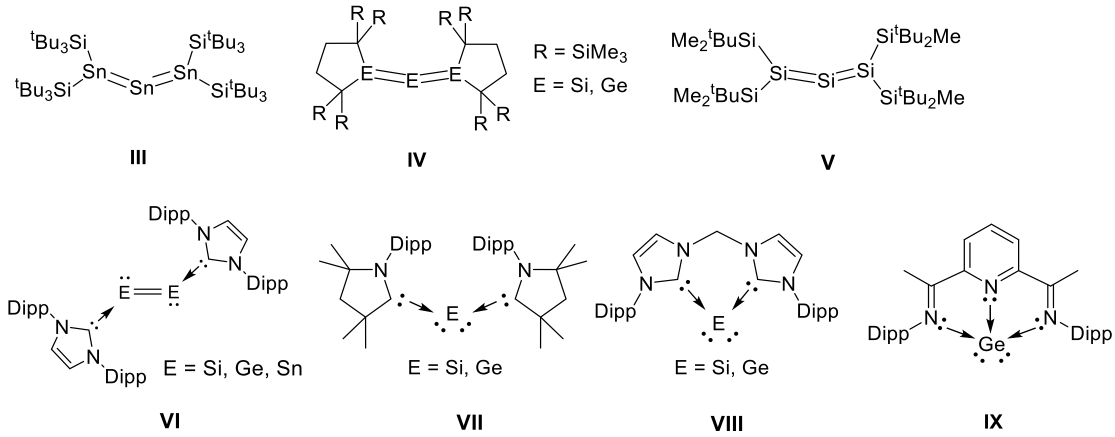

Figure 5.2 Structurally characterized heavier group 14 molecules featuring an element in the zero-oxidation state. Dipp = 2,6-diisopropylphenyl

5.2 Results and Discussions

The imino-N-heterocyclic carbene **1** was prepared according to the same procedures described in chapter 2. Treatment of **1** with two equivalents of germanium dichloride/1,4-dioxane complex afforded a white precipitate through autoionization[17] of germanium dichloride (Scheme 5.1). After the reaction completed overnight, the white solid was filtered and washed with cold toluene to give the targeted compound **2** in 67% yield. Compound **2** represents the first example of chloro-germyliumylidene ion chelated by an imino-N-heterocyclic carbene. In the ^{13}C NMR spectrum, the carbene peak around 198.4 ppm was observed, which is shifted upfield relative to that (242.3 ppm) of **1**. Compound **2** is thermally stable but it gradually decomposes upon exposure to air.

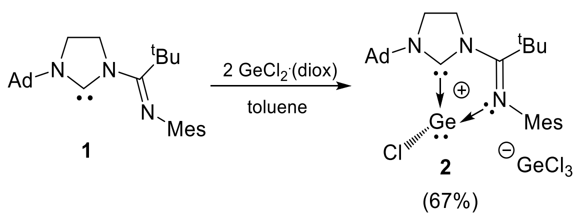

Scheme 5.1 Synthesis of **2**.

Single crystals of **2** were obtained by slow evaporation of an acetonitrile solution. The X-ray diffraction analysis disclosed that the shortest distance between the cation [**2**-$Ge^{II}Cl]^+$ and the anion $[Ge^{II}Cl_3]^-$ is greater than 6.5 Å, indicating there is no interaction between them (Figure 5.3). In the cation part, the Ge atom is tri-coordinated by the carbene carbon atom C1, the imine nitrogen atom N3 and one chlorine atom Cl1, and possesses a pyramidal geometry. The sum of the bond angles around the carbene carbon atom is 359.1°. All the five atoms (C1, N2, C4, N3, Ge1) of the central C_2N_2Ge ring are nearly coplanar (the sum of the internal pentagon angles = 537.38°), but the Ge1 slightly deviates from the plane in the opposite direction of the Ge1–Cl1 bonding vector. The Cl1 atom is located out of the C_2N_2Ge plane with bond angles of 95.25(5)° for C1–Ge1–Cl1 and 95.79(5)° for N3–Ge1–Cl1. The Ge1–Cl1 distance of 2.2646(6) Å is comparable to those (2.243–2.310 Å) observed in previously reported germyliumylidene ions.[14c, 17, 18] The Ge1–C1 distance of 2.0588(19) Å is nearly identical to those [2.058(3) and 2.057(3) Å] of a cyclic germadicarbene.[14c] The Ge1–N3 distance of 2.0560(16) Å is longer than those [1.981(3) and 1.960(3) Å][18b] of [LClGe:]+ [L = 1,8-bis(tri-nbutylphosphanzenyl) naphthalene] but slightly shorter than those [2.114(5)–2.428(5) Å][18c] in $[(pmdta)ClGe:]^+$ and those [2.071(2)–2.267(2) Å][17] in $[L'ClGe:]^+$ [L' = 2,6-diacetylpyridinebis(2,6-diisopropylanil)], thus suggesting a relatively strong interaction between the Ge1 atom and the N3 atom in **2**.

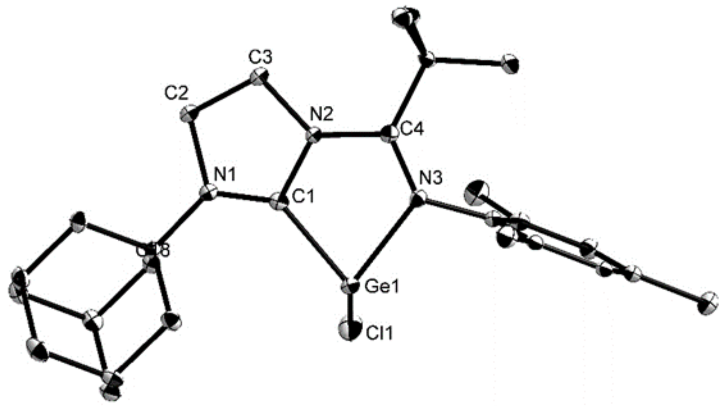

Figure 5.3 Solid-state structure of **2** (hydrogen atoms, solvent molecules, and counteranion $GeCl_3^-$) are omitted for clarity). Thermal ellipsoids are set at the 50% probability.

To gain a deeper understanding of the electronic property, we performed quantum chemical calculations for the cationic fragment of **2**. The optimized geometry is in good agreement with the experimental result. The frontier orbitals are shown in Figure 5.4. The HOMO–2 orbital mainly consists the lone-pair orbital on the Ge atom (Figure 5.4a), and the LUMO mainly corresponds to a π-type orbital over the C_2N_2Ge five-membered ring (Figure 5.4b). From the Natural Bond Order (NBO) analysis, Wiberg bond index (WBI) values of the Ge–C bond (0.61) and the Ge–N bond (0.39) were obtained, indicating a pronounced interaction between the imino-carbene ligand and $[:GeCl]^+$ fragment in **2**. Indeed, Natural Population Analysis (NPA) revealed an overall charge transfer of 0.57 *e* from the imino-carbene ligand **1** to $[:GeCl]^+$ in **2**.

(a) (b)

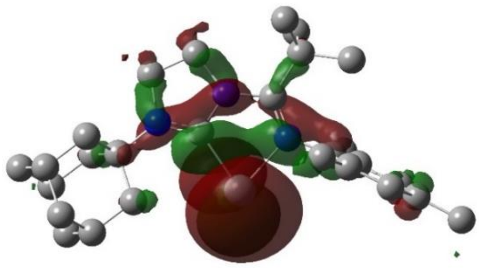

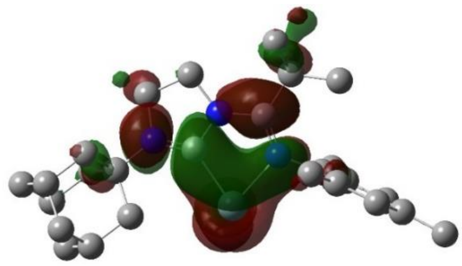

HOMO-2 (–8.2785 eV) LUMO (–5.8423 eV)

Figure 5.4 Plots of the HOMO–2 (a) and LUMO (b) of **2** calculated at the B3LYP/6-311G(d,p) level of theory.

With the compound **2** in hand, we next attempted the reduction of **2**. The mixture of **2** with five equivalents of potassium graphite in toluene was stirred at ambient temperature for 1 h. During this process, the color changed to light yellow. Upon completion of the reaction, the insoluble parts were filtered off and the solvent was removed in vacuum to afforded **3** as a yellow solid in 45% yield (Scheme 5.2). Note that **3** can be viewed as both an abnormal N-heterocyclic germylene **3a** and a Ge(0) species **3b**, which is the first example of a dicoordinate Ge(0) analogue supported by a carbene and an imine ligands.[19] In the ^{13}C NMR spectrum of **3**, the carbene peak appeared at 194.3 ppm which is similar to that (198.4 ppm) in **2** and shifted upfield with respect to that (242.3 ppm) of **1**. The complex **3** is thermally stable both in solid state and in solution, and even under heating at 110 ºC for several hours in toluene, no decomposition was detected. However, it rapidly decomposes to unidentified prodoucts upon exposure to air or moisture.

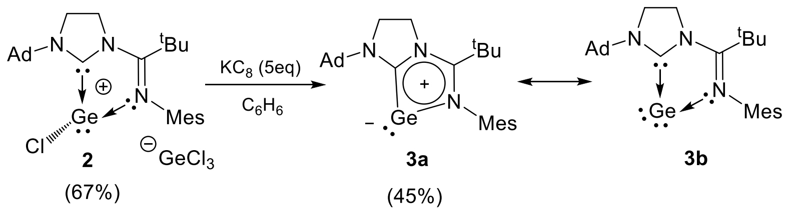

Scheme 5.2 Synthesis of **3**.

Single crystals suitable for X-ray diffraction analysis were obtained from a benzene solution of **3** stored at 10 °C under argon. In the solid state, the Ge1 atom is two-coordinated by the carbene carbon and the imine nitrogen atom, with a C1–Ge1–N1 angle of 80.59(6)° (Figure 5.5). This angle is slightly larger than that (76.88(7)°) of **2**, but smaller than the corresponding C–Ge–C angle (86.6(1)°) of a cyclic germadicarbene **VIII**[14c] or those [83.44(12)° and 85.62(7)°] of tetraphenylgermole dianions $(thf)_nLi_2[(PhC)_4Ge]$[20a] that are isoelectronic species of **4**. The five-membered C_2N_2Ge ring is nearly coplanar (the sum of internal pentagon angles = 539.97°) with a trigonal planar geometry around the carbene carbon (the sum of bond angles = 359.98°). The Ge1–C1 distance of 1.8870(15) Å is significantly shorter by 0.3776 Å than that in **2**, and it ranges between typical Ge–C single bonds and Ge=C double bonds.[21] The Ge1–N1 bond and the C4–N2 bond become shorter and the C4–N1 bond and the C1–N2 bond become slightly longer compared to those of **2**. These structural features suggest the delocalization of π-electrons over the five-membered C_2N_2Ge ring in **3**. The similar geometrical property has been reported on germole dianions $M_2[(RC)_4Ge]$ displaying a planar C_4Ge ring structure as well as cyclic C–C bond equalization, which indicates the delocalization of the negative charge over the entire ring system.[20] Similarly, cyclic delocalization of the π-electrons on the skeletal five-membered ring was also proposed in N-heterocyclic germanediyl derivatives $[(H)C(R)N]_2Ge$: that are alternative isomers of **3**, based on experimental analysis and theoretical studies.[22]

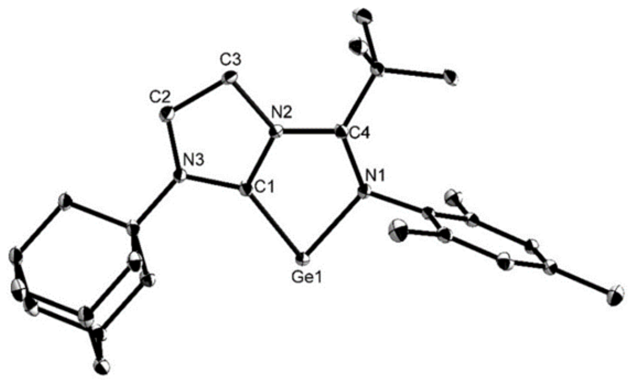

Figure 5.5 Solid-state structure of **3** (hydrogen atoms and solvent molecules are omitted for clarity). Thermal ellipsoids are set at the 50% probability level.

To gain further insight into the electronic features of **3**, we performed the DFT calculation including geometry optimization, NBO analysis, and NPA calculation. Geometry optimization provided similar structural parameters to those observed experimentally. The frontier orbitals are depicted in Figure 5.6**.** The LUMO is the π-type orbital over the C_2N_2Ge five-membered ring (Figure 5.6a). The HOMO is mainly a C–Ge π-bonding orbital which exhibits antibonding conjugation with the N=C(^{t}Bu) π orbital in the C_2N_2Ge ring (Figure 5.6b). Meanwhile, the HOMO−1 is a σ-type lone-pair orbital at the Ge atom (Figure 5.6c). WBI values of the Ge−C bond (1.21) supports the π-bonding property of the Ge−C bond. WBI values larger than 1 for the C(carbene)–N bond (1.08) and the N−C(^{t}Bu) bonds (1.20 and 1.35) in the C_2N_2Ge ring were also obtained, thus indicating the delocalization of the π system. In the UV-vis spectrum of **3**, a strong absorption band with λ_{max} = 415 nm was observed and corresponds to the π–π* transition (Figure 5.6d).

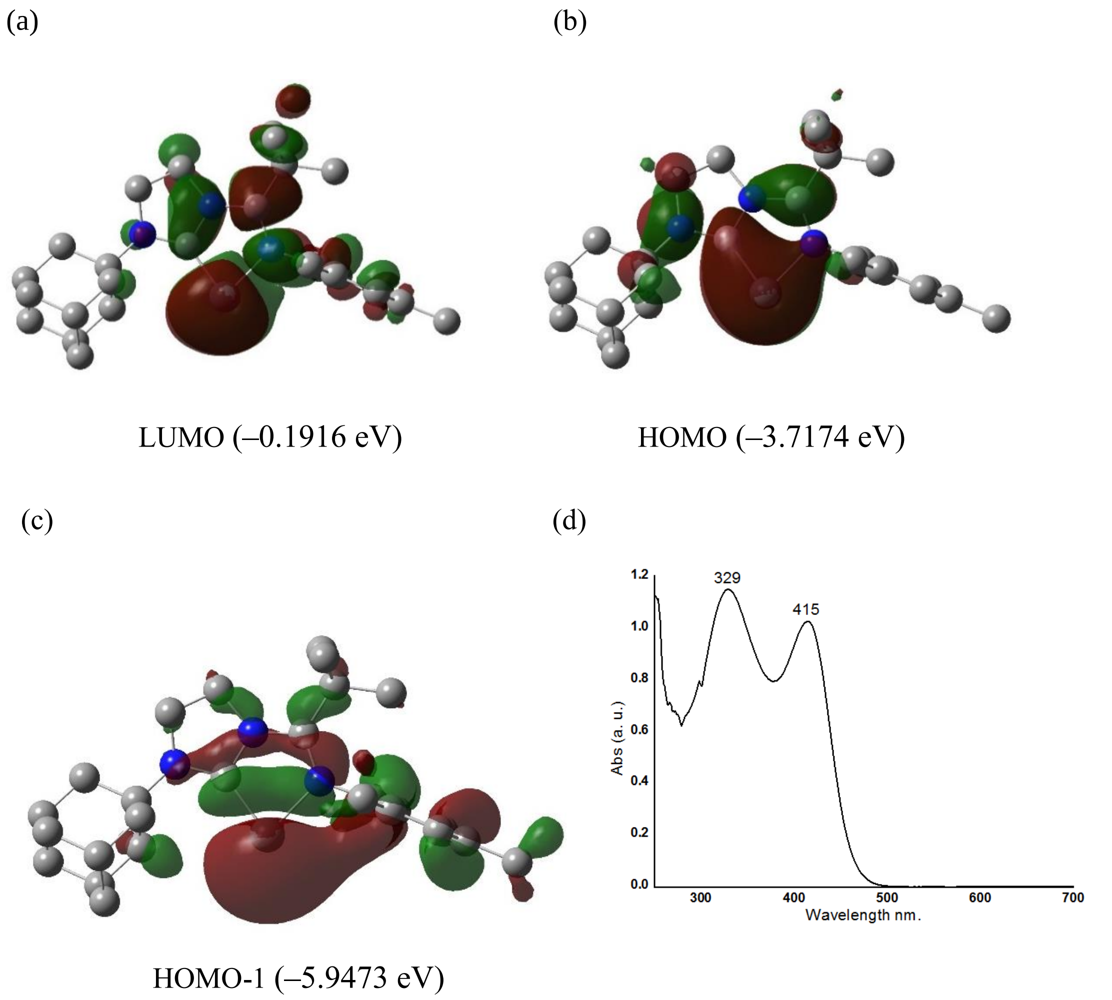

Figure 5.6 Plots of the LUMO (a), HOMO (b) and HOMO-1 (c) of **3** calculated at the B3LYP/6-311G(d,p) level of theory; (d) UV-vis spectrum of compound **3** in benzene.

5.3 Summary

In conclusion, we successfully prepared the chlorogermyliumylidene cation **2** which is supported by the imino-N-heterocyclic carbene ligand through autoionization of a germanium dichloride/1,4-dioxane complex. Reduction of **2** with potassium graphite afforded the novel germanium compound **3** which can be viewed as both a mesoionic germylene and a germanium(0) species. X-ray diffraction analysis and computational studies revealed the electron delocalization over the five-membered C_2N_2Ge ring involving one of the lone pairs on Ge, thus supporting the electronic properties of the resonance structure **3a**.

5.4 Experimental Sections

5.4.1 Synthesis of compounds 2 and 3 and their spectral data

General considerations: All reactions were performed under an atmosphere of argon or nitrogen by using standard Schlenk or dry box techniques; solvents were dried over Na metal, K metal, or CaH_2. Reagents were of analytical grade, obtained from commercial suppliers and used without further purification. ^{1}H and ^{13}C NMR spectra were obtained with a Bruker AVIII 400MHz BBFO1 spectrometer at 298 K unless otherwise stated. NMR multiplicities are abbreviated as follows: s = singlet, d = doublet, t = triplet, m = multiplet, br = broad signal. Coupling constants *J* are given in Hz. Electrospray ionization (ESI) mass spectra were obtained at the Mass Spectrometry Laboratory at the Division of Chemistry and Biological Chemistry, Nanyang Technological University. Melting points were measured with an OpticMelt Stanford Research System. UV−Vis absorption spectroscopic analyses were carried out with a Shimadzu UV-3600 spectrometer.

Compound 2: Toluene (30 mL) was added to a mixture of **1** (1.00 g, 2.47 mmol) and $GeCl_2$·dioxane (1.14 g, 4.92 mmol) at room temperature under argon. The mixture was stirred overnight, and the white precipitate was separated by filtration. After washing the residue with cold toluene (2×10 mL), **2** was obtained as a white solid. (1.14 g, 67%). Single crystals suitable for X-ray diffraction studies were grown from a saturated acetonitrile solution at −26 °C. M.p.: 102 °C (dec.); ^{1}H NMR ($CDCl_3$, 400 MHz, 298 K): δ 6.90 (s, 2H, *m*-C*H*), 4.78 (t, *J* = 7.7 Hz, 2H, NCH_2), 4.58 (t, *J* = 8.3 Hz, 2H, NCH_2), 2.30–2.85 (m, 12H, CH_3 & Ad–*H*), 2.24 (br, 6H, Ad–*H*), 1.75 (br, 6H, Ad–*H*), 1.35 (s, 9H, C(CH_3)$_3$); $^{13}C\{^{1}H\}$ NMR ($CDCl_3$, 100 MHz, 298 K):

δ 198.4 (N*C*N), 170.8 (*C*=N), 137.8 (C_{Ar}), 136.6 (C_{Ar}), 131.8 (C_{Ar}), 129.9 (C_{Ar}), 62.1 (Ad-*q*), 51.2 (N*C*H_2), 49.7 (N*C*H_2), 41.0 (Ad−*C*H_2), 40.1 (*C*(CH_3)$_3$), 35.5 (Ad−*C*H_2), 29.5 (Ad−*C*H), 28.9 (C(*C*H_3)$_3$), 21.0 (*p*-*C*H_3), 20.2 (*o*-*C*H_3); HRMS (ESI): *m/z* calcd for $C_{27}H_{39}ClGeN_3$: 514.2044 [(*M*–*GeCl*$_3$)]$^+$; found: 514.2034.

Compound 3: Benzene (10 mL) was added to a mixture of compound **2** (100 mg, 0.144 mmol) and KC_8 (97.6 mg, 0.722 mmol) at room temperature. After 1 h with stirring, the reaction mixture was filtered, and the filtrate was concentrated to 5 mL. The crude product was recrystallized at 10 ºC to afford **3** as a yellow crystalline solid (32.0 mg, 45%). M.p.: 140 ºC (dec.); ^{1}H NMR (C_6D_6, 400 MHz, 298 K): δ 6.75 (s, 2H, *m*-C*H*), 3.73 (t, *J* = 7.2 Hz, 2H, NC*H*$_2$), 3.08 (t, *J* = 7.2 Hz, 2H, NC*H*$_2$), 2.36 (s, 6H, *o*-CH_3), 2.20–2.19 (*m*, 6H, Ad–C*H*$_2$), 2.15 (s, 3H, *p*-C*H*$_3$), 2.02 (br, 3H, Ad–C*H*), 1.64 (d, *J* = 12.2 Hz, 3H, Ad–C*H*$_2$), 1.56 (d, *J* = 11.6 Hz, 3H, Ad–C*H*$_2$), 0.92 (s, 9H, C(C*H*$_3$)$_3$); ^{13}C{^{1}H} NMR (C_6D_6, 100 MHz, 298 K): δ 194.3 (N*C*N), 144.1 (*C*=N), 139.4 (C_{Ar}), 134.6 (C_{Ar}), 133.1 (C_{Ar}), 128.8 (C_{Ar}), 54.5 (Ad-*q*), 49.8 (N*C*H_2), 46.9 (N*C*H_2), 38.9 (Ad−*C*H_2), 38.0 (*C*(CH_3)$_3$), 37.2 (Ad−*C*H_2), 30.0 (Ad−*C*H), 29.4 (C(*C*H_3)$_3$), 21.0 (*p*-*C*H_3), 19.0 (*o*-*C*H_3); HRMS (ESI): *m/z* calcd for $C_{27}H_{40}GeN_3$: 480.2434 [(*M*+*H*)]$^+$; found: 480.2430.

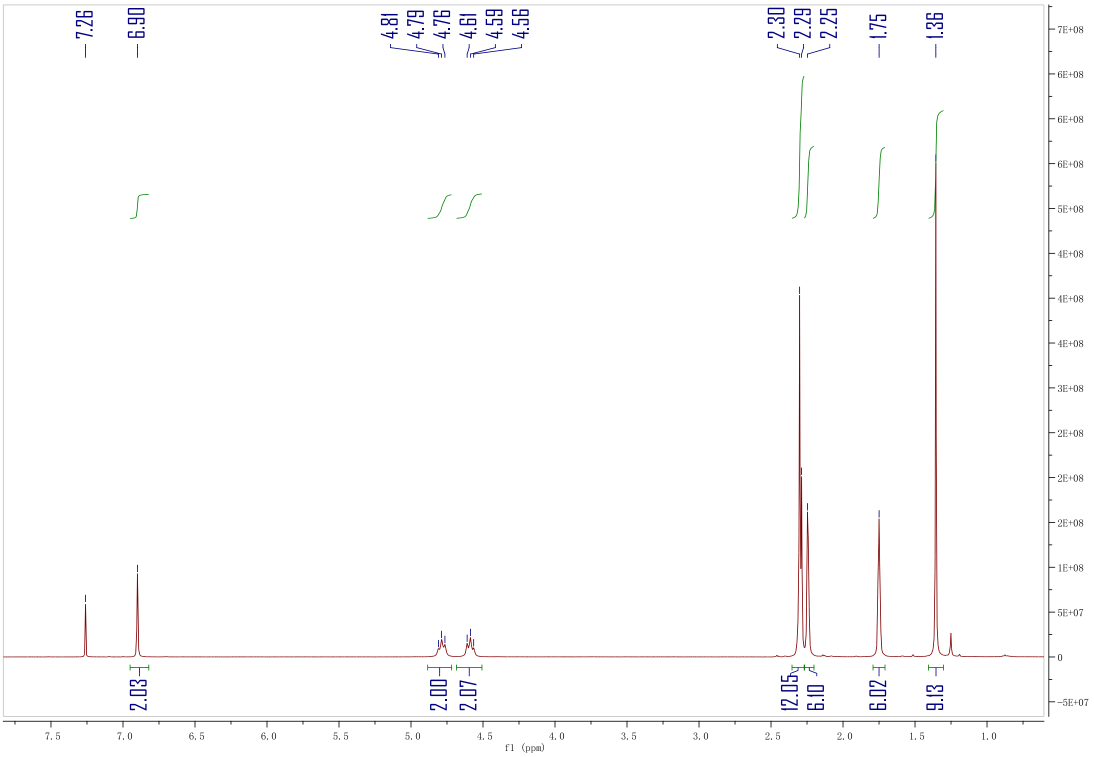

Figure 5.7 ^{1}H NMR spectrum of **2**.

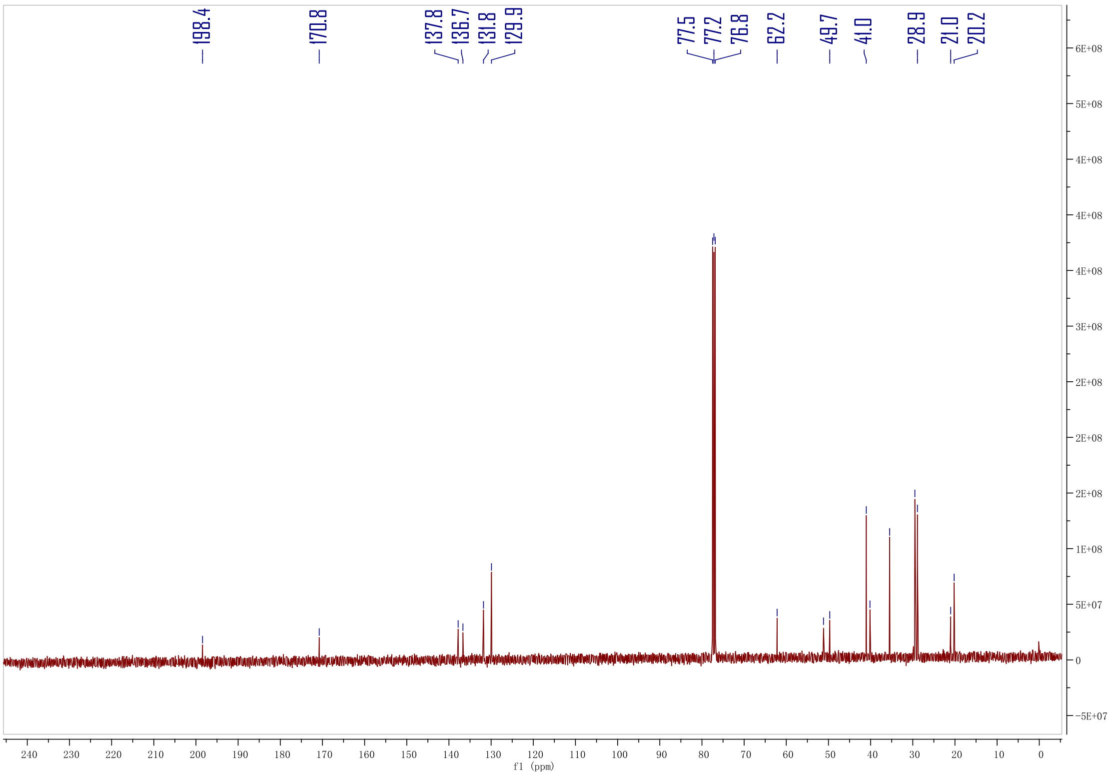

Figure 5.8 ^{13}C{^{1}H} NMR spectrum of **2**.

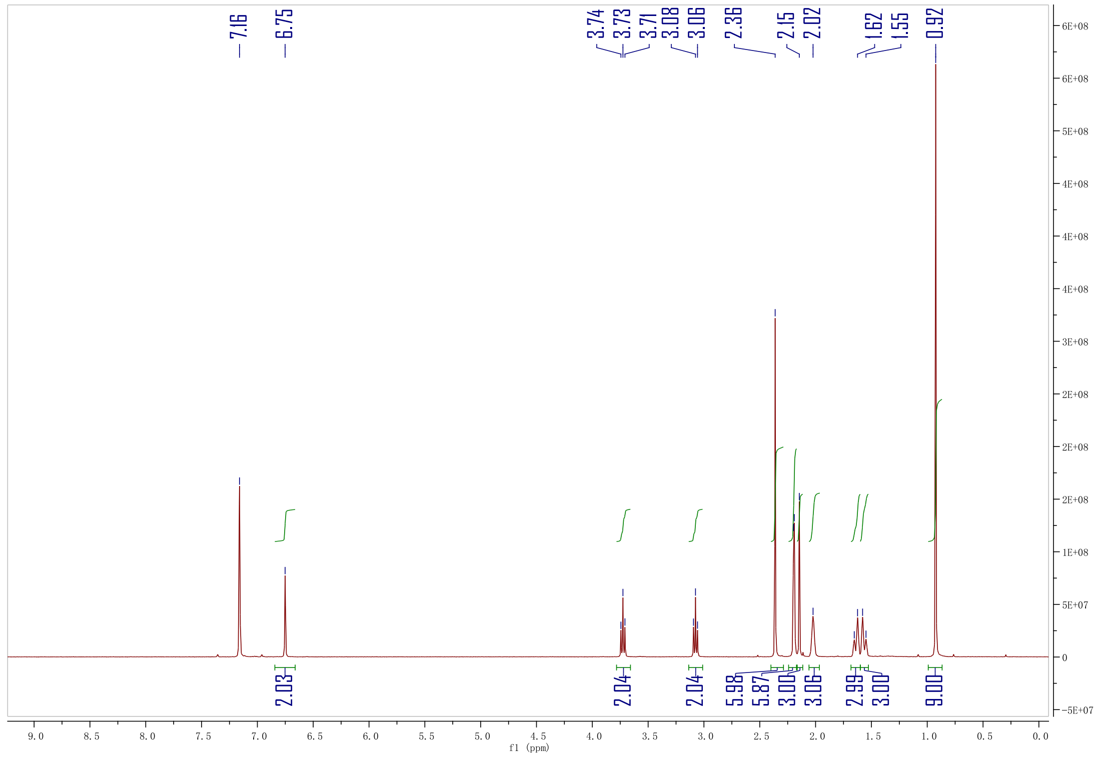

Figure 5.9 ^{1}H NMR spectrum of **3**.

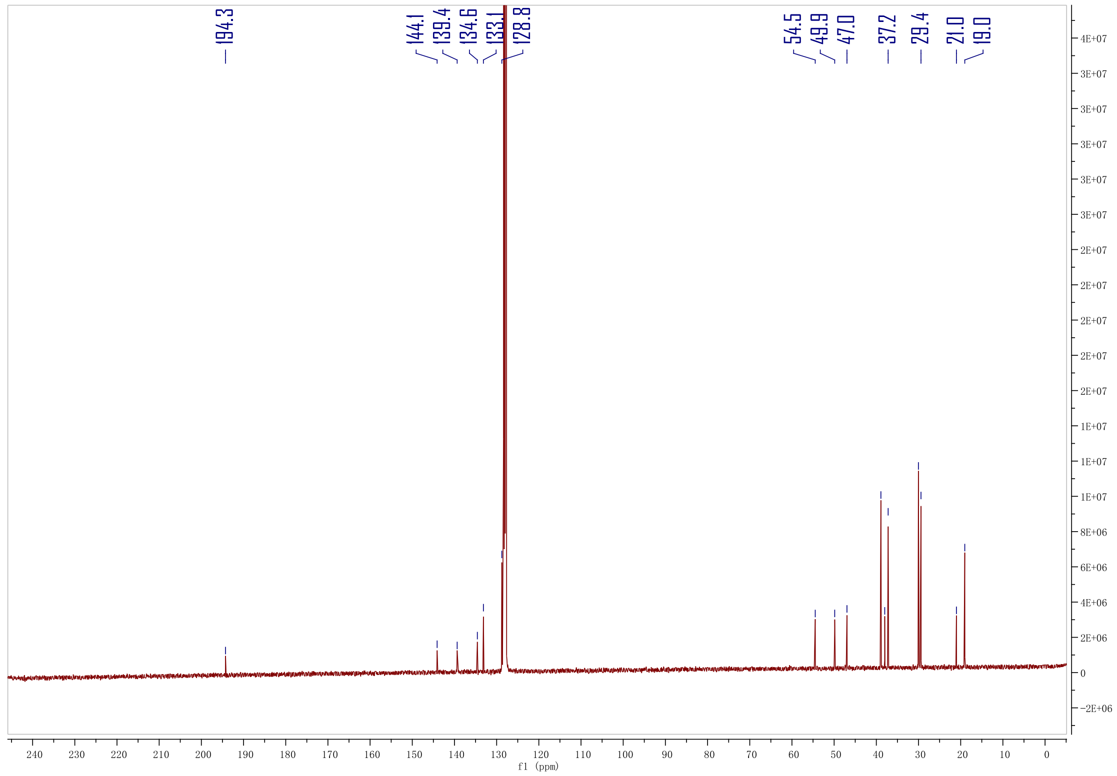

Figure 5.10 ^{13}C{^{1}H} NMR spectrum of **3**.

5.4.2 Crystal structural parameters

X-ray data collection and structural refinement. Intensity data for compounds **2** and **3** was collected using a Bruker APEX II diffractometer. The crystals of **2** and **3** were measured at 103(2) K. The structure was solved by direct phase determination (SHELX-2013) and refined for all data by full-matrix least squares methods on *F2*.[23] All non-hydrogen atoms were subjected to anisotropic refinement. The hydrogen atoms were generated geometrically and allowed to ride in their respective parent atoms; they were assigned appropriate isotropic thermal parameters and included in the structure-factor calculations. CCDC; 1012365 and 1012366 (**2** and **3**) contains the supplementary crystallographic data. The data can be obtained free of charge from the Cambridge Crystallography Data Center via www.ccdc.cam.ac.uk/data_request/cif.

Table 1 Crystallographic data for compounds 2 and 3.

Compounds	**2·(CH$_3$CN)$_2$**	**3·(C$_6$H$_6$)$_{0.5}$**
Formula	$C_{31}H_{45}Cl_4Ge_2N_5$	$C_{30}H_{42}GeN_3$
Fw	774.70	517.25
Cryst syst	monoclinic	triclinic
Space group	$P2_1/c$	*P*-1
Size (mm^3)	0.180 x 0.220 x 0.260	0.140 x 0.200 x 0.380
T, K	103(2)	103(2)
a, Å	13.7263(6)	7.7987(2)
b, Å	16.2786(6)	12.9356(5)
c, Å	15.8632(6)	13.2720(5)
α, deg	90	92.943(2)
β, deg	95.5530(17)	98.4185(18)
γ, deg	90	91.202(2)
V, Å^3	3527.9(2)	1322.17(8)
Z	4	2

d_{calcd} g·cm^{-3}	1.459	1.299
μ, mm^{-1}	2.036	1.181
Refl collected	60676	54964
T_{min}/T_{max}	0.7110/0.6200	0.8520/0.6620
N_{measd}	11290	8559
[R_{int}]	0.0605	0.0809
R [I>2sigma(I)]	0.0356	0.0392
R_w[I>2sigma(I)]	0.0735	0.0802
GOF	1.017	1.035
Largest diff. peak/hole[e·Å^{-3}]	0.999/-0.465	0.475/-0.417

5.4.3 Theoretical calculation

Gaussian 09 was used for all density functional theory (DFT) calculations.[24] Geometry optimization, frequency calculations, and Natural bond orbital (NBO) analysis on compound **2** and **3** were performed at the B3LYP/6-311G(d,p) level of theory.

Figure 5.11. Calculated optimized structures for **2** and **3** at B3LYP/6-311G(d,p) level of theory.

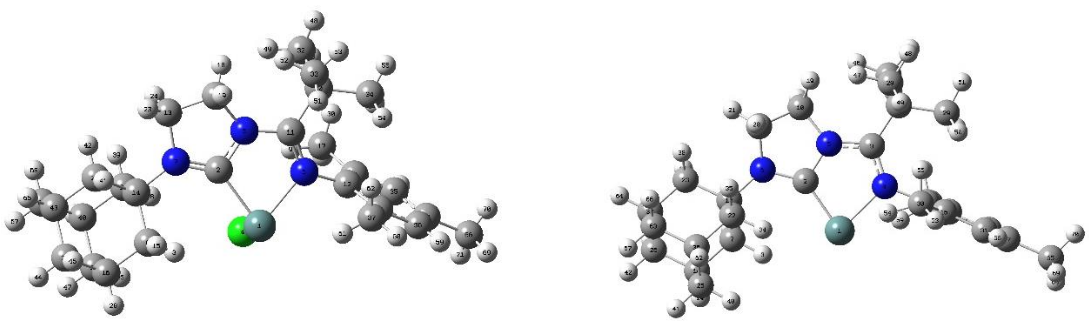

2 **3**

Table 2. Optimized structures of **2** and **3** (atom, x-, y-, z- positions in Å)

2

Ge	-0.198486	-1.200956	-0.124344
C	0.817221	0.647296	-0.066359
H	2.386460	-1.672554	0.347628
Cl	0.084624	-1.342622	2.144405
N	-0.050628	1.715335	0.000710
N	-1.755398	0.229353	-0.041471
N	2.061495	1.053756	-0.006150
C	3.003566	-1.229783	-0.439897
H	-2.326626	-0.007888	2.478954
C	0.727910	2.984651	-0.056313
C	-1.441760	1.487866	-0.040694
C	-3.051551	-0.411058	-0.135911
C	2.123699	2.503018	0.325267
C	3.320143	0.236563	-0.101285
H	2.456846	-1.288412	-1.387194
C	4.314812	-2.039424	-0.548521
C	-3.376090	-0.283747	2.406494
H	0.350180	3.734969	0.629097
H	0.711459	3.376632	-1.073540
C	-2.388378	2.712886	-0.034974
C	-3.773211	-0.735401	1.021284
C	-3.479565	-0.828036	-1.412443
H	2.903981	3.008254	-0.236997
H	2.324019	2.609491	1.393805
C	4.079382	0.297743	1.245978
C	4.208128	0.824297	-1.226330
C	5.193762	-1.450072	-1.665607
H	4.056630	-3.075542	-0.783580
C	5.062262	-1.978402	0.796944
H	-3.982041	0.574059	2.720341
H	-3.554244	-1.079913	3.131528
C	-2.308920	3.379398	1.364843
C	-2.004614	3.717815	-1.156728
C	-3.871865	2.357012	-0.278953
C	-4.953988	-1.470536	0.866426
C	-4.665642	-1.550537	-1.504740

C	-2.703897	-0.489067	-2.662701
H	3.445250	-0.106036	2.041367
H	4.316256	1.335231	1.503478
C	5.390386	-0.511061	1.129550
H	3.663987	0.794332	-2.176435
H	4.454726	1.869730	-1.019326
C	5.519302	0.015823	-1.329089
H	6.117495	-2.028625	-1.760104
H	4.678861	-1.514232	-2.630630
H	4.452792	-2.421798	1.591406
H	5.984103	-2.564879	0.738841
H	-2.953695	4.260949	1.366475
H	-1.308475	3.706625	1.647277
H	-2.668058	2.699887	2.139121
H	-1.838337	3.214011	-2.112736
H	-1.137359	4.331586	-0.929066
H	-2.840125	4.404809	-1.297505
H	-4.037419	1.894814	-1.251752
H	-4.433114	3.293426	-0.260174
H	-4.290976	1.710884	0.486449
H	-5.521757	-1.721130	1.756782
C	-5.419784	-1.888585	-0.376689
H	-5.008320	-1.863361	-2.485785
H	-3.204649	-0.891579	-3.543279
H	-1.692449	-0.908258	-2.643259
H	-2.604336	0.591840	-2.806612
H	5.915128	-0.455750	2.087297
C	6.269579	0.089438	0.015448
H	6.132943	0.453425	-2.121558
C	-6.681132	-2.704219	-0.509002
H	7.212881	-0.460677	-0.053090
H	6.527257	1.128116	0.251311
H	-7.301504	-2.345858	-1.334097
H	-7.276944	-2.670196	0.404272
H	-6.444678	-3.753588	-0.712224

3

Ge	0.107578	-1.12426	-0.35575
C	-0.79481	0.561384	-0.28684
N	1.681474	0.106218	-0.12078
N	0.076102	1.644314	-0.12341
N	-2.10601	1.074783	-0.38259
C	-3.28224	-0.96161	-1.12712
C	1.42289	1.420037	-0.04582
C	2.951058	-0.55087	-0.01799
C	-0.68913	2.902708	-0.21711
C	-2.08478	2.432936	0.16684
C	-3.28251	0.212714	-0.12319
C	-4.52216	-1.85399	-0.92446
C	2.40364	2.601125	0.152701
C	3.406147	-1.00026	1.233967
C	3.661462	-0.86869	-1.19118
C	-3.31502	-0.35084	1.32087
C	-4.57544	1.03051	-0.35623
C	-4.52082	-2.41078	0.513084
C	-5.7973	-1.02269	-1.15555
C	2.242845	3.64431	-0.9854
C	2.159634	3.263981	1.533714
C	3.892737	2.19358	0.129394
C	2.640171	-0.71451	2.501823
C	4.603447	-1.71863	1.292757
C	4.852142	-1.58683	-1.07947
C	3.157235	-0.4507	-2.55034
C	-4.55821	-1.24307	1.518404
C	-5.82236	0.145622	-0.15468
C	5.347787	-2.01584	0.152931
C	-5.83165	-0.40747	1.284201
C	6.65112	-2.77295	0.243906
H	-2.38124	-1.56846	-1.0015
H	-3.25265	-0.55732	-2.1443
H	-0.67675	3.261026	-1.25065
H	-0.31391	3.679959	0.440477
H	-2.20095	2.443063	1.263684
H	-2.85317	3.068003	-0.27259
H	-4.48407	-2.68193	-1.64004
H	-2.40071	-0.91994	1.510929
H	-3.33333	0.475862	2.040969
H	-4.625	1.871177	0.343237
H	-4.56025	1.448583	-1.36943
H	-3.62561	-3.01987	0.678686
H	-5.38728	-3.06483	0.664888
H	-6.68836	-1.64812	-1.02779
H	-5.81823	-0.64112	-2.1829
H	2.369429	3.171128	-1.96257
H	3.017728	4.40927	-0.88304
H	1.283985	4.157657	-0.98198
H	1.139598	3.620009	1.674149
H	2.828243	4.121853	1.652465
H	2.37413	2.558506	2.339205
H	4.156562	1.499147	0.923971
H	4.48636	3.101114	0.271032
H	4.189892	1.751378	-0.82095
H	2.997279	-1.34677	3.316765
H	1.570645	-0.88957	2.366351
H	2.758678	0.327678	2.818811
H	4.954696	-2.06359	2.260831
H	5.401559	-1.82649	-1.98526
H	2.164034	-0.86294	-2.74557
H	3.835094	-0.79341	-3.33412
H	3.066841	0.636842	-2.63494
H	-4.55867	-1.63775	2.540339
H	-6.71738	0.755135	-0.32046
H	-5.88082	0.417217	2.005192
H	-6.72421	-1.02358	1.443028
H	6.751538	-3.49298	-0.57248
H	6.72896	-3.31892	1.186594
H	7.508525	-2.09329	0.185096

Table 3. The NPA charges of **2** calculated at B3LYP/6-311G(d,p) level of theory.

Atom	No	Natural Charge	Core	Valence	Rydberg	Total
Ge	1	0.86899	27.99672	3.10490	0.02939	31.13101
C	2	0.18364	1.99912	3.76693	0.05030	5.81636
H	3	0.22139	0.00000	0.77392	0.00469	0.77861
Cl	4	-0.43928	9.99983	7.43116	0.00830	17.43928
N	5	-0.44212	1.99907	5.43066	0.01239	7.44212
N	6	-0.59071	1.99919	5.57170	0.01982	7.59071
N	7	-0.37219	1.99906	5.35410	0.01902	7.37219
C	8	-0.43137	1.99908	4.41300	0.01929	6.43137
H	9	0.21667	0.00000	0.78104	0.00229	0.78333
C	10	-0.18982	1.99917	4.17463	0.01602	6.18982
C	11	0.56744	1.99884	3.39908	0.03464	5.43256
C	12	0.10119	1.99864	3.87961	0.02056	5.89881
C	13	-0.19096	1.99917	4.17528	0.01651	6.19096
C	14	0.18967	1.99898	3.78958	0.02177	5.81033
H	15	0.21383	0.00000	0.78287	0.00329	0.78617
C	16	-0.18881	1.99913	4.17170	0.01798	6.18881
C	17	-0.60185	1.99919	4.59334	0.00932	6.60185
H	18	0.22413	0.00000	0.77263	0.00324	0.77587
H	19	0.21005	0.00000	0.78661	0.00334	0.78995
C	20	-0.08499	1.99908	4.07322	0.01268	6.08499
C	21	-0.01175	1.99883	3.99943	0.01350	6.01175
C	22	-0.01714	1.99884	4.00481	0.01349	6.01714
H	23	0.22601	0.00000	0.77186	0.00213	0.77399
H	24	0.21590	0.00000	0.78130	0.00281	0.78410
C	25	-0.40843	1.99907	4.39155	0.01781	6.40843
C	26	-0.40341	1.99908	4.38643	0.01791	6.40341
C	27	-0.39186	1.99915	4.37581	0.01690	6.39186
H	28	0.22098	0.00000	0.77646	0.00256	0.77902
C	29	-0.39247	1.99915	4.37635	0.01697	6.39247
H	30	0.20962	0.00000	0.78806	0.00232	0.79038
H	31	0.22667	0.00000	0.77160	0.00173	0.77333
C	32	-0.56606	1.99917	4.55462	0.01226	6.56606
C	33	-0.57848	1.99918	4.56704	0.01226	6.57848
C	34	-0.57864	1.99919	4.56574	0.01371	6.57864
C	35	-0.19379	1.99888	4.17961	0.01531	6.19379
C	36	-0.19550	1.99887	4.18128	0.01535	6.19550
C	37	-0.58950	1.99920	4.58156	0.00874	6.58950
H	38	0.22040	0.00000	0.77641	0.00319	0.77960

H	39	0.20217	0.00000	0.79489	0.00295	0.79783
C	40	-0.19559	1.99914	4.17845	0.01801	6.19559
H	41	0.20819	0.00000	0.78844	0.00336	0.79181
H	42	0.19983	0.00000	0.79678	0.00339	0.80017
C	43	-0.19509	1.99914	4.17781	0.01814	6.19509
H	44	0.21283	0.00000	0.78427	0.00291	0.78717
H	45	0.20161	0.00000	0.79565	0.00274	0.79839
H	46	0.20721	0.00000	0.79042	0.00237	0.79279
H	47	0.21226	0.00000	0.78497	0.00277	0.78774
H	48	0.22115	0.00000	0.77679	0.00206	0.77885
H	49	0.19181	0.00000	0.80664	0.00155	0.80819
H	50	0.21685	0.00000	0.78095	0.00219	0.78315
H	51	0.20832	0.00000	0.78933	0.00235	0.79168
H	52	0.19938	0.00000	0.79898	0.00164	0.80062
H	53	0.22476	0.00000	0.77315	0.00209	0.77524
H	54	0.21422	0.00000	0.78322	0.00256	0.78578
H	55	0.21405	0.00000	0.78360	0.00235	0.78595
H	56	0.21903	0.00000	0.77799	0.00298	0.78097
H	57	0.20770	0.00000	0.78856	0.00374	0.79230
C	58	0.01676	1.99894	3.97098	0.01331	5.98324
H	59	0.20654	0.00000	0.78969	0.00377	0.79346
H	60	0.22129	0.00000	0.77711	0.00160	0.77871
H	61	0.20943	0.00000	0.78858	0.00199	0.79057
H	62	0.19984	0.00000	0.79743	0.00273	0.80016
H	63	0.22173	0.00000	0.77574	0.00253	0.77827
C	64	-0.39277	1.99915	4.37670	0.01692	6.39277
H	65	0.22039	0.00000	0.77708	0.00254	0.77961
C	66	-0.59005	1.99919	4.58173	0.00913	6.59005
H	67	0.21287	0.00000	0.78424	0.00289	0.78713
H	68	0.20057	0.00000	0.79662	0.00281	0.79943
H	69	0.21434	0.00000	0.78385	0.00181	0.78566
H	70	0.21046	0.00000	0.78785	0.00169	0.78954
H	71	0.22048	0.00000	0.77758	0.00193	0.77952

===

* Total *	1.00000	97.96845	171.37194	0.65961	270.00000

Table 4. The NPA charges of **3** calculated at B3LYP/6-311G(d,p) level of theory.

Atom	No	Natural Charge	Core	Valence	Rydberg	Total
Ge	1	0.45288	27.99427	3.53136	0.02149	31.54712
C	2	-0.13649	1.99925	4.09671	0.04053	6.13649
H	3	0.20796	0.00000	0.78890	0.00314	0.79204
N	4	-0.69107	1.99929	5.67336	0.01842	7.69107
N	5	-0.42647	1.99907	5.41476	0.01264	7.42647
N	6	-0.53548	1.99921	5.51419	0.02208	7.53548
C	7	-0.39725	1.99911	4.37866	0.01948	6.39725
C	8	0.46338	1.99889	3.50156	0.03616	5.53662
C	9	0.14837	1.99869	3.83208	0.02086	5.85163
C	10	-0.17201	1.99920	4.15555	0.01726	6.17201
C	11	-0.17382	1.99922	4.15637	0.01824	6.17382
C	12	0.19868	1.99905	3.77898	0.02329	5.80132
H	13	0.20421	0.00000	0.79195	0.00384	0.79579
C	14	-0.19425	1.99917	4.17669	0.01839	6.19425
C	15	-0.07131	1.99914	4.05899	0.01318	6.07131
C	16	-0.00959	1.99886	3.99632	0.01441	6.00959
C	17	-0.00568	1.99886	3.99244	0.01438	6.00568
H	18	0.19244	0.00000	0.80323	0.00433	0.80756
H	19	0.20036	0.00000	0.79615	0.00350	0.79964
H	20	0.16757	0.00000	0.82667	0.00576	0.83243
H	21	0.19987	0.00000	0.79779	0.00234	0.80013
C	22	-0.41632	1.99912	4.39872	0.01848	6.41632
C	23	-0.40178	1.99913	4.38388	0.01877	6.40178
H	24	0.20472	0.00000	0.79257	0.00271	0.79528
C	25	-0.38572	1.99919	4.36906	0.01747	6.38572
C	26	-0.38440	1.99919	4.36762	0.01759	6.38440
C	27	-0.56721	1.99923	4.55543	0.01255	6.56721
C	28	-0.56098	1.99922	4.54903	0.01273	6.56098
C	29	-0.57222	1.99924	4.55894	0.01405	6.57222
C	30	-0.58696	1.99922	4.57837	0.00937	6.58696
C	31	-0.21337	1.99891	4.19876	0.01570	6.21337
C	32	-0.21244	1.99891	4.19771	0.01582	6.21244
C	33	-0.58538	1.99923	4.57690	0.00925	6.58538
H	34	0.21839	0.00000	0.77869	0.00291	0.78161
H	35	0.19099	0.00000	0.80560	0.00341	0.80901
C	36	-0.19403	1.99918	4.17659	0.01827	6.19403
C	37	-0.19214	1.99917	4.17446	0.01851	6.19214
H	38	0.19397	0.00000	0.80276	0.00328	0.80603

H	39	0.20120	0.00000	0.79462	0.00418	0.79880
H	40	0.20080	0.00000	0.79671	0.00249	0.79920
H	41	0.19287	0.00000	0.80408	0.00305	0.80713
H	42	0.19377	0.00000	0.80318	0.00305	0.80623
H	43	0.19404	0.00000	0.80331	0.00265	0.80596
H	44	0.20240	0.00000	0.79512	0.00248	0.79760
H	45	0.19833	0.00000	0.79905	0.00262	0.80167
H	46	0.19394	0.00000	0.80440	0.00166	0.80606
H	47	0.18838	0.00000	0.80998	0.00164	0.81162
H	48	0.19721	0.00000	0.80025	0.00255	0.80279
H	49	0.20153	0.00000	0.79596	0.00251	0.79847
H	50	0.21184	0.00000	0.78534	0.00282	0.78816
H	51	0.19600	0.00000	0.80141	0.00259	0.80400
H	52	0.20755	0.00000	0.78970	0.00275	0.79245
H	53	0.20040	0.00000	0.79785	0.00175	0.79960
H	54	0.22517	0.00000	0.77249	0.00234	0.77483
H	55	0.19640	0.00000	0.80082	0.00278	0.80360
H	56	0.19474	0.00000	0.80133	0.00393	0.80526
C	57	-0.00600	1.99896	3.99280	0.01424	6.00600
H	58	0.19480	0.00000	0.80132	0.00387	0.80520
H	59	0.22618	0.00000	0.77169	0.00213	0.77382
H	60	0.19815	0.00000	0.80008	0.00177	0.80185
H	61	0.19838	0.00000	0.79889	0.00273	0.80162
H	62	0.20241	0.00000	0.79466	0.00293	0.79759
C	63	-0.38477	1.99919	4.36794	0.01764	6.38477
H	64	0.20177	0.00000	0.79551	0.00271	0.79823
C	65	-0.57989	1.99923	4.57112	0.00954	6.57989
H	66	0.19208	0.00000	0.80524	0.00268	0.80792
H	67	0.19435	0.00000	0.80259	0.00306	0.80565
H	68	0.20328	0.00000	0.79479	0.00193	0.79672
H	69	0.20047	0.00000	0.79770	0.00184	0.79953
H	70	0.20481	0.00000	0.79312	0.00207	0.79519
* Total *		0.00000	87.96759	165.37086	0.66156	254.00000

5.5 References

(1) a) Igau, A.; Grutzmacher, H.; Baceiredo, A.; Bertrand, G. *J. Am. Chem. Soc.* **1988**, *110*, 6463 – 6466; b) Arduengo III, A. J.; Harlow, R. L.; Kline, M. *J. Am. Chem. Soc.* **1991**, *113*, 361 – 363.

(2) a) Herrmann, W. A.; Köcher, C. *Angew. Chem. Int. Ed. Engl.* **1997**, *36*, 2162 – 2187; b) Peris, E. *Chem. Rev.* **2017**, DOI: 10.1021/acs.chemrev.6b00695; c) Díez-González, S.; Marion, N.; Nolan, S. P. *Chem. Rev.* **2009**, *109*, 3612 – 3676; d) Hahn, F. E.; Jahnke, M. C. *Angew. Chem. Int. Ed.* **2008**, *47*, 3122 – 3172; e) Arnold, P. L.; Casely, I. J. *Chem. Rev.* **2009**, *109*, 3599 – 3611; f) de Frémont, P.; Marion, N.; Nolan, S. P. *Coord. Chem. Rev.* **2009**, *253*, 862 – 892; g) Crudden, C. M.; Allen, D. P.; *Coord. Chem. Rev.* **2004**, *248*, 2247 – 2273; h) Jacobsen, H.; Correa, A.; Poater, A.; Costabile, C.; Cavallo, L. *Coord. Chem. Rev.* **2009**, *253*, 687 – 703; i) Poyatos, M.; Mata, J. A.; Peris, E. *Chem. Rev.* **2009**, *109*, 3677 – 3707; j) Hindi, K. M.; Panzner, M. J.; Tessier, C. A.; Cannon, C. L.; Youngs, W. J. *Chem. Rev.* **2009**, *109*, 3859 – 3884.

(3) a) Enders, D.; Niemeier, O.; Henseler, A. *Chem. Rev.* **2007**, *107*, 5606 – 5655; b) Fevre, M.; Pinaud, J.; Gnanou, Y.; Vignolle, J.; Taton, D. *Chem. Soc. Rev.* **2013**, *42*, 2142 – 2172; (c) Naumann, S.; Dove, A. P. *Polymer Chemistry* **2015**, *6*, 3185 – 3200; d) Nair, V.; Menon, R. S.; Biju, A. T.; Sinu, C. R.; Paul, R. R.; Jose, A.; Sreekumar, V. *Chem. Soc. Rev.* **2011**, *40*, 5336 – 5346; e) Bugaut, X.; Glorius, F. *Chem. Soc. Rev.* **2012**, *41*, 3511 – 3522.

(4) a) Kuhn, N.; Al-Sheikh, A. *Coord. Chem. Rev.* **2005**, *249*, 829 – 857; b) Fuchter, M. J. *Chem. Eur. J.* **2010**, *16*, 12286 – 12294; c) Curran, D. P.; Solovyev, A.; Makhlouf Brahmi, M.; Fensterbank, L.; Malacria, M.; Lacôte, E. *Angew. Chem. Int. Ed.* **2011**, *50*, 10294 – 10317; d) Kolychev, E. L.; Theuergarten, E.; Tamm, M. In *Frustrated Lewis Pairs II: Expanding the Scope*; Erker, G., Stephan, D. W., Eds.; Springer Berlin Heidelberg: Berlin, Heidelberg, 2013, p 121 – 155; e) Martin, D.; Soleilhavoup, M.; Bertrand, G. *Chem. Sci.* **2011**, *2*, 389 – 399; f) Martin, C. D.; Soleilhavoup, M.; Bertrand, G. *Chem. Sci.* **2013**, *4*,

3020 – 3030; g) Murphy, L. J.; Robertson, K. N.; Masuda, J. D.; Clyburne, J. A. C. In *N-Heterocyclic Carbenes*; Wiley-VCH Verlag GmbH & Co. KGaA: 2014, p 427 – 498; h) Wang, Y.; Robinson, G. H. *Inorg. Chem.* **2011**, *50*, 12326 – 12337.

(5) a) Martin, D.; Melaimi, M.; Soleilhavoup, M.; Bertrand, G. *Organometallics* **2011**, *30*, 5304 – 5313; b) Melaimi, M.; Soleihavoup, M.; Bertrand, G. *Angew. Chem. Int. Ed.* **2010**, *49*, 8810 – 8849.

(6) Aldeco-Perez, E.; Rosenthal, A. J.; Donnadieu, B.; Parames-waran, P.; Frenking, G.; Bertrand, G. *Science* **2009**, *326*, 556 – 559.

(7) a) Crabtree, R. H. *Coord. Chem. Rev.* **2013**, *257*, 755 – 766; b) Drçge, T.; Glorius, F. *Angew. Chem. Int. Ed.* **2010**, *49*, 6940 – 6952; see also ref 5.

(8) For recent reviews, see: a) Asay, M.; Jones, C.; Driess, M. *Chem. Rev.* **2011**, *111,* 354 – 396; b) Mizuhata, Y.; Sasamori, T.; Tokitoh, N. *Chem. Rev.* **2009**, *109*, 3479 – 3511; c) Lappert, M. F.; Power, P. P.; Protchenko, A.; Seeber, A. *Metal Amide Chemistry*, Wiley, Chi-chester, UK, **2009**; c) Zabula, A. V.; Hahn, F. E. *Eur. J. Inorg. Chem.* **2008**, 5165 – 5179.

(9) a) Tonner, R.; Frenking, G. *Angew. Chem., Int. Ed.* **2007**, *46*, 8695 – 8698; b) Tonner, R.; Frenking, G. *Chem. Eur. J.* **2008**, *14*, 3260 – 3272; c) Tonner, R.; Frenking, G. *Chem. Eur. J.* **2008**, *14*, 3273 – 3289; d) Tonner, R.; Frenking, G. *Pure Appl. Chem*. **2009**, *81*, 597 – 614; e) Takagi, N.; Shimizu, T.; Frenking, *G. Chem. Eur. J.* **2009**, *15*, 3448 – 3456; f) Takagi, N.; Shimizu, T.; Frenking, G. *Chem. Eur. J.* **2009**, *15*, 8593 – 8604; g) Takagi, N.; Tonner, R.; Frenking, G. *Chem. Eur. J.* **2012**, *18*, 1772 – 1780; h) Kosa, M.; Karni, M.; Apeloig, Y. *J. Chem. Theory Comput*. **2006**, *2*, 956 – 964.

(10) Wiberg, N.; Lerner, H.-W.; Vasisht, S.-K.; Wagner, S.; Karaghiosoff, K.; Nöth, H.;

Ponikwar, W. *Eur. J. Inorg. Chem.* **1999**, *1999*, 1211 – 1218.

(11) a) Kira, M. *Chem. Commun.* **2010**, *46*, 2893 – 2903; b) Kira, M.; Iwamoto, T.; Ishida, S.; Masuda, H.; Abe, T.; Kabuto, C. *J. Am. Chem. Soc.* **2009**, *131*, 17135 – 17144; c) Iwamoto, T.; Masuda, H.; Kabuto, C.; Kira, M. *Organometallics* **2004**, *24*, 197 – 199; d) Ishida, S.; Iwamoto, T.; Kabuto, C.; Kira, M. *Nature* **2003**, *421*, 725 – 727.

(12) Tanaka, H.; Inoue, S.; Ichinohe, M.; Driess, M.; Sekiguchi, A. *Organometallics* **2011**, *30*, 3475 – 3478.

(13) a) Jones, C.; Sidiropoulos, A.; Holzmann, N.; Frenking, G.; Stasch, A. *Chem. Commun.* **2012**, *48*, 9855 – 9857; b) Sidiropoulos, A.; Jones, C.; Stasch, A.; Klein, S.; Frenking, G. *Angew. Chem. Int. Ed.* **2009**, *48*, 9701 – 9704; c) Wang, Y.; Xie, Y.; Wei, P.; King, R. B.; Schaefer, H. F.; von R. Schleyer, P.; Robinson, G. H. *Science* **2008**, *321*, 1069 – 1073; d) Dyker, C. A.; Bertrand, G. *Science* **2008**, *321*, 1050 – 1051.

(14) a) Mondal, K. C.; Roesky, H. W.; Schwarzer, M. C.; Frenking, G.; Niepötter, B.; Wolf, H.; Herbst-Irmer, R.; Stalke, D. *Angew. Chem. Int. Ed.* **2013**, *52*, 2963 – 2967; b) Li, Y.; Mondal, K. C.; Roesky, H. W.; Zhu, H.; Stollberg, P.; Herbst-Irmer, R.; Stalke, D.; Andrada, D. M. *J. Am. Chem. Soc.* **2013**, *135*, 12422 – 12428; c) Xiong, Y.; Yao, S.; Tan, G.; Inoue, S.; Driess, M. *J. Am. Chem. Soc.* **2013**, *135*, 5004 – 5007; d) Xiong, Y.; Yao, S.; Inoue, S.; Epping, J. D.; Driess, M. *Angew. Chem. Int. Ed.* **2013**, *52*, 7147 – 7150.

(15) Chu, T.; Belding, L.; van der Est, A.; Dudding, T.; Korobkov, I.; Nikonov, G. I. *Angew. Chem. Int. Ed.* **2014**, *53*, 2711 – 2715.

(16) Flock, J.; Suljanovic, A.; Torvisco, A.; Schoefberger, W.; Gerke, B.; Pöttgen, R.; Fischer, R. C.; Flock, M. *Chem. Eur. J.* **2013**, *19*, 15504 – 15517.

(17) Singh, A. P.; Roesky, H. W.; Carl, E.; Stalke, D.; Demers, J.-P.; Lange, A. *J. Am. Chem. Soc.* **2012**, *134*, 4998 – 5003.

(18) a) Khn, S.; Gopakumr, G.; Thiel, W.; Alcarazo, M. *Angew. Chem. Int. Ed*. **2013**, *52*, 5644 – 5647; b) Xiong, Y.; Yao, S.; Inoue, S.; Berkefeld, A.; Driess, M. *Chem. Commun*. **2012**, *48*, 12198 – 12200; c) Cheng, F.; Dyke, J. D.; Ferrante, F.; Hector, A. L.; Levason, W.; Reid, G.; Webster, M.; Zhang, W. *Dalton Trans*. **2010**, *39*, 847 – 856; d) Probst, T.; Steigelmann, O.; Riede J.; Schmidbaur, H. *Angew. Chem. Int. Ed.* **1990**, *12*, 1397 – 1398.

(19) For different viewpoints on the use of dative arrows, see: a) Himmel, D.; Krossing, I.; Schnepf, A. *Angew. Chem. Int. Ed.* **2014**, *53*, 370 – 374; b) Frenking, G. *Angew. Chem. Int. Ed.* **2014**, *53*, 6040 – 6046; c) Himmel, D.; Krossing, I.; Schnepf, A. *Angew. Chem. Int. Ed.* **2014**, *53*, 6047 – 6049.

(20) a) West, R.; Sohn, H.; Powell, D. R.; Müller, T.; Apeloig, Y. *Angew. Chem. Int. Ed.* **1996**, *35*, 1002 – 1004; b) Freeman, W. P.; Tilley, T. D.; Liable-Sand, L. M.; Rheingold, A. L. *J. Am. Chem. Soc.* **1996**, *118*, 10457 – 10468; For review, see: c) Lee, V. Ya.; Sekiguchi, A. *Angew. Chem. Int. Ed.* **2007**, *46*, 6596 – 6620.

(21) a) Lee, V. Ya.; Sekiguchi, A. *Comprehensive Inorganic Chemistry II*; Elsevier, Amsterdam, Netherlands, **2013**, *Vol.1*, 289 – 324; b) Fischer, R. C.; Power, P. P.; *Chem. Rev.* **2010**, *110*, 3877 – 3923; c) Lee, V. Ya.; Sekiguchi, A. *Organometallic Compounds of Low-Coordinate Si, Ge, Sn and Pb: From Phantom Species to Stable Compounds;* Wiley, Chichester, UK, **2010**, Chapter 5.

(22) a) Herrmann, W. A.; Denk, M.; Behm, J.; Scherer, W.; Klingan, F.-R.; Bock, H.; Solouki, B.; Wagner, M. *Angew. Chem. Int. Ed.* **1992**, *31*, 1485 – 1488; For reviews, see ref (8).

(23) Bruker AXS SHELXTL, Madison, WI; *SHELX-97G*. M. Sheldrick, Acta Crystallogr. A, **2008**, *64*, 112–122, *SHELX-2013*, http://shelx.uni-ac. gwdg.de/SHELX/index.php.

(24) Gaussian 09, Revision B.01, Frisch, M. J.; Trucks, G. W.; Schlegel, H. B.; Scuseria, G. E.; Robb, M. A.; Cheeseman, J. R.; Scalmani, G.; Barone, V.; Mennucci, B.; Petersson, G. A.; Nakatsuji, H.; Caricato, M.; Li, X.; Hratchian, H. P.; Izmaylov, A. F.; Bloino, J.; Zheng, G.; Sonnenberg, J. L.; Hada, M.; Ehara, M.; Toyota, K.; Fukuda, R.; Hasegawa, J.; Ishida, M.; Nakajima, T.; Honda, Y.; Kitao, O.; Nakai, H.; Vreven, T.; Montgomery, J. A. Jr.,; Peralta, J. E.; Ogliaro, F.; Bearpark, M.; Heyd, J. J.; Brothers, E.; Kudin, K. N.; Staroverov, V. N.; Keith, T.; Kobayashi, R.; Normand, J.; Raghavachari, K.; Rendell, A.; Burant, J. C.; Iyengar, S. S.; Tomasi, J.; Cossi, M.; Rega, N.; Millam, J. M.; Klene, M.; Knox, J. E.; Cross, J. B.; Bakken, V.; Adamo, C.; Jaramillo, J.; Gomperts, R.; Stratmann, R. E.; Yazyev, O.; Austin, A. J.; Cammi, R.; Pomelli, C.; Ochterski, J. W.; Martin, R. L.; Morokuma, K.; Zakrzewski, V. G.; Voth, G. A.; Salvador, P.; Dannenberg, J. J.; Dapprich, S.; Daniels, A. D.; Farkas, O.; Foresman, J. B.; Ortiz, J. V.;Cioslowski, J.; Fox, D. J. Gaussian, Inc., Wallingford CT, **2010**.

Chapter 6 Diverse reactivity of the Imino-N-heterocyclic Carbene/Germanium(0) Adduct†

6.1 Introduction

Germylenes bearing a Ge atom in the +2 oxidation state, as the analogue of the carbenes has been widely studied for a long time.[1] In particular, germylenes exhibit various chemical behaviours including activation of strong σ-bonds in inorganic and organic compounds,[2,3] coordination to metals[4-6] and cycloaddition reactions.[7] The unique chemical properties of germylenes are attributed to the electronic environment at the Ge center, which features a lone pair and an accessible vacant p-orbital (Figure 6.1a).

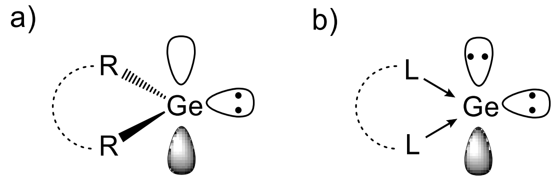

Figure 6.1 Schematic representation for the electronic states of germylene (a) and germylone (b).

In recent years, several groups reported a novel class of germanium species, namely, germylones.[8,9] Germylones retain their valence electrons at the germanium center, and involve a germanium atom in the zero-oxidation state.[10] Thus, the germanium center in germylones formally possesses two lone pairs (Figure 6.1b), which is in contrast to the electronic situation

† Portions of this chapter are taken with permission from: 1) Su, B.; Ganguly, R.; Li, Y.; Kinjo, R. *Angew. Chem. Int. Ed.* **2014**, *53*, 13106 – 130109. Copyright (2014) WILEY-VCH Verlag GmbH & Co. KGaA, Weinheim. 2) Su, B.; Ganguly, R.; Li, Y.; Kinjo, R. *Chem. Commun.* **2016**. 52, 613 – 616. Copyright (2015) Royal Society of Chemistry.

of germylenes. The unique electronic property might result in a diverse reactivity of the germylones. To the best of our knowledge, although various types of Ge(0) species have been developed thus far, their reactivity especially their ligand behaviours towards transition metals had rarely been studied when we started this project. In chapter 5, we reported the synthesis of a Ge(0) species **1** supported by a bidentate imino-N-heterocyclic carbene (Figure 6.2), which may also be deemed a mesoionic germylene **1'**, a heavier analogue of imidazol-5-ylidene.[11] It has been reported that the ligand nature of imidazol-5-ylidene is different from that of NHCs.[11,12] Hence, it is reasonable to envisage that compound **1** would show peculiar chemical properties. In this chapter, we report the synthesis and characterization of the mono- and di-cationic germanium species **2** and **3** as well as the germylone-transition metal (Cr, Mo, W) complexes **4**–**7**.

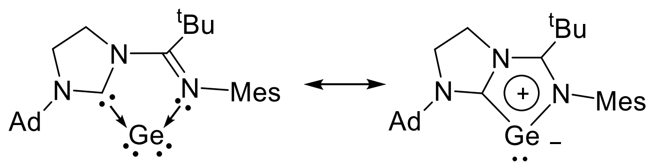

1 **1'**

Figure 6.2 Canonical forms of compound **1** (Ad = 1-admantyl, Mes = 2,4,6-trimethylphenyl).

When we completed the project mentioned in this chapter, the Driess group reported a series of studies on the reactivity of the germylones. For a better understanding of the recent progress in this research field, their research work is briefly introduced first. In 2016, the Driess group reported the first germylone-gallium trichloride adduct **I** by treatment of the germylone BisNHC-Ge(0) with $GaCl_3$ (Figure 6.3).[13] In the molecular structure, the Ge atom is tricoordinate with the carbon atoms of bisNHC and Ga atom, and adopts a pseudotetrahedral coordination geometry with a lone pair of electrons occupying the vertex. The reaction of **I** with Se (1 eq) or Te (1eq) afforded the germanium mono-chalcogenides **II**, but the reaction towards to S_8 gave the germanium disulfide **III** (X = S) exclusively. Compound **II** (X = Se) can be further oxidized by selenium to afford **III** (X = Se). Compound **II** and **III** represent novel classes of heavier congeners of CO and CO_2 complexes. Note that the presence of the Lewis acid $GaCl_3$ is essential for the stabilization of such species bearing highly polar Ge=X bonds. Very recently, the same group successfully isolated the first bis-NHSi supported zerovalent germanium complexes **IV**.[14] Attempts to synthesize the bis(silylene)pyridine-germanium(0) through the reductive dechlorination of its precursor $[LGeCl]^{+}Cl^{-}$ (L = bis(silylene)pyridine) failed, but the reaction with Collman's reagent, $K_2Fe(CO)_4$ successfully afforded the germylone-iron complex **IV**. In the molecular structure of **IV,** the Ge(0) center is coordinated by the two NHSi-silicon atoms and the iron atom, adopting a trigonal-pyramidal geometry. Interestingly, treatment of **IV** with one equivalent of $GeCl_2$(dioxane) resulted in the formation of the complex **V** by insertion of $GeCl_2$ into the dative Ge-Fe bond, which represents the push-pull germylone-germylene donor-acceptor complex.

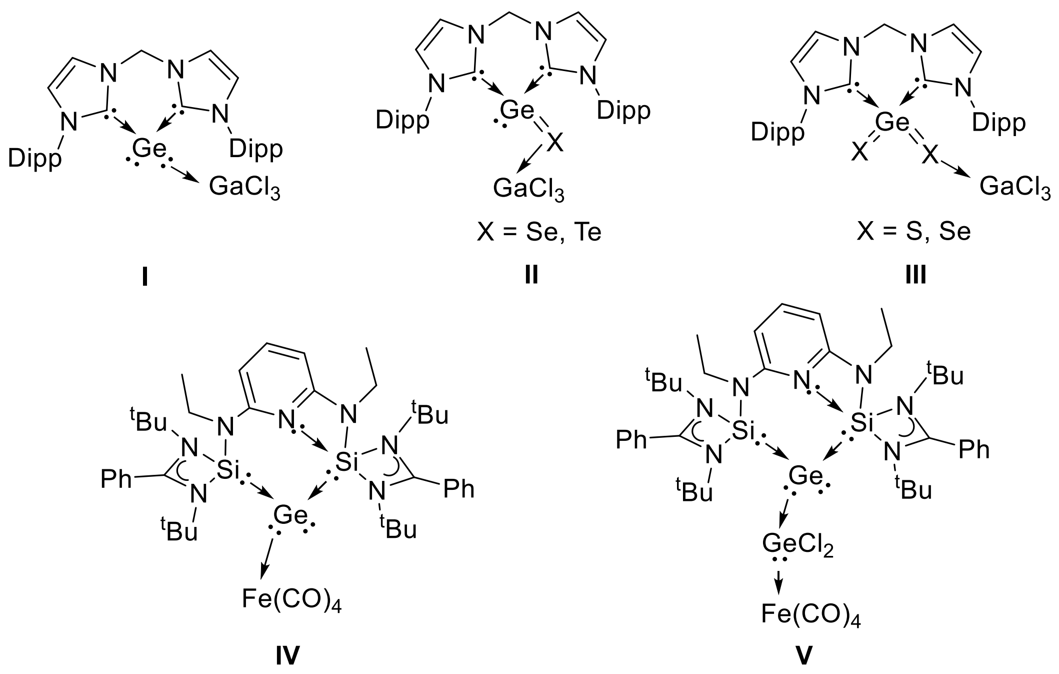

Figure 6.3 Reported gremylone adducts (**I**, **IV** and **V**) and germanium mono- and dichalcogenides (**II** and **III**).

6.2 Results and Discussions

6.2.1 Reactivity of germylone 1 towards one equivalent of MeOTf.

The germylone **1** was prepared according to the same procedures described in chapter 5. One equivalent of methyl trifluoromethanesulfonate (MeOTf) was added dropwise to a toluene solution of compound **1** at room temperature. Instantaneously, the colour of the solution darkened and changed from yellow to red. After work-up, compound **2** was obtained as a red solid in 65% yield (Scheme 6.1). In the ^{13}C NMR spectrum of **2**, the carbene peak appeared at 206.0 ppm which is slightly shifted downfield with respect to that (194.3 ppm) of **1**.

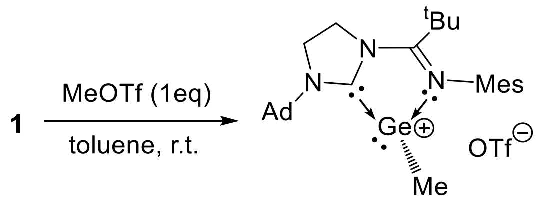

2 (65 %)

Scheme 6.1 Reaction of **1** with one equivalent of MeOTf.

Single crystals of **2** were obtained by slow evaporation of a toluene solution. The molecular structure of **2** was determined by X-ray diffraction analysis, which revealed the formation of a germyliumylidene ion (Figure 6.4). The five C_2N_2Ge atoms form a nearly planar five-membered ring (the sum of internal pentagon angles = 538.05°). The tricoordinate Ge center displays a pyramidal geometry (the sum of bond angles = 278.22°), and the Me group on the Ge atom is located nearly perpendicularly to the outside of the five-membered ring (C1–Ge1–N3: 98.28(9)°. C1–Ge1–C2: 101.71(10)°). The smaller C2–Ge1–N3 angle (78.23(9)°) and the longer Ge1–C2 (2.024(2) Å) and Ge1–N3 (2.040(2) Å) bond distances in **2** comparison to those of **1** (C–Ge–N: 80.59(6)°, Ge–C: 1.8870(15) Å, Ge–N: 1.9680(13) Å) are confirmed, and these metric parameters are similar to those of $[(L)GeCl]^+GeCl_3^-$ reported in chapter 5 (C–Ge–N: 76.88(7)°, Ge–C: 2.0588(19) Å, Ge–N: 2.0560(16) Å), indicating the loss of the electron delocalization over the five-membered C_2N_2Ge ring.

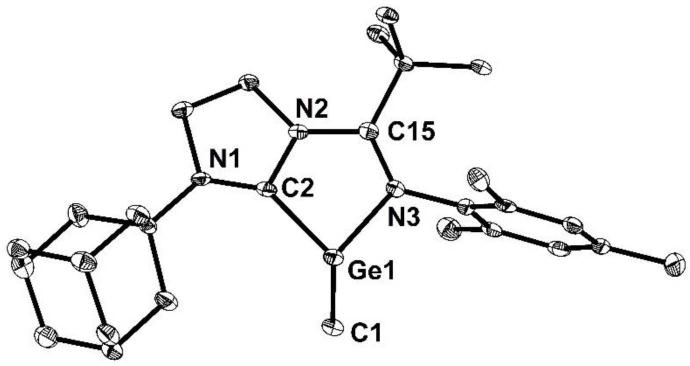

Figure 6.4 Solid-state structure of **2** (hydrogen atoms, solvent molecules, and OTf^-, are omitted for clarity). Thermal ellipsoids are set at the 50% probability.

To gain an insight into the electronic feature of **2,** quantum chemical density functional theory (DFT) calculation was performed for the cationic part of **2** (Figure 6.5). The HOMO displays a lone pair orbital which is mainly localized on the Ge atom. The LUMO is a π-type orbital and mainly locates on the C_2N_2Ge ring. Natural bond orbital (NBO) analysis showed Wiberg bond index (WBI) values of the Ge–$C_{carbene}$ bond (0.76) and the Ge–N bond (0.42) that are smaller than those in **1** (Ge–$C_{carbene}$: 1.21, Ge–N: 0.56) and comparable to those of $[(L)GeCl]^+GeCl_3^-$ (Ge–$C_{carbene}$: 0.61, Ge–N: 0.39), thus confirming the lack of electron delocalization over the five-membered C_2N_2Ge ring.

(a) (b)

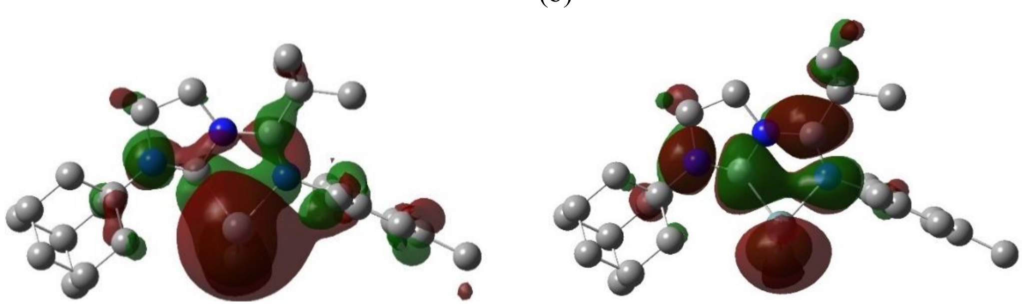

HOMO (–8.6573 eV) LUMO (–4.8330 eV)

Figure 6.5 The HOMO (a) and LUMO (b) of **2** calculated at the B3LYP/6-311G(d,p) level of theory.

6.2.1 Reactivity of germylone 1 towards two equivalents of MeOTf.

As the HOMO of **2** reveals the existence of a lone pair on the Ge atom, we postulated that it may further react with the electrophiles. Indeed, when two equivalents of MeOTf was added dropwise to a toluene solution of **1**, the colour change immediately from yellow to red, then to colourless (Scheme 6.2). In a short time, a lot of precipitation was formed. The solid was collected by filtration and washed with toluene to afforded the corresponding dicationic species **3** in 80% yield. In the ^{13}C NMR spectrum of **3**, the carbene peak appeared at 176.6 ppm which is significantly shifted upfield with respect to that (206.0 ppm) of **2**, indicating a more electron donating from carbene to Ge atom compared with that of **2**. Single crystals suitable for X-ray diffraction studies were grown by evaporation of a saturated acetonitrile solution. The solid-state structure of **3** was confirmed (Figure 6.6). The five atoms (Ge1, C3, N3, C6 and N1) are nearly coplanar with the sum of the internal angles = 539.14°. Both carbon atoms C1 and C2 are located at both sides of the C_2N_2Ge ring with the angle of 115.71(11)° for C1−Ge1−C2. The shorter distance of C3−Ge1 (1.962(2) Å) and Ge1−N1 (1.9399(19) Å) and the larger angle of C3−Ge1−N1 (82.29(8) °) are confirmed in comparison with those of **2**, supporting the stronger interaction between the carbene and $GeMe_2$ unit. The successful generation of **3** demonstrates a nucleophilic property of **1** where the Ge center donates two lone pairs to form two Ge−Me bonds of **3**.

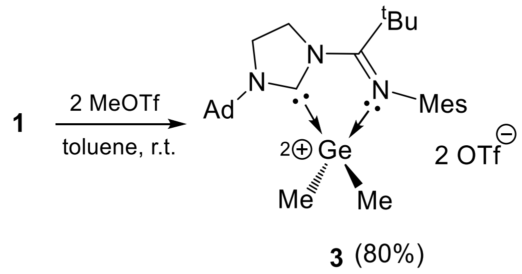

Scheme 6.2 Reaction of **1** with two equivalents of MeOTf.

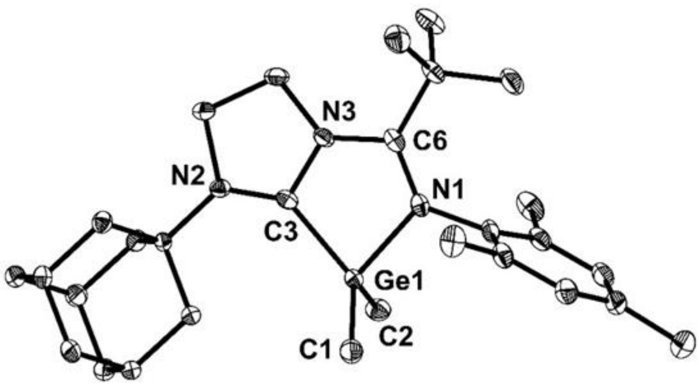

Figure 6.6 Solid-state structure of **3** (hydrogen atoms, the counteranions, and solvent molecules are omitted for clarity). Thermal ellipsoids are set at the 50% probability.

6.2.2 Reactivity of germylone 1 towards transition metals (M = Cr, Mo, W and Ir).

Germylenes, as the heavier carbene analogue, are widely applied in the coordination chemistry, due to their two-electrons donating property. In contrast to germylenes, compound **1** can be viewed as both mesoionic germylene and germylone, so we envisaged that **1** may express some unusual reactivity towards the transition metals.

First, we performed the reactions of **1** with group VI metals. Treatment of a THF solution of **1** with a stoichiometric amount of $M(CO)_5(thf)$ (M = Cr, Mo, W)[15] at room temperature proceeded immediately as indicated by the fast coloration of the reaction mixture to red. Red single crystals were obtained by recrystallization from a concentrated solution of THF at –26 ºC [**4** (M = Cr): 40%, **5** (M = Mo): 36%, **6** (M = W): 32% yields, respectively] (Scheme 6.3). Under an inert atmosphere, compounds **4**–**6** are thermally stable both in the solid state and in solution, and even under heating conditions at 80 ºC for several hours in toluene, no decomposition was detected. However, they rapidly decompose upon exposure to air. Note that compounds **4**–**6** represent the first examples of germylone–transition metal complexes. Compounds **4**–**6** have been fully characterized by NMR spectroscopy and a single-crystal X-ray diffraction analysis (Figure 6.7).

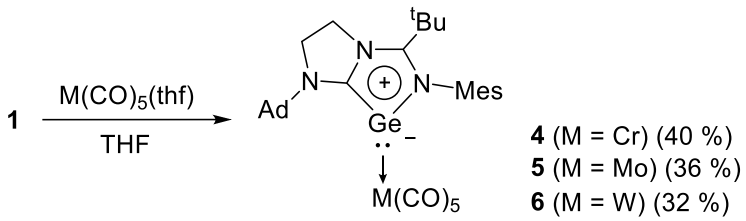

Scheme 6.3 Reaction of **1** with $M(CO)_5$(thf) (M = Cr, Mo, W).

The crystallographic studies revealed that complexes **4**–**6** exhibit a similar molecular geometry involving η^1-coordination of the Ge center to the $\{M(CO)_5\}$ (M = Cr, Mo, W) unit (Figure 6.7). The C_2N_2Ge five-membered rings persist their original coplanar geometries (the sum of internal pentagon angles = 539.90° (**4**), 539.9° (**5**), 539.90° (**6**), respectively). Notably, the Ge atoms in complexes **3**–**5** display a trigonal planar geometry (the sum of the bond angles around the Ge atom = 358.93° (**4**), 359.07° (**5**), 358.95° (**6**)), which is in marked contrast to the case of **2** (Figure. 6.4) and the germylone-iron complex **IV** (Figure. 6.3) where the Ge atoms adopt a trigonal-pyramidal geometry. The C–Ge–N bond angles in **4** (83.60(7)°), **5** (83.7(2)°) and **6** (83.70(16)°) are about 3° larger than that of **1** (80.59(6)°). Both Ge–C and Ge–N bond distances in **4** (1.8587(17) Å, 1.9303(14) Å), **5** (1.858(6) Å, 1.934(4) Å) and **6** (1.847(4) Å, 1.932(3) Å) are slightly shorter than those of **1** (1.8870(15) Å, 1.9680(13) Å). The Ge–Cr bond distance of 2.4883(3) Å is significantly shorter than the Ge–Mo bond (2.6176(8) A) in **5** and the Ge–W bond (2.6085(5) A) in **6**, suggesting a strong back-donation from the metal center to ligand **1** in complex **4**. However, these Ge–M bonds are longer than those of the relevant germylene-metal complexes such as $(ArS)_2GeCr(CO)_5$ (Ge–Cr: 2.367(2) Å),[5k] $(NHGe)_3Mo(CO)_3$ (Ge–Mo: 2.5452(3) Å),[7d] and $ArAr^*GeW(CO)_5$ (Ge–W: 2.5934(8) Å).[5i]

(a)

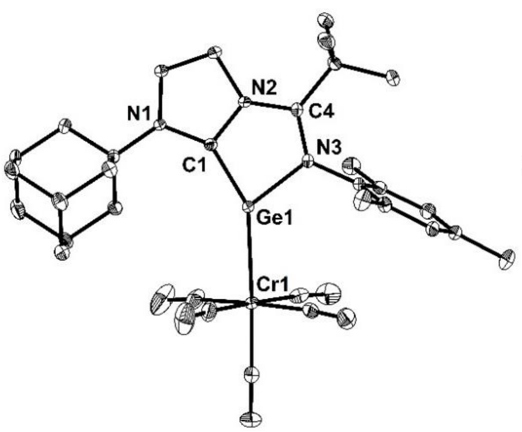

(b)

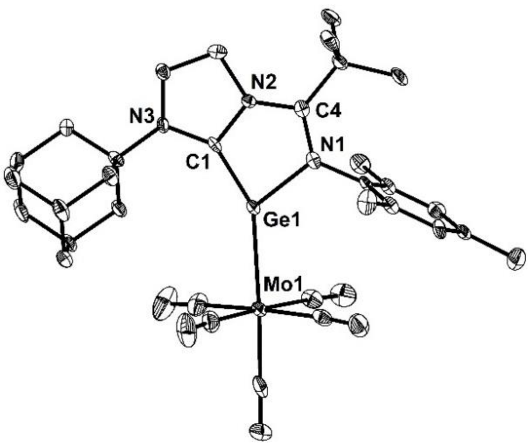

(c)

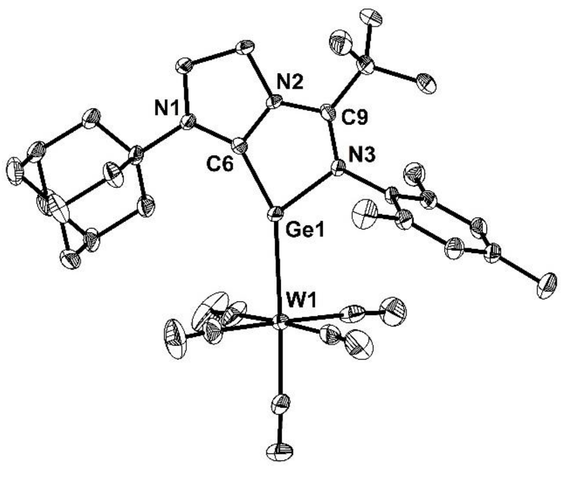

Figure 6.7 Solid-state structure of **4** (a), **5** (b), and **6** (c) (hydrogen atoms and solvent molecules are omitted for clarity). Thermal ellipsoids are set at the 50% probability.

To gain a deeper understanding of the electronic property, we performed quantum chemical calculations for the complexes **4**–**6**. The optimized geometries are in good agreement with the experimental results. The frontier orbitals of **4** are depicted in Figure 6.8. We also confirmed that complexes **5** and **6** show the similar MOs to **4**. The HOMO of **4** is mainly a C–Ge π-bonding orbital exhibiting antibonding conjugation with the p-orbitals of the carbon-bearing ^{t}Bu group (Figure 6.8a), thus, indicating the delocalization of π-electrons over the C_2N_2Ge five-membered ring. Interestingly, the HOMO−2 represents a d-orbital of the Cr atom that involves π-bonding interaction with the Ge atom through a back-donation (Figure 6.8b). It is inferred that the delocalization of π-electrons over the C_2N_2Ge five-membered ring allows the Ge center to accept d-electrons partially from the Cr atom. The planarity of the Ge center in complex **4** may presumably originate from the effective overlap of a d-orbital of the Cr atom and the p-orbital of the Ge atom. Indeed, germyliumylidene ion **2** in which no such d–p interaction is involved displays a contrasting pyramidal geometry at the Ge center. A donation of a σ-type lone pair from the ligand to the Cr center is confirmed in HOMO−7 (Figure 6.8c). The WBI value of the Ge–C1 bond is 1.11, indicating the partial Ge–C double bond character. WBI values larger than 1.0 for the C1–N2 (1.08), N2–C4 (1.23), and C4–N3 (1.33) bonds were also confirmed, which supports the delocalization of electrons in the C_2N_2Ge π-system. The WBI value of 0.77 for the Ge–Cr bond indicates the relatively strong interaction between them. The larger WBI value of the $Cr–CO_{trans}$ bond (1.15) than those of the $Cr–CO_{cis}$ bonds (1.03, 1.03, 1.04, and 1.05) is probably due to the greater σ-donating ability of **1** than CO. Natural Population Analysis (NPA) indicates an overall charge transfer of 0.70e (**4**), 0.71e (**5**), and 0.75e (**6**) from the ligand **1** to the $M(CO)_5$ fragment in complexes **4**–**6**.

(a) (b)

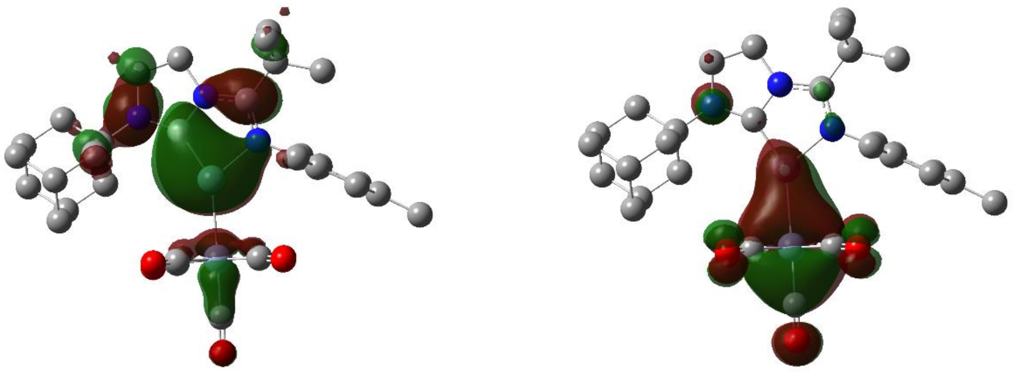

HOMO (−4.2776 eV) HOMO-2 (−5.8934 eV)

(c)

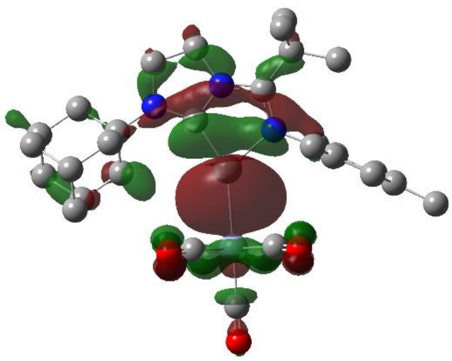

HOMO-7 (−7.4761 eV)

Figure 6.8 Plots of the HOMO (a), HOMO−2 (b) and HOMO−7 (c) of **4** calculated at the B3LYP/6-311G(d,p) level of theory, with the LANL2TZ(f) pseudo-potential applied for the Cr atom.

To evaluate the ligand donating/accepting ability of **1**, infrared spectra of complexes **4–6** were recorded (Figure 6.9). The ν(CO) frequencies were observed at 2048 (s), 1976 (m), 1917 (s), and 1899 (s) cm^{-1} for **4**, 2061 (s), 1985 (m), 1923 (s), and 1897 (s) cm^{-1} for **5**, and 2059 (s), 1978 (m), 1917 (s), and 1895 (s) cm^{-1} for **6**. The presence of four absorption bands ($A_1^{(2)}$, B_1, E, $A_1^{(1)}$) for ν(CO) frequencies indicates a distortion of the $M(CO)_5$ moiety.[16] Based on the $A_1^{(2)}$ bands of **4** and **5**, the Tolman Electronic Parameter (TEP) values for the ligand **1** were calculated.[17] The average of the TEP values estimated for **1** is 1868 cm^{-1}, which is significantly smaller than those for the reported N-heterocyclic germylenes (2073–2080 cm^{-1}),[5d] suggesting the strong σ-donating ability of **1**. The observed $A_1^{(1)}$ bands (**4**: 1899 cm^{-1}, **5**: 1895 cm^{-1}, and **6**: 1895 cm^{-1}) corresponding to the vibration of CO in the trans position to the donor ligand[18] are smaller than those of the reported germylene–$M(CO)_5$ complexes,[5,19] but comparable to those of pyridine–$M(CO)_5$ complexes (Cr: 1905 cm^{-1}, Mo: 1890 cm^{-1}, and W: 1895 cm^{-1}).[18c] These results indicate the poor π-acceptor ability of **1**, which might be due to the electron-richness of the 6π-system over the five-membered ring.

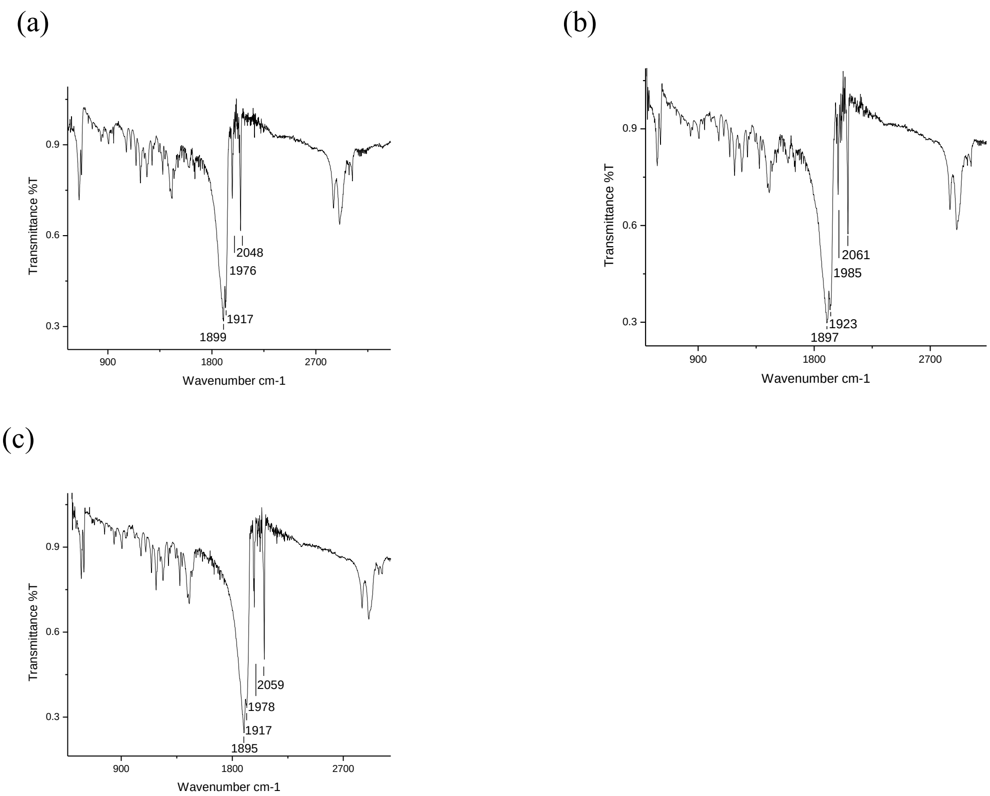

Figure 6.9 The IR spectra of **4** (a), **5** (b) and **6** (c) in the solid state.

Since the π bonding interaction between the metal atoms with Ge atom prevents the utility of the second lone pair to form the bimetallic complex, we proposed that the germanium bimetallic complexes may be formed by application of metals which show a week π back donating property. We are interested in the reaction of **1** with the iridium complex $[IrCl(COD)]_2$ (Scheme 6.4). Benzene was added to the mixture of **1** and one equivalent of $[IrCl(COD)]_2$ at room temperature. Immediately, the color changed to deep red. After work-up, the targeted complex **7** was obtained as the red crystalline solid in 86% yield. **7** was fully characterized by multiple spectroscopy and X-ray diffraction analysis.

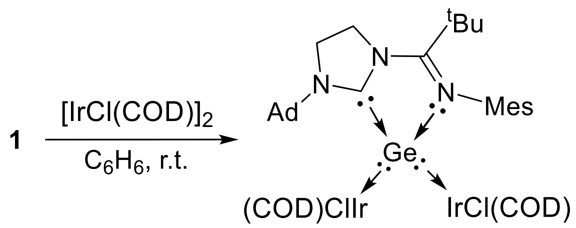

7 (86%)

Scheme 6.4 Reaction of **1** with $[IrCl(COD)]_2$.

The molecular structure of **7** shows that Ge atom is tetracoordinated with carbene carbon C1, imino nitrogen N3 and two iridium atoms Ir1 and Ir2 (Figure 6.10). The C_2N_2Ge ring persists the coplanar geometry (the sum of internal pentagon angles = 539.9°). The bond distances of 1.986(5) Å (Ge1–C1), 2.042(4) Å (Ge1–N3) and 1.391(7) Å (N2–C4) are longer than those (1.8870(15) Å, 1.9680(13) Å and 1.366(2) Å) of **1**, but comparable with those of $[$**1**-Cl$]^+(GeCl_3)^-$. The bond angle of 79.50(19) Å (C2–Ge1–N3) is slightly smaller than that (80.59(6)°) of **1**. Two iridium atoms Ir1 and Ir2 are located at both sides of the C_2N_2Ge ring. The distance of 4.746 Å between Ir1 and Ir2 atoms is significantly larger than the sum of its van der Waals radii (4.0 Å), indicating the absence of interaction between two Ir atoms.[20] The bond angle of 144.04(2)° for Ir1–Ge1–Ir2 is significantly larger than that (115.71(11)°) of C1–Ge1–C2 in **3**. The bond lengths of Ge1–Ir1 and Ge2–Ir2 are 2.4952(6) Å and 2.4942(6) Å, respectively, which are comparable with those (2.4103(2) − 2.5598(11) Å) of reported Germylene iridium complexes.[21] Note that **7** represents the first example of germylone bimetallic complex,[22]which perfectly demonstrates the two lone-pairs donating property of the germylone **1**.

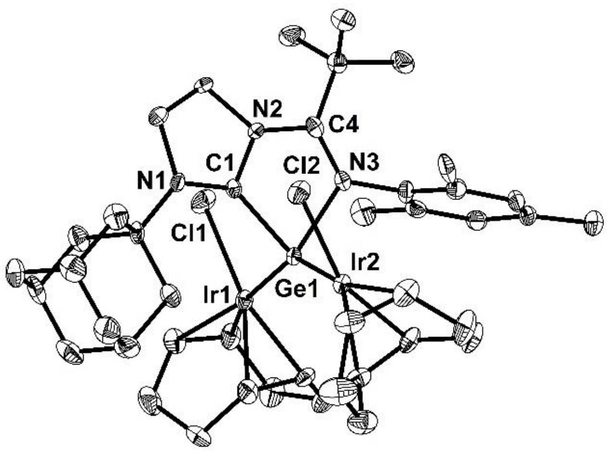

Figure 6.10 Solid-state structure of **7** (hydrogen atoms are omitted for clarity). Thermal ellipsoids are set at the 50% probability.

To get a deep understanding of the electronic structure of **7**, we performed the quantum chemical calculations. The optimized geometry is in good agreement with the metric data observed by X-ray analysis. The frontier orbitals are depicted in Figure 6.11. The HOMO mainly originates from the interaction between p orbitals of the Ge atom and the d orbitals of the Ir atoms. The LUMO is a π-type orbital on the C_2N_2Ge ring and the LUMO+1 majorly consists of the π-type orbital over the Ir1−Ge1−Ir2 bond. Wiberg Bond Index (WBI) values of 0.54 for the Ge1−C1 bond and 0.29 for the Ge1−N3 bond are significantly smaller than those (1.21, 0.56) of **1** but comparable with those (0.61, 0.39) of $[\mathbf{1}\text{-Cl}]^+(GeCl_3)^-$, indicating the loss of the aromatic property of the C_2N_2Ge ring in **7**. WBI values for the Ge1−Ir1 and Ge1−Ir2 bonds are 0.74 and 0.71 respectively, thus indicating a pronounced interaction between the gemylone ligand **1** and the [IrCl(COD)] fragments in **7**. Indeed, Natural Population Analysis (NPA) revealed an overall charge transfer of 0.80*e* and 0.79*e* from the ligand **1** to [Ir1Cl(COD)] and [Ir2Cl(COD)] fragments in **7**, respectively.

(a)

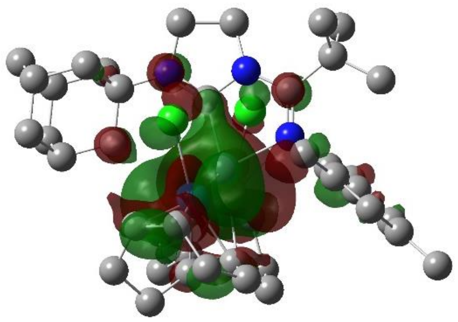

HOMO (−4.7712 eV)

(b)

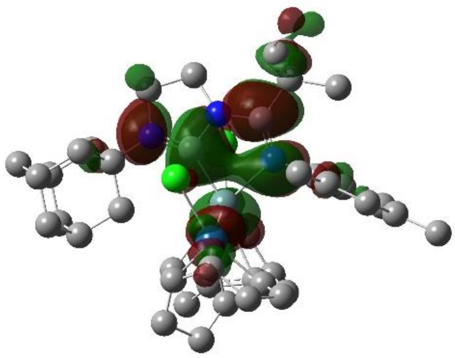

LUMO (−1.6436 eV)

(c)

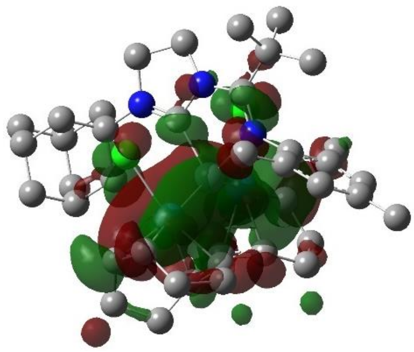

LUMO+1 (−1.0479 eV)

Figure 6.11 Plots of the HOMO (a), LUMO (b) and LUMO+1 (c) of **7** calculated at the B3LYP/6-311G(d,p) level of theory, with the LANL2TZ(f) pseudo-potential applied for the Ir atom.

6.3 Summary

In summary, we studied the reactivity of compound **1** towards MeOTf as well as the transition metal (Cr, Mo, W and Ir) complexes. The reaction of **1** with one equivalent of MeOTf afforded a germyliumylidene ion **2** bearing a pyramidal Ge center, whereas when two equivalents of MeOTf was applied, the dicationic species **3** was generated, thus demonstrating the property of **1** as a donor of one or two lone pairs. The reaction of **1** with group VI metal–pentacarbonyl complexes resulted in the complex **4**–**6** containing a trigonal planar germanium center. Computational studies showed that one of lone pairs on the Ge atom in **4**–**6** is involved in the π-system over the C_2N_2Ge five-membered ring. IR spectroscopic analysis suggests a strong σ-donating but weak π-accepting nature of **1**. Moreover, the reaction of **1** with $[IrCl(COD)]_2$ afforded the germylone bimetallic complex **7** with a relatively strong interaction between Ge atom with Ir atoms, which represents the first example of germylone bimetallic complex.

6.4 Experimental Sections

6.4.1 Synthesis of compounds 2–7 and their spectral data

General considerations: All reactions were performed under an atmosphere of argon or nitrogen by using standard Schlenk or dry box techniques; solvents were dried over Na metal, K metal, or CaH_2. Reagents were of analytical grade, obtained from commercial suppliers and used without further purification. ^{1}H and ^{13}C NMR spectra were obtained with a Bruker AVIII 400MHz BBFO1 spectrometer at 298 K unless otherwise stated. NMR multiplicities are abbreviated as follows: s = singlet, d = doublet, t = triplet, m = multiplet, br = broad signal. Coupling constants *J* are given in Hz. Electrospray ionization (ESI) mass spectra were obtained at the Mass Spectrometry Laboratory at the Division of Chemistry and Biological Chemistry, Nanyang Technological University. Melting points were measured with an OpticMelt Stanford Research System. UV−Vis absorption spectroscopic analyses were carried out with a Shimadzu UV-3600 spectrometer.

Compound 2: MeOTf (25 mg, 0.152 mmol) was added to a toluene solution of compound **1** (70 mg, 0.148 mmol) at room temperature. After 1 h with stirring, the solvent was removed under vacuum, and the residue was washed with hexane (3 × 2 mL) to afford **2** as a red solid (65%). Single crystals suitable for X-ray diffraction analysis were obtained by recrystallization from a saturated toluene solution of **2** at room temperature. M.p.:65 °C (decomposed); ^{1}H NMR (C_6D_6, 400 MHz, 298 K): δ 6.57 (s, 1H, Ar-C*H*), 6.55 (s, 1H, Ar-C*H*), 5.00–4.93 (m, 1H, NCH_2), 4.86–4.79 (m, 1H, NCH_2), 4.70–4.61 (m, 1H, NCH_2), 4.31–4.23 (m, 1H, NCH_2), 2.24 (s, 3H, Ar-CH_3), 2.08 (s, 3H, Ar-CH_3), 2.01−1.99 (m, 6H, Ar-CH_3 & Ad-C*H*), 1.93−1.86 (m, 6H, Ad-

CH_2), 1.41 (d, *J* = 12.7 Hz, 3H, Ad-CH_2), 1.35 (d, *J* = 12.1 Hz, 3H, Ad-CH_2), 1.12 (s, 9H, C(CH_3)$_3$), 0.77 (s, 3H, Ge-CH_3); ^{13}C{^{1}H} NMR (C_6D_6, 100 MHz, 298 K): δ 206.0 ($C_{carbene}$), 165.7 (*C*=N), 137.2 (C_{Ar}), 135.9 (C_{Ar}), 131.5 (C_{Ar}), 130.6 (C_{Ar}), 129.0 (C_{Ar}), 128.8 (C_{Ar}), 58.7 (Ad-*q*), 50.4 (N*C*H_2), 49.3 (N*C*H_2), 40.1 (Ad-*C*H_2), 39.2 (*C*(CH_3)$_3$), 34.9 (Ad-*C*H_2), 28.8 (Ad-*C*H), 27.8 (C(*C*H_3)$_3$), 20.0 (Ar-*C*H_3), 18.9 (Ar-*C*H_3), 18.3 (Ar-*C*H_3), 6.7 (Ge–*C*H_3), The signal for *C*F_3 could not be detected, presumably due to an overlap with other peaks; ^{19}F NMR (376 MHz, $CDCl_3$): δ −77.6. HRMS (ESI): *m/z* calcd for $C_{28}H_{42}GeN_3$: 494.2591 [(*M–OTf*)]$^+$; found: 494.2585.

Compound 3: MeOTf (50 mg, 0.304 mmol) was added to a toluene solution of compound **1** (70 mg, 0.148 mmol) at room temperature. A precipitate was formed immediately, and after 1 h with stirring, the solid was separated by filtration. The residue was then washed with toluene (3×2 mL) to afford **3** as a brown solid (80%). Single crystals suitable for X-ray diffraction studies were grown by evaporation of a saturated acetonitrile solution of **3**. M.p.: 237 ºC (dec.); ^{1}H NMR ($CDCl_3$, 400 MHz, 298 K): δ 6.99 (s, 2H, *m*-C*H*), 4.93 (t, *J* = 9.2 Hz, 2H, NCH_2), 4.76 (t, *J* = 8.9 Hz, 2H, NCH_2), 2.33–2.32 (m, 12H, CH_3 & Ad–*H*), 2.18–2.17 (m, 6H, Ad–*H*), 1.78 (d, *J* = 12.8 Hz, 3H, Ad–CH_2), 1.72 (d, *J* = 12.7 Hz, 3H, Ad–CH_2), 1.39 (s, 9H,C(CH_3)$_3$), 1.31 (s, 6H, Ge–CH_3); ^{13}C{^{1}H} NMR ($CDCl_3$, 100 MHz, 298 K): δ 177.4 (*C*=N), 176.6 ($C_{carbene}$), 140.0 (CAr), 133.6 (CAr), 133.2 (CAr), 130.8 (CAr), 63.6 (Ad-*q*), 53.4 (N*C*H_2), 49.9 (N*C*H_2), 41.1 (Ad–*C*H_2), 40.9 (*C*(CH_3)$_3$), 35.3 (Ad–*C*H_2), 29.4 (Ad–*C*H), 28.4 (C(*C*H_3)$_3$), 21.0 (*p*-*C*H_3), 18.8 (*o*-*C*H_3), 3.2 (Ge–*C*H_3), The signal for *C*F_3 could not be detected, presumably due to an overlap with other peaks; ^{19}F NMR (376 MHz, $CDCl_3$): δ −78.4; HRMS (ESI): *m/z* calcd for

$C_{30}H_{45}GeF_3N_3O_3S$: 658.2346 $[M–OTf]^+$; found: 658.2365.

General procedure for the synthesis of compound 4–6.

The respective $M(CO)_5(thf)$ (M = Cr, Mo, W) was prepared by UV-irradiation of the corresponding $M(CO)_6$ in THF.[15] A THF solution of the freshly prepared $M(CO)_5(thf)$ was added dropwise to a THF solution of compound **1** at room temperature. After 2 hours, the resulting solution was concentrated under reduced pressure and stored at –26 °C to afford red crystals. Compound **4–6** are very stable in THF, benzene and toluene solvents, and even after heating at 80 °C several hours no decomposition was detected.

Compound 4: Quantity used: $Cr(CO)_6$ (46 mg, 0.210 mmol), compound **1** (100 mg, 0.209 mmol), THF (15 mL); yield (40 %). M.p.:92 °C (decomposed); ^1H NMR (C_6D_6, 400 MHz, 298 K): δ 6.78 (s, 2H, Ar-CH), 3.50 (t, J = 7.3 Hz, 2H, NCH_2), 2.99 (t, J = 7.3 Hz, 2H, NCH_2), 2.13 (m, 12H, Ar-CH_3 & Ad-CH), 2.03 (m, 6H, Ad-CH_2), 1.75 (d, J = 11.9 Hz, 3H, Ad-CH_2), 1.62 (d, J = 12.1 Hz, 3H, Ad-CH_2), 0.77 (s, 9H, C(CH_3)$_3$); $^{13}C\{^1H\}$ NMR (C_6D_6, 100 MHz, 298 K): 225.9 (CO), 218.6 (CO), 195.5 ($C_{carbene}$), 145.1 (C=N), 140.2 (C_{Ar}), 136.8 (C_{Ar}), 133.9 (C_{Ar}), 129.7 (C_{Ar}), 54.7 (Ad-q), 49.9 (NCH$_2$), 46.8 (NCH$_2$), 39.7 (Ad-CH$_2$), 38.6 (C(CH$_3$)$_3$), 36.7 (Ad-CH$_2$), 29.8 (Ad-CH), 29.1 (C(CH$_3$)$_3$), 21.0 (Ar-CH$_3$), 19.0 (Ar-CH$_3$); IR ν/cm^{-1} (solid): 2048 (s), 1976 (m), 1917 (s), 1899 (s); UV-Vis (in THF): 402 nm, 465 nm; HRMS (ESI): m/z calcd for $C_{32}H_{40}CrGeN_3O_5$: 672.1585 $[(M+H)]^+$; found: 672.1594.

Compound 5: Quantity used: $Mo(CO)_6$ (56 mg, 0.210 mmol), compound **1** (100 mg, 0.209 mmol), THF (15 mL); yield (36 %). M.p.:95 ºC (decomposed); ^{1}H NMR (C_6D_6, 400 MHz, 298 K): δ 6.79 (s, 2H, Ar-C*H*), 3.53 (t, *J* = 7.3 Hz, 2H, NC*H*$_2$), 2.99 (t, *J* = 7.3 Hz, 2H, NC*H*$_2$), 2.15 (m, 6H, Ar-C*H*$_3$ & Ad-C*H*), 2.12 (s, 6H, Ar-C*H*$_3$), 2.05 (m, 6H, Ad-C*H*$_2$), 1.75 (d, *J* = 11.9 Hz, 3H, Ad-C*H*$_2$), 1.63 (d, *J* = 12.1 Hz, 3H, Ad-C*H*$_2$), 0.77 (s, 9H, C(C*H*$_3$)$_3$); ^{13}C{^{1}H} NMR (C_6D_6, 100 MHz, 298 K): 213.7 (*C*O), 206.7 (*C*O), 190.9 ($C_{carbene}$), 143.6 (*C*=N), 140.6 (C_{Ar}), 136.7 (C_{Ar}), 133.7 (C_{Ar}), 129.7 (C_{Ar}), 54.5 (Ad-*q*), 49.9 (N*C*H$_2$), 46.9 (N*C*H$_2$), 39.6 (Ad-*C*H$_2$), 38.3 (*C*(CH$_3$)$_3$), 36.7 (Ad-*C*H$_2$), 29.8 (Ad-*C*H), 29.1 (C(*C*H$_3$)$_3$), 21.0 (Ar-*C*H$_3$), 18.9 (Ar-*C*H$_3$); IR *v*/cm^{-1} (solid): 2061 (s), 1985 (m), 1923 (s), 1897 (s); UV-Vis (in THF): 327 nm, 430 nm; HRMS (ESI): *m/z* calcd for $C_{32}H_{40}MoGeN_3O_5$: 718.1234 [(*M*+*H*)]$^+$; found: 718.1251.

Compound 6: Quantity used: $W(CO)_6$ (73 mg, 0.208 mmol), compound **1** (100 mg, 0.209 mmol), THF (15 mL); yield (32 %). M.p.:105 ºC (decomposed); ^{1}H NMR (C_6D_6, 400 MHz, 298 K): δ 6.78 (s, 2H, Ar-C*H*), 3.51 (t, *J* = 7.3 Hz, 2H, NC*H*$_2$), 2.99 (t, *J* = 7.3 Hz, 2H, NC*H*$_2$), 2.15 (m, 6H, Ar-C*H*$_3$ & Ad-C*H*), 2.11 (s, 6H, Ar-C*H*$_3$), 2.05 (m, 6H, Ad-C*H*$_2$), 1.75 (d, *J* = 11.9 Hz, 3H, Ad-C*H*$_2$), 1.63 (d, *J* = 12.2 Hz, 3H, Ad-C*H*$_2$), 0.76 (s, 9H, C(C*H*$_3$)$_3$); ^{13}C{^{1}H} NMR (C_6D_6, 100 MHz, 298 K): 201.9 (*C*O), 197.5 (*C*O), 188.0 ($C_{carbene}$), 143.7 (*C*=N), 140.4 (C_{Ar}), 136.8 (C_{Ar}), 133.8 (C_{Ar}), 129.7 (C_{Ar}), 54.5 (Ad-*q*), 49.9 (N*C*H$_2$), 47.0 (N*C*H$_2$), 39.7 (Ad-*C*H$_2$), 38.3 (*C*(CH$_3$)$_3$), 36.7 (Ad-*C*H$_2$), 29.8 (Ad-*C*H), 29.1 (C(*C*H$_3$)$_3$), 21.0 (Ar-*C*H$_3$), 19.0 (Ar-*C*H$_3$); IR v/cm^{-1} (solid): 2059 (s), 1978 (m), 1917 (s), 1895 (s); UV-Vis (in THF): 328 nm, 434 nm; HRMS (ESI): *m/z* calcd for $C_{32}H_{40}WGeN_3O_5$: 804.1689 [(*M*+*H*)]$^+$; found: 804.1710.

Compound 7: Benzene (15 mL) was added to a mixture of **1** (143 mg, 0.3 mmol) and $[IrCl(COD)]_2$ (200 mg, 0.3 mmol) at room temperature. Immediately, the color changed to deep red. After completion of the reaction, all the solvent was removed in vacuum to afford a red solid as the crude product. Recrystallization of **7** by slow evaporation of a saturated benzene solution gave the red crystalline product in 86% yield (295 mg, 25.7 mmol). ^{1}H NMR (C_6D_6, 400 MHz, 298 K): δ 6.86 (s, 2H, Ar-C*H*), 4.51 (t, J = 8.8 Hz, 2H, NCH_2), 4.48–4.44 (m, 2H, COD-C*H*), 4.19–4.13 (m, 2H, COD-C*H*), 4.06 (t, J = 8.7 Hz, 2H, NCH_2), 3.93–3.89 (m, 2H, COD-C*H*), 3.33–3.30 (m, 2H, COD-C*H*), 2.76 (s, 6H, Ar-CH_3), 2.58 (br, 6H, Ad-CH_2), 2.27 (s, 3H, Ar-CH_3), 2.20 (br, 3H, Ad-C*H*), 2.01–1.88 (m, 8H, COD-CH_2), 1.85–1.79 (m, 6H, Ad-CH_2), 1.44–1.38 (m, 2H, COD-CH_2), 1.34–1.29 (m, 2H, COD-CH_2), 1.28 (s, 9H, C(CH_3)$_3$), 1.20–1.13 (m, 2H, COD-CH_2), 1.10–1.02 (m, 2H, COD-CH_2); ^{13}C{^{1}H} NMR (C_6D_6, 100 MHz, 298 K): δ 215.3 ($C_{carbene}$), 164.4 (*C*=N), 139.8 (C_{Ar}), 136.2 (C_{Ar}), 133.7 (C_{Ar}), 129.4 (C_{Ar}), 81.1 (COD-C*H*), 79.2 (COD-C*H*), 59.6 (Ad-*q*), 48.8 (N*C*H$_2$), 47.7 (N*C*H$_2$), 45.6 (COD-C*H*), 44.5 (COD-C*H*), 40.4 (Ad-*C*H$_2$), 40.1 (*C*(CH$_3$)$_3$), 37.1 (COD-CH_2), 36.9 (Ad-*C*H$_2$), 34.3 (COD-CH_2), 31.1 (COD-CH_2), 30.8 (Ad-*C*H), 29.7 (C(*C*H$_3$)$_3$), 27.7 (COD-CH_2), 21.1 (Ar-*C*H$_3$), 20.7 (Ar-*C*H$_3$); HRMS (ESI): *m/z* calcd for $C_{43}H_{64}N_3Cl_2Ge^{191}Ir^{193}Ir$: 1150.2925 $[(M+H)]^+$; found: 1150.2925.

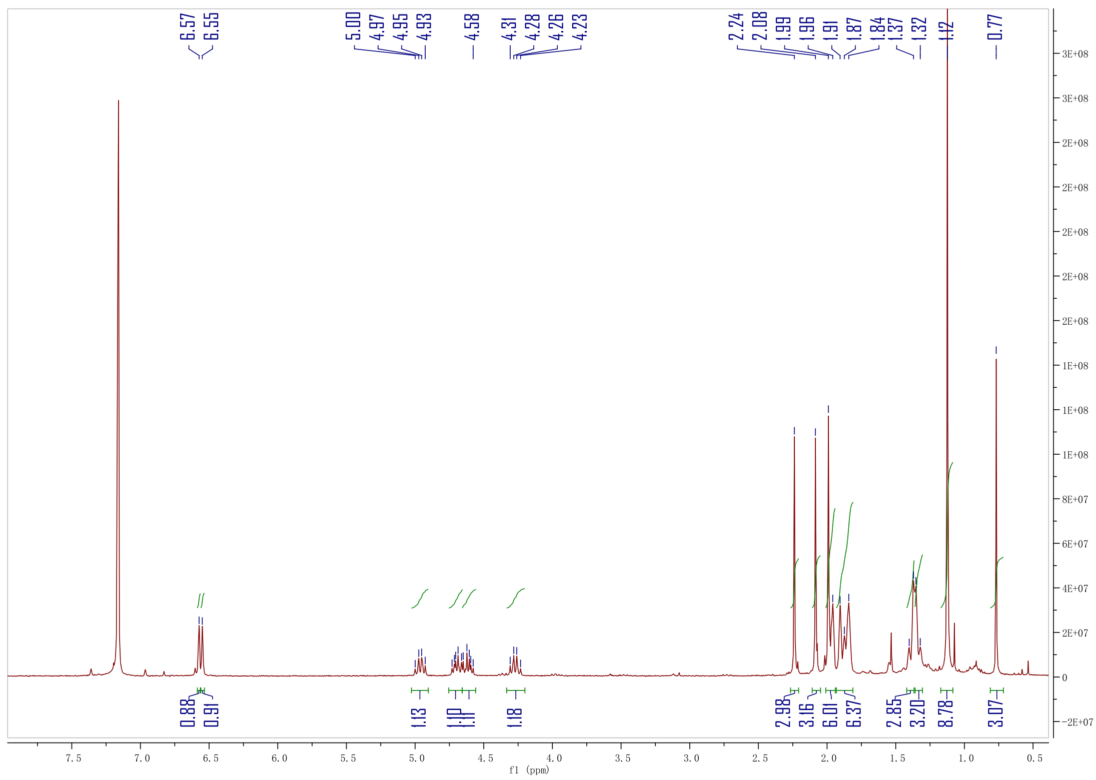

Figure 6.12 ^{1}H NMR spectrum of **2**.

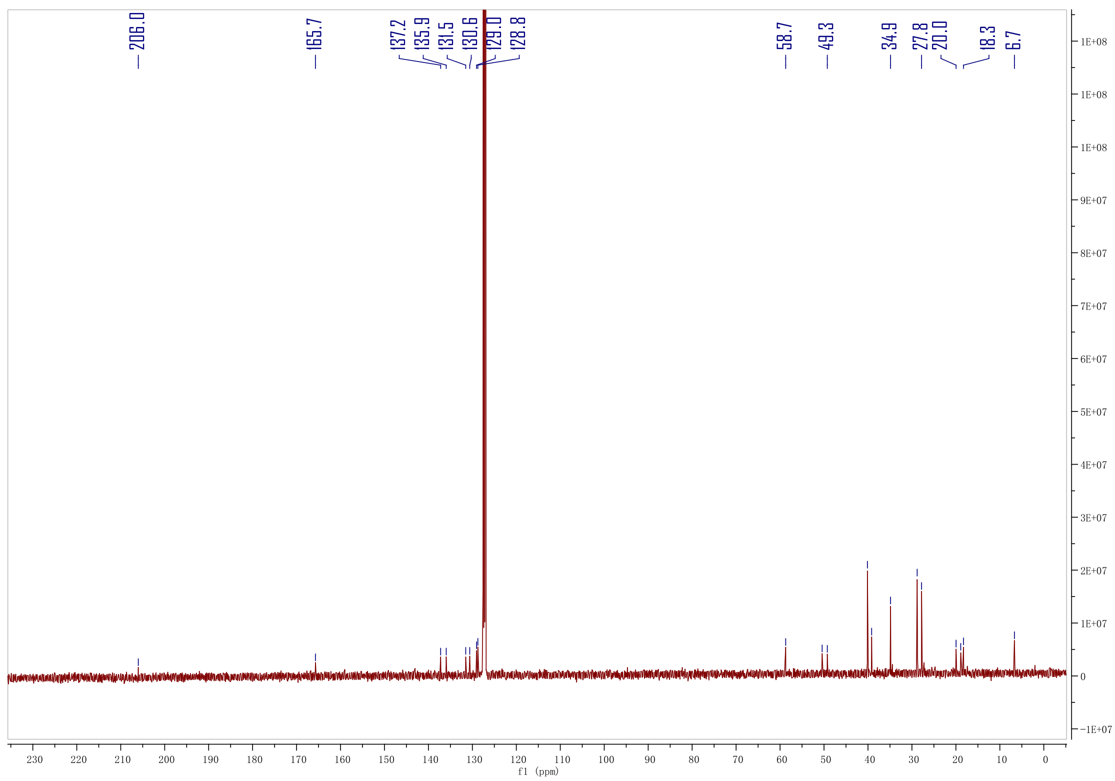

Figure 6.13 $^{13}C\{^{1}H\}$ NMR spectrum of **2**.

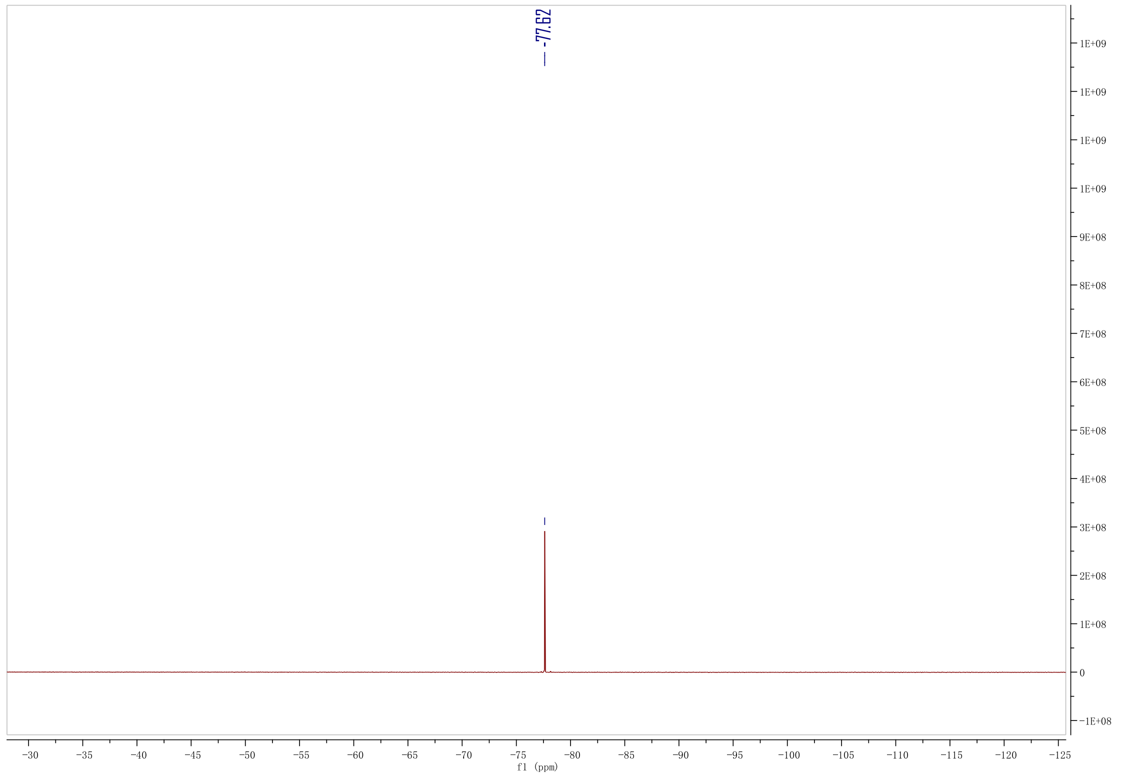

Figure 6.14 ^{19}F NMR spectrum of **2**.

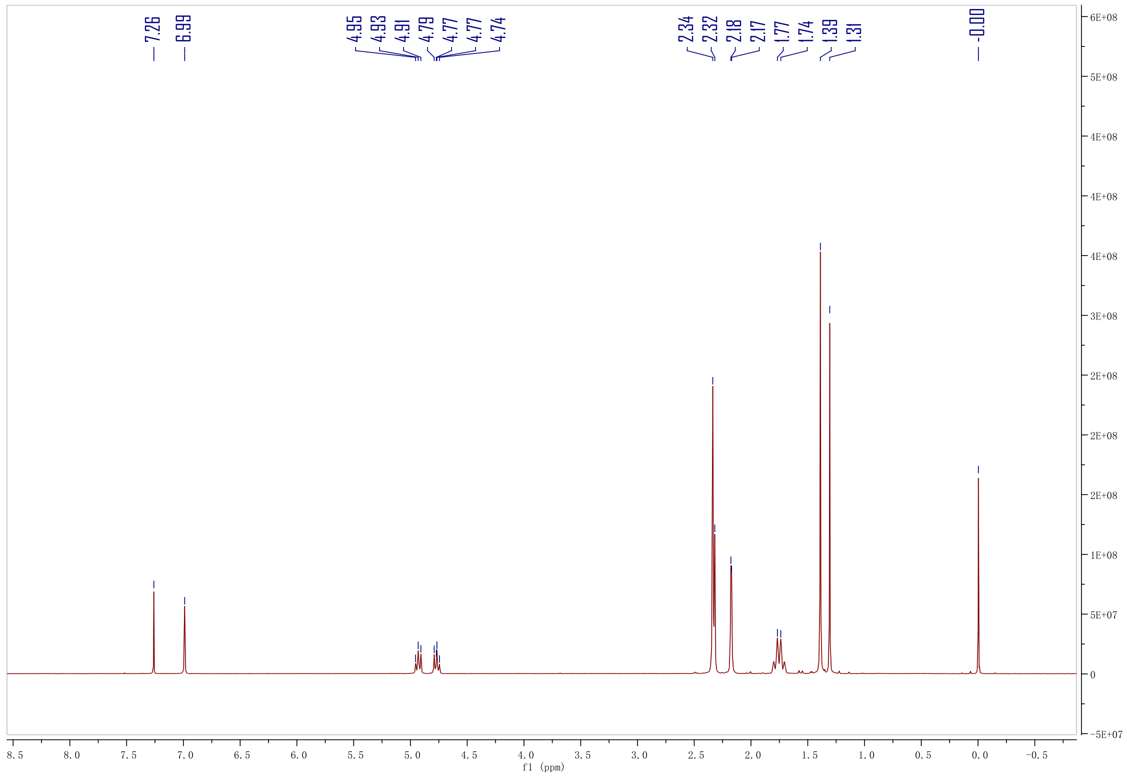

Figure 6.15 ^{1}H NMR spectrum of **3**.

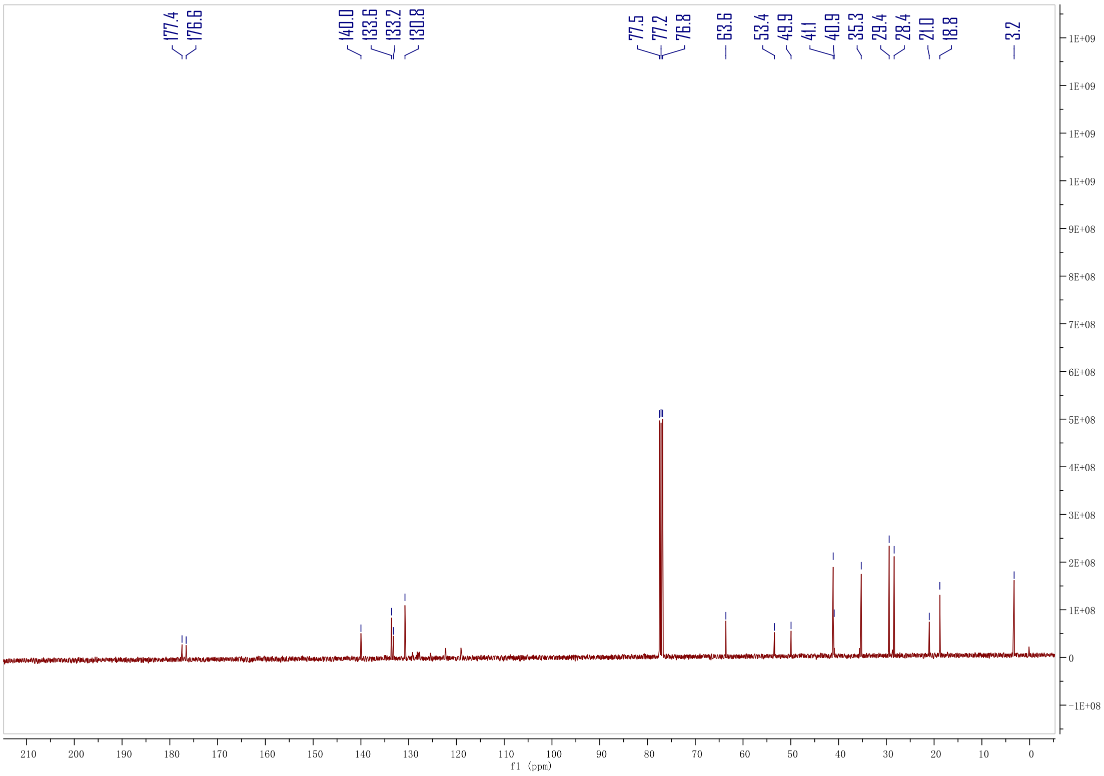

Figure 6.16 $^{13}C\{^{1}H\}$ NMR spectrum of **3**.

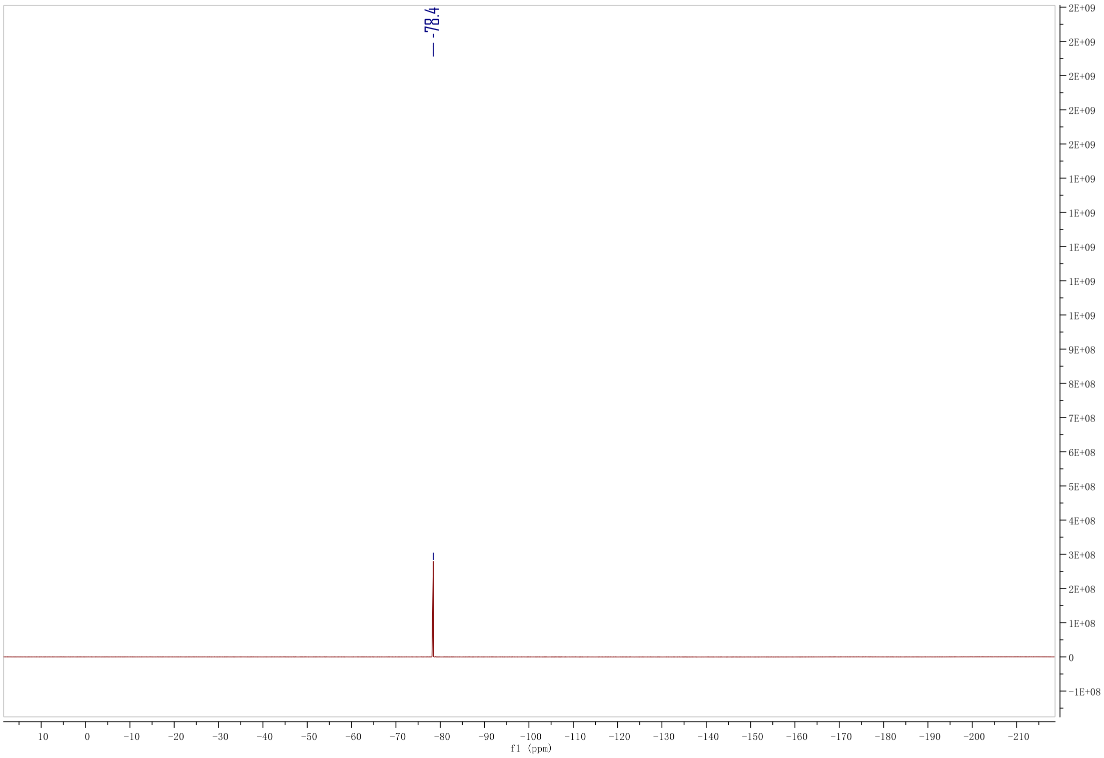

Figure 6.17 ^{19}F NMR spectrum of **3**.

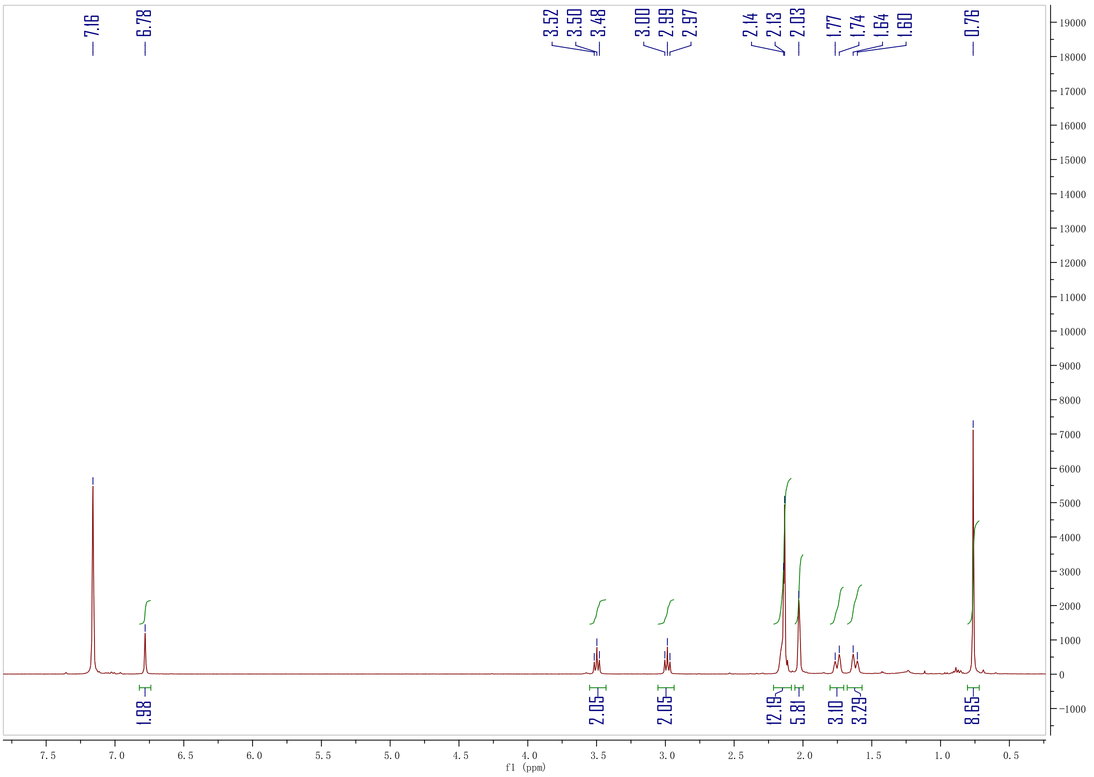

Figure 6.18 ^{1}H NMR spectrum of **4**.

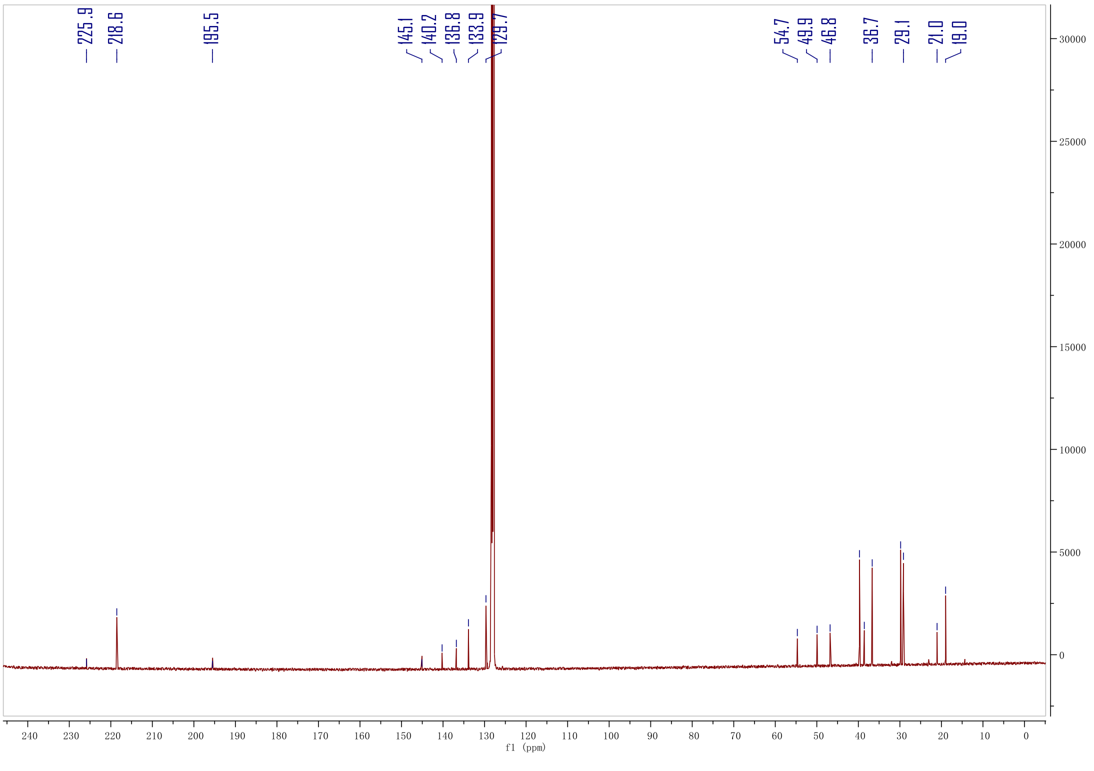

Figure 6.19 $^{13}C\{^{1}H\}$ NMR spectrum of **4**.

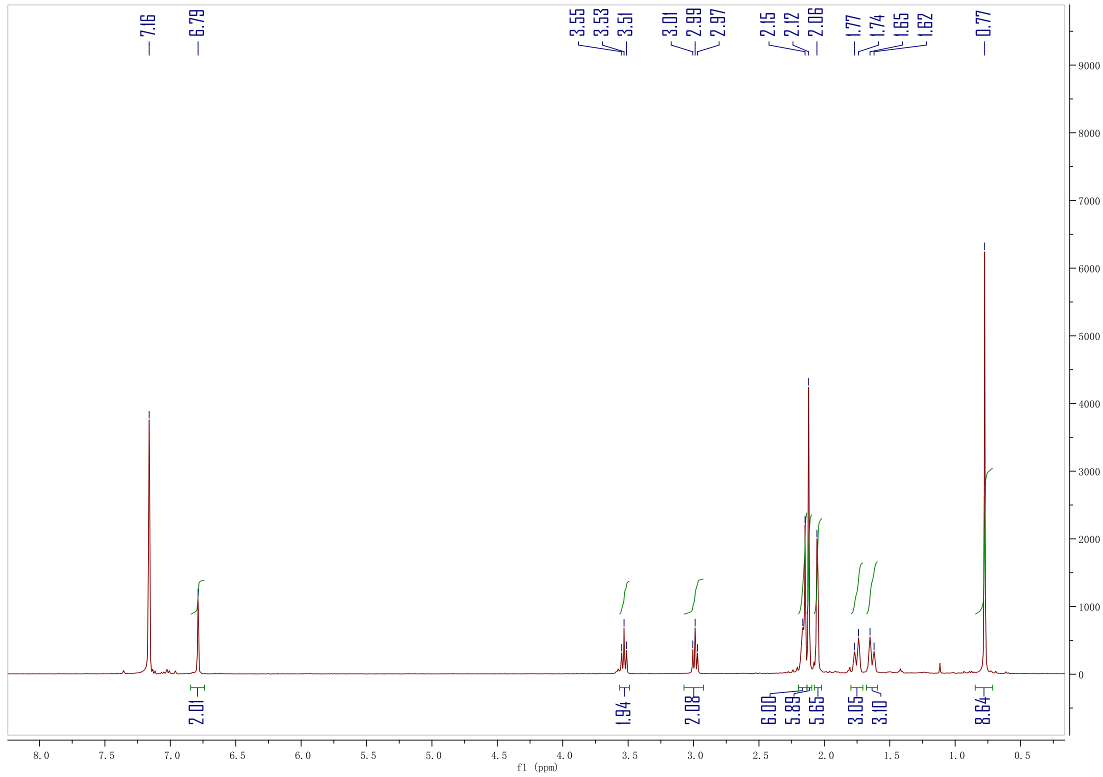

Figure 6.20 ^{1}H NMR spectrum of **5**.

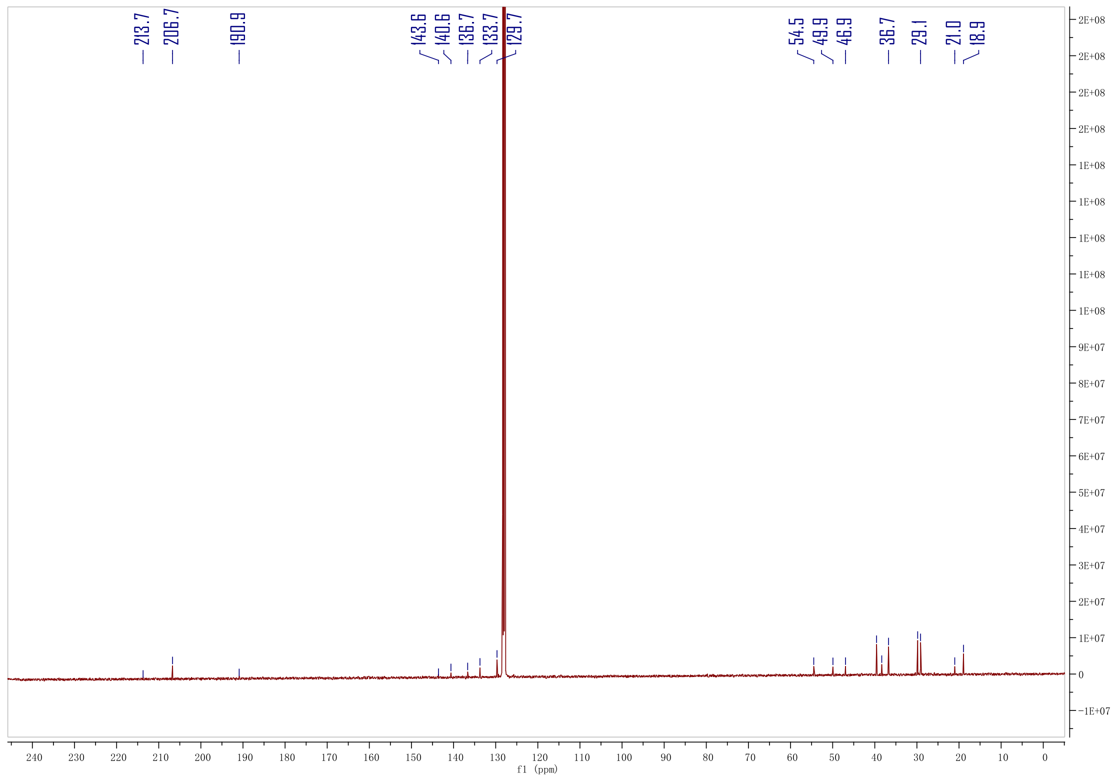

Figure 6.21 ^{13}C{^{1}H} NMR spectrum of **5**.

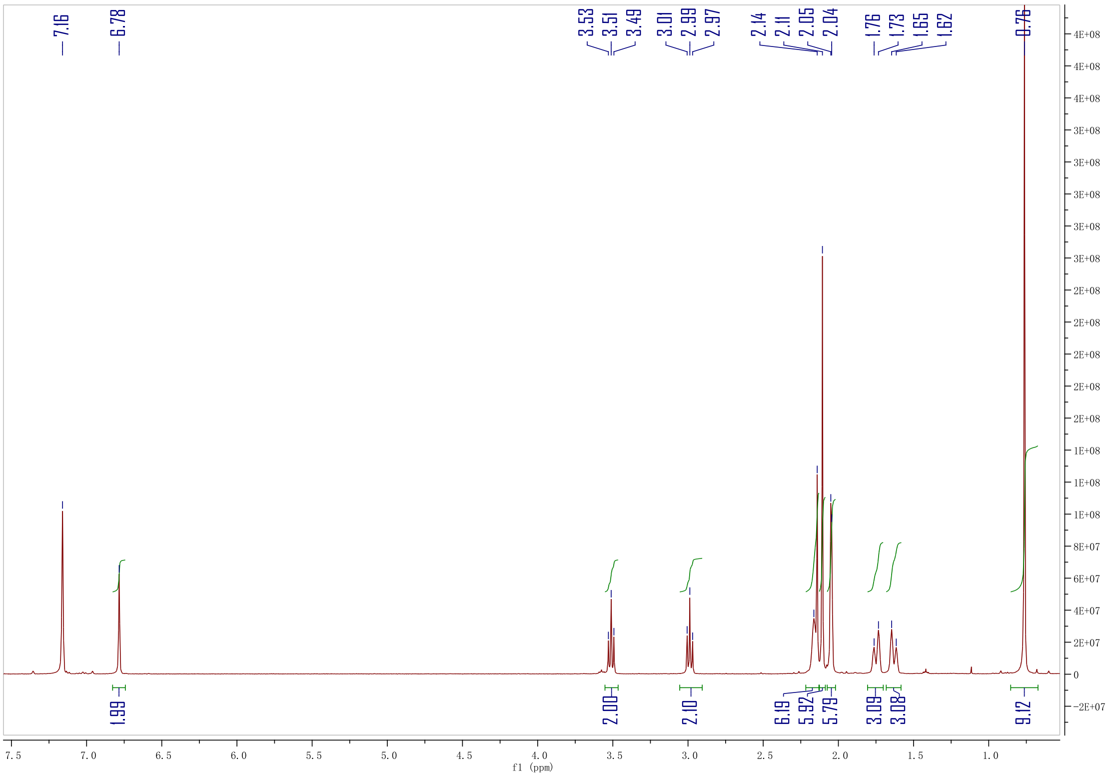

Figure 6.22 ^{1}H NMR spectrum of **6**.

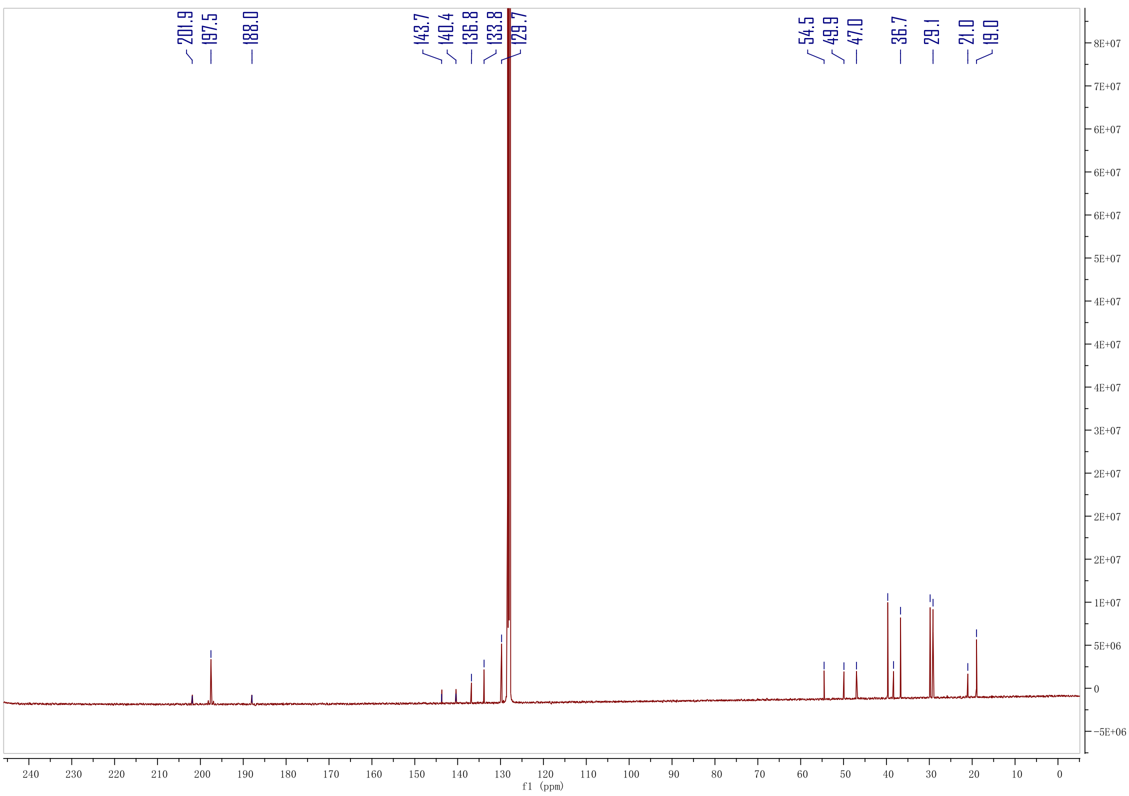

Figure 6.23 $^{13}C\{^{1}H\}$ NMR spectrum of **6**.

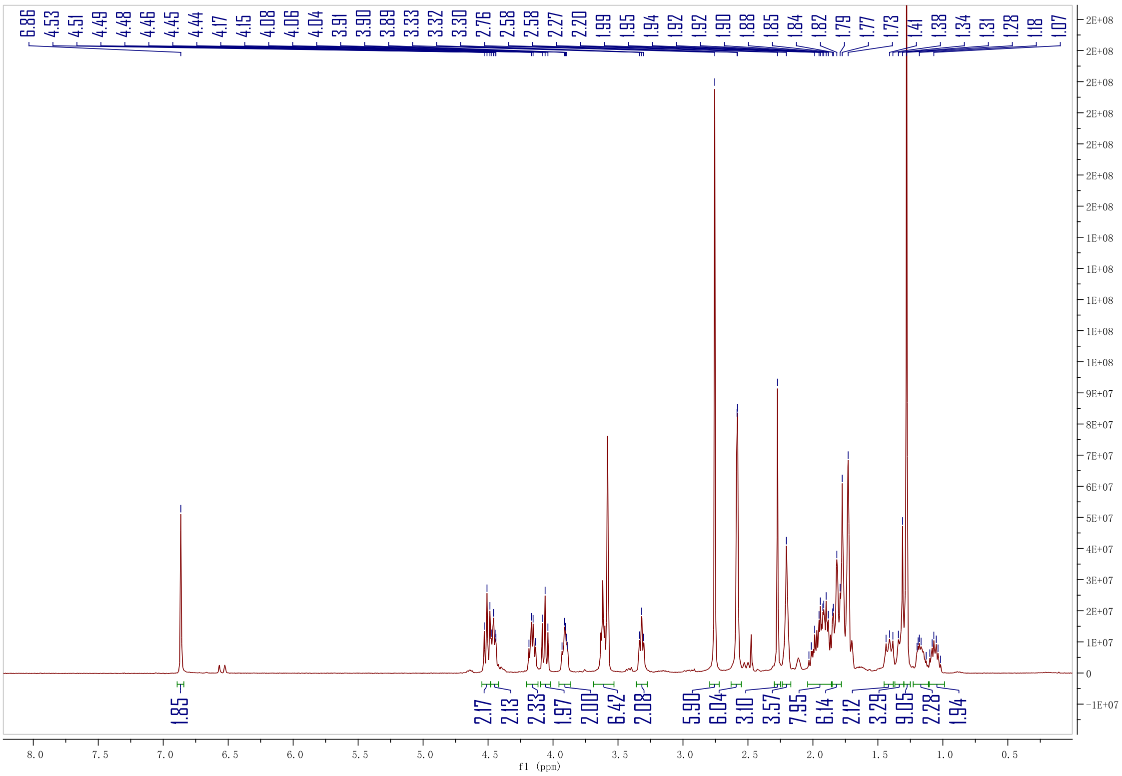

Figure 6.24 ^{1}H NMR spectrum of **7**.

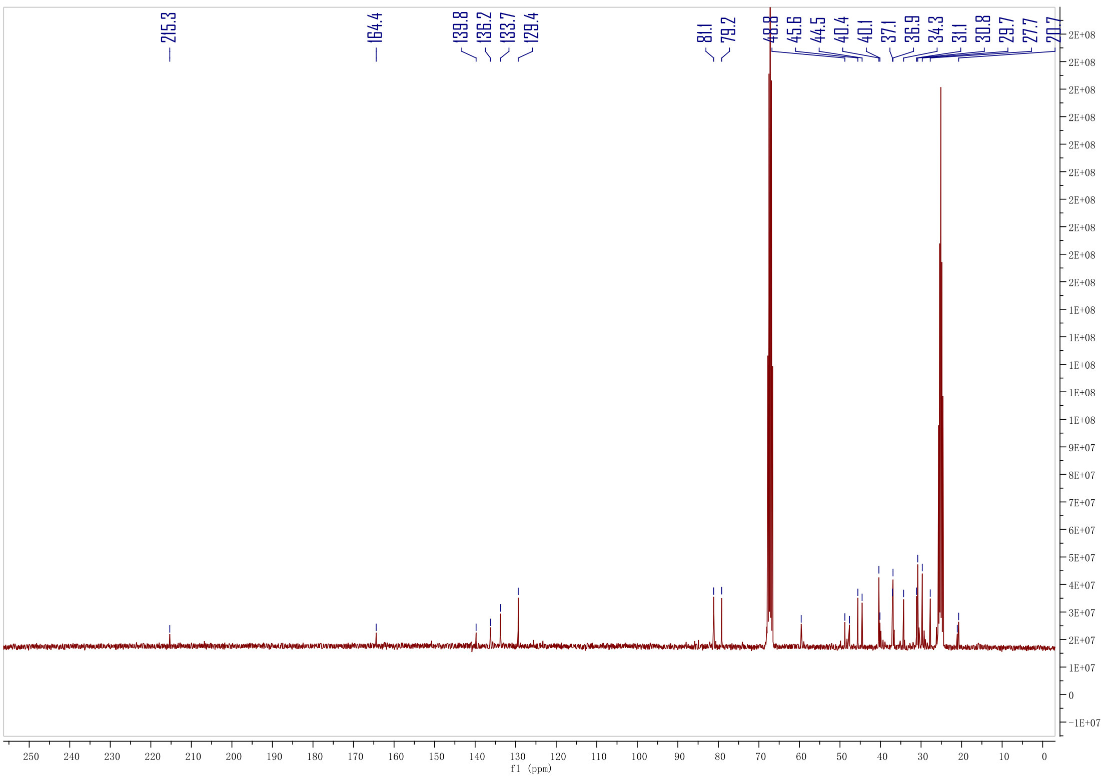

Figure 6.25 $^{13}C\{^{1}H\}$ NMR spectrum of **7**.

6.4.2 Crystal structure parameters

X-ray data collection and structural refinement. Intensity data for compounds **2–5** was collected using a Bruker APEX II diffractometer. The structures were solved by direct phase determination (SHELX-2013) and refined for all data by full-matrix least squares methods on F^2.[23] All non-hydrogen atoms were subjected to anisotropic refinement. The hydrogen atoms were generated geometrically and allowed to ride in their respective parent atoms; they were assigned appropriate isotropic thermal parameters and included in the structure-factor calculations. CCDC; 1429594-1429597(**2** and **4**–**6**), 1018493 (**3**) contains the supplementary crystallographic data. The data can be obtained free of charge from the Cambridge Crystallography Data Center via www.ccdc.cam.ac.uk/data_request/cif.

Table 6.1 Crystallographic data for compounds 2–5.

Compounds	**2**•$(C_6H_6)_1$	**3**•$(CH_3CN)_1$	**4**•(THF)$_1$
Formula	$C_{35}H_{48}F_3GeN_3O_3S$	$C_{33}H_{48}F_6Ge_1\,N_4O_6S_2$	$C_{36}H_{47}CrGeN_3O_6$
Fw	720.41	847.46	742.35
Cryst syst	monoclinic	monoclinic	monoclinic
Space group	$P2_1/n$	$P2_1/n$	$P2_1/c$
Size (mm^3)	0.120 x 0.180 x 0.320	0.240 x 0.300 x 0.420	0.180 x 0.200 x 0.200
T, K	103(2)	103(2)	103(2)
a, Å	11.7454(9)	15.6749(8)	10.2157(3)
b, Å	24.4796(19)	15.7685(7)	22.5884(5)
c, Å	13.3037(10)	16.6380(9)	15.2996(5)
β, deg	115.166(2)	112.057(3)	97.6480(13)
V, Å^3	3462.0(5)	3811.4(3)	3499.07(17)
Z	4	4	4

d_{calcd} g·cm^{-3}	1.382	1.477	1.409
μ, mm^{-1}	1.000	0.990	1.218
Refl collected	40551	65643	46257
T_{max}/T_{min}	0.8890/0.7400	0.7970/0.6810	0.8110/0.7930
N_{measd}	8645	16952	11215
[R_{int}]	0.0751	0.0991	0.0561
R [I>2sigma(I)]	0.0482	0.0572	0.0403
R_w[I>2sigma(I)]	0.1075	0.1350	0.0894
GOF	1.025	1.025	1.017
Largest diff. peak/hole[e·Å^{-3}]	1.357/-0.664	2.531/-1.033	1.325/-1.138

Compounds	**5**•(THF)$_1$	**6**•(THF)$_1$	**7**
Formula	$C_{36}H_{47}GeMoN_3O_6$	$C_{36}H_{47}GeWN_3O_6$	$C_{43}H_{63}Cl_2GeIr_2N_3$
Fw	786.29	874.20	1149.85
Cryst syst	monoclinic	monoclinic	monoclinic
Space group	$P2_1/c$	$P2_1/c$	$P2_1/n$
Size (mm^3)	0.100 x 0.120 x 0.180	0.060 x 0.080 x 0.120	0.160 x 0.180 x 0.220
T, K	103(2)	133(2)	153(2)
a, Å	10.3172(9)	10.3691(5)	12.4041(4)
b, Å	22.6231(18)	22.6170(7)	14.8542(5)
c, Å	15.3939(12)	15.3476(7)	22.8415(8)
β, deg	97.423(3)	97.055(3)	94.2923(18)
V, Å^3	3562.9(5)	3572.0(3)	4196.8(2)
Z	4	4	4
d_{calcd} g·cm^{-3}	1.466	1.626	1.820
μ, mm^{-1}	1.244	4.107	7.199
Refl collected	32532	50991	15842
T_{max}/T_{min}	0.8860/0.8070	0.7910/ 0.6380	0.3920/0.3000

N_{measd}	7754	9666	12979
[R_{int}]	0.1085	0. 0879	0.0902
R [I>2sigma(I)]	0.0512	0.0416	0.0467
R_w[I>2sigma(I)]	0.1292	0.0885	0.0997
GOF	1.024	1.001	1.038
Largest diff. peak/hole[e·Å^{-3}]	0.849/-1.298	1.397/-1.289	1.454/-1.451

6.4.3 Theoretical calculation

Gaussian 09 was used for all density functional theory (DFT) calculations.[24] Geometry optimization, frequency calculations and natural bond orbital (NBO) analysis of compounds **2** and **4**–**7** were performed at the B3LYP/6-311G(d,p) level of theory, with the LANL2TZ(f) pseudo-potential applied for the metal atoms.

Figure 6.26 Calculated optimized structures for **2** and **4**–**7**.

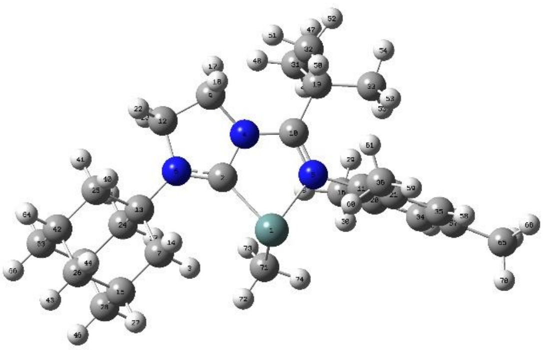

2

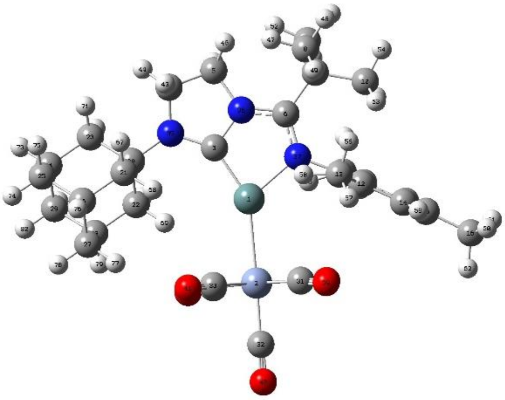

4

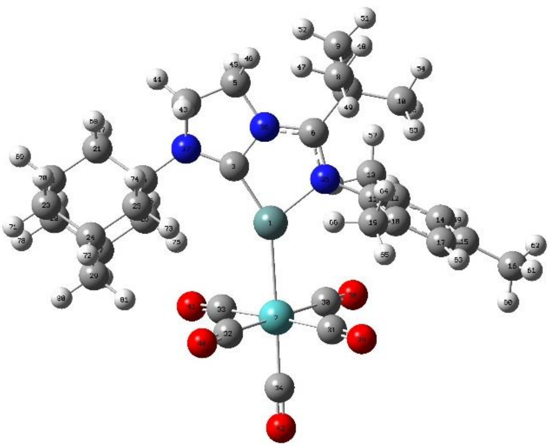

5

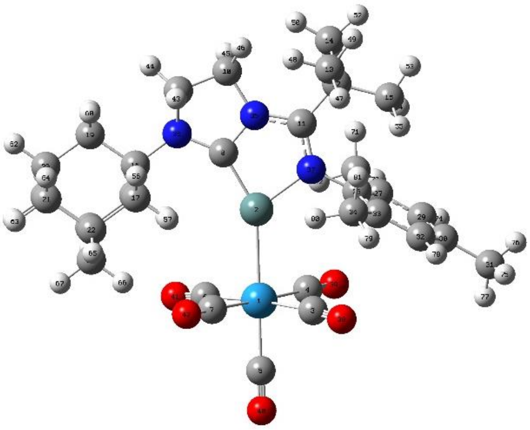

6

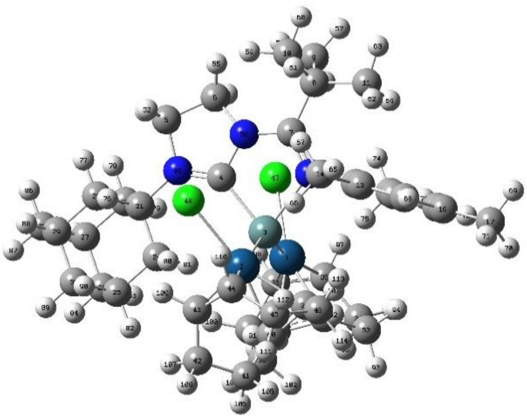

7

Table 6.2 Optimized structures of **2** and **4–7** (atom, x-, y-, z- positions in Å)

2

Ge	-0.160593	-1.079018	-0.603191
C	0.828228	0.643073	-0.133302
H	2.322121	-1.657319	-0.469518
N	-0.048857	1.707194	-0.038006
N	-1.722820	0.202143	-0.093956
N	2.078088	1.078868	-0.135769
C	3.152109	-1.063385	-0.863137
H	-1.820359	-0.221594	2.420471
C	0.702593	2.981516	-0.181708
C	-1.434255	1.467019	-0.010778
C	-3.010452	-0.452295	-0.029616
C	2.131806	2.538925	0.118045
C	3.319484	0.234473	-0.050772
H	2.923844	-0.824363	-1.906165
C	4.437284	-1.915184	-0.768683
C	-2.868873	-0.493889	2.528218
H	0.357675	3.750664	0.499973
H	0.611703	3.339677	-1.208207
C	-2.391802	2.673552	0.155468
C	-3.515835	-0.861763	1.213322
C	-3.664876	-0.782627	-1.232643
H	2.849028	3.029482	-0.534576
H	2.418203	2.720336	1.158264
C	3.610301	-0.116143	1.428231
C	4.516281	1.023093	-0.631812
C	5.622756	-1.123190	-1.347085
H	4.284893	-2.832213	-1.344641
C	4.712878	-2.263099	0.707321
H	-3.387004	0.351841	2.994126
H	-2.928642	-1.326163	3.232255
C	-2.150379	3.310012	1.549546
C	-2.166985	3.709541	-0.981150
C	-3.889176	2.300964	0.092849
C	-4.706363	-1.595053	1.229751
C	-4.850946	-1.509929	-1.154030
C	-3.142804	-0.343333	-2.579883
H	2.761905	-0.668110	1.845145
H	3.727870	0.799709	2.017789
C	4.898124	-0.964317	1.514940

H	4.312251	1.292279	-1.674176
H	4.671726	1.950720	-0.073301
C	5.801345	0.173675	-0.538851
H	6.535527	-1.724750	-1.299638
H	5.448153	-0.892966	-2.403710
H	3.887546	-2.853414	1.120665
H	5.611895	-2.882225	0.782754
H	-2.791486	4.188529	1.649155
H	-1.124405	3.633316	1.722439
H	-2.417196	2.611244	2.344578
H	-2.171621	3.231907	-1.964376
H	-1.254815	4.291867	-0.882799
H	-2.994575	4.420484	-0.962348
H	-4.176345	1.874972	-0.867547
H	-4.456238	3.225156	0.223524
H	-4.194231	1.616035	0.879217
H	-5.106581	-1.907835	2.189079
C	-5.390029	-1.931994	0.064411
H	-5.369301	-1.755027	-2.075354
H	-3.822362	-0.659076	-3.371647
H	-2.158768	-0.768198	-2.794203
H	-3.044278	0.745026	-2.645830
H	5.088329	-1.204000	2.565057
C	6.081727	-0.163571	0.938486
H	6.630258	0.756961	-0.949552
C	-6.657347	-2.748435	0.106971
H	7.003238	-0.747998	1.019771
H	6.238143	0.754438	1.515969
H	-7.380463	-2.398981	-0.633393
H	-7.128559	-2.704718	1.090291
H	-6.448734	-3.800500	-0.113370
C	-0.044664	-2.092758	1.145730
H	0.742209	-2.842446	1.040237
H	0.152115	-1.486199	2.028033
H	-0.989348	-2.624690	1.272764
Ge	-0.160593	-1.079018	-0.603191
C	0.828228	0.643073	-0.133302
H	2.322121	-1.657319	-0.469518
N	-0.048857	1.707194	-0.038006

N	-1.722820	0.202143	-0.093956
N	2.078088	1.078868	-0.135769
C	3.152109	-1.063385	-0.863137
H	-1.820359	-0.221594	2.420471
C	0.702593	2.981516	-0.181708
C	-1.434255	1.467019	-0.010778
C	-3.010452	-0.452295	-0.029616
C	2.131806	2.538925	0.118045
C	3.319484	0.234473	-0.050772
H	2.923844	-0.824363	-1.906165
C	4.437284	-1.915184	-0.768683
C	-2.868873	-0.493889	2.528218
H	0.357675	3.750664	0.499973
H	0.611703	3.339677	-1.208207
C	-2.391802	2.673552	0.155468
C	-3.515835	-0.861763	1.213322
C	-3.664876	-0.782627	-1.232643
H	2.849028	3.029482	-0.534576
H	2.418203	2.720336	1.158264
C	3.610301	-0.116143	1.428231
C	4.516281	1.023093	-0.631812
C	5.622756	-1.123190	-1.347085
H	4.284893	-2.832213	-1.344641
C	4.712878	-2.263099	0.707321
H	-3.387004	0.351841	2.994126
H	-2.928642	-1.326163	3.232255
C	-2.150379	3.310012	1.549546
C	-2.166985	3.709541	-0.981150
C	-3.889176	2.300964	0.092849
C	-4.706363	-1.595053	1.229751
C	-4.850946	-1.509929	-1.154030
C	-3.142804	-0.343333	-2.579883
H	2.761905	-0.668110	1.845145
H	3.727870	0.799709	2.017789
C	4.898124	-0.964317	1.514940

H	4.312251	1.292279	-1.674176
H	4.671726	1.950720	-0.073301
C	5.801345	0.173675	-0.538851
H	6.535527	-1.724750	-1.299638
H	5.448153	-0.892966	-2.403710
H	3.887546	-2.853414	1.120665
H	5.611895	-2.882225	0.782754
H	-2.791486	4.188529	1.649155
H	-1.124405	3.633316	1.722439
H	-2.417196	2.611244	2.344578
H	-2.171621	3.231907	-1.964376
H	-1.254815	4.291867	-0.882799
H	-2.994575	4.420484	-0.962348
H	-4.176345	1.874972	-0.867547
H	-4.456238	3.225156	0.223524
H	-4.194231	1.616035	0.879217
H	-5.106581	-1.907835	2.189079
C	-5.390029	-1.931994	0.064411
H	-5.369301	-1.755027	-2.075354
H	-3.822362	-0.659076	-3.371647
H	-2.158768	-0.768198	-2.794203
H	-3.044278	0.745026	-2.645830
H	5.088329	-1.204000	2.565057
C	6.081727	-0.163571	0.938486
H	6.630258	0.756961	-0.949552
C	-6.657347	-2.748435	0.106971
H	7.003238	-0.747998	1.019771
H	6.238143	0.754438	1.515969
H	-7.380463	-2.398981	-0.633393
H	-7.128559	-2.704718	1.090291
H	-6.448734	-3.800500	-0.113370
C	-0.044664	-2.092758	1.145730
H	0.742209	-2.842446	1.040237
H	0.152115	-1.486199	2.028033
H	-0.989348	-2.624690	1.272764

4

Ge	0.097271	-0.050560	-0.028143
Cr	0.289847	-2.612021	-0.042388
C	-0.936568	1.515844	-0.178296
C	-2.293230	3.370262	0.091746

C	-0.927213	3.859774	-0.351041
C	1.247163	2.515332	-0.078392
C	2.154386	3.766960	0.032578
C	1.868385	4.484933	1.379002

C	1.927036	4.728731	-1.165279
C	3.671551	3.473072	0.026101
C	2.924312	0.681195	0.033288
C	3.515144	0.365308	1.266754
C	2.845593	0.670417	2.585108
C	4.785296	-0.217752	1.264719
C	5.469891	-0.501267	0.085455
C	6.820782	-1.174353	0.107973
C	4.848470	-0.186219	-1.124634
C	3.582854	0.394844	-1.177629
C	2.964881	0.727180	-2.513492
C	-3.464831	1.135705	-0.099785
C	-3.696784	0.800330	1.395944
C	-3.341352	-0.178950	-0.891466
C	-4.706566	1.895024	-0.631247
C	-5.979241	1.041677	-0.471985
C	-6.190490	0.726032	1.021906
C	-4.974475	-0.054905	1.556013
C	-4.827585	-1.365632	0.760133
C	-4.610122	-1.039933	-0.730525
C	-5.827031	-0.266789	-1.267557
C	1.633205	-2.544126	-1.404459
C	1.627969	-2.567914	1.323043
C	0.394177	-4.473392	-0.029184
C	-1.028322	-2.669645	1.332933
C	-1.028560	-2.734718	-1.419164
N	-2.264177	1.970544	-0.336580
N	-0.105161	2.650323	-0.151644
N	1.587311	1.213362	-0.011097
O	2.420394	-2.567829	-2.236130
O	2.407083	-2.625140	2.161131
O	0.454986	-5.621137	-0.019886
O	-1.795973	-2.739716	2.182793
O	-1.797673	-2.870512	-2.258603
H	-2.401697	3.471127	1.184023
H	-3.089692	3.930653	-0.393598
H	-0.936309	4.118251	-1.413236

H	-0.577045	4.706309	0.228599
H	0.828663	4.783535	1.507710
H	2.482084	5.387454	1.448956
H	2.129001	3.835766	2.217514
H	2.082441	4.206881	-2.112829
H	2.656785	5.540452	-1.109729
H	0.942347	5.187962	-1.191282
H	3.993073	2.858599	0.862893
H	4.187391	4.433551	0.105512
H	4.004508	2.997461	-0.895032
H	3.145706	1.656308	2.959855
H	3.133621	-0.065410	3.337196
H	1.758334	0.667667	2.503243
H	5.241562	-0.468577	2.217324
H	7.317426	-1.040865	1.071210
H	7.476909	-0.778173	-0.671047
H	6.722141	-2.251157	-0.065552
H	5.355934	-0.412777	-2.057227
H	3.481178	0.199178	-3.315777
H	3.027304	1.800197	-2.727568
H	1.908057	0.456060	-2.549828
H	-3.798685	1.725072	1.975517
H	-2.829231	0.265346	1.793734
H	-2.482525	-0.746090	-0.529634
H	-3.156244	0.047527	-1.946145
H	-4.846287	2.829858	-0.080021
H	-4.542811	2.155380	-1.682956
H	-6.834058	1.610561	-0.853362
H	-7.103617	0.135394	1.155720
H	-6.325664	1.655206	1.588208
H	-5.118898	-0.283161	2.617227
H	-3.992352	-1.951545	1.150983
H	-5.728972	-1.977251	0.880547
H	-4.476652	-1.965846	-1.297541
H	-6.733877	-0.874342	-1.172827
H	-5.697535	-0.047229	-2.333455

5

Ge	0.075470	0.135497	-0.033753
Mo	0.322265	-2.563713	-0.041460
C	-0.980550	1.686098	-0.187211

C	-2.370499	3.517999	0.063972
C	-1.009095	4.028054	-0.371177
C	1.185921	2.718917	-0.079494

C	2.074255	3.983427	0.030056
C	1.770113	4.704848	1.370638
C	1.840228	4.935991	-1.173625
C	3.594776	3.708349	0.034152
C	2.886792	0.904998	0.040725
C	3.548055	0.620029	-1.169192
C	2.924300	0.937912	-2.505879
C	4.819927	0.052861	-1.114120
C	5.444391	-0.251669	0.097192
C	6.803454	-0.907995	0.122201
C	4.755194	0.025772	1.275180
C	3.478363	0.594337	1.275001
C	2.800242	0.887642	2.591630
C	-3.496535	1.256683	-0.105344
C	-4.760786	1.998432	-0.607390
C	-6.015642	1.121937	-0.432493
C	-6.194264	0.788986	1.061857
C	-4.955013	0.025485	1.566739
C	-3.696232	0.904617	1.391052
C	-3.365141	-0.048667	-0.913253
C	-4.615761	-0.932775	-0.735291
C	-5.856113	-0.176824	-1.242206
C	-4.798721	-1.275111	0.756227
C	1.744109	-2.478003	-1.544845
C	1.802975	-2.506456	1.402049
C	-1.066144	-2.658803	1.479133
C	-1.139847	-2.732957	-1.489865
C	0.469194	-4.567216	-0.031524
N	1.544546	1.422629	-0.006618
N	-0.168515	2.833606	-0.159673
N	-2.314586	2.115415	-0.353408
O	2.519577	-2.478083	-2.386857
O	2.603103	-2.551080	2.219939
O	-1.814411	-2.734390	2.344498
O	-1.933039	-2.879988	-2.303812
O	0.548220	-5.714440	-0.025959
H	-2.489887	3.624838	1.154540
H	-3.172206	4.061468	-0.431933

H	-1.014491	4.281089	-1.434727
H	-0.677580	4.883514	0.206492
H	0.726691	4.995151	1.488432
H	2.375169	5.613082	1.441597
H	2.028824	4.062087	2.214662
H	2.009366	4.412542	-2.117925
H	2.556875	5.759288	-1.117366
H	0.848543	5.379566	-1.207450
H	3.918406	3.102481	0.876535
H	4.098924	4.675210	0.111013
H	3.938704	3.230942	-0.882048
H	3.459631	0.429798	-3.308613
H	2.951449	2.013024	-2.716361
H	1.876741	0.632414	-2.545248
H	5.330341	-0.170623	-2.045854
H	6.718869	-1.985557	-0.053897
H	7.295592	-0.770363	1.087134
H	7.456855	-0.501895	-0.654012
H	5.212768	-0.219621	2.228518
H	3.065204	1.886348	2.958803
H	3.114693	0.168591	3.349559
H	1.713647	0.846099	2.510217
H	-4.621590	2.270489	-1.659723
H	-4.906570	2.925891	-0.045348
H	-6.886770	1.679592	-0.792936
H	-6.335659	1.710205	1.639486
H	-7.094208	0.180893	1.206324
H	-5.075854	-0.214874	2.628205
H	-2.812454	0.382142	1.769246
H	-3.803591	1.822788	1.980075
H	-2.488545	-0.606368	-0.578548
H	-3.207749	0.193646	-1.969092
H	-4.477926	-1.851389	-1.312840
H	-6.750229	-0.801014	-1.135548
H	-5.750745	0.053718	-2.308426
H	-5.685408	-1.905459	0.888381
H	-3.945378	-1.848761	1.126118

6

W	0.324024	-2.332169	-0.032048
Ge	0.050471	0.333801	-0.034959

C	1.800853	-2.257768	1.393930
C	1.733412	-2.233919	-1.526442

C	0.491009	-4.327208	-0.011947
C	-1.128515	-2.530760	-1.466985
C	-1.051638	-2.427447	1.481954
C	-1.030741	1.861827	-0.187454
C	-2.445525	3.672621	0.068575
C	-1.092704	4.202761	-0.368589
C	1.121296	2.926084	-0.079399
C	1.991136	4.203402	0.030785
C	1.676319	4.920020	1.371627
C	1.742633	5.152039	-1.173008
C	3.515662	3.951573	0.035055
C	-3.541439	1.396565	-0.105368
C	-3.730173	1.030604	1.388983
C	-3.397929	0.099342	-0.923981
C	-4.816572	2.127009	-0.596269
C	-6.060040	1.234263	-0.422681
C	-6.228091	0.887923	1.069834
C	-4.977708	0.135417	1.563481
C	-4.809550	-1.157096	0.742317
C	-4.636978	-0.801111	-0.747211
C	-5.888492	-0.056228	-1.243120
C	2.850830	1.138692	0.038913
C	3.516080	0.864744	-1.171257
C	2.887596	1.172417	-2.508140
C	4.797300	0.319266	-1.116127
C	5.427204	0.026330	0.095229
C	6.796846	-0.607453	0.120378
C	4.733943	0.292766	1.273344
C	3.447530	0.839022	1.273268
C	2.764905	1.120352	2.590200
N	-2.370813	2.271738	-0.351767
N	-0.234263	3.020567	-0.159211
N	1.499811	1.634742	-0.008258
O	2.609669	-2.289073	2.207046
O	2.511291	-2.220427	-2.369107
O	0.582342	-5.475602	-0.000399
O	-1.924054	-2.692753	-2.278959
O	-1.802569	-2.498033	2.348479
H	-2.564252	3.775625	1.159574

H	-3.255682	4.205487	-0.424859
H	-1.103383	4.455672	-1.432086
H	-0.772428	5.062606	0.208778
H	1.943713	4.280753	2.215599
H	0.629116	5.196341	1.489553
H	2.268999	5.836307	1.442714
H	0.743432	5.578125	-1.208550
H	1.922533	4.631856	-2.117104
H	2.444633	5.987752	-1.115300
H	4.004806	4.926240	0.110125
H	3.866699	3.477740	-0.880204
H	3.848675	3.352556	0.878668
H	-3.845280	1.942755	1.985872
H	-2.839408	0.514771	1.759571
H	-2.512946	-0.449261	-0.597097
H	-3.248282	0.351432	-1.978667
H	-4.971497	3.048226	-0.026460
H	-4.685566	2.408537	-1.647181
H	-6.939206	1.784345	-0.775135
H	-7.120135	0.268165	1.213631
H	-6.377921	1.803033	1.655038
H	-5.090602	-0.114396	2.623580
H	-3.948133	-1.723588	1.104249
H	-5.688278	-1.798775	0.873072
H	-4.489991	-1.713415	-1.332328
H	-5.790464	0.183819	-2.307949
H	-6.774497	-0.692037	-1.137624
H	2.904964	2.247095	-2.722160
H	1.842993	0.857128	-2.546179
H	3.426633	0.666390	-3.309634
H	5.311045	0.103520	-2.047808
H	7.289487	-0.455493	1.082902
H	7.441211	-0.196048	-0.660537
H	6.728895	-1.687366	-0.048217
H	5.195726	0.055323	2.226635
H	3.081226	0.397522	3.343665
H	1.678731	1.073629	2.506698
H	3.024268	2.117964	2.964166

7

Ir	0.659242	-2.212911	-0.973221

Ir	-0.661935	2.387054	-0.470773

Ge	-0.182051	-0.042784	0.094263
C	0.821808	-0.088646	1.851893
C	2.124220	-0.066620	3.753493
C	0.904573	-0.929093	4.024651
C	-1.309833	-0.872367	2.657138
C	-2.142584	-1.377424	3.870315
C	-1.517025	-2.690337	4.426000
C	-2.196594	-0.271934	4.957452
C	-3.612564	-1.727952	3.549372
C	-3.038267	-0.765805	0.903539
C	-3.884396	0.357166	0.959196
C	-3.476749	1.643505	1.624643
C	-5.146877	0.266458	0.366956
C	-5.586568	-0.886370	-0.280624
C	-6.965861	-0.963054	-0.889562
C	-4.721182	-1.978380	-0.318906
C	-3.450495	-1.948109	0.260980
C	-2.585144	-3.177194	0.204432
C	3.257409	0.602654	1.551037
C	3.763052	1.910223	2.206127
C	4.363467	-0.479554	1.631521
C	2.945754	0.870200	0.069461
C	4.215113	1.366078	-0.655470
C	5.314683	0.292287	-0.568593
C	5.634727	0.019239	0.912435
C	6.129430	1.317785	1.579419
C	5.034035	2.397544	1.480190
C	4.707534	2.669072	-0.000040
C	1.028654	-1.296950	-2.853168
C	-0.313947	-1.786560	-2.798819
C	-0.802695	-3.040591	-3.505294
C	0.116615	-4.262826	-3.274357
C	0.843973	-4.195461	-1.938369
C	2.122006	-3.637158	-1.769089
C	2.937052	-2.991455	-2.871290
C	2.128138	-1.960375	-3.687679
C	-2.126601	1.956894	-1.930855
C	-0.850633	2.017457	-2.568692
C	-0.407796	3.179389	-3.460884
C	0.363076	4.253606	-2.665754
C	-0.096490	4.356159	-1.225984
C	-1.434031	4.438338	-0.803302
C	-2.627819	4.459096	-1.747594

C	-3.186718	3.041715	-2.016618
Cl	1.038174	-3.234914	1.202516
Cl	0.115815	3.061474	1.722194
N	2.050583	0.118867	2.288580
N	0.030761	-0.554300	2.886761
N	-1.696672	-0.667137	1.431107
H	2.057482	0.908846	4.243607
H	3.048329	-0.557852	4.049190
H	1.146691	-1.989472	3.938225
H	0.460091	-0.716485	4.989431
H	-1.244284	-3.373619	3.618982
H	-2.261509	-3.186558	5.051897
H	-0.638688	-2.533843	5.046038
H	-1.225085	0.125869	5.244092
H	-2.668541	-0.683162	5.853502
H	-2.803222	0.569643	4.618423
H	-4.183662	-0.884632	3.170975
H	-4.074441	-2.045684	4.487718
H	-3.701823	-2.552693	2.844675
H	-4.341701	2.294758	1.762033
H	-2.737006	2.176867	1.012485
H	-3.006056	1.490874	2.596673
H	-5.802216	1.130380	0.418423
H	-7.681040	-1.408600	-0.189481
H	-6.968684	-1.577632	-1.792847
H	-7.339907	0.028421	-1.153416
H	-5.040258	-2.893027	-0.809024
H	-3.131005	-4.007891	-0.246232
H	-2.239912	-3.491638	1.192123
H	-1.673832	-3.001728	-0.382934
H	2.970571	2.661713	2.159606
H	4.000093	1.739754	3.261728
H	4.610447	-0.701548	2.674743
H	3.993906	-1.404407	1.179779
H	2.158442	1.623833	-0.016606
H	2.592208	-0.052768	-0.403348
H	3.960072	1.552425	-1.703283
H	4.982247	-0.629182	-1.058388
H	6.216071	0.629519	-1.092664
H	6.406500	-0.753655	0.989081
H	6.381507	1.130913	2.630065
H	7.045690	1.664804	1.089323
H	5.378592	3.319901	1.958819

H	5.597532	3.040478	-0.520568
H	3.938844	3.444619	-0.078768
H	1.158859	-0.223640	-2.748363
H	-1.101848	-1.045258	-2.681309
H	-0.930165	-2.853168	-4.581169
H	-1.800467	-3.266924	-3.117711
H	-0.482930	-5.176487	-3.307418
H	0.842912	-4.350092	-4.086885
H	0.524755	-4.911249	-1.186790
H	2.696417	-3.984147	-0.915175
H	3.361509	-3.759686	-3.533285
H	3.789209	-2.491310	-2.402366
H	2.805276	-1.189565	-4.065999

H	1.690079	-2.430756	-4.572790
H	-2.556589	0.966826	-1.786933
H	-0.414652	1.068385	-2.855566
H	-1.275091	3.619864	-3.960665
H	0.232204	2.794405	-4.259698
H	1.426085	3.995886	-2.653122
H	0.289561	5.231895	-3.162060
H	0.652794	4.730110	-0.533619
H	-1.603357	4.849088	0.187192
H	-2.350352	4.942347	-2.688042
H	-3.415130	5.079729	-1.311239
H	-3.951802	2.812278	-1.269354
H	-3.693958	3.006583	-2.991594

Figure 6.27 Plots of the frontier orbitals of compounds **4**–**7**.

4:

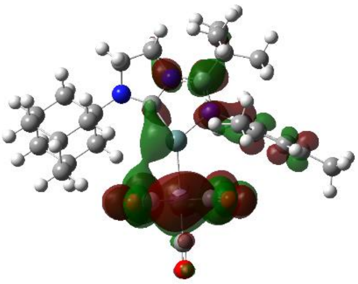

LUMO+3 (–0.3954 eV)

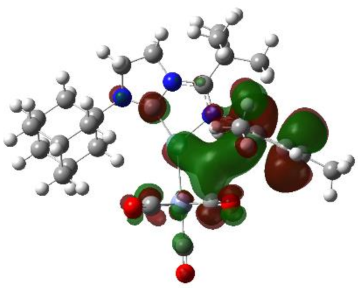

LUMO+2 (–0.4144 eV)

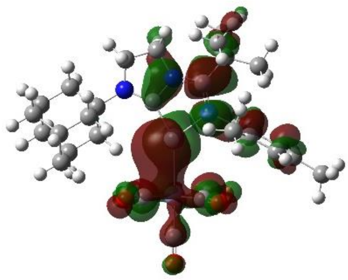

LUMO+1 (–0.7070 eV)

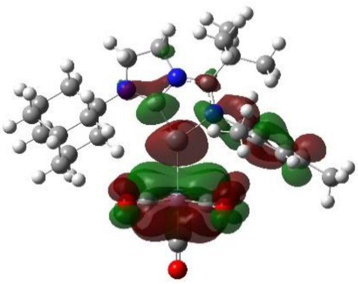

LUMO (–0.8419 eV)

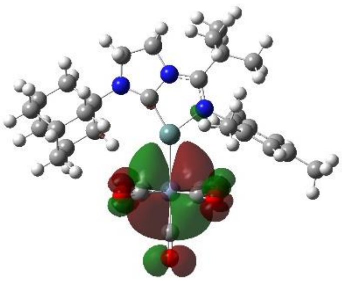

HOMO-1 (–5.7519 eV)

5:

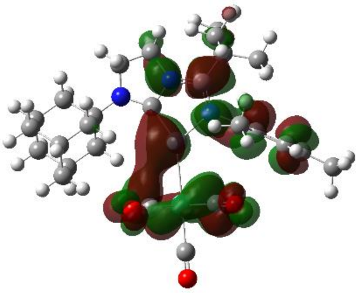

LUMO+3 (−0.5864 eV)

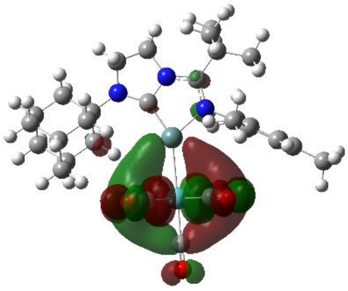

LUMO+2 (−0.7758 eV)

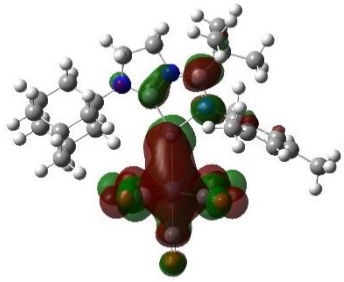

LUMO+1 (−0.9578 eV)

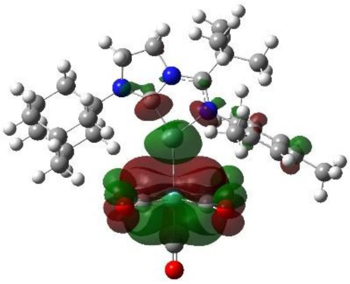

LUMO (−1.0735 eV)

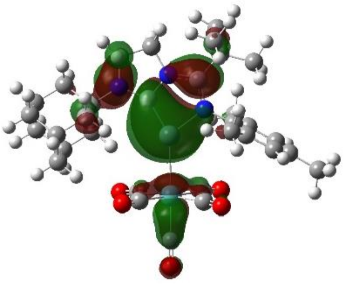

HOMO (−4.2719 eV)

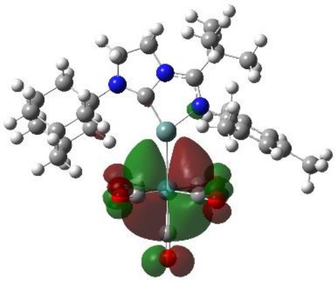

HOMO-1 (−5.7130 eV)

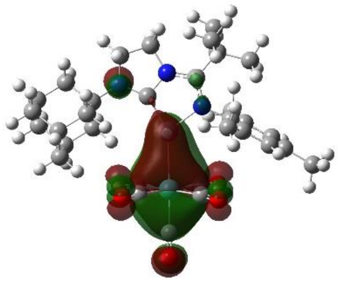

HOMO-2 (−5.8627 eV)

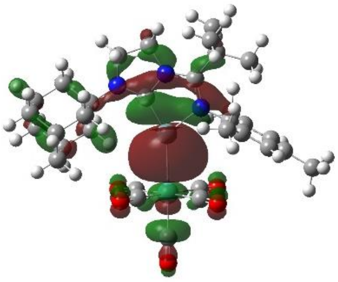

HOMO-7(−7.4807 eV)

6:

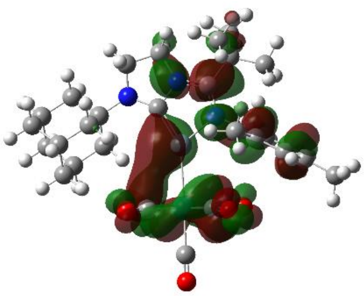

LUMO+3 (−0.6455 eV)

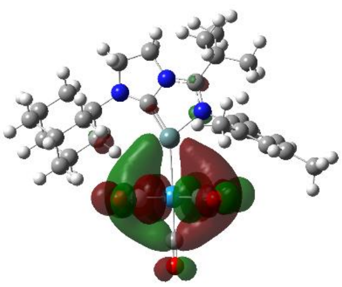

LUMO+2 (−0.8912 eV)

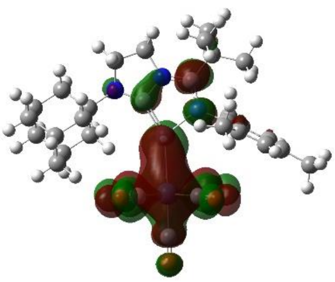

LUMO+1 (−1.0572 eV)

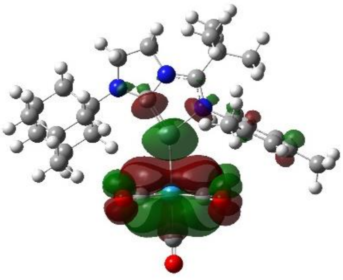

LUMO (−1.1557 eV)

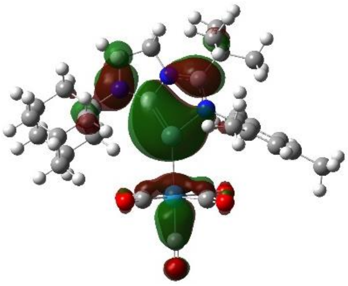

HOMO (−4.3095 eV)

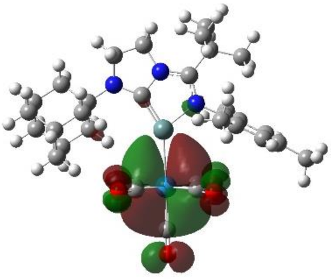

HOMO-1 (−5.6861 eV)

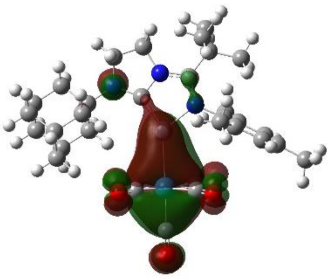

HOMO-2 (−5.8646 eV)

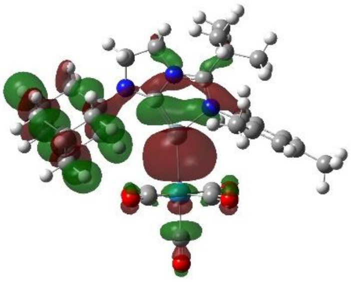

HOMO-7 (−7.7052 eV)

7:

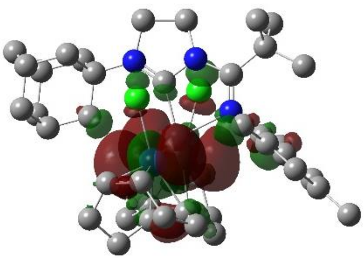

HOMO-1 (−4.9517 eV)

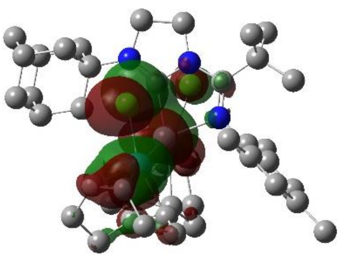

HOMO-2 (−5.3394 eV)

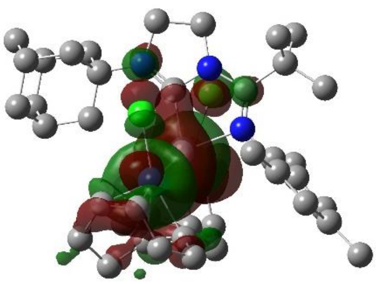

HOMO-3 (−5.3664 eV)

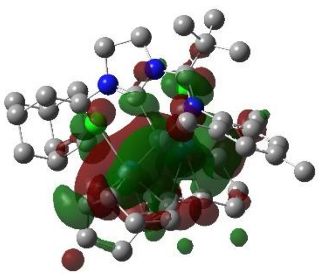

LUMO+2 (−0.6370 eV)

Table 6.3. The NPA charges of **4** calculated at the B3LYP/6-311G(d,p) level of theory, with the LANL2TZ(f) pseudo-potential applied for the Cr atom.

Atom	No	Natural Charge	Core	Valence	Rydberg	Total
Ge	1	1.16572	28.00000	2.81526	0.01902	30.83428
Cr	2	-2.62631	17.95983	8.61342	0.05307	26.62631
C	3	-0.21821	1.99908	4.18238	0.03675	6.21821
C	4	-0.18038	1.99943	4.16410	0.01685	6.18038
C	5	-0.18004	1.99941	4.16423	0.01640	6.18004
C	6	0.44634	1.99903	3.52166	0.03298	5.55366
C	7	-0.06207	1.99935	4.04942	0.01330	6.06207
C	8	-0.57130	1.99943	4.56078	0.01109	6.57130
C	9	-0.57742	1.99944	4.56687	0.01112	6.57742
C	10	-0.58013	1.99945	4.56811	0.01256	6.58013
C	11	0.12865	1.99886	3.85219	0.02029	5.87135
C	12	-0.00752	1.99906	3.99259	0.01587	6.00752
C	13	-0.60024	1.99943	4.59148	0.00933	6.60024
C	14	-0.20829	1.99908	4.19436	0.01484	6.20829
C	15	0.00360	1.99917	3.98265	0.01458	5.99640
C	16	-0.59058	1.99944	4.58229	0.00884	6.59058
C	17	-0.20860	1.99908	4.19466	0.01485	6.20860
C	18	-0.00394	1.99906	3.98914	0.01573	6.00394
C	19	-0.59527	1.99944	4.58660	0.00924	6.59527
C	20	0.19598	1.99927	3.78294	0.02182	5.80402
C	21	-0.41686	1.99933	4.40149	0.01604	6.41686
C	22	-0.40754	1.99933	4.39008	0.01813	6.40754
C	23	-0.40521	1.99934	4.38889	0.01698	6.40521
C	24	-0.19347	1.99942	4.17716	0.01689	6.19347
C	25	-0.39057	1.99941	4.37556	0.01560	6.39057
C	26	-0.19369	1.99942	4.17750	0.01676	6.19369
C	27	-0.39586	1.99940	4.38120	0.01526	6.39586
C	28	-0.19500	1.99941	4.17901	0.01658	6.19500
C	29	-0.38941	1.99941	4.37445	0.01555	6.38941
C	30	0.84444	1.99908	3.10053	0.05595	5.15556
C	31	0.84454	1.99907	3.10048	0.05591	5.15546
C	32	0.84078	1.99890	3.10402	0.05631	5.15922
C	33	0.83992	1.99907	3.10446	0.05655	5.16008
C	34	0.83677	1.99907	3.10771	0.05645	5.16323
N	35	-0.51624	1.99931	5.49484	0.02209	7.51624
N	36	-0.39452	1.99922	5.38331	0.01199	7.39452

N	37	-0.72730	1.99934	5.71014	0.01781	7.72730
O	38	-0.45335	1.99975	6.44250	0.01110	8.45335
O	39	-0.45493	1.99975	6.44407	0.01112	8.45493
O	40	-0.45660	1.99975	6.44619	0.01065	8.45660
O	41	-0.46172	1.99975	6.45083	0.01114	8.46172
O	42	-0.45632	1.99975	6.44551	0.01106	8.45632
H	43	0.17303	0.00000	0.82280	0.00417	0.82697
H	44	0.20707	0.00000	0.79126	0.00167	0.79293
H	45	0.19876	0.00000	0.79810	0.00314	0.80124
H	46	0.20678	0.00000	0.79061	0.00261	0.79322
H	47	0.19132	0.00000	0.80747	0.00122	0.80868
H	48	0.20249	0.00000	0.79552	0.00199	0.79751
H	49	0.20767	0.00000	0.79046	0.00187	0.79233
H	50	0.20614	0.00000	0.79189	0.00197	0.79386
H	51	0.20391	0.00000	0.79409	0.00200	0.79609
H	52	0.19714	0.00000	0.80165	0.00122	0.80286
H	53	0.21499	0.00000	0.78290	0.00211	0.78501
H	54	0.20052	0.00000	0.79739	0.00208	0.79948
H	55	0.21175	0.00000	0.78622	0.00203	0.78825
H	56	0.20262	0.00000	0.79543	0.00195	0.79738
H	57	0.21743	0.00000	0.78103	0.00154	0.78257
H	58	0.22133	0.00000	0.77754	0.00113	0.77867
H	59	0.20098	0.00000	0.79633	0.00268	0.79902
H	60	0.20440	0.00000	0.79434	0.00126	0.79560
H	61	0.20582	0.00000	0.79286	0.00132	0.79418
H	62	0.21459	0.00000	0.78396	0.00146	0.78541
H	63	0.20074	0.00000	0.79657	0.00269	0.79926
H	64	0.21237	0.00000	0.78629	0.00134	0.78763
H	65	0.20063	0.00000	0.79724	0.00213	0.79937
H	66	0.22286	0.00000	0.77584	0.00129	0.77714
H	67	0.19328	0.00000	0.80400	0.00271	0.80672
H	68	0.21420	0.00000	0.78353	0.00228	0.78580
H	69	0.20853	0.00000	0.78776	0.00371	0.79147
H	70	0.21092	0.00000	0.78548	0.00360	0.78908
H	71	0.19372	0.00000	0.80347	0.00281	0.80628
H	72	0.20499	0.00000	0.79169	0.00332	0.79501
H	73	0.20506	0.00000	0.79278	0.00216	0.79494
H	74	0.19875	0.00000	0.79884	0.00241	0.80125
H	75	0.19360	0.00000	0.80432	0.00209	0.80640
H	76	0.20719	0.00000	0.79052	0.00229	0.79281
H	77	0.21027	0.00000	0.78696	0.00277	0.78973
H	78	0.19674	0.00000	0.80073	0.00253	0.80326
H	79	0.21470	0.00000	0.78273	0.00257	0.78530
H	80	0.19792	0.00000	0.79967	0.00241	0.80208

H	81	0.19700	0.00000	0.80096	0.00205	0.80300
* Total *		0.00000	125.93265	221.07634	0.99102	348.00000

Table 6.4 The NPA charges of **5** calculated at the B3LYP/6-311G(d,p) level of theory, with the LANL2TZ(f) pseudo-potential applied for the Mo atom.

Atom	No	Natural Charge	Core	Valence	Rydberg	Total
Ge	1	1.15111	28.00000	2.83007	0.01882	30.84889
Mo	2	-2.34130	35.94126	8.36519	0.03485	44.34130
C	3	-0.20646	1.99909	4.17045	0.03692	6.20646
C	4	-0.18053	1.99943	4.16426	0.01683	6.18053
C	5	-0.18014	1.99941	4.16435	0.01638	6.18014
C	6	0.44763	1.99903	3.52076	0.03257	5.55237
C	7	-0.06222	1.99935	4.04957	0.01330	6.06222
C	8	-0.57118	1.99943	4.56067	0.01108	6.57118
C	9	-0.57738	1.99944	4.56683	0.01111	6.57738
C	10	-0.58017	1.99945	4.56820	0.01251	6.58017
C	11	0.13044	1.99886	3.85048	0.02021	5.86956
C	12	-0.00453	1.99906	3.99009	0.01537	6.00453
C	13	-0.59578	1.99944	4.58727	0.00907	6.59578
C	14	-0.20921	1.99908	4.19531	0.01482	6.20921
C	15	0.00324	1.99917	3.98301	0.01459	5.99676
C	16	-0.59058	1.99944	4.58230	0.00884	6.59058
C	17	-0.20831	1.99908	4.19437	0.01486	6.20831
C	18	-0.00813	1.99906	3.99350	0.01557	6.00813
C	19	-0.59984	1.99943	4.59125	0.00915	6.59984
C	20	0.19587	1.99927	3.78299	0.02187	5.80413
C	21	-0.40558	1.99934	4.38928	0.01696	6.40558
C	22	-0.19335	1.99942	4.17704	0.01689	6.19335
C	23	-0.39054	1.99941	4.37553	0.01561	6.39054
C	24	-0.19382	1.99942	4.17765	0.01674	6.19382
C	25	-0.41698	1.99933	4.40160	0.01604	6.41698
C	26	-0.40762	1.99933	4.39045	0.01785	6.40762
C	27	-0.19554	1.99941	4.17955	0.01658	6.19554
C	28	-0.38945	1.99941	4.37449	0.01555	6.38945
C	29	-0.39492	1.99941	4.38028	0.01523	6.39492
C	30	0.78445	1.99918	3.15476	0.06161	5.21555
C	31	0.78295	1.99917	3.15617	0.06171	5.21705

C	32	0.77871	1.99917	3.16055	0.06157	5.22129
C	33	0.77598	1.99917	3.16316	0.06170	5.22402
C	34	0.77082	1.99898	3.16771	0.06250	5.22918
N	35	-0.72126	1.99935	5.70446	0.01746	7.72126
N	36	-0.39440	1.99923	5.38328	0.01190	7.39440
N	37	-0.51480	1.99931	5.49367	0.02182	7.51480
O	38	-0.44799	1.99975	6.43788	0.01037	8.44799
O	39	-0.44955	1.99975	6.43937	0.01044	8.44955
O	40	-0.45477	1.99975	6.44463	0.01040	8.45477
O	41	-0.45156	1.99975	6.44143	0.01039	8.45156
O	42	-0.45558	1.99975	6.44555	0.01028	8.45558
H	43	0.17303	0.00000	0.82278	0.00419	0.82697
H	44	0.20716	0.00000	0.79117	0.00167	0.79284
H	45	0.19874	0.00000	0.79816	0.00310	0.80126
H	46	0.20684	0.00000	0.79056	0.00260	0.79316
H	47	0.19131	0.00000	0.80748	0.00121	0.80869
H	48	0.20256	0.00000	0.79545	0.00199	0.79744
H	49	0.20756	0.00000	0.79057	0.00187	0.79244
H	50	0.20607	0.00000	0.79196	0.00197	0.79393
H	51	0.20398	0.00000	0.79402	0.00200	0.79602
H	52	0.19711	0.00000	0.80167	0.00121	0.80289
H	53	0.21486	0.00000	0.78304	0.00210	0.78514
H	54	0.20062	0.00000	0.79729	0.00208	0.79938
H	55	0.21194	0.00000	0.78605	0.00201	0.78806
H	56	0.21189	0.00000	0.78678	0.00134	0.78811
H	57	0.20067	0.00000	0.79719	0.00214	0.79933
H	58	0.22352	0.00000	0.77526	0.00122	0.77648
H	59	0.20089	0.00000	0.79641	0.00270	0.79911
H	60	0.21460	0.00000	0.78394	0.00146	0.78540
H	61	0.20448	0.00000	0.79426	0.00126	0.79552
H	62	0.20588	0.00000	0.79280	0.00132	0.79412
H	63	0.20122	0.00000	0.79608	0.00269	0.79878
H	64	0.20254	0.00000	0.79549	0.00197	0.79746
H	65	0.21608	0.00000	0.78241	0.00151	0.78392
H	66	0.22189	0.00000	0.77701	0.00109	0.77811
H	67	0.20482	0.00000	0.79185	0.00333	0.79518
H	68	0.19412	0.00000	0.80309	0.00279	0.80588
H	69	0.20514	0.00000	0.79270	0.00216	0.79486
H	70	0.19371	0.00000	0.80421	0.00209	0.80629
H	71	0.19884	0.00000	0.79874	0.00241	0.80116
H	72	0.20736	0.00000	0.79032	0.00231	0.79264
H	73	0.21423	0.00000	0.78372	0.00205	0.78577
H	74	0.19344	0.00000	0.80383	0.00273	0.80656
H	75	0.20959	0.00000	0.78645	0.00396	0.79041

H	76	0.21002	0.00000	0.78658	0.00340	0.78998
H	77	0.21519	0.00000	0.78229	0.00253	0.78481
H	78	0.19798	0.00000	0.79961	0.00242	0.80202
H	79	0.19698	0.00000	0.80097	0.00205	0.80302
H	80	0.19714	0.00000	0.80033	0.00253	0.80286
H	81	0.20829	0.00000	0.78906	0.00265	0.79171
* Total *		0.00000	143.91456	221.09102	0.99442	366.00000

Table 6.5 The NPA charges of **6** calculated at the B3LYP/6-311G(d,p) level of theory, with the LANL2TZ(f) pseudo-potential applied for the W atom.

Atom	No	Natural Charge	Core	Valence	Rydberg	Total
W	1	-2.18292	67.94744	8.19983	0.03566	76.18292
Ge	2	1.17580	28.00000	2.80553	0.01867	30.82420
C	3	0.74305	1.99910	3.19460	0.06325	5.25695
C	4	0.74476	1.99911	3.19294	0.06319	5.25524
C	5	0.72887	1.99887	3.20830	0.06396	5.27113
C	6	0.73499	1.99909	3.20265	0.06326	5.26501
C	7	0.73775	1.99910	3.20012	0.06303	5.26225
C	8	-0.20138	1.99907	4.16541	0.03690	6.20138
C	9	-0.18045	1.99943	4.16418	0.01684	6.18045
C	10	-0.18009	1.99941	4.16425	0.01643	6.18009
C	11	0.44932	1.99904	3.51948	0.03216	5.55068
C	12	-0.06234	1.99935	4.04969	0.01329	6.06234
C	13	-0.57118	1.99943	4.56069	0.01107	6.57118
C	14	-0.57732	1.99944	4.56677	0.01111	6.57732
C	15	-0.58019	1.99945	4.56821	0.01252	6.58019
C	16	0.19570	1.99927	3.78319	0.02185	5.80430
C	17	-0.41701	1.99933	4.40165	0.01603	6.41701
C	18	-0.40787	1.99933	4.39058	0.01796	6.40787
C	19	-0.40571	1.99934	4.38943	0.01695	6.40571
C	20	-0.19327	1.99942	4.17696	0.01689	6.19327
C	21	-0.39059	1.99941	4.37557	0.01560	6.39059
C	22	-0.19374	1.99942	4.17756	0.01676	6.19374
C	23	-0.39503	1.99941	4.38039	0.01523	6.39503
C	24	-0.19569	1.99941	4.17967	0.01660	6.19569
C	25	-0.38948	1.99941	4.37452	0.01554	6.38948
C	26	0.12911	1.99886	3.85166	0.02036	5.87089

C	27	-0.00451	1.99906	3.98992	0.01553	6.00451
C	28	-0.59567	1.99944	4.58712	0.00911	6.59567
C	29	-0.20871	1.99908	4.19481	0.01482	6.20871
C	30	0.00413	1.99917	3.98213	0.01457	5.99587
C	31	-0.59067	1.99944	4.58239	0.00885	6.59067
C	32	-0.20764	1.99908	4.19369	0.01487	6.20764
C	33	-0.00785	1.99906	3.99305	0.01575	6.00785
C	34	-0.60016	1.99943	4.59154	0.00918	6.60016
N	35	-0.51382	1.99931	5.49255	0.02196	7.51382
N	36	-0.39312	1.99923	5.38210	0.01180	7.39312
N	37	-0.71935	1.99934	5.70289	0.01712	7.71935
O	38	-0.44863	1.99975	6.43777	0.01112	8.44863
O	39	-0.44658	1.99975	6.43582	0.01102	8.44658
O	40	-0.45564	1.99975	6.44516	0.01073	8.45564
O	41	-0.45062	1.99975	6.43977	0.01110	8.45062
O	42	-0.45420	1.99975	6.44335	0.01110	8.45420
H	43	0.17340	0.00000	0.82246	0.00414	0.82660
H	44	0.20767	0.00000	0.79067	0.00166	0.79233
H	45	0.19911	0.00000	0.79780	0.00309	0.80089
H	46	0.20724	0.00000	0.79016	0.00260	0.79276
H	47	0.20776	0.00000	0.79037	0.00186	0.79224
H	48	0.19127	0.00000	0.80753	0.00121	0.80873
H	49	0.20287	0.00000	0.79515	0.00198	0.79713
H	50	0.19709	0.00000	0.80169	0.00121	0.80291
H	51	0.20622	0.00000	0.79182	0.00196	0.79378
H	52	0.20426	0.00000	0.79375	0.00200	0.79574
H	53	0.20084	0.00000	0.79708	0.00208	0.79916
H	54	0.21214	0.00000	0.78585	0.00201	0.78786
H	55	0.21496	0.00000	0.78294	0.00210	0.78504
H	56	0.19345	0.00000	0.80382	0.00273	0.80655
H	57	0.21411	0.00000	0.78378	0.00211	0.78589
H	58	0.20905	0.00000	0.78670	0.00425	0.79095
H	59	0.21002	0.00000	0.78663	0.00335	0.78998
H	60	0.19412	0.00000	0.80309	0.00279	0.80588
H	61	0.20479	0.00000	0.79189	0.00331	0.79521
H	62	0.20518	0.00000	0.79266	0.00216	0.79482
H	63	0.19901	0.00000	0.79858	0.00241	0.80099
H	64	0.19364	0.00000	0.80427	0.00209	0.80636
H	65	0.20767	0.00000	0.79002	0.00231	0.79233
H	66	0.20870	0.00000	0.78851	0.00279	0.79130
H	67	0.19721	0.00000	0.80025	0.00253	0.80279
H	68	0.21587	0.00000	0.78160	0.00252	0.78413
H	69	0.19692	0.00000	0.80103	0.00205	0.80308
H	70	0.19813	0.00000	0.79946	0.00241	0.80187

H	71	0.20067	0.00000	0.79721	0.00212	0.79933
H	72	0.22280	0.00000	0.77599	0.00121	0.77720
H	73	0.21267	0.00000	0.78599	0.00134	0.78733
H	74	0.20112	0.00000	0.79618	0.00270	0.79888
H	75	0.20459	0.00000	0.79415	0.00126	0.79541
H	76	0.20590	0.00000	0.79278	0.00132	0.79410
H	77	0.21498	0.00000	0.78355	0.00146	0.78502
H	78	0.20151	0.00000	0.79580	0.00269	0.79849
H	79	0.21721	0.00000	0.78125	0.00154	0.78279
H	80	0.22104	0.00000	0.77788	0.00108	0.77896
H	81	0.20276	0.00000	0.79529	0.00195	0.79724
* Total *		0.00000	175.92034	221.07352	1.00614	398.00000

Table 6.6 The NPA charges of **7** calculated at the B3LYP/6-311G(d,p) level of theory, with the LANL2TZ(f) pseudo-potential applied for the Ir atom.

Atom	No	Natural Charge	Core	Valence	Rydberg	Total
Ir	1	-0.44271	67.97178	9.42751	0.04342	77.44271
Ir	2	-0.46023	67.97175	9.44474	0.04373	77.46023
Ge	3	1.23757	28.00000	2.72718	0.03525	30.76243
C	4	0.13742	1.99914	3.81447	0.04897	5.86258
C	5	-0.18910	1.99942	4.17371	0.01597	6.18910
C	6	-0.19001	1.99941	4.17486	0.01574	6.19001
C	7	0.55985	1.99894	3.40674	0.03447	5.44015
C	8	-0.07162	1.99933	4.05866	0.01363	6.07162
C	9	-0.58293	1.99942	4.57213	0.01138	6.58293
C	10	-0.57265	1.99943	4.56196	0.01126	6.57265
C	11	-0.58172	1.99945	4.56987	0.01240	6.58172
C	12	0.11820	1.99881	3.86200	0.02099	5.88180
C	13	-0.00293	1.99907	3.98811	0.01574	6.00293
C	14	-0.58959	1.99940	4.57941	0.01077	6.58959
C	15	-0.21917	1.99908	4.20526	0.01483	6.21917
C	16	0.00056	1.99916	3.98544	0.01484	5.99944
C	17	-0.59003	1.99944	4.58174	0.00885	6.59003
C	18	-0.21525	1.99909	4.20150	0.01466	6.21525
C	19	-0.00055	1.99907	3.98618	0.01530	6.00055
C	20	-0.58752	1.99941	4.57784	0.01027	6.58752
C	21	0.19859	1.99924	3.78039	0.02177	5.80141

C	22	-0.41618	1.99932	4.40057	0.01629	6.41618
C	23	-0.40660	1.99933	4.39081	0.01646	6.40660
C	24	-0.43093	1.99931	4.41393	0.01768	6.43093
C	25	-0.18746	1.99942	4.17130	0.01675	6.18746
C	26	-0.39127	1.99941	4.37650	0.01536	6.39127
C	27	-0.19425	1.99942	4.17804	0.01679	6.19425
C	28	-0.39174	1.99941	4.37672	0.01561	6.39174
C	29	-0.19316	1.99942	4.17700	0.01674	6.19316
C	30	-0.39125	1.99941	4.37645	0.01540	6.39125
C	31	-0.21152	1.99892	4.18887	0.02372	6.21152
C	32	-0.19739	1.99893	4.17457	0.02389	6.19739
C	33	-0.39376	1.99941	4.37869	0.01566	6.39376
C	34	-0.40280	1.99941	4.38905	0.01434	6.40280
C	35	-0.21331	1.99898	4.18972	0.02461	6.21331
C	36	-0.19422	1.99897	4.17044	0.02481	6.19422
C	37	-0.39924	1.99941	4.38456	0.01528	6.39924
C	38	-0.39674	1.99942	4.38255	0.01477	6.39674
C	39	-0.19108	1.99892	4.16833	0.02382	6.19108
C	40	-0.21143	1.99893	4.18853	0.02397	6.21143
C	41	-0.39663	1.99942	4.38249	0.01471	6.39663
C	42	-0.39854	1.99941	4.38376	0.01536	6.39854
C	43	-0.18672	1.99896	4.16284	0.02492	6.18672
C	44	-0.22184	1.99898	4.19804	0.02482	6.22184
C	45	-0.40212	1.99941	4.38848	0.01423	6.40212
C	46	-0.39504	1.99941	4.38003	0.01560	6.39504
Cl	47	-0.44626	10.00000	7.43707	0.00919	17.44626
Cl	48	-0.42567	10.00000	7.41568	0.00999	17.42567
N	49	-0.40428	1.99918	5.38502	0.02007	7.40428
N	50	-0.44277	1.99916	5.43092	0.01269	7.44277
N	51	-0.63203	1.99927	5.61326	0.01950	7.63203
H	52	0.20552	0.00000	0.79219	0.00228	0.79448
H	53	0.21451	0.00000	0.78378	0.00171	0.78549
H	54	0.22299	0.00000	0.77452	0.00249	0.77701
H	55	0.21026	0.00000	0.78760	0.00214	0.78974
H	56	0.22653	0.00000	0.77194	0.00153	0.77347
H	57	0.20789	0.00000	0.79036	0.00175	0.79211
H	58	0.19837	0.00000	0.80031	0.00132	0.80163
H	59	0.19637	0.00000	0.80228	0.00135	0.80363
H	60	0.20694	0.00000	0.79129	0.00177	0.79306
H	61	0.21178	0.00000	0.78688	0.00135	0.78822
H	62	0.21843	0.00000	0.77979	0.00178	0.78157
H	63	0.20224	0.00000	0.79574	0.00202	0.79776
H	64	0.21519	0.00000	0.78289	0.00192	0.78481
H	65	0.20380	0.00000	0.79478	0.00143	0.79620

H	66	0.24809	0.00000	0.74925	0.00266	0.75191
H	67	0.20410	0.00000	0.79345	0.00245	0.79590
H	68	0.19981	0.00000	0.79738	0.00281	0.80019
H	69	0.20969	0.00000	0.78887	0.00144	0.79031
H	70	0.20715	0.00000	0.79155	0.00130	0.79285
H	71	0.20574	0.00000	0.79299	0.00128	0.79426
H	72	0.19915	0.00000	0.79814	0.00271	0.80085
H	73	0.20245	0.00000	0.79613	0.00143	0.79755
H	74	0.21181	0.00000	0.78616	0.00203	0.78819
H	75	0.24139	0.00000	0.75530	0.00331	0.75861
H	76	0.23829	0.00000	0.75991	0.00180	0.76171
H	77	0.19221	0.00000	0.80534	0.00245	0.80779
H	78	0.19070	0.00000	0.80639	0.00292	0.80930
H	79	0.22527	0.00000	0.77258	0.00215	0.77473
H	80	0.24213	0.00000	0.75365	0.00423	0.75787
H	81	0.23489	0.00000	0.76081	0.00430	0.76511
H	82	0.21015	0.00000	0.78723	0.00262	0.78985
H	83	0.20190	0.00000	0.79564	0.00246	0.79810
H	84	0.19757	0.00000	0.79998	0.00244	0.80243
H	85	0.20807	0.00000	0.78978	0.00214	0.79193
H	86	0.19436	0.00000	0.80358	0.00206	0.80564
H	87	0.19950	0.00000	0.79813	0.00237	0.80050
H	88	0.20875	0.00000	0.78913	0.00212	0.79125
H	89	0.19687	0.00000	0.80070	0.00242	0.80313
H	90	0.20683	0.00000	0.79133	0.00184	0.79317
H	91	0.21094	0.00000	0.78617	0.00289	0.78906
H	92	0.21305	0.00000	0.78416	0.00279	0.78695
H	93	0.20212	0.00000	0.79528	0.00259	0.79788
H	94	0.19945	0.00000	0.79837	0.00217	0.80055
H	95	0.20746	0.00000	0.79079	0.00175	0.79254
H	96	0.19588	0.00000	0.80179	0.00232	0.80412
H	97	0.23027	0.00000	0.76826	0.00147	0.76973
H	98	0.23230	0.00000	0.76574	0.00196	0.76770
H	99	0.20607	0.00000	0.79133	0.00260	0.79393
H	100	0.19945	0.00000	0.79836	0.00219	0.80055
H	101	0.20359	0.00000	0.79461	0.00179	0.79641
H	102	0.19493	0.00000	0.80272	0.00235	0.80507
H	103	0.21408	0.00000	0.78279	0.00312	0.78592
H	104	0.21242	0.00000	0.78492	0.00266	0.78758
H	105	0.19389	0.00000	0.80380	0.00230	0.80611
H	106	0.20378	0.00000	0.79449	0.00173	0.79622
H	107	0.20139	0.00000	0.79692	0.00169	0.79861
H	108	0.20557	0.00000	0.79188	0.00256	0.79443
H	109	0.23012	0.00000	0.76780	0.00208	0.76988

H	110	0.23142	0.00000	0.76711	0.00148	0.76858
H	111	0.19558	0.00000	0.80211	0.00231	0.80442
H	112	0.20678	0.00000	0.79148	0.00175	0.79322
H	113	0.19992	0.00000	0.79784	0.00225	0.80008
H	114	0.20189	0.00000	0.79553	0.00258	0.79811

===

* Total *	-0.00000	275.90884	284.98591	1.10525	562.00000

6.5 References

(1) a) Rivard, E. *Chem. Soc. Rev*. **2016**, *45*, 989 – 1003; b) Asay, M.; Jones, C.; Driess, M. *Chem. Rev.* **2011**, *111*, 354 – 396; c) Mizuhata, Y.; Sasamori, T.; Tokitoh, N. *Chem. Rev.* **2009**, *109*, 3479 – 3511; d) Zabula, A. V.; Hahn, F. E. *Eur. J. Inorg. Chem.* **2008**, 5165 – 5179; e) Boehme, C.; Frenking, G. *J. Am. Chem. Soc.* **1996**, *118*, 2039 – 2046.

(2) a) Dube, J. W.; Brown, Z. D.; Caputo, C. A.; Power, P. P.; Ragogna, P. *J. Chem. Commun.* **2014**, *50*, 1944 – 1946; b) Brown, Z. D.; Power, P. P. *Inorg. Chem.* **2013**, *52*, 6248 – 6259; c) Power, P. P. *Nature* **2010**, *463*, 171 – 177; d) Peng, Y.; Guo, J.-D.; Ellis, B. D.; Zhu, Z.; Fettinger, J. C.; Nagase, S.; Power, P. P. *J. Am. Chem. Soc.* **2009**, *131*, 16272 – 16282.

(3) a) Inomata, K.; Watanabe, T.; Miyazaki Y.; Tobita, H. *J. Am. Chem. Soc*. **2015**, *137*, 11935 – 11937; b) Erickson, J. D.; Fettinger, J. C.; Power, P. P. *Inorg. Chem.* **2015**, *54*, 1940 – 1948; c) Cabeza, J. A.; Fernández-Colinas, J. M.; Garcıía -Álvarez, P.; Polo, D. *Inorg. Chem.* **2012**, *51*, 3896 – 3903.

(4) a) Álvarez-Rodríguez, L.; Cabeza, J. A.; García-Álvarez, P.; Polo, D. *Coord. Chem. Rev.* **2015**, *300*, 1 – 28; b) Rivard, E. *Dalton Trans.* **2014**, *43*, 8577 – 8586.

(5) Germylene-group VI metal complexes: a) Al-Rafia, S. M. I.; Momeni, M. R.; Ferguson, M. J.; McDonald, R.; Brown, A.; Rivard, E. *Organometallics* **2013**, *32*, 6658 – 6665; b)

Bonnefille, E.; Saffon-Merceron, N.; Couret, C.; Mazières, S. *Eur. J. Inorg. Chem.* **2012**, 5771 – 5775; c) Matioszek, D.; Katir, N.; Saffon, N.; Castel, A. *Organometallics* **2010**, *29*, 3039 – 3046; d) Ullah, F.; Kühl, O.; Bajor, G.; Veszprémi, T.; Jones, P. G.; Heinicke, J. *Eur. J. Inorg. Chem.* **2009**, 221 – 229; e) Kühl, O.; Lönnecke, P.; Heinicke, J. *Inorg. Chem.* **2003**, *42*, 2836 – 2838; f) Du Mont, W. W.; Lange, L.; Pohl, S.; Saak, W. *Organometallics* **1990**, *9*, 1395 – 1399; g) Saur, I.; Rima, G.; Miqueu, K.; Gornitzka, H.; Barrau, J. *J. Organomet. Chem.* **2003**, *672*, 77 – 85; h) Bibal, C.; Mazières, S.; Gornitzka, H.; Couret, C. *Organometallics* **2002**, *21*, 2940 – 2943; i) Tokitoh, N.; Manmaru, K.; Okazaki, R. *Organometallics* **1994**, *13*, 167 – 171; j) Jutzi, P.; Hampel, B.; Stroppel, K.; Krüger, C.; Angermund, K.; Hofmann, P. *Chem. Ber.* **1985**, *118*, 2789 – 2797; k) Jutzi, P.; Steiner, W.; König, E. *Chem. Ber.* **1978**, *111*, 606 – 614; l) Marks, T. J. *J. Am. Chem. Soc.* **1971**, *93*, 7090 – 7091; m) Zabula, A. V.; Hahn, F. E.; Pape, T.; Hepp, A. *Organometallics* **2007**, *26*, 1972 – 1980; n) Hahn, F. E.; Zabula, A. V.; Pape, T.; Hepp, A. *Z. Anorg. Allg. Chem.* **2008**, *634*, 2397 – 2401.

(6) Selected recent examples of germylene-transition metal complexes: (a) El Ezzi, M.; Kocsor, T.-G.; D'Accriscio, F.; Madec, D.; Mallet-Ladeira, S.; Castel, A. *Organometallics* **2015**, *34*, 571 – 576; (b) Hlina, J.; Arp, H.; Walewska, M.; Flörke, U.; Zangger, K.; Marschner, C.; Baumgartner, J. *Organometallics* **2014**, *33*, 7069 – 7077; (c) Gallego, D.; Brück, A.; Irran, E.; Meier, F.; Kaupp, M.; Driess, M.; Hartwig, J. F. *J. Am. Chem. Soc.* **2013**, *135*, 15617 – 15626; (d) Brück, A.; Gallego, D.; Wang, W.; Irran, E.; Driess, M.; Hartwig, J. F. *Angew. Chem., Int. Ed.* **2012**, *51*, 11478 – 11482; (e) Wang, W.; Inoue, S.; Enthaler, S.; Driess, M. *Angew. Chem., Int. Ed.* **2012**, *51*, 6167 – 6171; (f) Cygan, Z. T.; Bender, J. E.;

Litz, K. E.; Kampf, J. W.; Banaszak Holl, M. M. *Organometallics* **2002**, *21*, 5373 – 5381; (g) Bazinet, P.; Yap, G. P. A.; Richeson, D. S. *J. Am. Chem. Soc.* **2001**, *123*, 11162 – 11167.

(7) a) Arii, H.; Amari, T.; Kobayashi, J.; Mochida, K.; Kawashima, T. *Angew. Chem., Int. Ed.* **2012**, *51*, 6738 – 6741; b) Koch, R.; Bruhn, T.; Weidenbruch, M. *Organometallics* **2004**, *23*, 1570 – 1575; c) Sekiguchi, A.; Izumi, R.; Ihara, S.; Ichinohe, M.; Lee, V. Ya. *Angew. Chem., Int. Ed.* **2002**, *41*, 1598 – 1600; d) Meiners, F. Saak, W.; Weidenbruch, M. *Z. Anorg. Allg. Chem.* **2002**, *628*, 2821 – 2822; e) Fukaya, N.; Ichinohe, M.; Kabe, Y.; Sekiguchi, A. *Organometallics* **2001**, *20*, 3364 – 3371; f) Ando, W.; Ohgaki, H.; Kabe, Y. *Angew. Chem., Int. Ed. Engl.* **1994**, *33*, 659 – 661.

(8) a) Chu, T.; Belding, L.; van der Est, A.; Dudding, T.; Korobkov, I.; Nikonov, G. I. *Angew. Chem., Int. Ed.* **2014**, *53*, 2711 – 2715; b) Xiong, Y.; Yao, S.; Tan, G.; Inoue, S.; Driess, M. *J. Am. Chem. Soc.* **2013**, *135*, 5004 – 5007; c) Li, Y.; Mondal, K. C.; Roesky, H. W.; Zhu, H.; Stollberg, P.; Herbst-Irmer, R.; Stalke, D.; Andrada, D. M. *J. Am. Chem. Soc.* **2013**, *135*, 12422 – 12428; d) Iwamoto, T.; Masuda, H.; Kabuto C.; Kira, M. *Organometallics* **2005**, *24*, 197 – 199.

(9) For other heavier group 14 analogues, see: a) Mondal, K. C.; Roesky, H. W.; Schwarzer, M. C.; Frenking, G.; Niepötter, B.; Wolf, H.; Herbst-Irmer, R.; Stalke, D. *Angew. Chem., Int. Ed.* **2013**, *52*, 2963 – 2967; b) Xiong, Y.; Yao, S.; Inoue, S.; Epping, J. D.; Driess, M. *Angew. Chem., Int. Ed*. **2013**, *52*, 7147 – 7150; c) Flock, J.; Suljanovic, A.; Torvisco, A.; Schoefberger, W.; Gerke, B.; Pöttgen, R.; Fischer, R. C.; Flock, M. *Chem. – Eur. J.* **2013**, *19*, 15504 – 15517; d) Ishida, S.; Iwamoto, T.; Kabuto, C.; Kira, M.; *Nature* **2003**, *421*, 725 – 727; e) Wiberg, N.; Lerner, H.-W.; Vasisht, S.-K.; Wagner, S.; Karaghiosoff, K.; Nöth,

H.; Ponikwar, W. *Eur. J. Inorg. Chem.* **1999**, 1211 – 1218.

(10) a) Takagi, N.; Tonner, R.; Frenking, G. *Chem. – Eur. J.* **2012**, *18*, 1772 – 1780. See also: b) Petz, W.; Frenking, G. *Top. Organomet. Chem.* **2010**, *30*, 49 – 92.

(11) Aldeco-Perez, E.; Rosenthal, A. J.; Donnadieu, B.; Parameswaran, P.; Frenking, G.; Bertrand, G. *Science* **2009**, *326*, 556-559.

(12) Crabtree, R. H. *Coord. Chem. Rev.* **2013**, *257*, 755-766.

(13) Xiong, Y.; Yao, S.; Karni, M.; Kostenko, A.; Burchert, A.; Apeloig, Y.; Driess, M. *Chem. Sci.* **2016**, *7*, 5462 − 5469.

(14) Zhou, Y. -P.; Karni, M.; Yao, S.; Apeloig, Y.; Driess, M. A. *Angew. Chem., Int. Ed.* **2016**, *55*, 15096 − 15099.

(15) Strohmeier, W. *Angew. Chem., Int. Ed. Engl.* **1964**, *3*, 730 – 737.

(16) a) Kitschke, P.; Mertens, L.; Rüffer, T.; Lang, H.; Auer, A. A.; Mehring, M. *Eur. J. Inorg. Chem.* **2015**, 4996 – 5002; b) Cotton, F. A.; Kraihanzel, C. S. *J. Am. Chem. Soc.* **1962**, *84*, 4432 – 4438.

(17) a) Kühl, O. *Coord. Chem. Rev.* **2005**, *249*, 693 – 740; b) Gillespie, A. M.; Pittard, K. A.; Cundari, T. R.; White, D. P. *Internet Electron. J. Mol. Des.* **2002**, *1*, 242 – 251.

(18) a) Timney, J. A. *Encyclopedia of Inorganic and Bioinorganic Chemistry*, John Wiley & Sons, Ltd, **2011**; b) Gädt, T.; Eichele, K.; Wesemann, L. *Organometallics* **2006**, *25*, 3904 – 3911; c) Kraihanzel, C. S.; Cotton, F. A. *Inorg. Chem.* **1963**, *2*, 533 – 540.

(19) Petz, W. *Chem. Rev.* **1986**, *86*, 1019 – 1047.

(20) Batsanov, S. S. *Inorg. Mater.* **2001**, *37*, 871 – 885; Batsanov, S. S. *Neorg. Mater.* **2001**, *37*, 1031 – 1046.

(21) a) Mobarok, M. H.; McDonald, R.; Ferguson, M. J.; Cowie, M. *Inorg. Chem.* **2012**, *51*, 9249–9258; b) Mobarok, M. H.; McDonald, R.; Ferguson, M. J.; Cowie, M. *Inorg. Chem.* **2012**, *51*, 4020–4034; c) Hall, M. B.; Trufan, E. *Organometallics* **2012**, *31*, 2621–2630; d) Adams, R.; Captain, B.; Smith, J. L. Jr. *Inorg. Chem.* **2005**, *44*, 1413−1420.

(22) For silicon(0) bimetallic complex, see: a)Yao, S.; Xiong, Y.; Driess, M. *Acc. Chem. Res.* **2017**, *50*, 2026 − 2037; for carbon(0) bimetallic complexes, see: b) Vicente, J.; Singhal, A. R.; Jones, P. G. *Organometallics* **2002**, *21*, 5887 − 5900. c) Alcarazo, M.; Lehmann, C. W.; Anoop, A.; Thiel, W.; Fürstner, A. *Nat. Chem.* **2009**, *1*, 295 − 301. d) Reitsamer, C.; Schuh, W.; Kopacka, H.; Wurst, K.; Peringer, P. *Organometallics* **2009**, *28*, 6617 − 6620. e) Alcarazo, M.; Radkowski, K.; Mehler, G.; Goddard, R.; Fürstner, A. *Chem. Commun.* **2013**, *49*, 3140 − 3142.

(23) Bruker AXS SHELXTL, Madison, WI; *SHELX-97G*. M. Sheldrick, Acta Crystallogr. A, **2008**, *64*, 112–122, *SHELX-2013*, http://shelx.uni-ac. gwdg.de/SHELX/index.php.

(24) Gaussian 09, Revision B.01, Frisch, M. J.; Trucks, G. W.; Schlegel, H. B.; Scuseria, G. E.; Robb, M. A.; Cheeseman, J. R.; Scalmani, G.; Barone, V.; Mennucci, B.; Petersson, G. A.; Nakatsuji, H.; Caricato, M.; Li, X.; Hratchian, H. P.; Izmaylov, A. F.; Bloino, J.; Zheng, G.; Sonnenberg, J. L.; Hada, M.; Ehara, M.; Toyota, K.; Fukuda, R.; Hasegawa, J.; Ishida, M.; Nakajima, T.; Honda, Y.; Kitao, O.; Nakai, H.; Vreven, T.; Montgomery, J. A. Jr.,; Peralta, J. E.; Ogliaro, F.; Bearpark, M.; Heyd, J. J.; Brothers, E.; Kudin, K. N.; Staroverov, V. N.; Keith, T.; Kobayashi, R.; Normand, J.; Raghavachari, K.; Rendell, A.; Burant, J. C.; Iyengar, S. S.; Tomasi, J.; Cossi, M.; Rega, N.; Millam, J. M.; Klene, M.; Knox, J. E.; Cross, J. B.; Bakken, V.; Adamo, C.; Jaramillo, J.; Gomperts, R.; Stratmann, R. E.; Yazyev,

O.; Austin, A. J.; Cammi, R.; Pomelli, C.; Ochterski, J. W.; Martin, R. L.; Morokuma, K.; Zakrzewski, V. G.; Voth, G. A.; Salvador, P.; Dannenberg, J. J.; Dapprich, S.; Daniels, A. D.; Farkas, O.; Foresman, J. B.; Ortiz, J. V.;Cioslowski, J.; Fox, D. J. Gaussian, Inc., Wallingford CT, **2010**.

Conclusion

The chemistry of aromatic five-membered heterocyclic rings involving the boron, silicon, and germanium elements has been briefly summarized in Chapter 1. Given the importance of the preparation and utilization of such novel aromatic molecules, we successfully developed several unknown aromatic molecules through several alternative synthetic routes.

In Chapter 2, we reported a novel aromatic 1,4,2-diazaborole species through reduction of boronium cation which is stabilized by a bidentate imino-N-heterocyclic carbene. X-ray diffraction analysis and computational studies revealed its aromatic nature. Meanwhile, owing to the unique electronic structure, the formal nucleophilic nature of the boron center has been demonstrated by the formation of B–F bond after the reaction with Selectfluor, which is very diffenent from the reactivity of 1,3,2-diazaboroles and its all-carbon anolgues.

In Chapter 3, we demonstrated the skeletal transformation of the B,N-heterocyclic skeleton of 1,4,2-diazaborole derivatives advantageously having the annulated C_3N_2 five-membered ring. A remarkable borylene **:**BBr insertion into the C-N bond was observed, and the resulting product could further undergo regiospecific substitution to afford the functionalized B,N-dihydroindole derivatives.

In Chapter 4, we described the photo-induced skeletal transformation of the 1,4,2-diazaborole derivatives. Based on the intrinsic electronic structure or the bulkiness of the substitutes on the boron center, the photo-reactions of these 1,4,2-diazaborole derivatives lead to the formation of different skeletal isomer via either the rearrangement of the BN_2C_2 five-membered ring or retro-cyclization of the N_2C_3 five-membered ring followed by 1,3-dipolar cycloaddition.

In Chapter 5, we successfully prepared the imino--N-heterocyclic carbene supported chlorogermyliumylidene cation which is further reduced by potassium graphite to afford the novel germanium(0) species**.** X-ray diffraction analysis and computational studies revealed the electron delocalization over the five-membered C_2N_2Ge ring involving one of the lone pairs on Ge, thus it can also be viewed as a mesoionic germylene species possessing a considerable aromaticity.

In Chapter 6, we studied the reactivity of germanium(0) species towards MeOTf as well as the transition metal (Cr, Mo, W and Ir) complexes. The reaction of germanium(0) species with one or two equivalents of MeOTf afforded the germyliumylidene ion or the dicationic species, respectively, thus demonstrating the property of the germanium(0) species as a donor of one or two lone pairs. Treatment of the germanium(0) species with complexes $M(CO)_5(THF)$ (M = Cr, Mo, W) resulted in the monometallic complexes containing a trigonal planar germanium center. Moreover, the reaction of the germanium(0) species with $[IrCl(COD)]_2$ afforded the germylone bimetallic complex with a relatively strong interaction between Ge atom with Ir atoms, which represents the first example of germylone bimetallic complex.

As mentioned above, we have developed the new methods for the preparation of two kinds of main group molecules (1,4,2-diazaboroles, germanium(0) species) which show the unusal electronic properties and reactivity. We envisage that 1,4,2-diazaboroles will show some unique photophysical properties when π-conjugated functionality is substituted at the boron atom due to the stronger π-electron-donating ability of 1,4,2-diazaboroles than reported 1,3,2-diazaboroles. Owing to the two lone pairs donating ability, the germanium(0) compound is very likely to be the supporting ligand for the stabilization of low-valent main group elements, such as B, Al, Ga. Meanwhile, this germanium(0) compound is a potential coordinated ligand for the transion-metal complexes, which are expected to possess some unique catalytic performances.

The structures of all new compounds synthesized in this thesis.

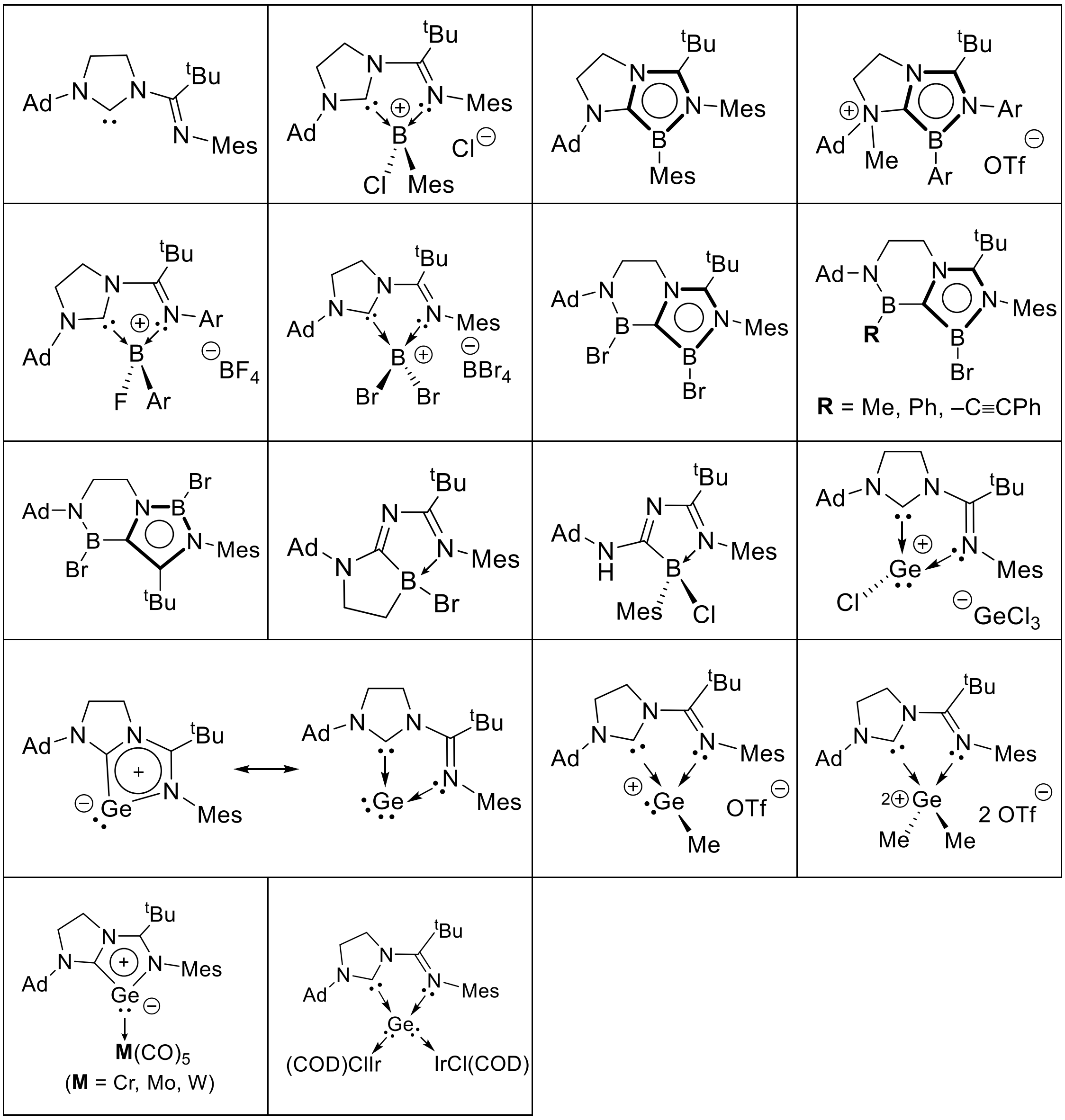

List of Publications related to this Thesis

1. **Bochao Su**, Yongxin Li, Rakesh Ganguly, Rei Kinjo,* "Ring expansion, photo-isomerization, and retro-cyclization of 1,4,2-diazaboroles" *Angew. Chem. Int. Ed.* **2017**, *56*, 14572 – 14576.

2. **Bochao Su**, Rei Kinjo,* "Construction of boron-containing aromatic heterocycles" *Synthesis* **2017**,*49*, 2985 – 3034.

3. **Bochao Su**, Rakesh Ganguly, Yongxin Li, Rei Kinjo,* "Synthesis, characterization, and electronic structures of a methyl germyliumylidene ion and germylone-group VI metal complexes" *Chem. Commun.* **2016**. 52, 613 – 616.

4. **Bochao Su**, Yongxin Li, Rakesh Ganguly, Jenny Lim, Rei Kinjo,* "Isolation and reactivity of 1,4,2-diazaborole" *J. Am. Chem. Soc.* **2015**, *137*, 11274 – 11277.

5. **Bochao Su**, Rakesh Ganguly, Yongxin Li, Rei Kinjo,* "Isolation of an imino-N-heterocyclic carbene/germanium(0) adduct: a mesoionic germylene equivalent" *Angew. Chem. Int. Ed.* **2014**, *53*, 13106 – 13109.